Understanding the Post-Harvest Disorder Blackheart in *Solanum tuberosum*



Lottie Chapman
Department of Plant Sciences
Worcester College

Thesis submitted for the degree of
Doctor of Philosophy

University of Oxford

Michaelmas term 2018

Abstract

Over a third of the food produced globally for human consumption is wasted each year, representing huge economic losses and limiting the security and efficiency of our food systems. In the UK, almost a half of potato tubers are lost after harvest, with the post-harvest disorder Blackheart accounting for a significant proportion of this wastage. Despite the importance of Blackheart, the underlying cause of the disorder is unclear, preventing its reliable prediction and management in industry.

Utilisation of a Blackheart induction method enabled improved characterisation of Blackheart in *Solanum tuberosum*, identifying it as a tissue specific condition that originates in tuber pith tissues. Although high temperatures and the abundances of CO_2 and O_2 have long been attributed to causing Blackheart, it was shown that none are necessary for the disorder to develop and instead, multiple conditions influence Blackheart development. Blackheart was associated with a decrease in the ATP:ADP ratio below a threshold level in affected tissues. The production of ATP did not appear to be limited in Blackheart affected tissues, as demonstrated by flux analysis and the abundance of respiratory substrates. Altered redistribution of labelled precursors into lipids and increased lipid acyl hydrolase activity of the potato storage protein, patatin, suggested that that active phospholipid breakdown was responsible for observed increases in membrane leakage. The resulting increased maintenance costs and consumption of ATP are proposed to drive cell death and the polyphenol-oxidase catalysed pigmentation that is observed in Blackheart affected tissues.

Acknowledgements

I'd like to thank my supervisors Professors Lee Sweetlove and Nick Kruger, for their help, supervision and teaching, which goes far beyond the pages of this thesis.

I would like to thank Manor Fresh Ltd for funding of three years of this industrial CASE studentship, provision of biological material, and managing of field trials. The practical support and industrial insight provided by Manor Fresh Ltd, particularly David Wright, Mike Scott and Chris Goodliff, was invaluable to the success of this thesis.

Thanks to: J.R.Simplot Ltd for financing a visit to Idaho and allowing me to work on their Innate® potato lines; Maria Font Farre and Professor Renier van der Hoorn, for the training in ABPP; Dr Jack Miller, for his interest in investigating Blackheart via MRI; the Advanced Proteomics Facility, University of Oxford for protein ID; and to Professor James McCullagh and his lab for MS training.

I'd like to thank the Department of Plant Sciences, University of Oxford, for such an inspiring work environment. Particular thanks to: Gem Toes-Crichton for her constant encouragement; to both the current and past Biochemistry lab members, from who I have learnt so much; to Pedro Bota for his lab management; and to the Oxford Interdisciplinary Bioscience Doctoral Training Programme and BBSRC for additional training and funding my iCASE studentship for an additional year.

Lastly, thank you to Mum, Dad, Jen and Ed, for keeping my priorities in check and offering emotional support, advice and assurances throughout the last four years.

Contents

Abstract 2

Acknowledgements 3

Contents 4

Abbreviations 7

1 Introduction 9

1.1 The Importance of This Research 9

1.2 Potatoes: An Important Crop with Significant Post-Harvest Difficulties 11

1.3 The Post-Harvest Potato Disorder Blackheart and its Commercial Importance 13

1.4 Current Understanding of Blackheart 15

1.5 Involvement of Polyphenol Oxidase and Cell Death in Blackheart 19

1.6 The Role of Anoxia in Blackheart 20

1.7 The Role of Storage Temperature in Blackheart and Tuber Metabolism 23

1.8 The Role of Membrane Integrity in Blackheart and Tuber Physiology 26

1.9 The Role of Storage Duration on the Occurrence of Blackheart 28

1.10 Research Hypothesis and Aims 29

2 Materials and Methods 31

2.1 Plant Material 31

2.2 Blackheart Induction 33

2.3 Destructive Blackheart Imaging 33

2.4 Non-Destructive Blackheart Imaging 34

2.5 Tissue Extraction 35

2.6 Histochemical and Histological Stains 35

2.7 Electrolyte Leakage Measurements 36

2.8 Respiration Rate 37

2.9 Adenylate Quantification 37
2.10 Metabolomics 38
2.11 Quantification of Starch, Sucrose, Glucose and Fructose 41
2.12 Carbon Flux Analysis 44
2.13 Maximum Catalytic Activity of Glycolytic Enzymes 59
2.14 Lipid Quantification and Identification 62
2.15 Activity Based Protein Profiling 66
2.16 Statistical Analysis Methods 70
3 Induction and Characterisation of Blackheart 71
3.1 Introduction 71
3.2 Results 82
3.3 Discussion 110
3.4 Summary 117
4 Blackheart Physiology and Biochemistry 119
4.1 Introduction 119
4.2 Results 132
4.3 Discussion 164
4.4 Summary 174
5 Does Insufficient Energy Production Lead to Blackheart? 176
5.1 Introduction 176
5.2 Results 182
5.3 Discussion 193
5.4 Summary 196
6 What Causes Increased Energy Demands in Blackheart Susceptible Tissues? 198
6.1 Introduction 198
6.3 Results 206

6.4 Discussion 227

6.5 Summary 232

7 Discussion 234

7.1 Summary of Research 234

7.2 Proposed Cause of Blackheart and Role of Patatin 235

7.3 Research Discussion: Future Work and Industrial Impact 237

7.4 Limitations of This Research 240

7.5 Wider Impact of This Work 241

Supplementary Data 244

Bibliography 247

Abbreviations

Activity Based Protein Profilling	ABPP
Apparent Difusion Coefficient	ADC
Adenosine diphosphate	ADP
Adenylate Energy Charge	AEC
Adenosine monophosphate	AMP
Alternative oxidase	AOX
Adenosine triphosphate	ATP
Beats per minute	BPM
Bovine serum albumin	BSA
Cold Induced Sweetening	CIS
3,3'-Diaminobenzidine	DAB
Disintegrations per minute	DPM
Dimethyl sulfoxide	DSMO
Fatty Acid Metyl Ester	FAME
Free Fatty Acid	FFA
Fluorophosphonate	FP
Gas Chromatography	GC
Gel loading buffer	GLB
Genetic Modificaton	GM
4-(2-hydroxyethyl)-1-piperazineethanesulfonic acid	Hepes
Infrared	IR
Liquid Chromatography	LC
Mass charge ratio	m/z

2-(*N*-morpholino)ethanesulfonic acid	MES
Modified Look-Locker Inversion	MOLLI
Mass Spectroscopy	MS
Trimethylsilyl-*N*-methyl trifluoroacetamide	MSTFA
3-(4,5-Dimethylthiazol-2-yl)-2,5-Diphenyltetrazolium Bromide	MTT
Nicotinamide adenine dinucleotide	NADH/NAD
Nicotinamide adenine dinucleotide phosphate	NADP/NADPH
Nitro blue tetrazolium	NBT
Oxidative Pentose Phosphate Pathway	OPPP
Polyacrylamide gel electrophoresis	PAGE
Phenylalanine Ammonia Lyase	PAL
Polyethylene/Polyamide	PE/PA
Phosphofructokinase	PFK
Fructose-6-phosphate 1-phosphotransferase	PFP
Polyphenol Oxidase	PPO
Reactive Oxygen Species	ROS
Sodium dodecyl sulfate	SDS
Solid Phase Extraction	SPE
Tricarboxylic acid	TCA
Tetramethylethylenediamine	TEMED
Polyoxyethylene octyl phenyl ether	TRITON
2,3,5-Triphenyltetrazolium Chloride	TTC

1 Introduction

1.1 The Importance of This Research

With the global population set to reach 9.8 billion by 2050 (United Nations DESA, 2017), current food supply must be increased by 50-60% to avoid a Malthusian crisis (Tilman et al., 2011; Foley et al., 2011; Alexandratos & Bruinsma, 2012; United Nations FAO & OECD, 2012; United Nations DESA, 2017) . The United Nations sustainable development goals identify food security as one of the most pressing global issues, aiming to "*end hunger, achieve food security and improved nutrition, and promote sustainable agriculture*" by 2030, via a "*doubling of agricultural productivity*" (United Nations DESA, 2015). This production-orientated approach to improving food security is prevalent; over 95% of recent agricultural research funding has gone towards increasing pre-harvest yields (Aulakh & Regmi, 2013; Kader, 2003), propagated by the stance of scientific funding bodies that "*global food security ultimately depends on growing enough crops"* (BBSRC, 2017).

This emphasis on improving in-field productivity has led to record global use of fertilizer, herbicides, and pesticides (FAO, 2018). Despite this, global crop productivity is stagnating (Foley et al., 2011), particularly in rice, wheat, maize and soybean, the four key crops that produce 67% of the worlds agricultural calories (Ray et al., 2012). This global decline in productivity has been compensated by an increase in land conversion to agriculture (Gibbs & Greenway, 2003; Foley et al., 2005; Foley et al., 2011), bringing with it dramatic effects on biodiversity (Pimm & Raven, 2000), water availability and soil erosion (Pimentel et al., 1995). The

impacts of climate change are expected to exacerbate the situation (Lobell et al., 2011). Genetic modification (GM) of crops to increase productivity has not yet achieved yield increases close to those required to sustain future populations (Klümper & Qaim, 2014; Miflin, 2000; Sinclair et al., 2004; Jordan, 2002; Halket et al., 2005; Paul et al., 2018), and their widespread adoption has been met with public resistance (Godfray et al., 2010). Without significant advances and a second green revolution, meeting food security demands by solely increasing crop productivity by 60-110% appears to be idealistic (Godfray et al., 2010; Sinclair et al., 2004; Miflin, 2000; Jordan, 2002; Paul et al., 2018).

A paradigm shift which considers the efficiency and sustainability of the whole food system has been recommended (Foley et al., 2011). It is estimated that 33-50% of the current food produced for consumption globally is thrown away (Gustavsson et al., 2011; Arbon et al., 2013). Reducing this percentage of wasted food could help feed a growing population, without the need for additional: agricultural land; fertiliser; herbicides and pesticides; human effort; carbon inputs; genetic modification; water; or large industrial and social changes. Reducing the amount of food lost or wasted could be "*one of the leading global strategies for achieving a sustainable food future*" (Lipinski et al., 2013) and help meet the required increases in food. Not only could reducing food waste and loss account for a sustainable way to meet some of the growing demands for food, but the effectiveness of current food production efforts are impeded unless this issue is tackled.

Post-harvest yield loss occurs at each stage of the food system; the food that is lost through harvest, handling, storage, processing, and distribution is referred to as food

loss and that from sales and consumption, food waste (Hodges et al., 2011). Food loss is largely invisible to consumers and is an unintended consequence of improper storage or physical damage, whereas food waste comprises produce that is in excess, has expired or does not meet aesthetic standards. The ratio of food waste and food loss differs geographically, based on environmental and social contexts; more food is lost in developing countries, due to financial and technical limitations around storage and post-harvest processing, as well as the high proportion of crops grown on smallholdings. In industrialised countries, higher levels of food waste are driven by uncoordinated supply chains and consumer behaviour (Gustavsson et al., 2011). Therefore, tackling issues that cause food loss and waste are of global importance.

1.2 Potatoes: An Important Crop with Significant Post-Harvest Difficulties

Potatoes are the world's most important vegetable crop, and the third most consumed crop, second only to that of rice and corn (Camire et al., 2009; FAO-STAT, 2018; FAO, 2009). Moreover, demand for tuber crops has been growing while that for cereal crops has begun to plateau (FAO-STAT, 2018). This is largely due to higher yields of tuber crops per hectare, and harvest reliability under variable climatic conditions (Scott et al., 2000; FAO, 2009). Climatic variability has been driving global food price inflation and in turn, food shortages in low income countries; in 2007-2008 the average global rice price tripled (FAO-STAT, 2018) causing widespread famine (Slayton, 2009). However, tuber crops such as potatoes are not internationally traded commodities; 95% of potatoes are consumed in the country of harvest (FAO-STAT, 2018), making the crop price less prone to market fluctuations and inflation.

Potatoes are highly nutritious; approximately 80% of potato dry matter is starch and the calorie density is equivalent to that of cereals (King & Slavin, 2013). However, potatoes provide far more protein, fibre and micronutrients than equivalent amounts of cereal grains. Just 100 g of potato provides 50% of the recommended daily intake of vitamin C, and more potassium than any other vegetable (FAO-STAT, 2018). The high, reliable yields, nutritional value, water use efficiency and resistance to economic fluctuations make the potato an ideal target crop for improving future food security; the FAO have described potatoes as *"a solution to increasing global food security"* (UN FAO, 2009).

However, storage of a tuber crop poses difficulties; 63% of roots and tuber calories produced for consumption globally are lost or wasted, as opposed to only 26% of cereals (Lipinski et al., 2013). Depending on the climate of a country, harvests may only occur once a year; for example, in the UK tubers are harvested in autumn and stored in long-term cold storage for up to 12 months, to meet year round consumer demand (Terry et al., 2011). The relatively high respiration rates of dormant tubers, as compared to grains (Diop & Caverly, 1998), means that storage conditions must be monitored more closely and that the maximum possible lifespan of the crop is shortened. The soft tissues of tubers are more prone to mechanical damage, causing increased transportation and processing losses, as well as specific storage requirements. The high water content of tubers increases the likelihood of microbial and fungal infections as well as damage by pests. This high water content also necessitates humidity and temperature control of the stores, to avoid drying or freezing. Additionally, as tubers are normally relatively short-lived overwintering

storage organs, stores must be kept cool and dark to avoid a breaking of dormancy or greening, although this ectodormancy is not preventable indefinitely (Diop & Caverly, 1998).

Consequently, almost all potato yield loss occurs beyond the field; in the UK 25-46% of tuber losses occur between harvest and retail and an additional 49-74.5% of tuber waste occurs after purchasing (Terry et al., 2011). Almost half of UK potatoes purchased are thrown away, at a weight of 2.12 billion tonnes each year (Quested & Parry, 2015) and similar losses are seen across North America and Europe (Lipinski et al., 2013). With a growing global demand for potatoes, the volume and duration of crops in storage will increase (FAO, 2009) and post-harvest potato losses will become an increasingly significant issue.

1.3 The Post-Harvest Potato Disorder Blackheart and its Commercial Importance

Blackheart is a non-pathogenic, storage disorder of potato crops (Stewart and Mix, 1917; Davis, 1926) that results in dark grey-black pigmentation of central tuber tissues that are firm to the touch and can also contain small cavities. Anecdotal evidence suggests a significant recent increase in the occurrence of the disorder and thus crop wastage, which has resulted in problems for agricultural potato growers and consumers (Briddon, 2015; Kiaitsi, 2015; David Wright, Manor Fresh Ltd., pers. comm., 2014). The internal pigmentation cannot be detected by external inspection and therefore existing quality control methods are unable to detect the disorder; this results in producers relying on destructive methods to sample crops for

Blackheart which introduces a trade-off between waste, and reliability of detection, resulting in Blackheart-affected tubers frequently being bought by consumers. Blackheart accounts for up to 30-40% of total vegetable related consumer complaints (Kiaitsi, 2015) and the dark tissue pigmentation is a cause of consumer food waste.

To avoid consumer complaints, growers regularly destructively sample their stored stocks for Blackheart; above a certain incidence rate the entire stock will be deemed unsellable and the material used for animal feed or wasted. In the UK, towards the end of the storage period or when Blackheart incidences are high, supermarkets will preferentially stock imported younger tubers from the Mediterranean. These practices result in significant reductions in UK potato yield and economic returns. Yet, the incidence of Blackheart complaints and occurrence in stores is increasing (Briddon 2015; Kiaitsi 2015). Despite its prevalence, no underlying cause of Blackheart has yet been proven, resulting in an inability to predict the varying prevalence of the disorder in tuber crops from year to year and continued crop waste and loss.

These high levels of consumer complaints and limited shelf life have driven supermarket preferences for late season imported potatoes and generated commercial concern around the issue of Blackheart. The supermarkets have therefore put both direct and competitive pressure on UK suppliers to reduce the incidence of Blackheart. This research, which aims to identify the cause of Blackheart and offer preventative measures, has been funded by the vegetable growers and suppliers Manor Fresh, the providers of fresh produce to the UK food

retailer Marks and Spencer. Offering Blackheart free potatoes would be a significant competitive advantage for a supplier, driving increased sales and stocking by supermarkets, as well as reducing crop waste and its associated economic losses.

1.4 Current Understanding of Blackheart

Blackheart was first characterised in 1913 (Bartholomew, 1913). With the advent of the railways in America, potato harvests began to be transported in refrigerated train carts. Temperature regulation of these carts was ineffective, particularly in the winter, and stoves were periodically lit within the carts to prevent material freezing. On arrival to the destination, the tubers closest to these stoves were frequently found to have dark pigmented central tissues when cut open, giving the disorder the name Blackheart. Blackheart could be replicated in the laboratory in tubers kept at high temperatures (38-44°C) for up to 24 hours. Further investigation showed that the affected tissues remained sterile, suggesting that the disorder is non-pathogenic (Bartholomew, 1913). The high temperatures (above 32°C) and CO_2 concentrations caused by stove combustion were proposed to increase tuber respiration rates, resulting in CO_2 accumulation in central tissues which caused cell death.

Stewart & Mix (1917) tested this hypothesis and found they were able to induce Blackheart by storing tubers in hermetically sealed jars at high temperatures, further supporting a metabolic, rather than pathogenic cause of the disorder. However, Blackheart could also be induced in tubers stored at temperatures below 6°C when oxygen was excluded, replicating common deep-piling storage conditions at the time. This suggested that high temperatures were not necessary for Blackheart

incidence and instead oxygen exclusion, rather than CO_2 accumulation, was the cause of central tissue "*asphyxiation*" (Stewart & Mix, 1917), a hypothesis that was further supported by Singh & Mathur (1937).

However, Davis (1926) found that even with an abundance of oxygen Blackheart could be induced in tubers at high temperatures. Davis suggested that gaseous diffusion was limited by tuber tissue, causing CO_2 to accumulate at the tuber centre. The cause of Blackheart was proposed to be a response of both high respiratory rates and insufficient gaseous exchange. More recently, gaseous exchange was indicated as limited within tuber tissues; oxygen tension falls from 15% in the cortex, to just 2-5% in the pith (Geigenberger, 2003), giving some support to Davis' (1926) hypothesis. No tissue-specific differences in tuber ultrastructure have been recorded (Kiaitsi, 2015) suggesting that any observed oxygen gradients and position of Blackheart affected tissues are a result of diffusion distance. This is further supported by anecdotal evidence that Blackheart incidence is higher in larger tubers (Kiaitsi, 2015; Briddon, 2015). Yet in the first photographs of Blackheart used to characterise the disorder (Stewart & Mix, 1917) (Figure 1.1), the region of affected tissues extends along the pith tissue of the tuber towards the periderm and along medullary rays towards the buds/eyes. As pigmentation does not spread concentrically from the centre of the tuber, Blackheart does not appear to be a function of diffusion gradients and instead appears to be tissue specific. In summary, high and low storage temperatures, CO_2 accumulation and oxygen exclusion have been shown as sufficient factors in driving Blackheart development, but none have been proven essential. Despite the lack of a clear understanding of the cause of Blackheart, the inconclusive results of past studies have strongly influenced

current research directions (Kiaitsi, 2015; Briddon, 2015) and industrial best-practice. For example, current recommendations for reducing Blackheart propose that tubers are stored in cool, well-aerated conditions with close monitoring of changes in CO_2 (Potato Research Council, 2016). The conflicting conclusions on the role of oxygen exclusion and high temperature (Stewart & Mix, 1917; Davis, 1926) in the development of Blackheart mean that there is still no clear cause of the disorder and an unreliable scientific basis for these measures.

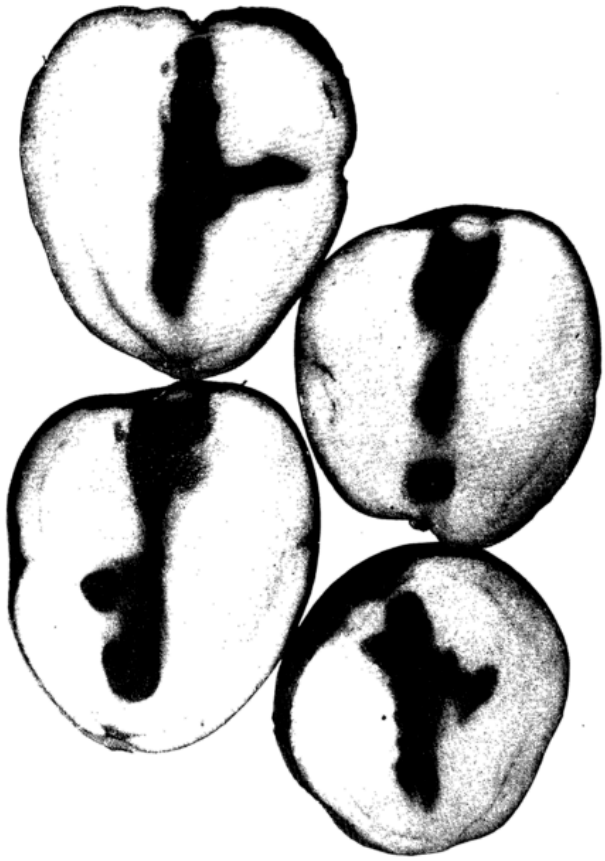


PLATE III.— BLACKHEART OF POTATOES CAUSED BY EXCLUSION OF THE AIR.
(For explanation of plate, see page 351.)

Figure 1.1 Blackheart affected tubers during characterisation (Taken from Stewart & Mix, 1917)

Blackheart has been increasing in incidence in the UK for the last five years (Briddon, 2015; Kiaitsi, 2015; David Wright, Manor Fresh Ltd. Pers. Comm) and this has led to a renewed interest in understanding the causative factors of the disorder (Kiaitsi, 2015; Briddon, 2015), but little progress has been made. The relatively low incidence rates of Blackheart during storage, require enormous amounts of tuber material for any measurements or observations to be statistically significant. This affected the recent work of Kiaitsi (2015) where due to the low incidence of Blackheart, tubers with slightly discoloured piths were considered as pre-Blackheart and counted as being affected with the disorder. However the variation in pith tissues colouration can be explained by differences in tissue water content (Burton, 1989) and this Blackheart misidentification appeared to hamper further statistical analysis and reliability. More recent research by the UK Potato Research Council has avoided these issues by using an experimental method to induce Blackheart (Briddon, 2015) similar to those seen in the historical literature. Additionally, the focus of Blackheart research internationally has shifted away from cause and prevention, and focussed instead on non-destructive imaging methods to improve quality control (Mohamed et al., 2016; Zhou et al., 2015). It should be noted that Blackheart incidence is less prevalent in countries with multiple harvests or greater demand for processed potato products, which contribute to reduced tuber storage (J.R.Simplot Ltd, pers. comm.).

There is some evidence to suggest that there are varietal differences in Blackheart susceptibility (Kiaitsi, 2015); Maris Piper accounts for the largest proportion of UK customer Blackheart complaints, but is also the most frequently purchased variety in the UK (Kiaitsi, 2015; Briddon, 2015). Despite these potential varietal differences,

there is no known characterisation or robust ranking of the Blackheart susceptibility of modern potato varieties.

1.5 Involvement of Polyphenol Oxidase and Cell Death in Blackheart

Bartholomew (1913) first suggested that Blackheart pigmentation was caused by the production of melanin from tyrosinase enzymes. Polyphenol oxidases (PPOs) are a collective term for the enzymes involved in production of phenolic pigments from aromatic substrates (Vámos-Vigyázó & Haard, 2009; Yoruk & Marshall, 2003). A broad selection of aromatic monophenol substrates, such as tyrosine, can be converted to *o*-quinones by PPO activity. These red-brown pigments are then non-enzymatically oxidised to dark brown-black polyphenols, such as melanins (Yoruk & Marshall, 2003; Steffens et al., 1994), a process which is dependent on the presence of oxygen (Jolley et al., 1974).

Under normal conditions, PPO enzymes are localised within plastids (Vámos-Vigyázó & Haard, 2009; Yoruk & Marshall, 2003; Tolbert, 1973; Czaninski & Catesson, 1974) and are therefore physically separated from their phenolic substrates, which are predominantly found in the vacuole (Vámos-Vigyázó & Haard, 2009; Czaninski & Catesson, 1974). Thus, PPO activity and subsequent enzyme-substrate mixing is only generally observed after subcellular compartmentalisation has been lost. Considering the catastrophic changes in cell ultrastructure that would be associated with PPO as a cause for Blackheart pigmentation, additional research explicitly testing the role of PPO and the loss of subcellular compartmentalisation is essential.

Physical damage to cells during potato processing can lead to bruising via changes in subcellular compartmentalisation and PPO activity (Busch, 1999). Cell damage through alternative pathways, such as necrosis can account for diseases such as Blackspot (Stevens & Davelaar, 1997), heat necrosis and internal brown spot (Chi et al., 2015), which are observationally similar to Blackheart. Blackheart has long been assumed to consist of a region of necrosis within a tuber (Stewart & Mix, 1917; Bartholomew, 1913). However, it is a mark of how little is understood about Blackheart that the involvement of cell death has also never been experimentally explored.

1.6 The Role of Anoxia in Blackheart

The occurrence of Blackheart has previously been attributed to anoxic conditions (Bartholomew, 1913; Bartholomew, 1914) and current storage practice involves frequent storage ventilation and monitoring (Briddon, 2015; Kiaitsi, 2015; David Wright, Manor Fresh Ltd, pers. comm., 2014). Oxygen is a key component of plant cellular respiration; under aerobic conditions carbohydrates are catabolised in glycolysis and the TCA cycle which produces energy, in the form of ATP, and reducing power, in the form of NADH. Oxidative phosphorylation in mitochondria uses this NADH to generate a chemiosmotic potential across the inner mitochondrial membrane, driving the synthesis of ATP via the F_1F_0 ATPase and using oxygen as a terminal electron acceptor (Plaxton, 1996).

The bulky tuber organ creates varying diffusion pathway lengths which affect oxygen tension levels; oxygen constitutes approximately 15-5% of the intercellular peridermal atmosphere, falling to only 5-2% oxygen in the centre of the tuber (Geigenberger, 2003a). This low internal oxygen concentration can be coupled with a low external oxygen concentration when tubers are in kept in deep-piling and long-term cold storage. Such conditions may cause central tuber cells to switch from aerobic respiration to fermentation with a consequent lower yield of ATP synthesised per carbohydrate catabolised. Further evidence of this comes from observations of the ATP: ADP ratio of different tuber tissues, with the lowest ATP: ADP ratio found in central pith tissue, correlating with oxygen levels (Geigenberger, 2003a).

Under anoxic conditions, ATP is produced by substrate level phosphorylation alone. NAD^+ is regenerated during the conversion of pyruvate to lactic acid or ethanol. Fermentation lacks the additional ATP produced in downstream respiratory pathways and thus the process is significantly less energy efficient than aerobic respiration, producing only 2 ATP per glucose. To avoid an energy deficit and meet cellular demands, fermenting cells use up to 20 times more glucose than respiring cells in a process known as the Pasteur effect (for reviews see Kennedy et al., 1992). Even under hypoxia (rather than anoxia), the cellular adenylate energy charge declines due to a hypoxic inhibition of glycolysis and the TCA cycle (Geigenberger, 2003a). The addition of respiratory substrates to hypoxic tissues can stimulate oxygen consumption, suggesting that hypoxic tissues are not limited by insufficient oxygen for mitochondrial respiration (Zabalza et al., 2009). Instead, a decline in flux through central metabolism occurs which may act as a mechanism to limit the

accumulation of pyruvate (Zabalza et al., 2009). High concentrations of pyruvate activate the mitochondrial alternative oxidase (AOX). Flux through central metabolism may therefore limited during hypoxia to avoid AOX activation, ensuring efficient ATP synthesis via transfer of electrons through the terminal cytochrome c oxidase of the mitochondrial electron transport chain. This results in more proton pumping and improved oxygen-use efficiency of ATP synthesis (Zabalza et al., 2009; Millar et al., 2011).

Prolonged hypoxia, anoxia, and fermentation ultimately cause cell death. There are several potential causes of fermentative necrosis: Firstly, in an attempt to meet energy demands, cellular carbohydrate reserves can be rapidly depleted via the Pasteur effect. This rapid catabolism may use cellular carbohydrates faster than any regeneration, ultimately exhausting respiratory reserves and causing an energy crisis (Gibbs and Greenway, 2003). Secondly, due to the decrease in mitochondrial oxidative phosphorylation, fermentation results in cellular acidification via production of excess protons, affecting both pH homeostasis and electrochemical proton gradients between cellular compartments (Couldwell et al., 2008). Lastly, accumulation of toxic metabolites such as acetaldehydes and ethanol may cause necrosis (Pfister-Sieber & Brändle, 1995).

Despite the clear propensity of central tuber tissues to experience hypoxia and utilise fermentation, lack of oxygen does not seem to be a prerequisite for occurrence of Blackheart (Bartholomew, 1913; Davis, 1926). Additionally, Blackheart pigmentation does not appear to be a function of gaseous diffusion gradients, affecting pith tissues close to the periderm (Stewart & Mix, 1917) (Figure 1.1).

Thus, it is not yet clear if oxygen availability is a factor in Blackheart development during commercial storage, despite current prevention methods focussing on aeration of tuber stores.

1.7 The Role of Storage Temperature in Blackheart and Tuber Metabolism

High temperature alone (Bartholomew, 1913; Davis, 1926) and in combination with anoxia (Stewart & Mix, 1917) has been shown to induce Blackheart in potatoes. Elevations in temperature will increase the rate of all metabolic reactions. The elevated temperatures used to induce Blackheart are insufficient to denature enzymes, but would be expected to increase enzyme catalytic activity, and thus potentially change mass action ratios of metabolites due to differential effects of temperature on different enzymes. An increase in temperature e.g. removal of tubers from cold storage, is likely to increase tissue respiration rate and high respiration rates have been identified as a possible cause of Blackheart (Bartholomew, 1913; Davis, 1926; Stewart & Mix, 1917).

Conversely, tubers stored at lower temperatures (1.5°C) have been demonstrated to develop Blackheart at higher incidences than those tubers stored at warmer temperatures (3.5°C) (Briddon, 2015). Long-term storage temperatures of potato stocks vary between UK growers, and are typically between 2°C to 4°C (Briddon, 2015; Kiaitsi, 2015; David Wright, Manor Fresh Ltd., pers. comm., 2014). This increase in Blackheart susceptibility at low temperatures has also been proposed to be a result of increased respiration rates (Briddon, 2015; Burton, 1989). Tuber storage temperatures and CO_2 release (as a proxy for respiration) display a non-

linear relationship (Burton, 1989) whereby CO_2 declines with temperature until approximately 3°C and increase at temperatures below that; the rate of CO_2 release from tubers stored at 1.5°C is equivalent to that released from tubers stored at 22°C (Burton, 1989). Briddon (2015) previously explored the relationship between CO_2 release in tubers stored at 1.5°C and 3.5°C with Blackheart susceptibility, however due to large variability, no correlation was found between Blackheart and CO_2 release rates. Moreover, respiration rates are not equivalent to CO_2 release; many other metabolic reactions beyond the TCA cycle can produce CO_2, for example flux through the oxidative pentose-phosphate pathway (oxPPP) increases at low temperatures (Malone et al., 2006). Therefore, oxygen consumption would be a more appropriate measure of cellular respiration. Malone et al. (2006) demonstrated that oxygen uptake in tuber discs taken from tubers stored at 4°C and 25°C display similar respiratory rates (Figure 1.2), supporting the proposed non-linear relationship between tuber respiration and temperature (Burton, 1989). Therefore, without further oxygen consumption measurements it is difficult to conclude if low temperatures increase respiration rates and/or Blackheart susceptibility.

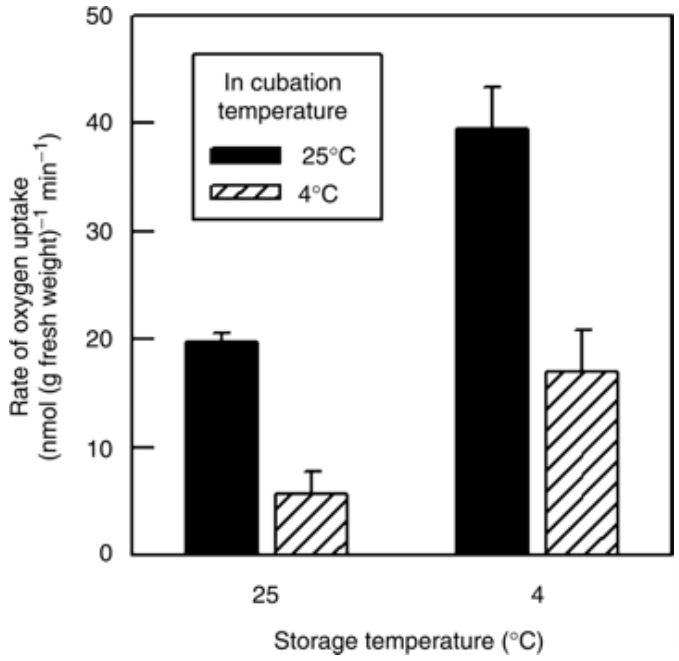


Figure 1.2 Effect of low temperature on respiration by potato tubers (taken from Malone et al., 2006)

Malone et al. (2006) demonstrated that discs taken from tubers stored at 25°C or 4°C and then incubated under different temperatures undergo dramatic respiratory changes (Figure 1.2) and flux redistribution. These results suggest that variations in temperature affect the respiratory rate more than the absolute temperature, as oxygen consumption is comparable in tissues stored and incubated at 25°C vs. 4°C (Figure 1.2). Respiration rate declined when tuber material was transferred from 25°C storage to 4°C incubation, conditions comparable to the process of transferring harvested material into cold stores in industry. Conversely, respiration rate increased in tuber material which was transferred from 4°C storage to 25°C incubation, comparable to removal of material from cold stores in industry. Both of these metabolic responses persisted for at least 4 h after the temperature transfer had occurred. Variations in temperature are an additional source of metabolic stress, arising within poorly managed long-term stores, movement of material between

stores and within downstream processing steps and could therefore be a significant factor in the occurrence of Blackheart.

1.8 The Role of Membrane Integrity in Blackheart and Tuber Physiology

Electrical conductivity of tuber tissues increases during Blackheart development (Davis, 1926) which suggests that Blackheart involves changes to cell membrane permeability. The potential involvement of loss of membrane integrity in the formation of the pigmentation associated with Blackheart pigmentation has already been discussed previously (1.5) and appears to be an important factor in Blackheart development.

Potato tuber plasma membranes increase in permeability at low temperatures due to an increase in the ratio of unsaturated:saturated fatty acids (Spychalla and Desborough, 1990). These changes ensure membrane fluidity and function at low temperatures but are also associated with increased electrolyte leakage across plasma membranes due to the decreased organization of the acyl chains. To maintain membrane electrochemical gradients under such circumstances, it is likely that ATP expenditure will increase via increased activity of ATPase proton pumps. This energy dependent process normally requires approximately 20% of the plant maintenance costs (Penning, 1975; Woods, 2014).

Changes in membrane permeability during storage of potato tubers are also thought to be a causative factor in Cold Induced Sweetening (CIS), a process where soluble

sugars accumulate in in potato tubers stored at low temperatures. The high sugar content acts as a cryoprotectant and prevents tissues freezing (Stitt & Hurry, 2002). However, CIS is an undesirable effect of cold storage for the potato industry; during cooking reducing sugars can interact with amino acids to form dark brown polymers in a process called the Maillard reaction, which affects the aesthetics and taste of potato products. Additionally, a by-product of these reactions is acrylamide, a potent carcinogen and neurotoxin (Serpen & Gökmen, 2009).

CIS is caused by increased conversion of starch to fructose and glucose. Glucose is the predominant sugar found in cold stored potatoes as high levels of fructokinase in potatoes cycle fructose back into the hexose-phosphate pool (Renz et al., 1993). Multiple factors influence CIS, and starch degradation is of key importance (Sowokinos, 2001); a cold inducible β-amylase increases starch hydrolysis at low temperatures (Nielsen et al., 1997) and changes in membrane permeability may increase access of enzymes to amyloplast starch reserves (Malone et al., 2006).

If cell membranes become too permeable then cell integrity can be lost, eventually resulting in cell death. Regions of polyphenolic pigmentation, physiologically similar to Blackheart, can be observed in soft fruit that has undergone chilling injuries. One of these disorders, also named Blackheart, is found in pineapples and is caused by improper membrane function and degradation at low temperatures (Zhou et al., 2003; Zhou et al., 2014). Changes to potato tuber membrane permeability at low temperatures could help explain the increased susceptibilities of cold stored tubers to Blackheart (Briddon, 2015).

1.9 The Role of Storage Duration on the Occurrence of Blackheart

Blackheart susceptibility has also been linked to prolonged storage length and tuber age (Singh & Mathur, 1937; Davis, 1926, Briddon, 2015). This is also apparent in industry; consumer related Blackheart complaints begin after four months of storage and peak after ten months (Briddon, 2015; David Wright, Manor Fresh Ltd. pers. comm). Very few incidences of Blackheart prior to storage have been observed (David Wright, Manor Fresh Ltd. pers. comm), suggesting that Blackheart may be largely driven by industrial storage, processing conditions and physiological age.

A significant effect of tuber aging is increased membrane permeability. Changes in cell compartmentalization drive processes such as senescence sweetening, allowing starch-degrading enzymes come into contact with amyloplast contents (Marangoni, 2017). These membrane changes occur due to several factors; firstly, as dormancy breaks, hormonal changes drive sprouting at tuber buds/eyes. This growth process requires tuber storage reserves requiring additional sugars. Additionally, Reactive Oxygen Species (ROS) levels can increase in tubers as they age (Suzuki and Mittler, 2006). Autocatalytic peroxidation of membrane lipids is a direct consequence of ROS production and results in modification of membrane function and permeability. As previously discussed, membrane permeability is a possible factor Blackheart susceptibility with storage duration. Aging also appears to increase tuber respiration rate, although this may be a consequence of oxidative stress and electrolyte leakage covered above. Nevertheless, high respiration rates have been previously linked with Blackheart.

1.10 Research Hypothesis and Aims

There is a dearth of research around post-harvest food waste and loss reduction and this is particularly evident with the lack of information on the underpinning molecular-biochemical causes of Blackheart. From the existing literature it is not clear which conditions are necessary or sufficient to induce Blackheart. Multiple storage conditions appear to increase Blackheart susceptibility and further work is required to understand what aspects of these are the causative factors.

Identifying the underlying biochemical and physiological changes in tubers during Blackheart development will help to understand the driving factors of the disorder. This will in turn allow post-harvest management measures to be put in place, with the aim of predicting the likelihood of a tuber store to develop Blackheart or reducing the disorder occurrence. This will help reduce consumer complaints and crop loss and food waste in the industry. To achieve this, my project will pursue the following research objectives:

A. **To develop a robust method for inducing Blackheart and to use this to characterise the development of Blackheart**

   Previous studies have been limited by low endogenous rates of Blackheart in long-term storage (section 1.4) (Kiaitsi, 2015) and thus development of a reliable method to induce Blackheart is necessary. Using controlled induction of Blackheart will enable measurements to be taken throughout the Blackheart development process, aiding identification of changes that occur both during and before the onset of Blackheart. Determination of the

necessary and sufficient induction conditions (e.g. high or low temperature, anoxia) will be useful in understanding the cause of Blackheart. As there is so little information about Blackheart, varietal differences in Blackheart susceptibility will be recorded, as well as changes between harvests and with tuber age.

B. **To test the involvement of PPO and cell death in Blackheart**

The involvement of cell death and PPO in Blackheart has long been assumed, the first steps of this project should aim to experimentally test the involvement of these processes. This, coupled with the induction conditions involved in Blackheart development (section 1.10.A) will feed in to developing a hypothesis about the biochemical cause of Blackheart.

C. **To identify the metabolic changes that occur in Blackheart affected tissue.**

Blackheart has been characterised as a metabolic disorder and has previously been associated with high respiration rates. Factors that have induce Blackheart (anoxia, temperature) appear to increase the respiratory rate of tubers and this correlation needs to be explored further. However, a high respiratory rate alone may not cause Blackheart, and thus an underlying mechanism would then need to be identified (section 1.6). One possibility is that tissues are unable to maintain high respiratory rates induced by Blackheart induction conditions, for example via carbohydrate reserve exhaustion or inhibitions in flux through central metabolism.

2 Materials and Methods

All chemicals, enzymes, standards and kits were purchased from Sigma Aldritch, (St. Louis, USA) unless otherwise stated

2.1 Plant Material

2.1.1 Annual Potato Harvests

Potato tuber material for the project was grown in collaboration with Manor Fresh (Holbeach Hurn, UK) at Manor Farm, Holbeach Hurn, Lincolnshire, in fields also containing potato produce for commercial sale. Fields were irrigated if necessary. The details of each annual field trial were as follows:

Year 1: 2014 Harvest

Location: Multiple

Cultivars: B, A, Maris Piper, C, E, D and King Edward.

Year 2: 2015 Harvest

Location: 52.842975, 0.073780

Cultivars: B, A, Maris Piper, C, E, D, King Edward and F.

Year 3: 2016 Harvest

Location: 52.838866, 0.094341

Cultivars: B, A, Maris Piper, King Edward.

Year 4: 2017 Harvest

Location: 52.838866, 0.094341

Cultivars: B, A, Maris Piper, King Edward.

2.1.2 Potato Harvesting and Storage

Tubers were harvested by hand and stored in 1 m^3 slatted wooden crates in dark, well ventilated conditions. Material was immediately transferred to a 10°C store for skin curing and temperatures slowly reduced by approximately 0.5-1°C each day until store temperature was at 4°C. Tubers were then stored for up to 12 months at 2-4°C.

For transportation to the Department of Plant Sciences, University of Oxford material was portioned into paper bags or cardboard boxes containing 5 kg of tubers and transported via refrigerated courier or car, ensuring that the tuber temperature never rose above 4°C during the journey. Potato material was then stored in the dark in one of three locations and conditions; 4°C for a maximum of 12 months in a laboratory cold room; 2°C for a maximum of nine months in a temperature-controlled cabinet (Weiss Technik, Loughborough UK, INF600010R); 22°C for a maximum of one month in a temperature-controlled room.

2.1.3 Tuber Grading and Washing

All experiments were conducted on tubers within the size range of 6.5 cm wide by 7.5 cm long, ± 0.5 cm, and displayed no greening, physical damage or disease

symptoms. Material was washed before use (unless stated otherwise) via submergence in water at 13°C for 2 min, to replicate industry washing conditions. Tubers were dried thoroughly before use.

2.2 Blackheart Induction

Tubers were placed in a PE/PA composite plastic bag (Sousvide, Broomfield, USA) and a 0.75 bar vacuum packer (Andrew James, Seaham UK, 170) was used to create an anoxic environment and hermetic seal. Tubers were then stored in the dark and incubated at 37°C (Memmert, Schwabach, Germany, ICOmed) for 1-34 h to induce Blackheart. Tubers were then used for either Blackheart imaging (2.3) or tissue sampling (2.5).

2.3 Destructive Blackheart Imaging

After removal from Blackheart induction conditions (2.2), tubers were kept in the dark at 22°C for 12 h for Blackheart pigmentation to develop. Tubers were then cut in half, longitudinally from the stolon to terminal bud and imaged using a flat-bed scanner (Epson, Suwa, Japan, expression 1600Pro) in 24-bit colour and 600dpi.

2.3.1 Image Analysis

The proportion of Blackheart affected tissue in each tuber was quantified using ImageJ/Fiji software (Schindelin et al., 2012). The same in-built macro was used on

all samples to avoid user bias. This macro converted images (2.3) to 16-bit greyscale and binary before applying two different thresholding limits to measure the both area of the cut tuber and any Blackheart affected tissue.

2.4 Non-Destructive Blackheart Imaging

The following work (section 2.4) was conducted by Dr Jack Miller, Department of Physiology, Anatomy and Genetics, University of Oxford.

Tubers were imaged throughout Blackheart development using an MRI system (Agilent, Santa Clara, USA, 7 T-Varian) at the Department of Physiology, Anatomy and Genetics, University of Oxford. Potatoes were placed supine inside a 72 mm ^{1} $^{h}/^{13}$C birdcage coil and temperature was monitored via IR pyrometry. A modified water-jacket maintained anoxia and 37°C water around the tuber to maintain Blackheart induction conditions throughout imaging. A scanning protocol acquiring ADC and T1 maps were undertaken hourly for 24 h.

Tubers were also imaged on a clinical MRI system (Siemens, Munich, Germany, 3T Tim Trio) at the John Radcliffe Hospital, Oxford. A double-blind randomised trial in a clinic was conducted on four potatoes, two of which had previously been stored under 24 h of Blackheart induction conditions (2.2). T1 maps were obtained via MOLLI from isothermal potatoes at rest (8 readouts, 60 bpm nominal heart rate, 0.86 mm^3 in-plane resolution).

2.5 Tissue Extraction

All tissues were taken from tubers stored for a minimum of three months after harvest (unless stated otherwise). After removal from Blackheart induction conditions (section 2.2), tubers were cut in half, longitudinally from the stolon to terminal bud and immediately sliced using a mandolin into 4-mm thick slices. A 4 mm or 6 mm diameter core borer was then rapidly used to punch discs from the pith, parenchyma, and cortex. Care was taken so discs were only comprised of single tissue types. Depending on use discs were either:

Fresh tissue: Used immediately as whole discs of fresh tissue.

Ground tissue: Immediately dropped into a bath of liquid N_2 to quench metabolism and stored at -80°C for up to eight months. Before use, tissues were ground using a Cellcrusher tissue pulveriser (Cellcrusher, Cork, Ireland) that had been pre-cooled in a bath of liquid N_2.

Lyophilised tissue: Immediately dropped into a bath of liquid N_2 to quench metabolism before lyophilisation (CHRiST, Osterode am Harz, Germany, Alpha 2-4 LD). Tissue was then ground using a ball mill (Qiagen, Hilden, Germany, TissueLyser) to a fine powder.

2.6 Histochemical and Histological Stains

2.6.1 Enzymatic Activity Stain

TTC salt was dissolved in deionised water to form a 2% (w/v) solution. Tissue was bathed in the solution for 30 min for staining to develop before being washed in deionised water to remove excess stain and then imaged (2.3).

2.6.2 Cell Viability Stain

Evans blue was dissolved in deionised water to form a 1% (w/v) solution. Tissue was bathed in the solution for 30 min for staining to develop before being washed in deionsised water to remove excess stain and then imaged (2.3).

2.7 Electrolyte Leakage Measurements

Tissue discs (2.5) were incubated in 5 mL deionised water. The conductivity of the deionised water was recorded using a microprocessor conductivity and TDS meter with automatic temperature compensation (Hanna, Woonsocket, USA, primo 5) before use. Discs were incubated for 10 min at 22°C and 150 rpm before the conductivity of the solution was measured a second time, representing the electrolyte leakage of the tissue. Vials were then incubated for 10 min in a waterbath at 100°C to lyse cells before allowing to cool and a third conductivity measurement, representing the total electrolyte content, was taken. Electrolyte leakage was quantified as follows:

$$Electrolyte\ leakage\ \% = \frac{(EC_{Initial} - EC_{water})}{(EC_{total} - EC_{water})} \times 100$$

EC_{water}= Electrical conductivity of the water in which the discs were immersed indicating background conductivity.

$EC_{initial}$ =Electrical conductivity of the water after incubation of the discs indicating electrolyte leakage.

EC_{total}= Electrical conductivity of the water after cell death indicating total electrolyte content of the tissue.

Electrolyte leakage = the proportion of tissue electrolytes leaked due to storage/incubation conditions, expressed as a percentage.

2.8 Respiration Rate

Tubers in long-term storage (2.1.2) were sealed in hermetically sealed containers containing an O^2xyDot®, which was used to measure oxygen concentrations via OxySense (OxySense, New Castle, USA, 325I) immediately after sealing. The sealed boxes were then returned to storage conditions (2.1.2) for 1-2 h before a second oxygen reading was taken and the rate of oxygen consumption calculated.

2.9 Adenylate Quantification

2.9.1 Adenylate Extraction

Method modified from (Sweetlove, 1995). All work was conducted at 4°C. Approximately 0.2 g (FW) of ground tissue (2.5) was mixed with 1 mL of 1.41 M perchloric acid and chilled on ice for 5 min. Samples were centrifuged at 10,000 g

for 5 min to pellet the cell debris and the supernatant was retained. The pellet was resuspended in 0.5 mL of 1.41 M perchloric acid, centrifuged again at 10,000 g for 5 min and the supernatants combined. 5 M K_2CO_3 was added until each sample had a neutral pH. The samples were centrifuged at 10,000 g for 10 min to remove precipitates and assayed immediately.

2.9.2 ATP, ADP and AMP Assay

Modified from (Valero et al., 2000). Extracted adenylates (2.9.1) were assayed using a modified kit (ATP:ADP ratio kit, MAK135) by the addition of 5 U of Myokinase to each well. Negative controls contained no extracted adenylate sample. ATP was measured by recording the production of luminescence from the conversion of D-Luciferin to Oxyluciferin using a spectrophotometric platereader (Beckman Coulter, Brea, USA, DTX 880 Multimode detector). ADP and AMP were then sequentially converted to ATP, and quantified. Therefore, the second luminescence reading represented the amount of ATP and ADP, and the third luminescence reading represented the amount of ATP, ADP and AMP. These luminescence values were compared to a standard curve of known ATP concentrations.

Adenylate energy charge was calculated from adenylate abundances as follows:

$$Adenylate\ Energy\ Charge = \frac{ATP + \frac{1}{2}ADP}{ATP + ADP + AMP}$$

2.10 Metabolomics

Modified from (Lisec et al., 2006).

2.10.1 Extraction of Metabolites

1.4 mL of precooled methanol was added to 0.1 g (DW) of powdered tissue sample (2.5) to quench enzymatic activity and vortexed. Negative controls omitted tissue sample material. 60 µl of 0.2 mg /mL ribitol and norvaline in water was added as an internal standard to each sample before vortexing. Samples were heated for 10 min at 70°C while shaking at 950 rpm. Samples were then centrifuged for 10 min at 11,000 g and the supernatant transferred to a glass vial. 750 µl of precooled chloroform and 1.5 mL of precooled deionised water was added before vortexing. The samples were centrifuged at 2,200 g for 15 min and the upper polar phase was retained. 500 µl aliquots were flash frozen in in liquid N_2 and kept in -80°C for up to three months.

2.10.2 Derivatisation

Prior to derivatization, 15 µl of sample was dried in a speed vacuum for 3 h and re-suspended in 40 µl of 20 mg /mL methoxyamine hydrochloride in pyridine before incubation at 37°C, 900 rpm for 2 h. 10 µL MSTFA and alkane time standards preheated to 70°C were added. Samples were incubated at 37°C, 900 rpm for 30 min before transfer to glass vials with sealed septum caps (Chromacol, Welwyn Garden City, UK) for injection.

2.10.3 Gas Chromatography Mass Spectrometry Analysis

Analysis was carried out on a GC (Agilent, Santa Clara, USA, 79890) and a connected quadrupole MS detector (Agilent, Santa Clara, USA, 5975) at 70 eV. The mass spectrometer was calibrated before each run using the inbuilt autotune method. A HP 5-ms column (Agilent, Santa Clara, USA) (30 m long, 0.25 mm inner diameter) was used and 1 µl of sample was injected into the MS each time. The GC column temperature was raised to 70°C for 5 min, increased by 5°C per min until a temperature of 280°C, which was maintained for 3 min. The temperature was then decreased by 120°C per min to 70°C degrees with a solvent delay of 10 min and a helium gas flow of 0.6 mL per min.

Mass spectra were acquired using a SIM and scan method with a dwell time of 10-30 ms for each ion group. Elution times and mass fragments were determined by comparison with standard curves of pure compounds.

2.10.4 High-Throughput GC-MS Spectra Analysis

MetAlign (Lommen, 2009) assisted baseline corrections were conducted on spectra to remove noise and TagFinder software (Luedemann et al., 2008) was used to identify metabolites in GC-MS spectra. The elution times of internal alkane time standards, added in the derivatization process (2.10.2), were used to align all GC-MS chromatograms. Analytes were then classed by their retention times and simultaneously identified in all samples based on the comparison of mass spectral tags to the NIST library (Luedemann et al., 2008; Halket et al., 2005; Ausloos et al., 1999). Abundances were expressed relative to both internal standards (2.3.1) and tissue weight. The mean abundances of metabolites found in negative controls were

subtracted from all other samples. Statistical analysis was conducted using Significant Analysis of Microarrays (SAM) software (Tusher et al., 2001).

2.11 Quantification of Starch, Sucrose, Glucose and Fructose

Modified method from (Hargreaves & ap Rees, 1988). Ground tissue (2.5) was divided into two separate vials, each containing approximately 1 g (FW) of tissue. Half of the sample was used to quantify the sugars (2.11.2) and the other half used to quantify starch (2.11.1).

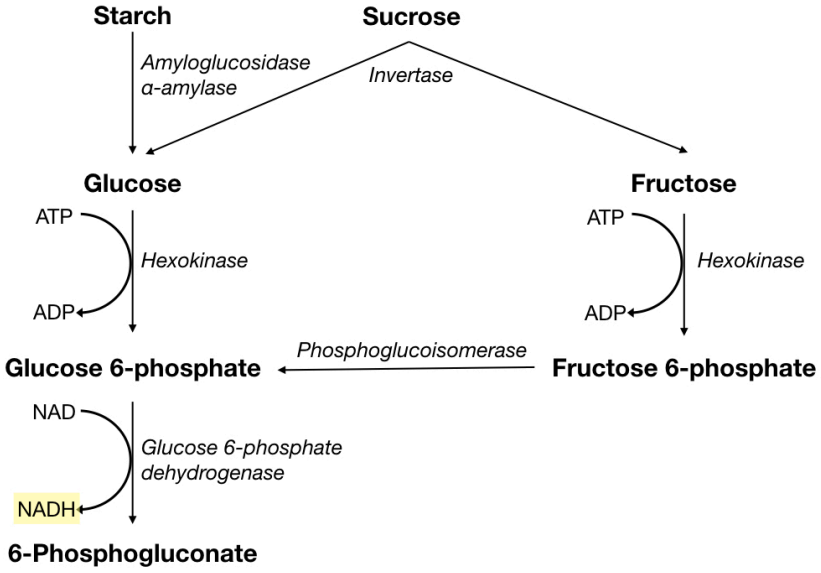


Figure 2.1: Enzymatic conversion of carbohydrates to 6-Phosphogluconate and the production of NADH which, as it is produced in a known stoichiometry, is used to quantify the amount of carbohydrates present in each sample.

2.11.1 Starch Hydrolysis to Glucose Monomers

Approximately 1 g (FW) of ground tissue (2.5 and 2.11) was mixed with 1 mL of ice cold 45% (w/v) perchloric acid and incubated on ice for 5 min to break starch granules open. Negative controls contained no sample. 9 mL of distilled water was added and mixed forming a dilute solution of starch. Complete gelatinisation was confirmed by staining an aliquot with 1% (w/v) Lugols iodine solution and visually checking for the absence of starch granules using a light microscope (Zeiss, Oberkochen, Germany, Stemi 508).

50 µl of the dilute starch solution was mixed with 2 units of amyloglucosidase (*Aspergillus niger*), 20 units of α-amylase (porcine pancreas), 0.2 M sodium acetate buffer (pH 5.5) to make 1 mL volume total. Amyloglucosidase and α-amylase enzymes were omitted from control samples. Samples were incubated for 16 h at 37°C and 50 µl of the solution was assayed as per glucose (2.11.4). The endogenous amount of glucose from each sample (2.11) was subtracted before the amount of starch was calculated (Figure 2.1).

2.11.2 Glucose, Fructose and Sucrose Perchloric Acid Extraction

Modified from (Sweetlove et al., 1996a), all work was conducted at 4°C. Approximately 0.1 g (FW) of ground tissue (2.5 and 2.11) was mixed with 0.5 mL of 1.41 M perchloric acid and chilled on ice for 2 h. Negative controls contained no tissue sample. Samples were then processed as per (2.9.1) before being immediately used or stored at -80°C for up to 1 month.

2.11.3 Sucrose Hydrolysis to Hexoses

Approximately 100 µl of extract was mixed with 200 mM Sodium acetate (pH 5.5) and 30 U Invertase (yeast concentrate, BDH Chemicals, Poole, UK) to a total volume of 1 mL before incubation at 100°C for 2 min before assaying as per glucose (2.11.4). The endogenous amount of glucose from each sample (2.11.1) was subtracted before the amount of sucrose was calculated (Figure 2.1).

2.11.4 Sucrose, Glucose and Fructose assay

Extracted samples (2.11.2) were mixed with 100 mM Tris-HCl (pH 8.0), 5 mM $MgCl_2$, 0.25 mM NAD^+, 1 mM ATP and 0.7 U hexokinase in a 96 well plate to make a total 200 µl volume. Using a spectrophotometer plate reader (Beckman Coulter, Brea, USA, DTX 880 Multimode detector) the background absorbance of light (wavelength of 340 nm) was measured before the addition of either:

Glucose: 0.56 U of glucose 6-phosphate dehydrogenase

Fructose: 0.7 U of phosphoglucoisomerase

The absorbance was measured until it was stable. The difference in the background and final absorbance was calculated and compared against a standard curve of absorbance from known amounts of NADH. This was then used to calculate the amount of each sugar present, based on the stoichiometry of the reaction (Figure 2.1).

2.12 Carbon Flux Analysis

Method modified from (Malone et al., 2003). Fluxes to biosynthetic products were estimated from the redistribution of label following the metabolism of [U-^{14}C]-glucose by potato tuber discs.

2.12.1 [U-^{14}C]-Glucose Feeding

Tubers were either incubated under Blackheart induction conditions (2.2) for 8 h (Treatment 2), or immediately sampled (Treatment 1). Discs of 5 mm in diameter and 3 mm thick were sampled as per (2.5) in an anoxic chamber, heated to 37°C to maintain Blackheart induction conditions. Five discs were taken from the pith and cortex and pooled for each measurement. Discs were washed in 10 mM MES-KOH (pH 6.5) buffer and blotted dry. These were then added to a 100 mL conical flask, containing 5 mL of deoxygenated 10 mM MES-KOH (pH 6.5). To trap CO_2, a 2 mL eppendorf tube containing 0.5 mL of 10% (w/v) KOH was suspended in each flask via a paperclip. A suba seal lid tightly sealed the flask and held the CO_2 trap in place (Figure 2.2). The sealed flasks were then removed from the anoxic chamber and incubated in a 37°C water bath at 90 rpm for 30 min to reach a steady metabolic state.

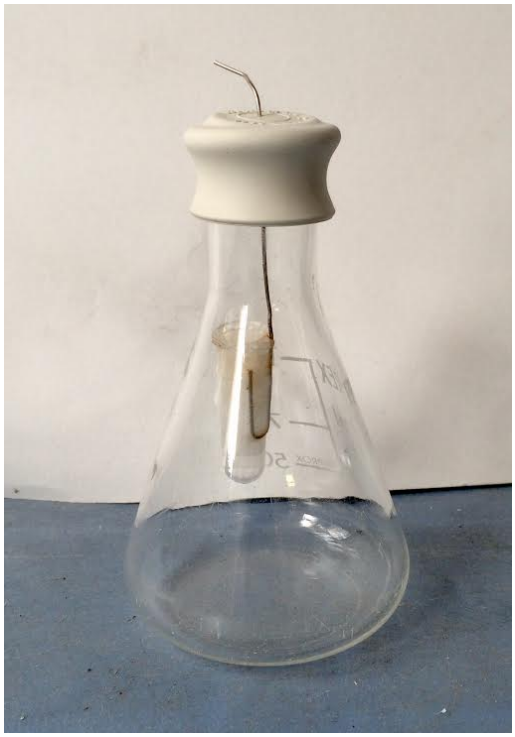


Figure 2.2: Arrangement of flasks used for incubation of tissue for radiolabelling illustrating the CO_2 trap.

The radioactivity of the [U-^{14}C]-Glucose substrate stock was measured prior to use by liquid scintillation counting (section 2.12.3). To begin the incubation, 100 µL of 100 mM [U-^{14}C]-Glucose was injected into the flask, through the suba seal. 100 µL of 100 mM unlabelled glucose was added to negative controls. The flasks were then incubated for a further 3 h to reach an isotopic steady state. At the end of the incubation, the flasks were opened and the CO_2 trap tube was sealed. The potato discs were then washed in unlabelled 10 mM MES-KOH buffer (pH 6.5), blotted dry and weighed, before being flash-frozen in a bath of liquid N_2 and stored at -20°C for up to one week before processing. The buffer used to wash the discs was combined with the labelled buffer, frozen in a bath of liquid N_2 and also stored at -20°C for up to one week before processing.

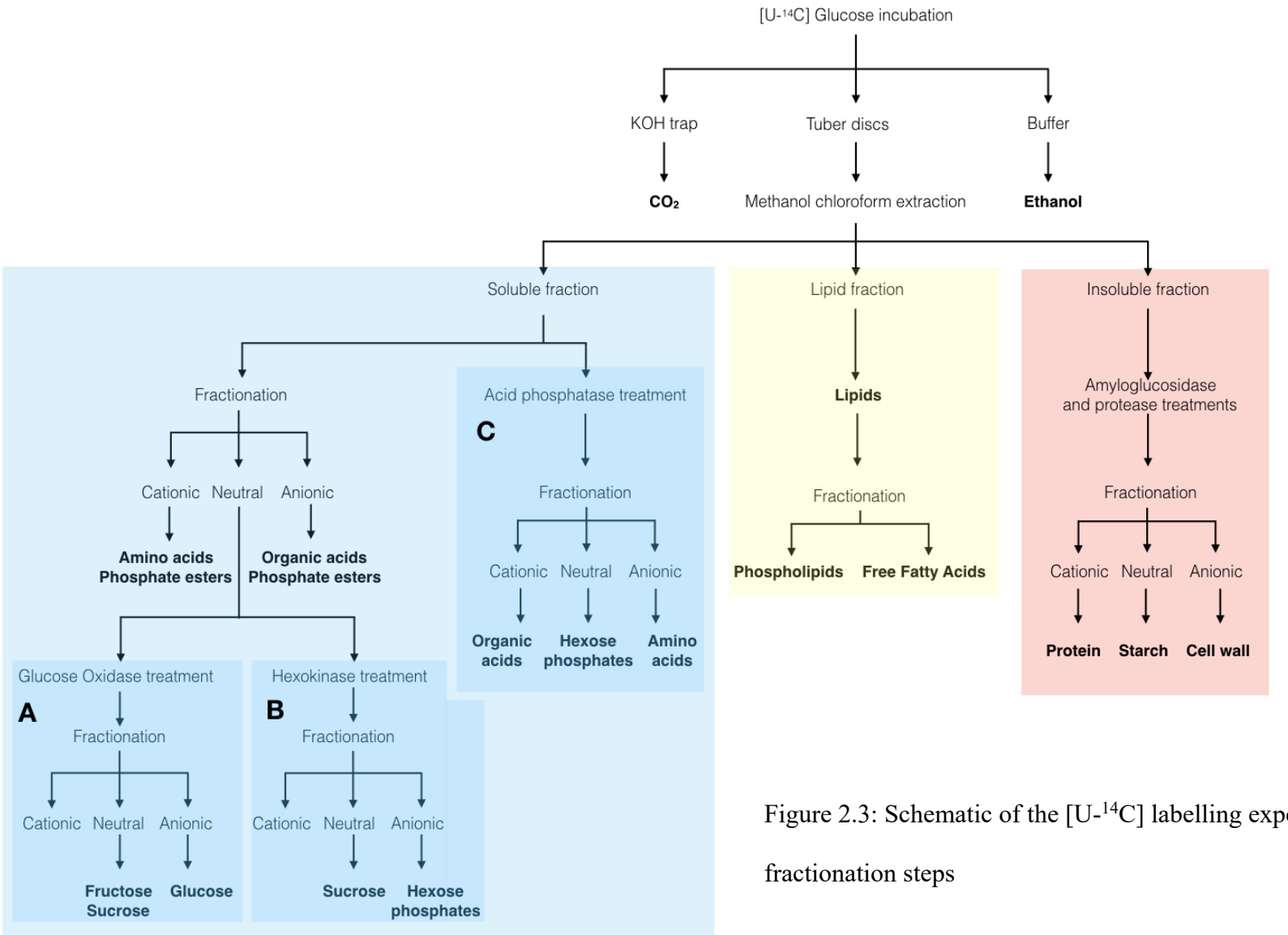


Figure 2.3: Schematic of the [U-^{14}C] labelling experiment fractionation steps

2.12.2 Radioactivity Measurements

To measure the [^{14}C] radioactivity, samples were mixed in a 1:4 volume ratio with scintillation fluid (Optiphase, Los Angeles, USA, HiSafe) and shaken vigorously. To avoid interference from chemiluminescence, samples were left in the dark for a minimum of 12 h before measurements were taken. Total dpm were measured over 5 min using a scintillation counter (Beckman, Brea, USA, LS 6500).

2.12.3 CO_2 Fraction

450 µL of the KOH CO_2 trap was used to measure the radioactivity (2.12.2) in the CO_2 fraction. The dpm corresponded to 90% of the radioactivity released as [^{14}C]-CO_2 (Figure 2.3).

2.12.4 Ethanol Fraction

The buffer washings from each flask were transferred to a round-bottomed flask and 1 mL of 100% (v/v) ethanol added to aid recovery. The mixture was gently heated to < 90°C to evaporate ethanol off from the sample and using a Liebig condenser, the distilled ethanol was collected. The total recovered sample was used to measure the radioactivity (2.12.2) and therefore the corresponding dpm equated to the total radioactivity released as [^{14}C]-ethanol (Figure 2.3).

2.12.5 Extraction of Radiolabelled Metabolites and Separation into Soluble, Insoluble and Lipid Fractions

For all following methods referring to mixtures containing chloroform, no plastic was used in order to prevent contamination. Instead the following were used: glass Pasteur-, Mohr- and serological-pipettes; Hamilton syringes with metal needles; glass centrifuge tubes with Teflon coated screw-cap lids. Prior to use, this equipment was first washed in an acetic acid-based acid rinse (LCA-A, Lancer, USA) without detergent, before a second rinse in chloroform to remove any contaminants.

Frozen discs were ground into a fine powder (2.5) and mixed with 5 mL of 100% (v/v) methanol, cooled to -20°C. The sample was left to thaw on ice for 2 h, vortexed and then centrifuged at 2,200 g for 20 min at 5°C. The resulting supernatant was retained and stored on ice whilst the pellet was resuspended in 5 mL of 100% (v/v) methanol (pre-cooled to -20°C), incubated on ice for 5 min and centrifuged at 2,200 g for 20 min at 5°C. The two methanolic supernatants were combined and kept on ice whilst the pellet (comprising of the insoluble cell residue) was bathed, without re-suspension, in 5 mL of 100% (v/v) methanol at 70°C. The pellet mixture was allowed to cool and briefly centrifuged and this third supernatant was combined with the two existing supernatants on ice. The remaining insoluble residue, comprising the **insoluble fraction**, was resuspended in 0.5 mL of water and stored at -20°C for up to a week before use (Figure 2.3).

The methanolic supernatants were combined with distilled water and chloroform in a ratio of 2:4:4 $CHCl_3$:CH_3OH:H_2O (v/v). The mixture was shaken and centrifuged at

3,500 g for 10 min at 20°C to promote phase separation. The upper aqueous methanol phase, comprising the **soluble fraction** was transferred to a separate 50 mL tube and stored at -20°C for up to a week before use (Figure 2.3).

The lower chloroform phase comprising the **lipid fraction** was rinsed with 2 mL of water and 4 mL of methanol, shaken and allowed to separate. The upper phase was pipetted off and the washing process was repeated a total of three times. This was then evaporated under N_2 before re-suspension in 2 mL of chloroform. This sample was flushed with N_2 and stored at -20°C for up to two weeks before further fractionation (2.12.6) (Figure 2.3).

2.12.6 Total Lipid Fraction and Component Fractionation by Solid-Phase Extraction

Method modified from (Kim & Salem, 1993). 500 µL of the chloroform phase from (2.12.5) was taken for scintillation counting (2.12.2), and the corresponding dpm equated to 25% of the total radioactivity released as [^{14}C]-lipids (Figure 2.3).

The remaining 1.5 mL of sample was used to further fractionate lipids and free fatty acids by solid-phase extraction on aminopropyl columns (Supelco LC-NH_2 columns with 0.5 g resin). The columns were first reconditioned by washing twice with 2 mL hexane using a Visiprep SPE Vacuum Manifold (Supelco) system, immediately before use. The sample was applied to the column before it was washed four times with 1 mL chloroform:propan-2-ol (2:1) and the elute, comprising **neutral lipids** was collected, flushed with N_2, and stored at -20°C for up to 2 days prior to use. Next, the

columns were washed four times with 1 mL 2% (v/v) acetic acid in diethyl ether and the elute, comprising **free fatty acids**, collected, flushed with N_2, and stored at -20°C for up to 2 days prior to use (Figure 2.3). After this, the columns were washed four times with 1 mL methanol and the elute, comprising **neutral phospholipids**, was collected and flushed with N_2. Lastly, columns were washed four times with 1 mL wash mix A (Hexane:propan-2-ol:ethanol:0.1 M ammonium acetate:formic acid combined in a 350:420:100:50:0.5 ratio made up to a 5% (v/v) phosphoric acid solution). 1 mL of this mix was used to wash the columns four times. The elute, comprising **acidic phospholipids**, collected in the same vial as the elute containing neutral phospholipids so that the combined elutes compromised **total phospholipids** (Figure 2.3). These were then flushed with N_2 and either stored at -20°C for up to 2 days before further analysis.

For determination of radioactivity, each fraction was evaporated to dryness under N_2 and then resuspended in 500 µL of chloroform before addition of scintillation fluid (2.12.2). The dpm values recorded were equivalent to the 75% of the radioactivity in each [^{14}C]-lipid type.

2.12.7 Preparation and Charging of the Anion and Cation Exchange Columns for Ion Exchange Chromatography of the Soluble and Insoluble Fractions

The Cation exchange resin (Dowex-50, 50*8-200) was prepared by incubating with two volumes of 4 M HCl for 1 h in a 100°C water bath. The resin was repeatedly rinsed with deionised water, the suspension allowed to settle, and the liquid poured off until this elute was neutral. The resin was then resuspended in two volumes of

10% (v/v) NaOH before further incubation for 1 h in a 100°C waterbath. The resin was again rinsed with deionised water until the elute was neutral as previously described. The resin was then re-suspended in 2x volumes of 2 M HCl and kept at 4°C until use. Immediately before use the cation exchange resin was charged by washing with an excess volume of 2 M HCl four times. The resin was again rinsed with deionised water until the elute was neutral as previously described and immediately used. The Anion exchange resin (Dowex-1, 1*8-200) was washed in deionised water three times, discarding any unsettled resin at each stage. The resin was charged by washing in 1 M sodium acetate followed by washing five times with 0.1 M acetic acid, or until the elute became acidic and the resin was immediately used.

Anionic and cationic exchange columns were prepared by pipetting approximately 500 μL of the charged resins into empty solid phase extraction (SPE) columns with a frit covering the elute hole so that the resin bed was approximately 1.5 cm in height. These SPE columns were stacked using an SPE column adaptor so that the SPE column containing the cationic resin was on top of that containing the anionic resin, allowing the flow to drop directly from one to the other. The stacked SPE columns were placed in a Visiprep SPE Vacuum Manifold (Supelco) system and vials were placed underneath to catch the elutes. The columns were washed twice with 1 mL of deionised water using a vacuum manifold to speed up the process (Figure 2.4), and were immediately used to avoid resin desiccation.

2.12.8 Total Soluble Fraction and Further Fractionation

The methanol phase (2.12.5) was dried by rotary evaporation at 37°C. The pellet was resuspended in 5 mL of water by shaking at 1,000 g. To measure the total radioactivity in the soluble fraction, the dpm from 50 µL from each sample was measured (2.12.2), corresponding to 1% of radioactivity in the total soluble fraction (Figure 2.3)..

To further fractionate into acid, basic and neutral fractions, 750 µL of the soluble fraction was applied to a new set of anionic/cationic exchange columns (as arranged in Figure 2.4). Once the sample had run into the resins, 1 mL of deionized water was used to wash the column three times and the elute retained as the **soluble neutral fraction** (Figure 2.3).

The columns were then separated. The cationic column was washed three times with 1 mL of 1 M NH_4OH, and the elute retained as the soluble basic fraction, predominantly comprising **amino acids** (Figure 2.3). The anionic column was washed three times with 1 mL of 4 M formic acid, and the elute retained as the soluble acidic fraction, predominantly comprising **organic acids and phosphate ester** components (Figure 2.3).

To measure the radioactivity in each of the fractions, the dpm from 500 µL of each sample was measured (2.12.2), corresponding to 2.5% of the [^{14}C] radioactivity of each component.



Figure 2.4: Vacuum manifold illustrating the set up for the fractionation of lipid products (columns one and two from the left) and labeled metabolites (columns 3 and 4 from the left)

2.12.9 Fractionation of the Soluble Neutral Fraction into Hexose Sugars and Sucrose

200 µL of the soluble neutral fraction was treated with 200 µL of a solution containing 8 U /mL hexokinase, 100 mM TRIS-HCl (pH 8.0), 27 mM $MgCl_2$ and 6

mM ATP. The reaction was incubated for 4 h at 25°C with shaking at 400 rpm, before stopping the reaction by heating to 95°C for 5 min and briefly centrifuging. This hexokinase treatment phosphorylated the hexose sugars in the sample, allowing the uncharged sucrose component to be separated from the newly negatively charged hexose sugars. The hexokinase treated fraction was applied to a new set of anionic/cationic exchange columns (as arranged in Figure 2.4) and the neutral and acidic fractions obtained as described in 2.12.8. Due to the hexokinase treatment, the neutral fraction comprised the **sucrose** fraction and the acidic fraction comprised the **hexose sugar** components (Figure 2.3).

To measure the radioactivity in each of the fractions, the dpm from 500 µL of each sample was measured (2.12.2), corresponding to 0.156% of the [^{14}C] radioactivity of each component (Figure 2.3).

2.12.10 Fractionation of the Soluble Neutral Fraction and into Fructose and Sucrose

200 µL of the soluble neutral fraction was treated with 200 µL of a solution containing 2 U /mL glucose oxidase and 64 U /mL peroxidase with 200 mM potassium phosphate buffer (pH 6.0). The reaction was incubated for 6 h at 25°C and 400 rpm, before stopping by heating to 95°C for 5 min and briefly spinning down. This glucose oxidase treatment converted glucose to D-glucono-1,5-lactone, allowing the uncharged fructose and sucrose sugars to be separated from the newly negatively charged glucose component. The glucose oxidase treated fraction was applied to a new set of anionic/cationic exchange columns (as arranged in Figure 2.4) and neutral

fraction and acidic fractions obtained as described in section 2.12.8. Due to the glucose oxidase treatment, the acidic fraction comprised the **glucose** component and the neutral fraction comprised the **fructose and sucrose** components (Figure 2.3). To measure the radioactivity in each of the fractions, the dpm from 500 µL of each sample was measured (2.12.2), corresponding to 0.156% of the [^{14}C] radioactivity of each component.

2.12.11 Fractionation of the Total Soluble Fraction into Hexose Phosphates and Organic Acids

150µL of the total soluble fraction was mixed with 50 µL of a solution containing 20 U /mL acid phosphatase and 10 mM MES-KOH (pH 6.0). The reaction was incubated for 3 h at 37°C and 400 rpm, before stopping by heating the sample to 95°C for 3 min and briefly centrifuging. This treatment cleaved the orthophosphate from hexose phosphates, allowing the charged organic acids and amino acids to be separated from the newly uncharged hexose phosphate component. The acid phosphatase treated fraction was applied to a new set of anionic/cationic exchange columns (as arranged in Figure 2.4) and fractionated into neutral, acidic and basic fractions as described in section 2.12.8. Due to the acid phosphatase treatment, the neutral fraction comprised the **hexose phosphates** component, the acidic fraction the **organic acids, and the basic fraction** the **amino acids** (Figure 2.3). To measure the radioactivity in each of the fractions, the dpm from 200 µL of each sample was measured (2.12.2), corresponding to 0.123% of the [^{14}C] radioactivity of each component.

2.12.12Total Insoluble Fraction and Further Fractionation

The ethanol insoluble fraction comprises the starch, protein and cell wall. The resuspended insoluble pellet (2.12.5) was vortexed and ground using a ball mill (Qiagen, Hilden, Germany, TissueLyser). To measure the total radioactivity in the insoluble fraction, the dpm from 20 µL of each sample was measured (2.12.2), corresponding to 0.4% of radioactivity in the total insoluble fraction.

For further fractionation, 200 µL of the insoluble fraction was added to 200 µL of a solution containing 5 U /mL amyloglucosidase from (*Aspergillus nidulans*, Roche, Basel, Switzerland) in 0.4 M sodium acetate (pH 5.5). This was incubated for 12 h at 37°C with shaking at 400 rpm to hydrolyse starch molecules into glucose monomers. After incubation, 100 µL of a solution containing 10 U /mL pronase (*Streptomyces griseus*, Roche, Basel, Switzerland) in 0.5 M Tris-HCl (pH 7.8), was added to digest protein into amino acids monomers. This was incubated for 12 h at 37°C with shaking at 400 rpm. The reaction was stopped by heating the samples for 5 min at 95°C, before briefly centrifuging.

The remaining insoluble residue in the enzyme treated samples comprised the cell wall, which was separated by filtration; a small hole was made in a 0.5 mL centrifuge tube, and covered with a small piece of miracloth, before placing the 0.5 mL centrifuge tube into a larger 1.5 mL centrifuge tube (Figure 2.5). The enzyme treated aliquot was applied to the smaller 0.5 mL centrifuge tube and the whole system centrifuged briefly. The enzyme treated aliquot (now in the larger 1.5 mL centrifuge tube) was applied to a new set of anionic/cationic exchange columns to obtain neutral, acidic and basic fractions as described in section 2.12.8. The small piece of miracloth,

containing the insoluble cell wall was retained and added to the insoluble anionic/acidic fraction prior to scintillation counting.



Figure 2.5: Arrangement of centrifuge tubes and miracloth for filtration of the total insoluble fraction for cell wall components.

2.12.13Total Insoluble Fraction and Further Fractionation

The neutral fraction comprised radioactivity from **starch,** the basic fraction radioactivity from **protein** (Figure 2.3).

The columns were then separated. The cationic column alone was washed with three volumes of 1 mL of 1 M NH_4OH, and the elute retained as the insoluble cationic/basic fraction, comprising the **amino acids**. The anionic column was washed 3x with 1 mL of 4 M formic acid, and the elute retained as the insoluble

anionic/acidic fraction. This, combined with the small piece of miracloth comprised the **cell wall** components.

The radioactivity in the neutral, basic and anionic elutes was measured (2.12.2) and the dpm measured corresponded to 40% of the [^{14}C] radioactivity in the **starch**, **amino acid** and **cell wall** respectively (Figure 2.3).

2.12.14Quantification of the Hexose Phosphate Pool Size

A solution containing 50 mM Tricine KOH (pH 9.0), 2.5 mM $MgCl_2$, 0.1 mM $NADP^+$, 0.1 mM glucose-1,6-bisphosphate, 2.5 U glucose 6-phosphate dehydrogenase (yeast, Roche, Basel, Switzerland), 1.0 U phosphoglucose isomerase (yeast, Roche, Basel, Switzerland) and 1.0 U phosphoglucomutase (rabbit muscle, Roche, Basel, Switzerland) was added to a 5 µL aliquot of the total soluble fraction (2.12.8) (Figure 2.3) to make a total final volume of 75 µL in a 96 well plate. This converted both fructose 6-phosphate, and glucose 1-phosphate, to glucose 6-phosphate. The reaction was incubated for 30 min at 22°C to convert the endogenous and converted glucose 6-phosphate into an equivalent amount of NADPH. 20 µL of 0.5 M KOH was added to stop the reaction before the 96 well plate was sealed, spun down and incubated at 95°C for 5 min. HCl was mixed with 1.0 M Tricine KOH (pH 9.0) and diluted with deionised water until the solution had 0.5 M HCl and 0.2 M Tricine KOH, the pH was not adjusted after mixing. The plate containing the samples was then allowed to cool before the addition of 20 µL of the 0.5 M HCl and 0.2 M Tricine mixture and the pH confirmed to be pH 9.0. The heating and pH ensured endogenous NADH degradation in the sample, leaving the NADPH remaining.

The NADPH was then quantified using a cycling assay based on the reduction of phenazine methosulphate by NADPH; 50 µL of a solution containing 300 mM Tricine KOH (pH 9.0), 12 mM EDTA, 9 mM glucose 6-phosphate (Roche, Basel, Switzerland) 100 U /mL glucose 6-phosphate dehydrogenase (yeast, Roche, Basel, Switzerland) 1.8 mM MTT and 0.3 mM PMS was added to each reaction. The MTT and PMS stock solutions were prepared fresh daily and were stored in the dark prior to use. The change in absorbance of light at a wavelength of 570 nm was recorded using a spectrophotometric platereader (Beckman Coulter, Brea, USA, DTX 880 Multimode detector) until the slope became stable after 20 min.

The rate of change in absorbance was proportional to the cycling reaction velocity, and this was used to calculate the amount of hexose phosphate by comparison to velocities obtained from standard samples containing known glucose 6-phosphate concentrations.

2.13 Maximum Catalytic Activity of Glycolytic Enzymes

Methods modified from (Rossouw et al., 2010; Sweetlove et al., 1996 ; Appeldoorn et al., 1997).

2.13.1 Enzyme Extraction

To assay glycolytic enzyme activity, approximately. 1 g (FW) of frozen potato material (2.5) was resuspended at 4°C in 5 mL of extraction medium, containing 100

mM Hepes (pH 7.5), 10 mM EDTA, 5 mM dithiothreitol and 0.5% (w/v) BSA which contained 0.1% (w/v) polyvinylpyrrolidone. Negative controls omitted the ground tissue. After 5 min the suspension was centrifuged at 10,000 g for 5 min at 4°C. Extracts were desalted using NAP-5 columns (GE Lifesciences, Amersham, UK, Illustra) which were equilibrated first with 1 mL of extraction medium and again with 1 mL deionised water, before the total supernatant was applied to the column for desalting and the elute/protein extract stored on ice before use.

2.13.2 Glycolytic Enzyme Activity Assays

The rate of change in absorbance of light at a wavelength of 340 nm from 145 µL of each reaction mix and 50 µL sample (2.13.1) was recorded using a spectrophotometric platereader (Beckman Coulter, Brea, USA, DTX 880 Multimode detector) prior to the addition of 5 µL of substrate or coenzyme to start the reaction (represented in bold) (Total reaction mixture 200 µL) (2.13.1). The subsequent change in absorbance at 340 nm, representing coenzyme consumption or production, (Figure 2.6) was recorded until stable, and the gradient of this change was used to measure the activity of each glycolytic enzyme (Figure 2.6). Each of the assay mixtures were optimised with respect to the concentration of each component and pH for this experiment, using starting reference points from published methodologies (Rossouw et al., 2010; Sweetlove et al., 1996 ; Appeldoorn et al., 1997).

Invertase: 50 mM Tris-HCl (pH 7.0), 5 mM **$MgCl_2$**, 2.5 mM ATP, 0.33 mM $NADP^+$, 1 U glucose 6-phosphate dehydrogenase, 1.2 U Hexokinase, 1 mM sucrose.

Hexokinase: 50 mM Tris-HCl (pH 8.0), 5 mM $MgCI_2$, 2.5 mM ATP, 0.33 mM $NADP^+$, 1 U **glucose 6-phosphate dehydrogenase** and 3 mM glucose.

PFK: 100 mM Tris-HCl (pH 8.0), 2 mM **$MgCl_2$**, 5 mM fructose 6- phosphate, 0.1 mM NAD^+, 1 mM ATP, 1 mM ADP, 1 U aldolase, 10 U triosephosphate isomerase and 1.3 U of glycerol-3-phosphate dehydrogenase.

PFP: 100 mM Tris-HCl (pH 7.5), 2 mM $MgCl_2$, 5 mM fructose 6- phosphate, 10 μM fructose 2,6 bisphosphate, 0.1 mM NAD^+, 1 mM ADP, 1 U aldolase, **10 U triosephosphate isomerase**, 1 mM PPi and 1.3 U of glycerol-3-phosphate dehydrogenase.

Pyruvate kinase: 50 mM MOPS (pH 7.0), 100 mM KCl, 15 mM **$MgCl_2$**, 0.15 mM NADH, 5.0 mM phosphoenolpyruvate, 1.0 mM ADP and 0.15 U lactate dehydrogenase.

Lactate dehydrogenase: 100 mM TRIS (pH 7.0), 0.2 mM NADH, 10 mM **pyruvate**.

Pyruvate decarboxylase: 100 mM TRIS (pH 8.5), 0.2 mM NADH, 30 mM pyruvate and 1 U **alcohol dehydrogenase**.

Alcohol dehydrogenase: 50 mM Hepes (pH 8.0), **2 mM NAD^+** and 150 mM ethanol.

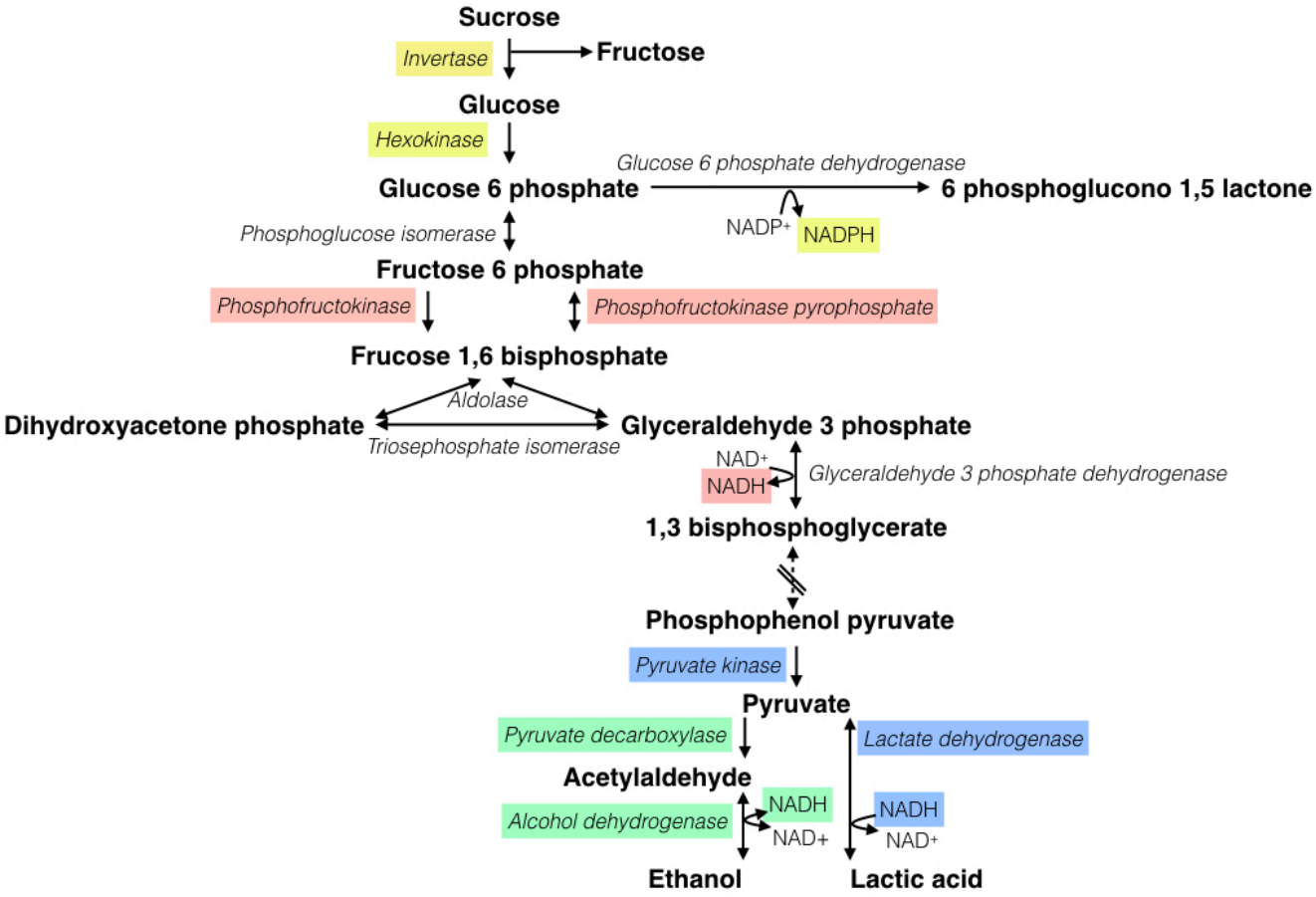


Figure 2.6: Schematic diagram demonstrating the coupled enzyme assays to quantify maximum catalytic activity of different glycolytic enzymes and where changes in coenzyme abundance are measured. Each colour represents which coenzyme abundance is measured to calculate the activity of each enzyme.

2.14 Lipid Quantification and Identification

Method modified from (Kim & Salem, 1993).

2.14.1 Lipid Extraction and Component Fractionation by Solid-Phase Extraction

Equipment was prepared prior to use as in (2.12.6). Approximately 0.2 g (FW) of ground potato tissue (2.5) was mixed with 1.5 mL hot isopropanol and 0.01% (w/v) butylated hydroxytoluene. Negative controls omitted the ground tissue. Samples were heated at 75 °C for 15 min to denature enzymes (particularly plant phospholipases) and allowed to cool before addition of 750 µL chloroform and 300 µL deionised water. The vials were flushed with N_2 and shaken for 1 h at 400 rpm before the phases separated by centrifugation at 2,200 g for 10 min at 5°C.

The lower organic phase, consisting of the lipids and chloroform, was removed and flushed with N_2 before retaining on ice. The remaining polar phase was washed a further two times using 750 µL chloroform and 300 µL deionised water, with 30 min of agitation and centrifugation at 2,200 g for 10 min at 5°C. All lower organic phases were combined before washing with 1 mL of 1 M KCl, and the upper phase discarded. The lower organic phases were lastly washed with 2 mL deionised water, and the upper phase discarded before flushing with N_2 and retaining on ice.

The combined lower polar phases were then evaporated under N_2 using a manifold system (Figure 2.4). Once completely evaporated samples were resuspended in in 0.5 mL of chloroform, flushed with N_2 and stored at -20°C for up to 2 days before use. Entire samples were applied to aminopropyl columns (Supelco LC-NH_2 columns with 0.5 g resin) for solid-phase fractionation (as per 2.12.6).

2.14.2 Sulphuric-Phosphoric-Vanillin Assay for Lipid Quantification

Method modified from (McMahon et al., 2013).100 µL of lipid samples were pipetted into a 96 well plate and evaporated under a stream of N_2 before 100 µL of concentrated sulphuric acid was added. The added 96 well plate was then sealed and incubated on a heat block at 90°C for 10 min to form a carbonium ion from unsaturated lipids. After the plate had completely cooled to room temperature, the background absorbance of light at a wavelength of 540 nm was measured using a spectrophotometric platereader (Beckman Coulter, Brea, USA, DTX 880 Multimode detector). 50 µL of the vanillin-phosphoric acid reagent was added to each well (4 mL of 85% (v/v) phosphoric acid, 6 mL 80°C deionised water and 2 mg vanillin) which formed a phosphate ester, increasing carbonyl group reactivity before reacting with the phosphovanillin to form a pink colour. Final absorbances of the sulphuric-phosphoric-vanillin (SPV) assays after 5 and 10 min were measured and compared against a standard curve of known concentrations of oleic acid.

2.14.3 GC-MS analysis for Lipid Quantification and Identification

2.14.4 Fatty Acid Methyl Ester Formation

The elutes (2.14.1) compromising the total phospholipids and free fatty acids were each evaporated under N_2 using a manifold system and then subsequently resuspended in 300 µL of 5 % (v/v) HCl in methanol. A 15 µg internal standard of heptadecanoic acid (C17:0) was added before the samples were flushed with nitrogen and heated for 1 h at 85 °C for transesterification. Samples were allowed to cool and 800 µL hexane was added. The samples were once again flushed with nitrogen and capped, before

incubation at 25°C for 1 h at 200 rpm. After this, 500 µL of the hexane upper phase, containing the FAMEs, was transferred into GC-MS vials for analysis. These vials were flushed with N_2 before being sealed.

2.14.5 GC-MS Quantification and Identification of FAMEs

Analysis was carried out on a GC system (Agilent, Santa Clara, USA, 9000 Intuvo GC), coupled to a single quadrupole detector (Agilent, Santa Clara, USA, 5977B). The MS was calibrated before each run using the inbuilt autotune method. An Agilent 5-ms Ultra Inert column (Agilent, Santa Clara, USA, Intuvo GC) (15 m long, 0.25 mm inner diameter) was used and 1 µl of sample was injected into the MS each time. Column temperature was raised to 80°C for 2 min, increased by 7°C per min until 140°C and maintained for 4 min before a second ramp, increasing temperature by 4°C per min to 240°C which was held for 12.5 min, with a solvent delay of 10 min and a helium gas flow of 1 mL /min. Elution times and mass fragments of each fatty acid was determined by comparison with standard curves of pure compounds obtained from a plant FAME mixture. Fatty acids in each sample and fraction were identified and quantified using the MassHunter Workstation (Agilent, Santa Clara, USA). Analytes were classed by their retention times and simultaneously identified in all samples based on the comparison of Mass Spectral Tags to the NIST library (Luedemann et al., 2008; Halket et al., 2005; Ausloos et al., 1999).

2.14.6 Double Bond Index

The double bond index is a measure of the degree of saturation of each fatty acid and was measured from a modified method from (Cequier-Sánchez et al., 2011).

$$Double\ Bond\ Index = \%\ FA * (C + D)$$

% FA = the percentage of each fatty acid

C = the number of carbons/length of each fatty acid

D = the number of double bonds/degree of desaturation

2.15 Activity Based Protein Profiling

2.15.1 *In Vivo* Labelling of Active Serine Hydrolases Enzymes Under Blackheart Induction Conditions

Tissue sampling was done under a stream of N_2 and a heater set to 37°C to maintain Blackheart induction conditions (2.2). 2 mm thick discs (2.5) were taken from potato tubers stored under Blackheart induction conditions (2.2) for 0 h or 8 h. Discs were simultaneously added to a 24 well plate containing 300 µL of 0.2 µM TAMARA FP Serine Hydrolase probe (Thermofisher, Waltham, USA, in DSMO) in MES-KOH (10 mM, 6.5 pH). Negative controls contained DSMO in place of the FP probe. The 24 well plate was immediately flushed with a stream of N_2 and sealed, before incubation at 37°C to best maintain the anoxic Blackheart induction conditions (2.2). After 15 min from the start of incubation, discs were removed from wells and washed 3 times in MES-KOH (10 mM, 6.5 pH) to remove excess probe and wounded cells. Discs were blotted dry and dropped into baths of liquid N_2 to quench enzyme activity. Discs were kept frozen at -80°C for up to 2 weeks before use, or processed into ground tissue (2.5) immediately.

2.15.2 Protein Extraction

All following extraction work was completed at 4°C. Approximately 0.1 g (FW) of ground tissue (2.15.1) was added to 500 µL of ice cold 1% (v/v) PBS with 0.8% (v/v) Triton-X100 detergent, incubated on ice for 2 min and vortexed. Samples were then centrifuged at 10,000 g for 10 min. The tissue pellet was discarded and the supernatant kept on ice for further analysis.

2.15.3 Assay to Determine Protein Concentration

15 µL of each sample (2.15.2) was used to quantify total protein abundance via the Pierce™ Detergent Compatible Assay (Thermofisher, Waltham, USA) and measuring absorbance at 595 nm using a spectrophotometric platereader (Beckman Coulter, Brea, USA, DTX 880 Multimode detector). These absorbances were compared against a standard curve of known BSA concentrations to calculate the total protein concentration in each sample.

2.15.4 Resolving Proteins by SDS-Page Gel Electrophoresis

Samples were standardised by protein concentration (2.15.3) by mixing 1-100 µl of sample (2.15.2) with 50 µL of 2x Gel Loading Buffer (New England BioLabs, Ipswich, USA) before vortexing and incubation at 90°C, 200 rpm for 6 min to ensure total protein denaturation. 5 µL of sample was then run on an SDS-PAGE gel comprising:

15% (w/v) polyacrylamide separation gel: 1.5 Tris-HCl (pH 8.8), 10% (w/v) SDS, 30% (w/v) Acrylamide, 10% ammonium persulphate (w/v), 10 µl TEMED

5% (w/v) polyacrylamide stacking gel: 0.5 Tris-HCl (pH 6.8), 10% (w/v) SDS, 30% (w/v) Acrylamide, 10% ammonium persulphate (w/v), 10 µl TEMED

Electrophoresis was conducted in a 10% (w/v) glycine running buffer (25 mM TRIS, 192 mM glycine, 1% (v/v) SDS) and using an ice pack to avoid gel melting. Gels were run at 80 V in the dark, until the markers neared the end of the gel.

Resolved gels were imaged for in-gel fluorescence on a Typhoon scanner (GE lifesciences, Amersham, UK, Typhoon 9400) using a 526 shortpass filter, green laser at 532 nm and a 600 V photomultiplier tube. After imaging for protein activity, the gels were then stained with 0.1% (w/v) Coomassie Brilliant Blue for 8-12 h and then de-stained in deionised water : methanol : acetic acid (50:40:10 v/v/v) for another 4-8 h. Gels were then imaged using a flat-bed scanner (Epson, Suwa, Japan, expression 1600Pro) in 24 bit colour and 600 dpi to visualise corresponding in-gel protein abundance.

2.15.5 Gel Quantification

Images of both the fluorescence and Coomassie staining of each gel were analysed using ImageJ/Fiji software (Schindelin et al., 2012) to quantify the intensity of each band using the in built gel analysis settings.

2.15.6 Mass Spectrometry Identification of Proteins of Interest

Bands of interest were excised from gels made with ingredients filtered through 0.2 μM filters to avoid contamination (2.15.4).

The following work (2.17.6) was conducted by Dr Sabrina Liberatori at the Advanced Proteomics Facility at the Department of Biochemistry, University of Oxford.

Gel bands were subjected to in-gel trypsin digestion and peptides were separated by nano-flow reversed-phase LC coupled to a Q Exactive Hybrid Quadrupole-Orbitrap MS (Thermo Fisher Scientific, Waltham, USA). Peptides were loaded on a PepMap100 pre-column (inner diameter 300 μm x 5 mm, 3 μm C18 beads) (Thermo Fisher Scientific, Waltham, USA) and separated on a 50 cm reversed-phase C18 column (inner diameter 75 μm, 2 μm C18 beads) (Thermo Fisher Scientific, Waltham, USA) using a linear gradient from 10 to 35% of B for 30 min at a flow rate of 200 nL /min (A: 0.1% (v/v) formic acid, B: 0.1% (v/v) formic acid in acetonitrile). All data was acquired in a data-dependent mode, automatically switching from MS to collision-induced dissociation MS/MS on the top ten most abundant ions with a precursor scan range of 350–2000 m/z. MS spectra were acquired at a resolution of 70,000 and MS/MS scans at 17,500. Dynamic exclusion was enabled with an exclusion duration of 5 s and charge exclusion was applied to unassigned, and mono-charged ions. Raw data files were processed for protein identification using MaxQuant (Cox & Mann, 2008) integrated with the Andromeda search engine (Cox et al., 2011).

The MS/MS spectra were searched against the *Solanum tuberosum* and *Arabidopsis thaliana* Uniprot databases (Bateman et al., 2016) (UP000011115 and UP000006548respectively); precursor mass tolerance was set to 20 ppm and MS/MS tolerance to 0.05 Da. Enzyme specificity was set to trypsin with a maximum of two missed cleavages. False discovery rate for protein and peptide spectral matches was set at 0.01.

2.15.7 Further Identification of Serine Hydrolase Candidates

The list of candidate proteins was reduced by first ignoring any non-enzymatic proteins, before searching the remaining candidates for enzymes in the EC 3 hydrolase family. This shortened list was further reduced to those enzymes in the serine hydrolase family though individual literature searches.

2.16 Statistical Analysis Methods

Statistical analysis of results and parametric assumption testing was conducted using SPSS (IBM Corp. New York, USA).

3 Induction and Characterisation of Blackheart

3.1 Introduction

The work described in this chapter aims to determine the necessary and/or sufficient conditions required to induce Blackheart. These conditions will be used to develop a robust method that can rapidly and reliably induce Blackheart in the laboratory. This chapter aims to utilise such an induction method to assess and record any variation in Blackheart susceptibilities between tuber varieties, annual harvests and different industrial practices. The objectives of this work are to better characterise Blackheart and provide information to the UK potato industry on best practice to reduce the disorder incidence.

3.1.1 A Systematic Exploration of the Conditions Required to Induce Blackheart is Necessary

Anecdotal evidence suggests a significant increase in the occurrence of Blackheart over the last eight years (Briddon, 2015; Kiaitsi, 2015; David Wright, Manor Fresh Ltd., pers. comm., 2014) causing issues for both potato producers, sellers and consumers. Despite its ever-growing prevalence, the underlying conditions required for Blackheart to develop have not yet been robustly or systematically tested.

High storage temperatures, CO_2 accumulation and oxygen exclusion have all been shown as contributing factors in driving Blackheart development, but none have been proven essential for the disorder to develop (Chapter 1). Despite a lack of consensus in the existing literature (Table 3.1) the Potato Research Council (2016) suggests that

to minimise Blackheart incidence, stores should be cool and well-aerated, with close monitoring of CO_2 changes. However, despite consistent storage conditions, Blackheart complaints and incidence vary both within and between years (Briddon, 2015; Kiaitsi, 2015; David Wright, Manor Fresh Ltd., pers. comm., 2014; Potato Research Council, 2016). Indeed, since the Potato Research Council storage conditions recommendations have been in place, Blackheart incidence has been increasing (Briddon, 2015; Kiaitsi, 2015; David Wright, Manor Fresh Ltd., pers. comm., 2014). More recently, low storage temperatures have been implicated in driving Blackheart rates (Briddon, 2015). Therefore, it is likely that there are additional unknown factors that both cause and influence Blackheart development, other than high temperature and low oxygen concentrations.

Table 3.1: Summary of conditions previously linked to Blackheart induction.

Publication	Conditions shown to induce Blackheart	Proposed cause of Blackheart
Bartholomew (1913 & 1914)	High CO_2 and 38-44°C for 24 h	A combination of high temperature and CO_2 accumulation
Stewart & Mix (1917)	Anoxia and high temperature Anoxia and temp below 6°C	Oxygen exclusion alone
Singh & Mathur (1937)	Anoxia	Oxygen exclusion alone
Davis (1926)	Abundance of oxygen, high temp	Reduced gaseous diffusion
Briddon (2015)	Storage at 30°C in a non-airtight container for 60 h.	A combination of high storage temperature, low oxygen and high CO_2 accumulation, exacerbated by washing and <3.5°C long-term storage

The lack of consensus on the conditions that drive Blackheart has moved research focus away from identifying a cause of Blackheart, or prevention of the disorder, towards research directed on improving quality control methods and non-destructive detection of affected tubers (Mohamed et al., 2016; Zhou et al., 2015). The growing incidence of Blackheart in industry, confusion in the existing Blackheart literature (Table 3.1) and lack of headway in recent research efforts on Blackheart (Kiaitsi, 2015) mean that a robust and systematic exploration of causative factors in Blackheart is essential. Such a characterisation would need to distinguish between the necessary conditions for Blackheart to develop in tubers, versus those that are simply sufficient. This will in turn provide information on the underlying biochemical cause of the

disorder, as well as identifying practices in industry that might be responsible for increasing Blackheart incidence rates.

3.1.2 A Robust Induction Method is Required for Blackheart Characterisation

The relatively low incidence rates of Blackheart during storage are a barrier to research into the disorder (Kiaitsi, 2015); the problem being that very large numbers of tubers must be sampled in order to observe sufficient occurrences of Blackheart for observations to be statistically analysed. There are obvious practical limitations to such an approach and more headway has been made through use of a method to induce Blackheart within the laboratory (Briddon, 2015).

There are several requirements for an optimal method to induce Blackheart in the laboratory, which will be referred to as a Blackheart induction method throughout the rest of this thesis: firstly, the chosen Blackheart induction method needs to be sufficiently rapid that experiments and tests can be conducted and reproduced within the timeframe of a D.Phil. project; secondly, the induction method needs to produce Blackheart in a consistent, time-dependent manner; thirdly the induction method needs to reliably induce Blackheart in all tubers with a coordinated onset of the disorder. These last two requirements are integral to the success of the project as both imaging Blackheart and sampling tissues are destructive processes, and the two measurements cannot be done simultaneously in a single tuber. Therefore, a reliable and time dependent induction method would make it possible to determine the degree of Blackheart progression in tubers used for tissue analysis, without also imaging them. This would provide the first opportunity to measure the changes in tuber tissues

prior to the onset of Blackheart. This is particularly important because Blackheart appears to be a region of necrosis (Stewart & Mix, 1917; Bartholomew, 1913) meaning that biochemical analysis of (dead) tissue that is already affected would not be informative. Measurements throughout the onset of the disorder will be helpful in identifying changes that occur before Blackheart, and thus will help elucidate the underlying biochemical cause of the disorder, as well as characterising the spread and tissue-origin of the disorder.

The objective of this chapter is to first characterise what conditions induce Blackheart (3.1.1) and then utilise these to develop an optimal Blackheart induction method. A Blackheart induction method will provide sufficient Blackheart affected tubers for additional observations to be made, including if there are multiple or single origins and how the disorder spreads through tissues. Destructive sampling and non-destructive imaging, will be used to better characterise the disorder.

3.1.3 Varietal and Annual Differences in Blackheart Susceptibility

The work in this chapter aims to utilise a Blackheart induction method (3.1.2) as an experimental tool; highly susceptible tubers are likely to develop Blackheart faster than resistant tubers, and display larger pigmented regions. Therefore differences to the time of onset of Blackheart, and/or the area of Blackheart affected tissues may be utilised to compare Blackheart susceptibility between varieties, annual harvests and different storage conditions.

Blackheart complaint rates vary each year and are greater in certain varieties, (Briddon, 2015; Kiaitsi, 2015; David Wright, Manor Fresh Ltd., pers. comm., 2014), however no known robust characterisation of modern UK varieties Blackheart susceptibilities has been published. Although Maris Piper tubers have the highest number of Blackheart related complaints, this may not relate to a greater Blackheart susceptibility, as it is also one of the most frequently purchased varieties in the UK and complaints are not standardised by volume of varieties sold (David Wright, Manor Fresh Ltd., pers. comm., 2014; Kiaitsi, 2015).

Additionally, it is not known what causes this annual variability in Blackheart susceptibility; a Blackheart induction method would provide an experimental system where the effect of different storage or industry conditions on Blackheart susceptibility can be tested. This will, in turn, help identify factors that may reduce Blackheart incidence.

3.1.4 Effect of Industry Practices on Blackheart Susceptibility

There are various industrial practices that could potentially effect Blackheart incidence; sampling of tubers held in UK potato industry stores suggests that Blackheart incidence increases during long-term storage of potato crops (Potato Research Council, 2016; Briddon, 2015; David Wright, Manor Fresh Ltd., pers. comm., 2014). Although it is widely believed that storage conditions cause Blackheart, there are alternative explanations for this correlation. Firstly, Blackheart incidence could be exacerbated, rather than caused, by storage conditions. Although it is rare, Blackheart in freshly harvested tubers has been recorded (Briddon, 2015;

Kiaitsi, 2015)(Briddon, 2015; Kiaitsi, 2015)(Briddon, 2015; Kiaitsi, 2015)(Briddon, 2015; Kiaitsi, 2015)(Briddon, 2015; Kiaitsi, 2015)(Briddon, 2015; Kiaitsi, 2015)(Briddon, 2015; Kiaitsi, 2015)(Briddon, 2015; Kiaitsi, 2015)(Briddon, 2015; Kiaitsi, 2015)(Briddon, 2015; Kiaitsi, 2015) (Briddon, 2015; Kiaitsi, 2015; David Wright, Manor Fresh Ltd, pers. comm., 2014) suggesting the disorder is not caused by storage conditions alone. Secondly, Blackheart may instead be an age-related disorder and its incidence simply coincides with long-term storage, which accounts for the majority of a tubers life-span. Thirdly, most quality control checks occur during long-term storage, which may represent a measurement bias. Lastly, Blackheart complaints and industrial incidence tends to vary year-on-year (Potato Research Council, 2016; Briddon, 2015; Kiaitsi, 2015; David Wright, Manor Fresh Ltd., pers. comm., 2014) despite annual consistency in tuber storage conditions. Therefore, storage conditions alone are unlikely to explain Blackheart incidence variations and a whole system approach, from field to fork, must be considered.

UK potatoes are planted in the late spring, using small, disease free “seed” tubers. These seed tubers are planted along ridges which aid in soil aeration, drainage and ease of harvesting. Growers are warned that Blackheart incidence is exacerbated in waterlogged or tightly packed soil (Burton, 1989; Potato Research Council, 2016; David Wright, Manor Fresh Ltd., pers. comm., 2014) based on the previously reported connection between Blackheart and gaseous exchange (Table 3.1) (Davis, 1926). However, no correlation has been found between tuber gaseous exchange limitations and Blackheart incidence (Kiaitsi, 2015) indicating this practice may not affect Blackheart incidence. After two to three weeks the potato plant emerges from the seed tuber, and below ground stolons and roots begin to grow (Burton, 1989).

Tuberisation at the tips of each stolon occurs after 11-13 weeks and is initiated in part by changes in day length and flowering (Burton, 1989).

Measures to reduce Blackheart incidence often focus on reducing stress conditions to the tubers and mother plant and potato fields may be irrigated or treated with herbicides or pesticides during this growing period depending on conditions. For example, drought stress increases plant respiration (Flexas et al., 2005) and as high respiration rates have previously been linked to Blackheart (Stewart & Mix, 1917) irrigation under drought conditions is recommended. Additionally, high soil temperatures have also been thought to influence Blackheart induction and therefore warm growing summers are believed to increase Blackheart incidence (Potato Research Council, 2016, David Wright, Manor Fresh Ltd., pers. comm., 2014).

In the late summer, between 17-18 weeks since planting, the haulm is removed via chemical or manual defoliation. This practice reduces incidence of late tuber blight and controls final tuber size by preventing further bulking (Burton, 1989; Potato Research Council, 2016). Although defoliation methods have not been directly attributed to Blackheart, chemical treatments are likely to induce stress; a commonly used defoliant, Diquat, specifically increases plastid membrane permeability (Funderburk & Lawrence, 1964) and although defoliants are applied to above-ground growth, it has been indicated that foliar treatments are able to directly enter the tuber through the stem and stolon, causing necrosis (Headford and Douglas, 1967). Due to the link between plastid integrity and PPO-substrate mixing (Chapter 1) it is reasonable to consider the influence of diquat, and other chemical treatments, on tuber Blackheart development. After defoliation, tubers remain in the soil for three to four

weeks to encourage ‘skin set’ via periderm suberisation (Burton, 1989; David Wright, Manor Fresh Ltd., pers. comm., 2014.) The length of time mature tubers are left in the field, and the temperature during, is another possible factor thought to potentially affect Blackheart susceptibility (David Wright, Manor Fresh Ltd., pers. comm., 2014).

In the early autumn, approximately three months after planting, tubers are harvested. In the UK average potato yields are approximately 460 tonnes/ha (FAO-STAT, 2018). After harvest, stones and soil are mechanically removed before tubers are distributed into crates or stored as deep piling. Tubers are placed into “warm stores” kept at 10°C which are pulled down towards approximately 2-4°C over the course of several days. Rapid temperature transitions have been demonstrated to increase tuber respiration rates (Chapter 1) (Malone et al., 2006; Schippers, 1977) and similarly, high respiration rates have been linked to Blackheart (Stewart & Mix, 1917).

Long-term storage of potato harvests occurs in “cold stores”, maintained at 1.5-5°C for up to 14 months. Significant increases in Blackheart incidence occur when tubers were stored at 1.5°C versus 3.5°C (Briddon, 2015), suggesting that low temperature storage influences Blackheart incidence in industry. However, low storage temperatures (<3°C) are used in industry to maintain tuber dormancy and reduce pathogenic tuber skin diseases (Burton, 1989; David Wright, Manor Fresh Ltd., pers. comm., 2014; Potato Research Council, 2016). Stores are also kept dark to avoid greening, accumulation of glycoalkaloids and sprouting (Potato Research Council, 2016; Burton, 1989).

Stores are monitored for CO_2 concentrations, and ventilated by fans to remove the heat generated by respiring tubers, supply oxygen, and remove CO_2. CO_2 accumulation has previously been linked to Blackheart incidence (Bartholomew, 1913; Briddon, 2015; Davis, 1926). Sprout suppressors or chemicals for disease control can be added to stores as the crop ages and are distributed via the ventilation system. One widely used sprout suppressor is ethylene, which causes rapid increases in potato respiration after application (Reid and Pratt, 1972) and as a result may therefore influence Blackheart incidence.

To meet year-round consumer demand, tubers are stored for up to 12 months in cold stores. Blackheart incidence increases with length of storage (Potato Research Council, 2016; Briddon, 2015; David Wright, Manor Fresh Ltd., pers. comm., 2014). Prior to sale, boxes of tubers are removed from cold stores and transferred to warm stores (10°C) for several days, to reduce bruising during subsequent washing, sorting and packing (David Wright, Manor Fresh Ltd., pers. comm., 2014; Potato Research Council, 2016; Burton, 1989) and to decrease the levels of reducing sugars which accumulate during cold term storage via cold induced sweetening (Malone, 2006). Tubers are then washed, which can include periods of submergence (and thus anoxia), before automated and/or manual grading, which removes green, diseased, or mechanically damaged tubers (David Wright, Manor Fresh Ltd., pers. comm., 2014). Anecdotally, tubers that are left unwashed appear to have fewer Blackheart complaints (David Wright, Manor Fresh Ltd., pers. comm., 2014), and it is possible this is due to anoxia during the washing process, which is a reported factor in Blackheart development (Stewart & Mix, 1917; Singh & Mathur, 1937; Briddon, 2015). Packaging has also long been thought to affect Blackheart incidence via

reduced gaseous diffusion and the accumulation of CO_2, although its role is unclear as no correlation between gaseous diffusion and Blackheart has been found (Kiaitsi, 2015). A similar reasoning has led to the belief that increased tuber size correlates with Blackheart incidence (Kiaitsi, 2015; David Wright, Manor Fresh Ltd., pers. comm., 2014), although there is little supporting evidence for this (Kiaitsi, 2015). Finally, potatoes are stored in supermarkets, or with consumers, at room temperature for approximately 1-3 weeks, which introduces additional temperature transitions.

This chapter aims to explore the effect of the various conditions that have been suggested to increase Blackheart incidence, or the conditions that may affect potato tuber respiration, based on the prevailing thought that Blackheart is caused by high respiratory rates (3.1.1). This will be achieved by utilising a Blackheart induction method and identifying what conditions drive differences in Blackheart occurrence. These results can then be used to advise industry on best practice to reduce Blackheart incidence.

3.2 Results

3.2.1 Characterising the Necessary and Sufficient Conditions for Blackheart Development

Control storage conditions for tubers were chosen to mimic industrial cold store conditions (4°C, dark and well ventilated) (Chapter 2), to which Blackheart incidence rates would be compared. Different conditions were systematically applied to tubers for various durations before the percentage of tubers affected with Blackheart was quantified (Chapter 2).

Incubation conditions included the proposed causes of Blackheart in literature (Table 3.1). Tubers were incubated at various temperatures: 2°C was chosen in light of the finding that low cold store temperatures increase Blackheart incidence (Briddon, 2015); room temperature (22°C) was used to represent the temperature that tubers are frequently kept at by consumers; 37°C was chosen in line with previous literature (Bartholomew, 1913; Stewart & Mix, 1917; Davis, 1926; Briddon, 2015) where high temperatures induce Blackheart; and lastly, a the mid point between 22°C and 37°C (29.5°C) was also included as an additional measurement. As Blackheart has been linked to limited gaseous exchange (Briddon, 2015; Singh & Mathur, 1937; Stewart & Mix, 1917; Bartholomew, 1913; Kiaitsi, 2015) tubers were incubated whilst loosely wrapped with cling film to reduce, but not eliminate, gaseous diffusion. Tubers were also vacuum packed to eliminate oxygen, to explore the role of anoxia, or incubated with KOH to avoid the accumulation of CO_2.

Four King Edward tubers, that had been stored under control conditions for 3 months, were used for each induction condition and duration, and the experiment was repeated four times resulting in a total of 16 tubers for each condition. Simple presence or absence of Blackheart was used, rather than the quantification of the disorder (Chapter 2) and one tailed z tests used to identify any significant increases in Blackheart incidence between conditions.

Some conditions resulted in tuber heat necrosis, sprouting, or reduced tubers to pulp (recorded as "-", Table 3.2) due to the extent of tissue necrosis, rendering Blackheart identification futile. Blackheart was not found in any of the 16 tubers in some conditions (as recorded "0%", Table 3.2). For any tubers incubated under anoxia (not including the cling film wrapped tubers), Blackheart was not immediately evident after removal from induction conditions, only after re-aeration for 5-12 hours was Blackheart pigmentation visible (Chapter 2).

After 36 h incubation, tubers stored at 37°C had significantly more Blackheart than other temperatures (1 tailed z test, $p<0.00$) and after 48 h, tubers stored at 29.5°C also developed the disorder. Higher temperatures appeared to increase Blackheart incidence rates, for example only 12.5% of tubers had Blackheart after 36 h of 4°C and anoxia, compared to 100% of tubers with Blackheart if stored at 37°C with anoxia. Similarly, tubers that were stored under anoxia at 4°C, significantly increased in Blackheart incidence between 36-48 h (1 tailed z test, $p = 0.049$), indicating that incubation time increases Blackheart incidence (Table 3.2).

Gaseous diffusion does not appear to affect Blackheart incidence and no significant difference was found in Blackheart incidence between tubers stored for 36 h with reduced gaseous diffusion at 37°C versus aerated tubers incubated at 37°C (2 tailed z test, p =0.326). Additionally, CO_2 accumulation does not appear to increase Blackheart incidence; tubers stored at 4°C, under anoxia versus those with 1.5 g of KOH to scrub CO_2 had no significant difference in Blackheart after 48 hours (Table 3.2) (2 tailed z test, p =0.71). Additionally, there was no difference in Blackheart susceptibility in tubers that had the evolved ethylene removed (data not shown).

Table 3.2: Effect of storage conditions and length on Blackheart incidence. Percentages represent the presence of Blackheart in King Edward tubers stored at 4 °C for a minimum of 3 months unless otherwise stated (n=16). Tubers were either: loosely wrapped in clingfilm to reduce gaseous diffusion at the tuber surface; anoxia applied by vacuum packing and sealing in an airtight bag; stored with KOH to remove evolved CO_2. "-" indicates Blackheart incidence was unable to be measured due to complete necrosis or development of other disorder

	Tubers with Blackheart present (%)			
	Induction duration			
Induction conditions	**24 h**	**36 h**	**48 h**	**30 days**
2 °C	0%	0%	0%	0%
4 °C	0%	0%	0%	0%
22 °C	0%	0%	0%	0%
29.5°C	0%	0%	18.8%	-
37°C	0%	12.5%	25%	-
4 °C + reduced gaseous diffusion at tuber surface	0%	0%	0%	0%
37 °C + reduced gaseous diffusion at tuber surface	0%	12.5%	18.8%	-
4 °C + anoxia	0%	12.5%	37.5%	-
37 °C + anoxia	100%	100%	-	-
4 °C + anoxia + removal of evolved CO_2	0%	12.5%	31.3%	-
37 °C + anoxia + removal of evolved CO_2	100%	100%	-	-
37 °C + anoxia. After 1 month of 4 °C storage	0%	0%	-	-
37 °C + anoxia. After 2 months of 4 °C storage	0%	0%	-	-
37 °C + anoxia. After 3 months of 4 °C storage	100%	100%	-	-

3.2.2 Developing a Blackheart Induction Method and Blackheart Characterisation

King Edward tubers, stored at 4°C for at least three months after harvest, were incubated at 37°C under anoxic conditions for up to 32 h. Tubers were then removed from the Blackheart induction conditions, left for 12 h for pigmentation to develop and imaged (Figures 3.2 & 3.2). These images were then used to calculate the average percentage area of Blackheart affected tissue (Chapter 2) (Figure 3.3).

Blackheart occurred in King Edward tubers after 12 h of Blackheart induction conditions before spreading in area over time (Figures 3.1 & 3.3). Heat damage appeared in tubers incubated under Blackheart induction conditions for longer than 30 h, resulting in a large amount of variation and potential miscalculation of Blackheart affected areas due to the inclusion of other necrotic tissue in the measurements (Figure 3.3).

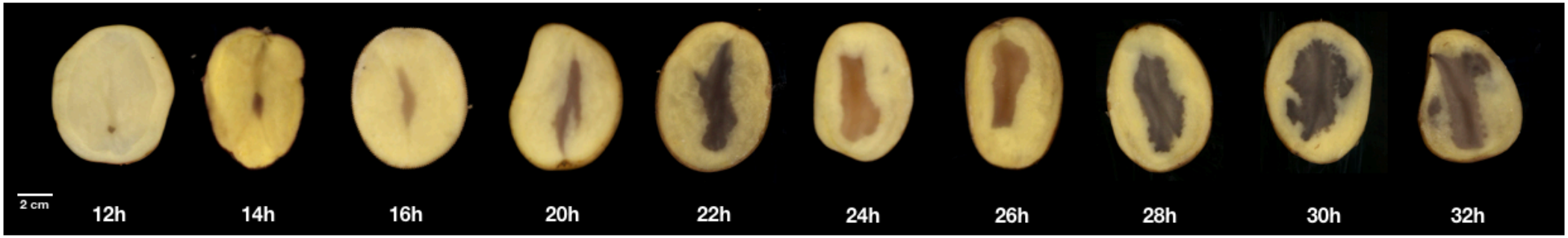


Figure 3.1: Tubers of the cultivar King Edward were incubated under Blackheart induction conditions (anoxia, 37°C) for the times indicated. Tubers were then incubated for 12 h at 22°C before cutting in half longitudinally and imaging Blackheart visible at the cut surface.

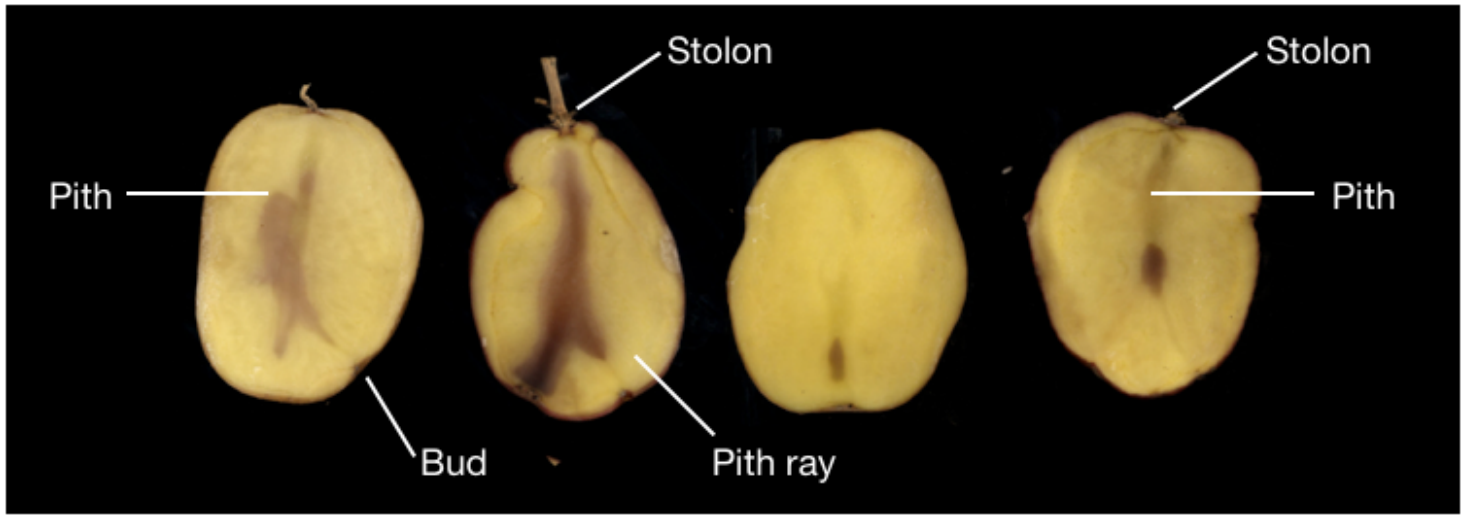


Figure 3.2: Characterisation of Blackheart demonstrating the single origin of the disorder and non-centric spread of affected tissue throughout the pith and pith rays to the peridermal buds. Tubers of the cultivar King Edward were incubated under Blackheart induction conditions (anoxia, 37°C) for 14 h. Tubers were then incubated for 12 h at 22°C before cutting in half longitudinally and imaging Blackheart visible at the cut surface.

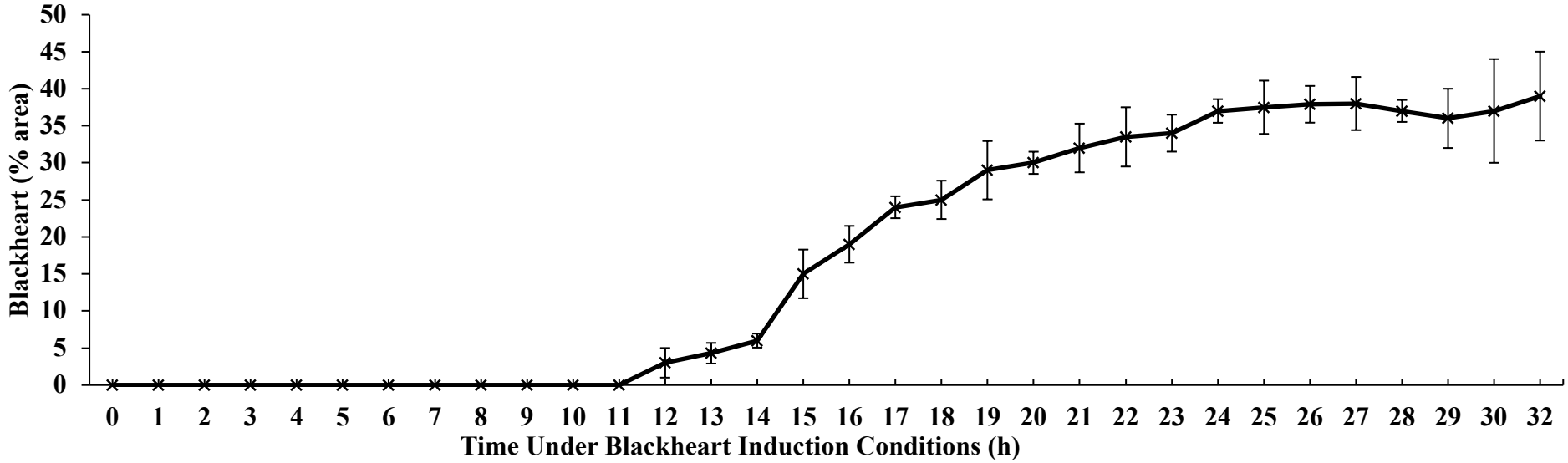


Figure 3.3: Quantitative development of Blackheart with time. Tubers of the cultivar King Edward were incubated under Blackheart induction conditions (anoxia, 37°C) for the times indicated. The tubers were then incubated for 12 h at 22°C before cutting in half longitudinally and

imaging Blackheart visible at the cut surface. Blackheart was quantified as the percentage of the total cut surface area that had black pigmentation (see Chapter 2). Error bars ± standard deviation, n=6.

3.2.3 Blackheart Characterisation and Non-Destructive Imaging

King Edward tubers incubated under Blackheart induction conditions were imaged by using proton MRI (Chapter 2). The resulting images clearly show the different tissue types within tubers, with the pith tissue spreading from the stolon, through the parenchyma and cortex, to the peripheral buds on the periderm (Figure 3.4). Variations within Blackheart affected, and Blackheart unaffected tubers are visible (Figure 3.4).

T1 represents the time taken for an excited proton to realign with the external magnetic field and therefore is often used as a measure of water movement (Ratcliffe, 1994; Van As, 2006). T1 weighted images show changes in the T1 of a pith of a single tuber under Blackheart induction conditions and fewer changes occurring in the cortex (Figures 3.4, 3.5 & 3.6). Blackheart appears to originate from a single region in the pith tissue, spreading into surrounding parenchymal tissue over time (Figures 3.4 3.5 & 3.6). Graphical representations of the T1 changes (as represented pictorially in Figure 3.5) indicate that, during Blackheart induction conditions, the median cortex and parenchyma T1 values remain consistent (between 2.8-2.9) and few changes are observed (Figure 3.7). However, in the pith tissues, the median T1 value increases by approximately 0.3 units between 8 h-11 h of Blackheart induction conditions (Figure 3.7) whereas the visible onset of Blackheart occurs at 12 h.

ADC is a measure of the ability of water molecules to diffuse (Van as, 2007). The ADC increases in the pith tissue from approximately 2.5E-7 mm/s^2 to 3.4E-7 mm/s^2

(+ 0.74E-7 mm/s^2 between 8-17 h) during incubation under Blackheart induction conditions. The ADC of the parenchyma and cortex combined increases from 2.7E-7 mm/s^2 to 3.15E-7 mm/s^2 (+ 0.36E-7 mm/s^2), however this change occurs 4 h later than in the pith (Figure 3.8).

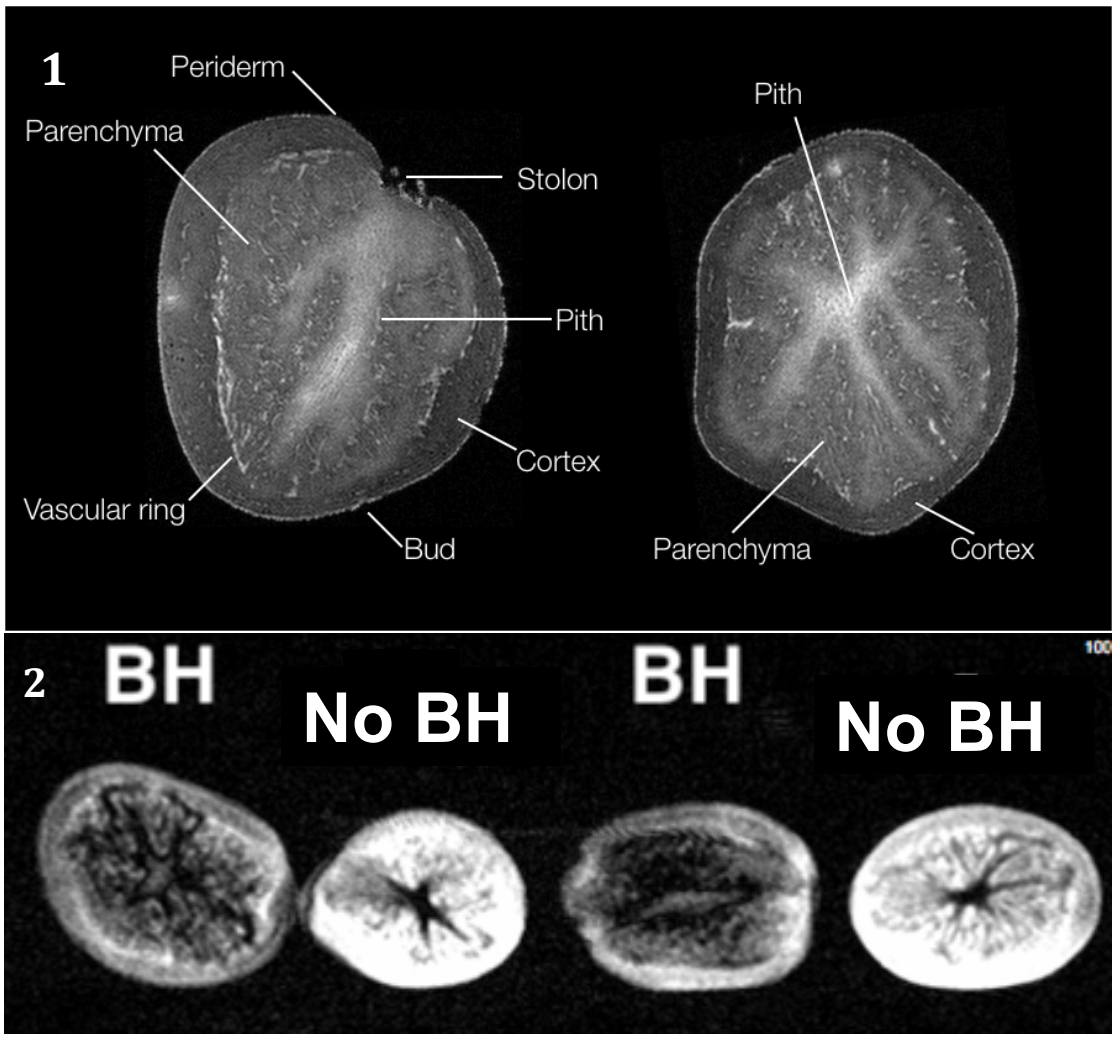


Figure 3.4: Anatomy of tubers with and without Blackheart, all T1 weighted images from a 7 T preclinical MRI system. Annotated transverse (1, right) and longitudinal (1, left) cross sections of a King Edward tuber prior to Blackheart induction. Then,

two King Edward tubers after 12 h of Blackheart induction conditions (2, “BH”) and two control tubers (no Blackheart induction conditions, “No BH”).

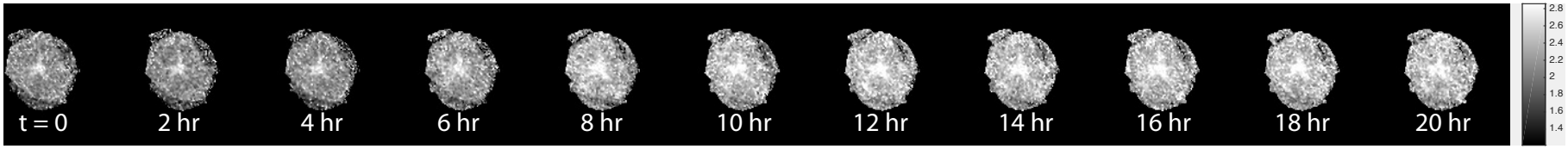


Figure 3.5: T1 weighted images of a King Edward tuber taken during incubation under Blackheart induction conditions for 0 h-20 h.

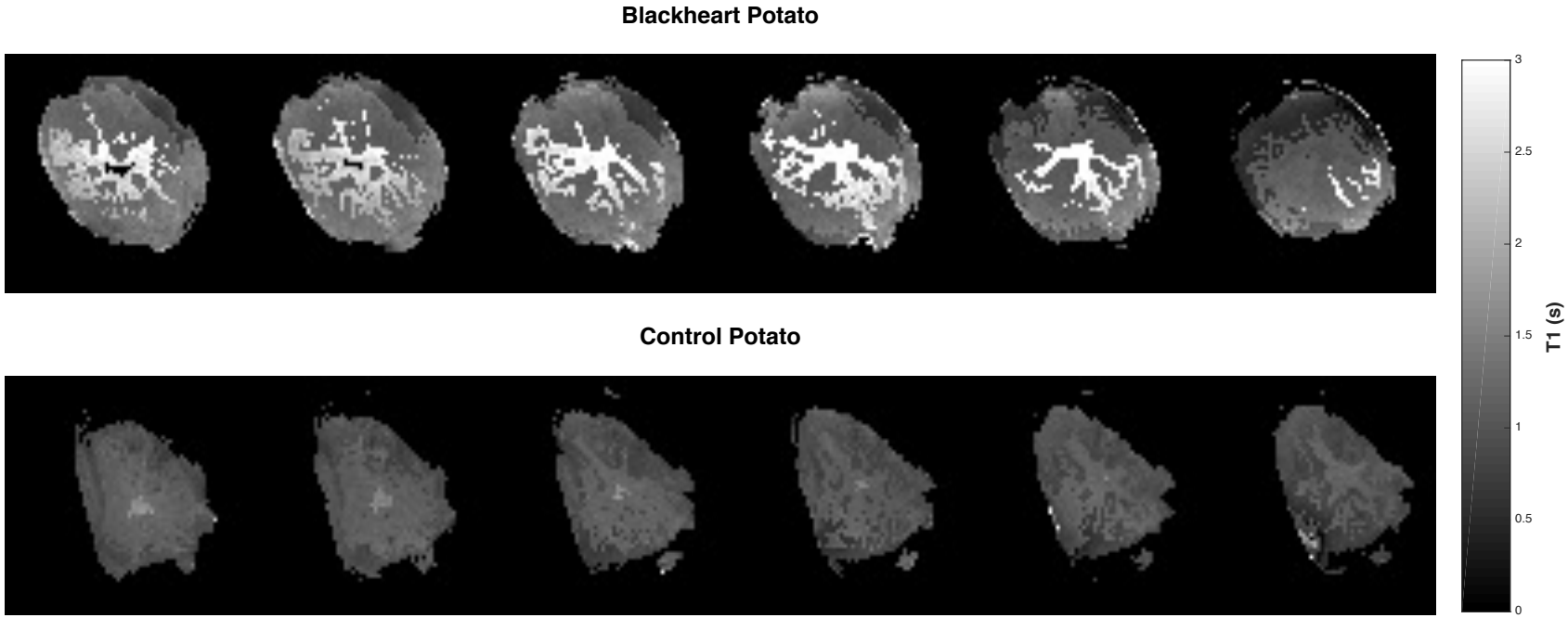


Figure 3.6: Mapped T1 values in transverse MRI slices of a King Edward tuber incubated under Blackheart induction conditions for 12 h ("Blackheart Potato" and prior to induction of Blackheart ('Control Potato')

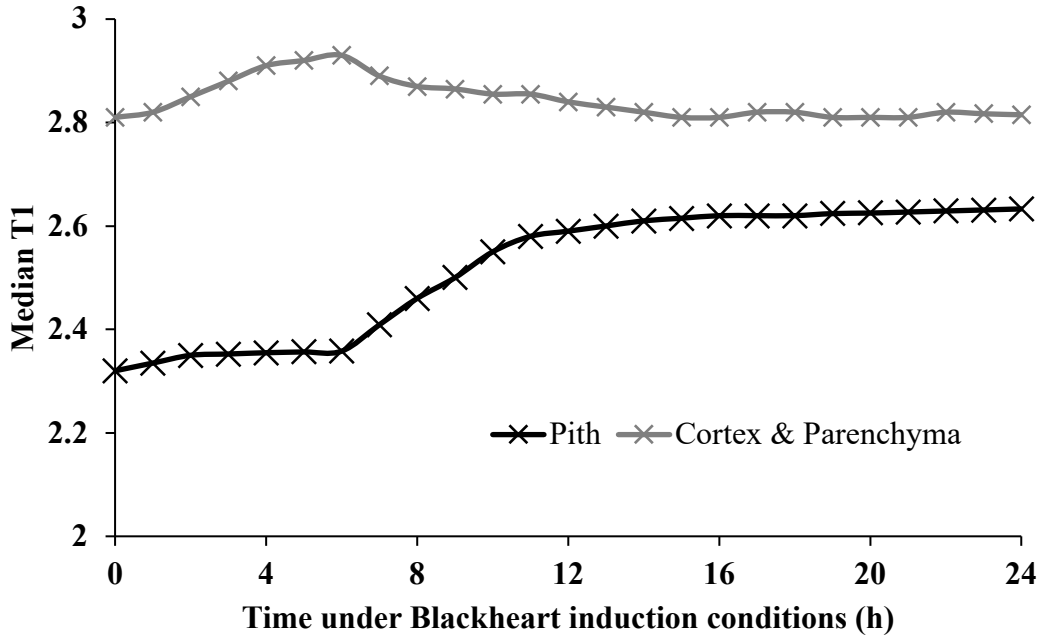


Figure 3.7: Changes to the T1 of King Edward tuber tissues during incubation of a single tuber under Blackheart induction conditions (n=1)

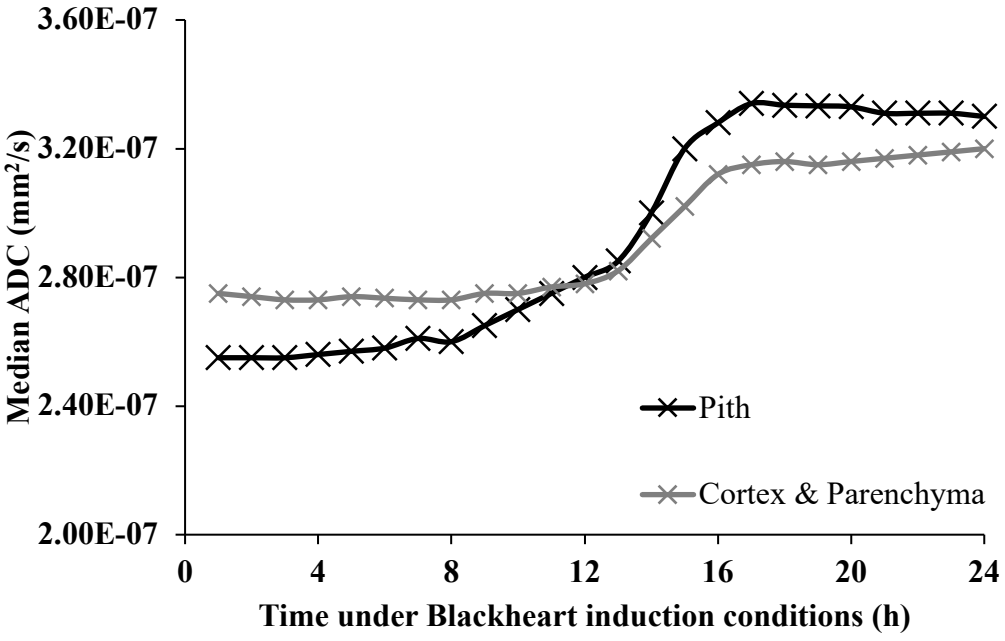


Figure 3.8: ADC in King Edward tuber tissues during incubation of a single tuber under Blackheart induction conditions.

3.2.4 Varietal Variations in Blackheart Susceptibilities

The Blackheart susceptibility of eight current commercial UK potato varieties (Chapter 2), stored under long term storage conditions (4°C) was measured throughout 2014 (Figure 3.9). Varietal susceptibility was inferred by observing both the extent of Blackheart (a high percentage area of affected tissue), and the time of onset of Blackheart (how long tubers need to be stored under Blackheart induction conditions before they develop the disorder). N.B. Due to commercial sensitivity, some names have been replaced with code names (A-F). Maris Piper and B both display low extent of Blackheart and late onset of the disorder; both Maris Piper and B only develop Blackheart after 24 h of Blackheart induction conditions (Figures 3.9, 3.10 & 3.11). Alternatively, D, King Edward, A and E all show rapid onset, and greater extent of Blackheart affected tissues; Blackheart can be observed in both D and E tubers after 8 h of induction conditions (Figure 3.10), and the area of affected tissue in one D tuber was as high as 78% (Figure 3.11).

All varieties increase in Blackheart susceptibility over time, as seen by the increasing percentage area of affected tuber tissues (Figures 3.9, 3.10 & 3.11). The relative susceptibilities between varieties do not appear to vary; for example, King Edward remains one of the most susceptible varieties, and Maris Piper one of the least susceptible after both three, six and nine months of long term storage (Figures 3.9, 3.10 & 3.11).

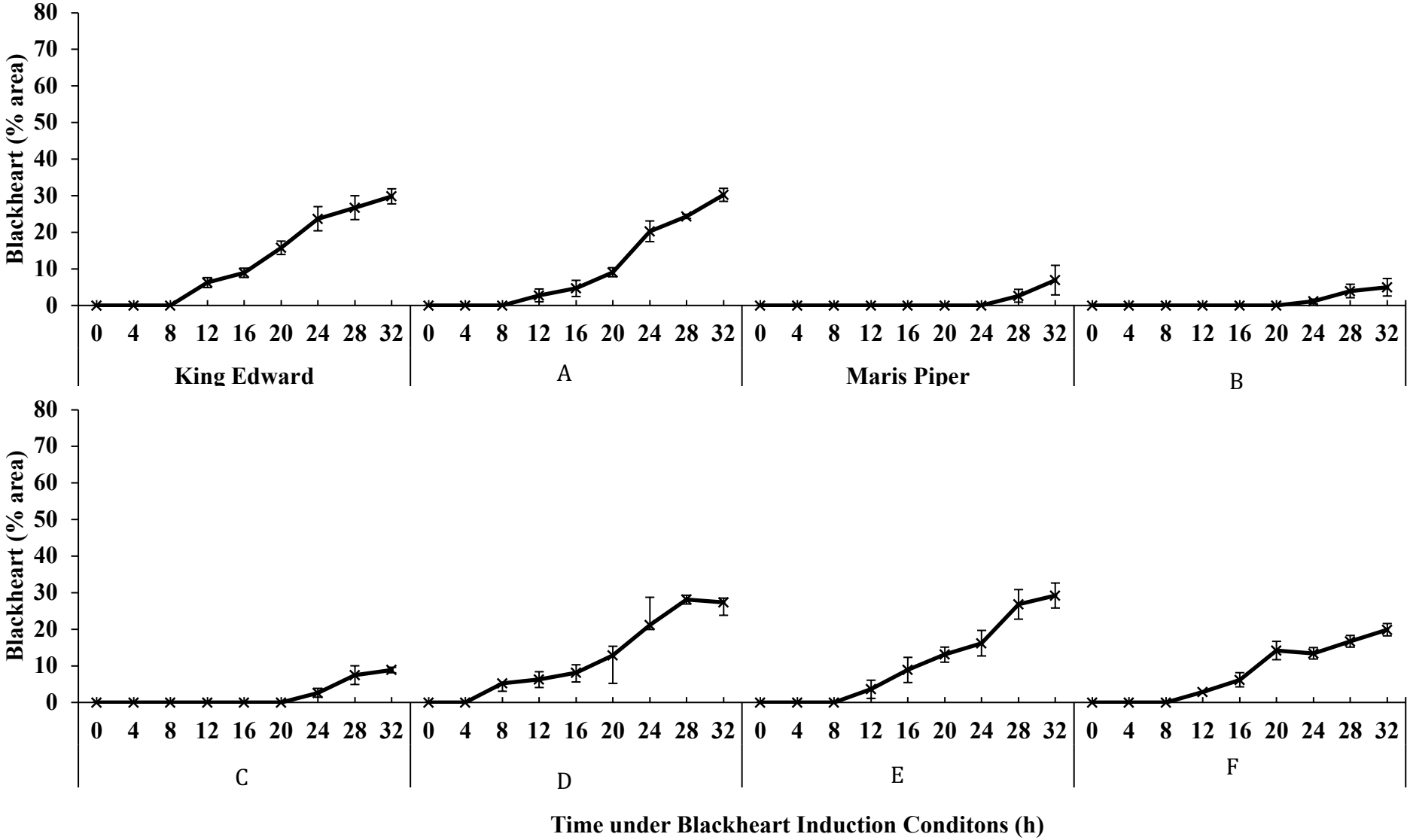


Figure 3.9: Varietal differences of Blackheart susceptibility in tubers stored for three months at 4°C prior to Blackheart induction conditions (Anoxia, 37°C) for 0-32 h. A-F represent UK tuber varieties obscured due to commercial sensitivity. Error bars ± standard deviations, n>5.

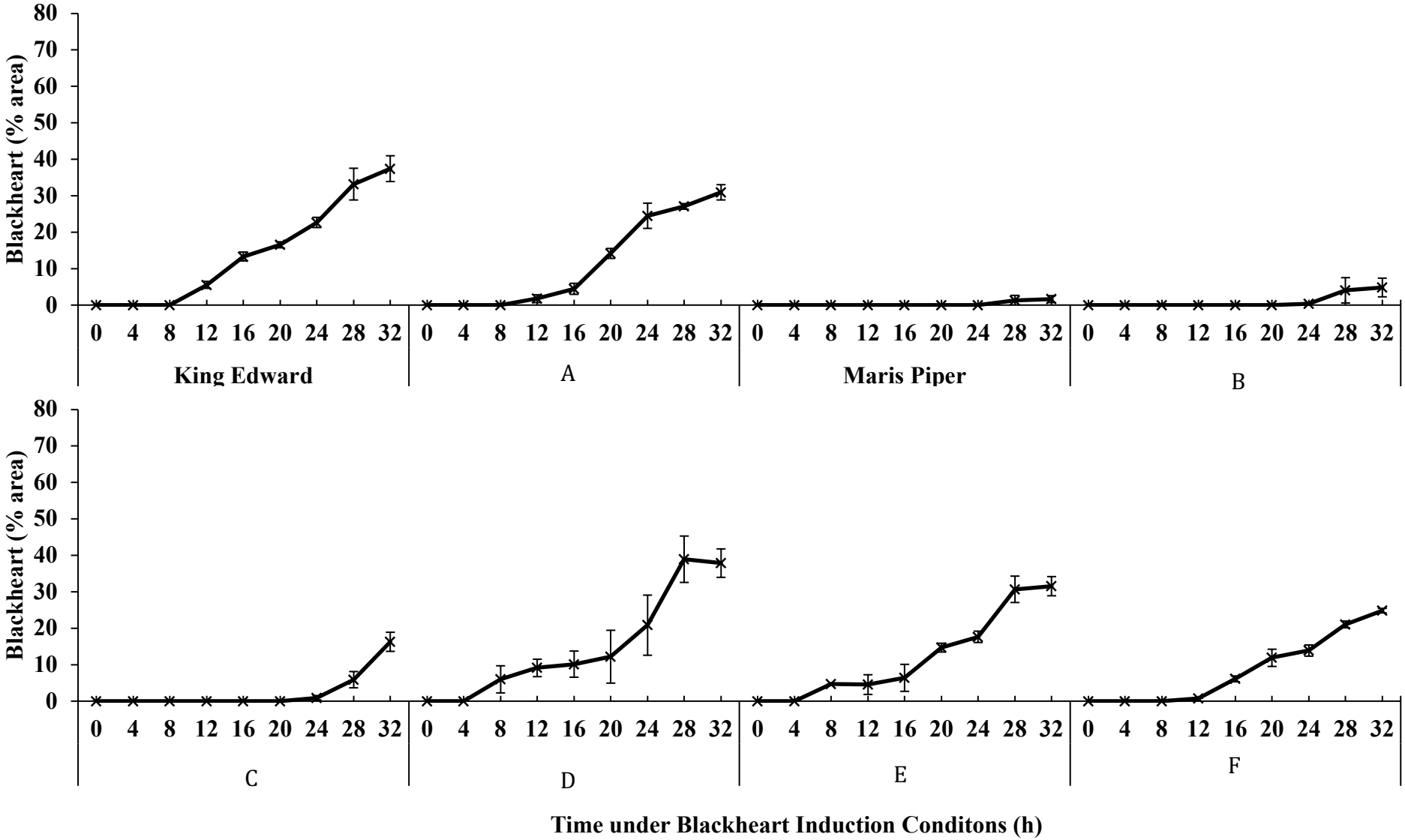


Figure 3.10: Varietal differences of Blackheart susceptibility in tubers stored for six months at 4°C prior to Blackheart induction conditions (Anoxia, 37°C) for 0-32 h. A-F represent UK tuber varieties obscured due to commercial sensitivity. Error bars ± standard deviations, n>4.

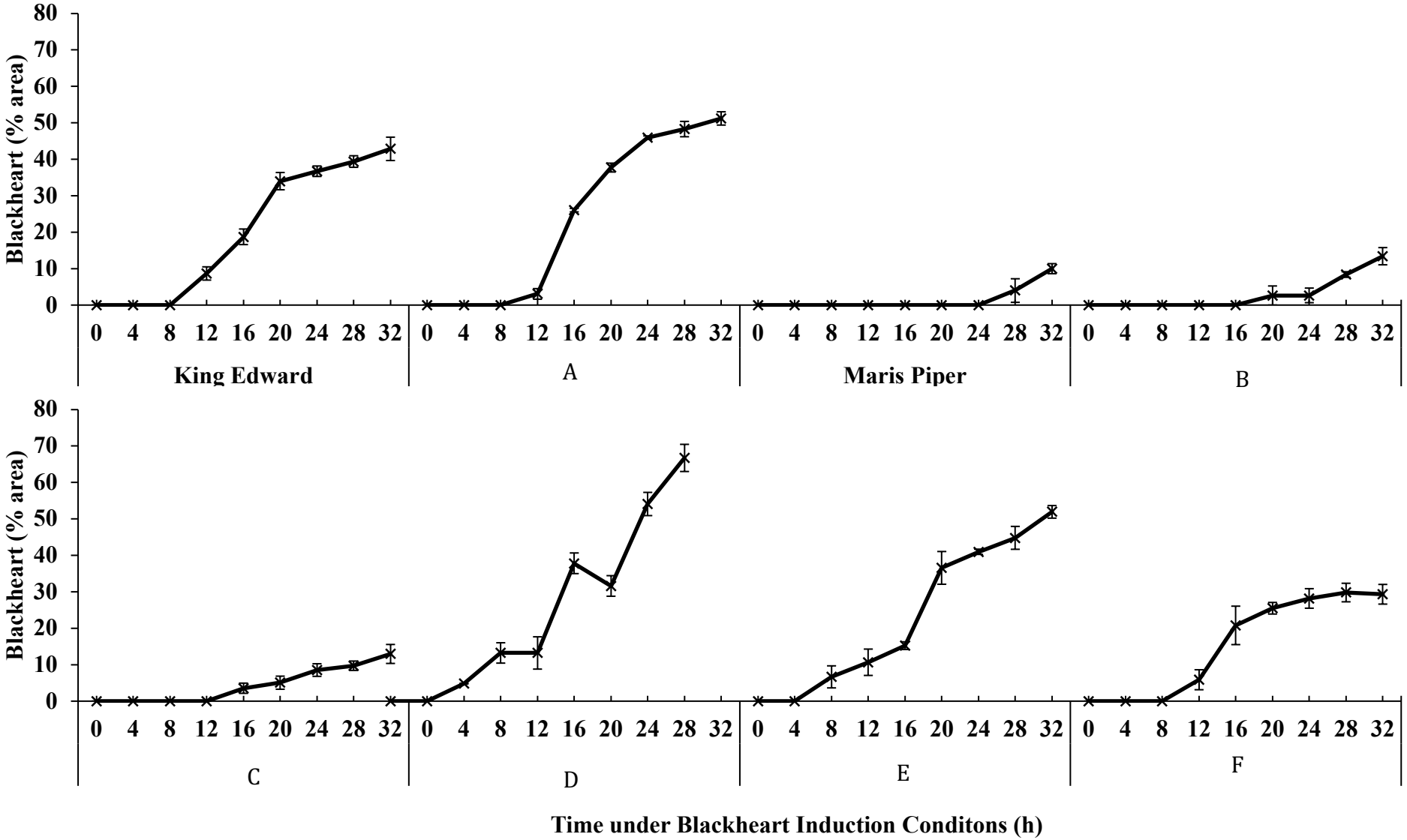


Figure 3.11: Varietal differences of Blackheart susceptibility in tubers stored for nine months at 4°C prior to Blackheart induction conditions (Anoxia, 37°C) for 0-32 h. A-F represent UK tuber varieties obscured due to commercial sensitivity. Error bars ± standard deviations, n=6

3.2.5 Annual Variations in Blackheart Susceptibilities

Annual field trials (Chapter 2) provided four harvests over the course of this DPhil project. Blackheart was induced in tubers every three months after each harvest, resulting in 12 Blackheart induction trials for each variety. Comparing induction trials within a variety between years indicated annual variations in Blackheart susceptibility (Figures 3.12, 3.13, 3.14 & 3.15); for example, King Edward tubers from 2016 showed larger areas of Blackheart affected tissue as compared to the year before and after (Figure 3.12). Variations were consistent across all varieties; for example, Blackheart susceptibility was also higher in Maris Piper (Figure 3.14), A (Figure 3.13) and B (Figure 3.15) varieties in 2016.

Relative susceptibilities between the varieties did not appear to change annually; Maris Piper and B remained the more resistant varieties to Blackheart (Figures 3.14 & 3.15) and King Edward and A remain highly susceptible in each year (Figures 3.12 & 3.13).

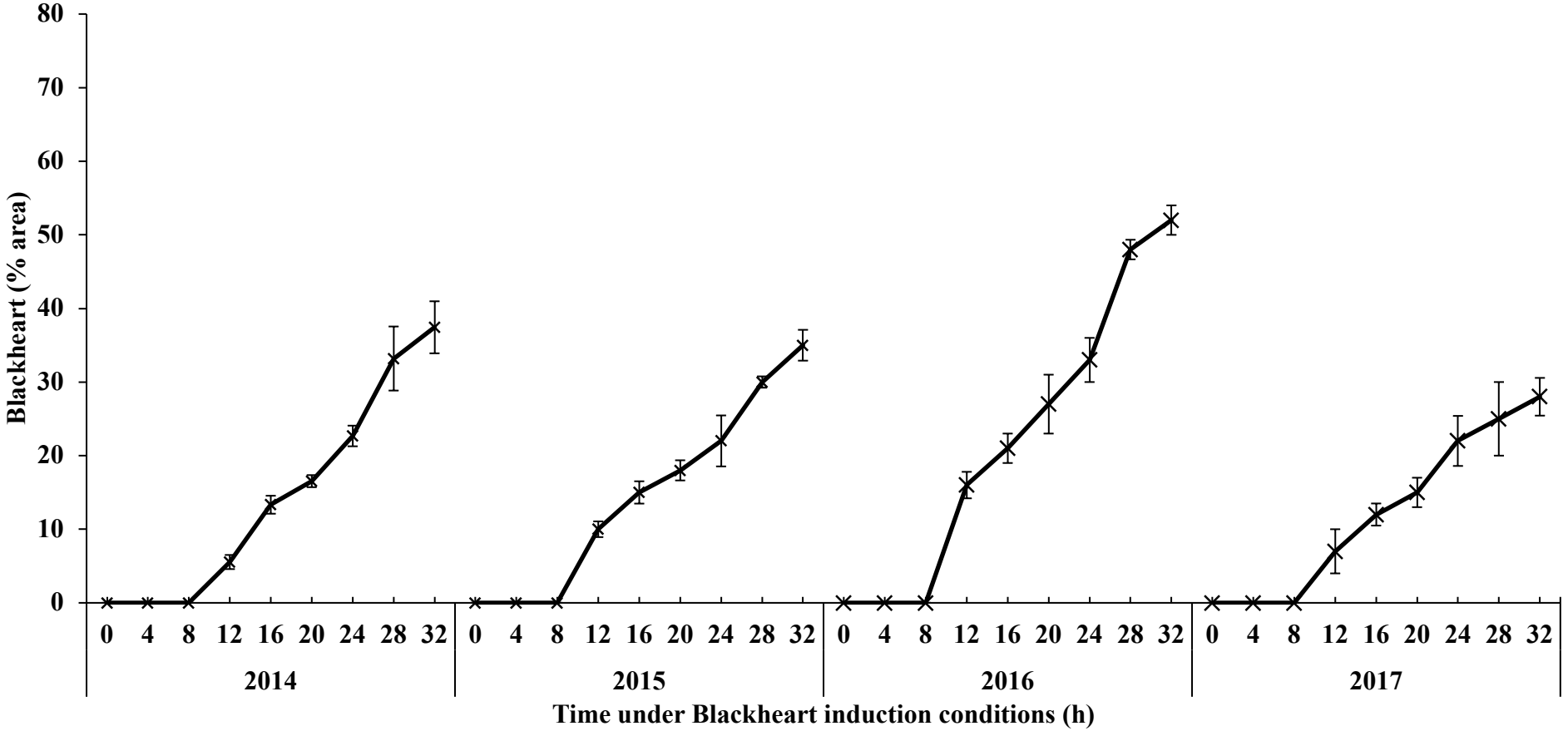


Figure 3.12: Annual differences in Blackheart susceptibility in King Edward tubers stored for six months at 4°C prior to incubation under Blackheart induction conditions (Anoxia, 37°C) for 0-32 h. Error bars ± standard deviations , n=6

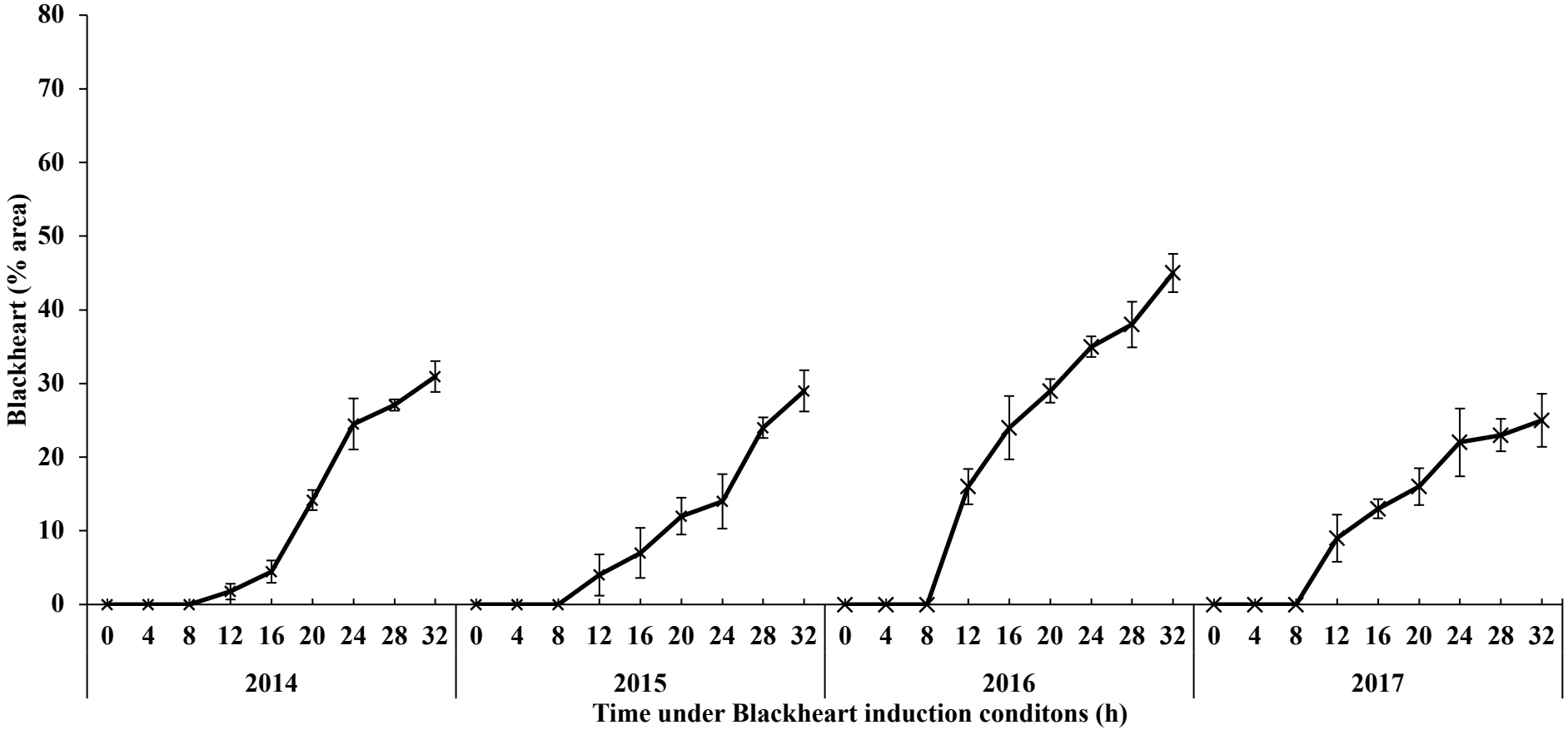


Figure 3.13: Annual differences in Blackheart susceptibility in "A" tubers stored for six months at 4°C prior to incubation under Blackheart induction conditions (Anoxia, 37°C) for 0-32 h. Error bars represent ± standard deviation from the mean, n=6. Variety name obscured due to commercial sensitivity.

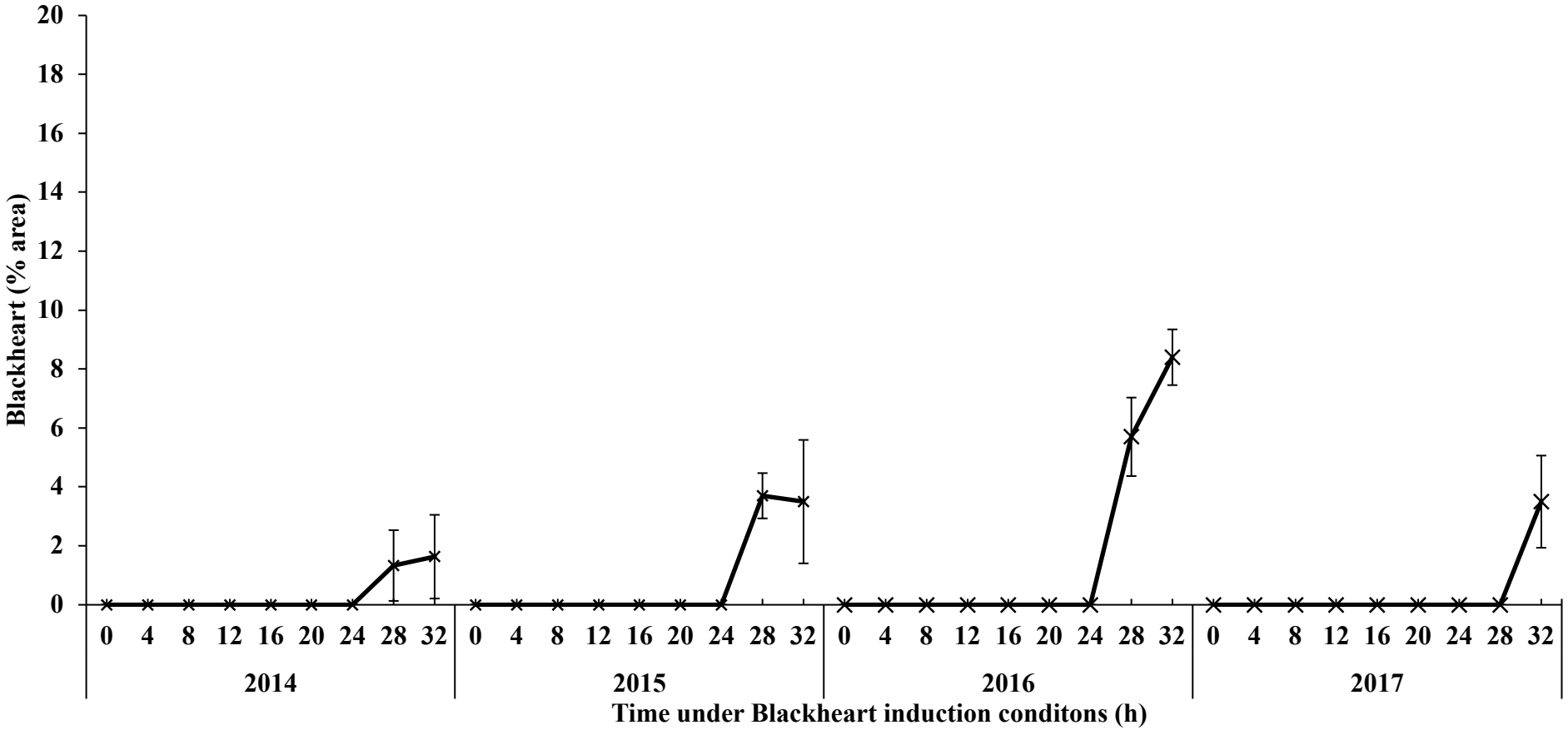


Figure 3.14: Annual differences in Blackheart susceptibility in Maris Piper tubers stored for six months at 4°C prior to incubation under Blackheart induction conditions (Anoxia, 37°C) for 0-32 h. Error bars represent ± standard deviation from the mean, n=6

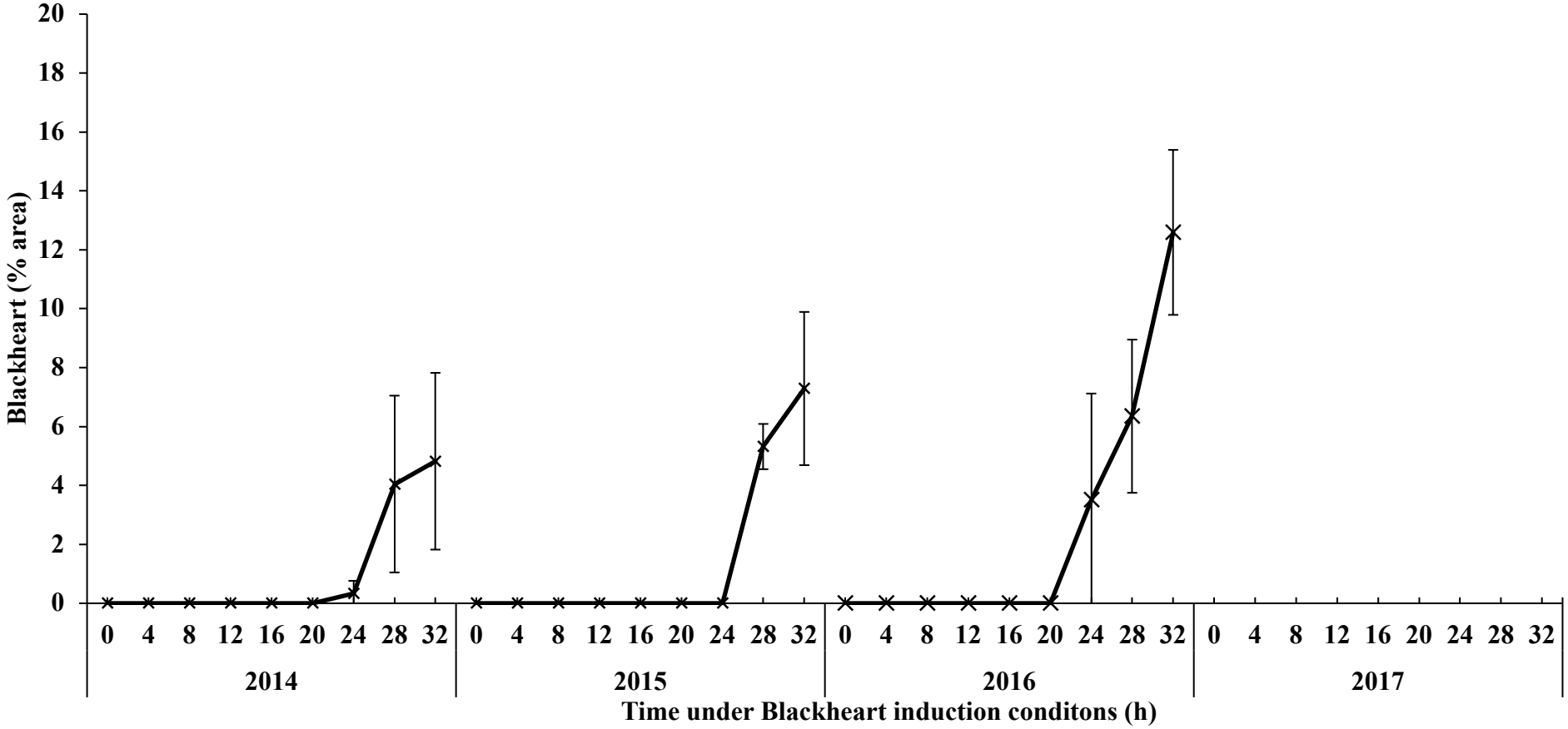


Figure 3.15: Annual differences in Blackheart susceptibility in "E" tubers stored for six months at 4°C prior to incubation under Blackheart induction conditions (Anoxia, 37°C) for 0-32 h. No measurements were made in 2017.Error bars represent ± standard deviation from the mean, n=6. Variety name obscured due to commercial sensitivity.

3.2.6 Effect of Industrial Factors on Blackheart Susceptibility

There was no variation on the development of Blackheart by tuber size (Figure 3.16); tubers were graded prior to the induction of Blackheart into: “Small”, measuring 5 cm width by 5 cm length; “Medium”, measuring 6.5 cm width by 7.5 cm length, as used as the standard size throughout this thesis (Chapter 2); or “Large”; 10 cm width by 12 cm length (all ± 0.5 cm).

Tubers were washed via submergence (Chapter 2), showering (avoiding total submergence) or left unwashed, were stored under Blackheart induction conditions. There was no variation in the development of Blackheart between washing type or no washing indicating the development of Blackheart was unaffected by these conditions (Figure 3.17). However, tubers washed via submergence did become significantly heavier (t test, $p = 0.03$) after washing and drying (Supplementary data) indicating the uptake of water.

Potato plants were defoliated in the field either by chemical defoliation, using two applications of carfentrazone-ethyl, or manual removal of the plant haulm. There was no apparent variation on the development of Blackheart in tubers with the different defoliation treatments (Figure 3.18). Additionally, neither irrigation nor duration of skin set (the length of time mature tubers remain in field) appeared to have an effect on Blackheart (data not shown).

However, the storage temperature of the long term "cold store" had a significant effect on Blackheart susceptibilities in all tuber varieties measured (Figure 3.19). Tubers stored at 2°C developed Blackheart earlier than those stored at 4°C; this was particularly apparent in the resistant varieties, where Maris Piper tubers developed Blackheart after 24 h if stored at 2°C. The extent of Blackheart was significantly lower in tubers stored at 4°C in all varieties (ANOVA, $F=4.2$, $p<0.024$).

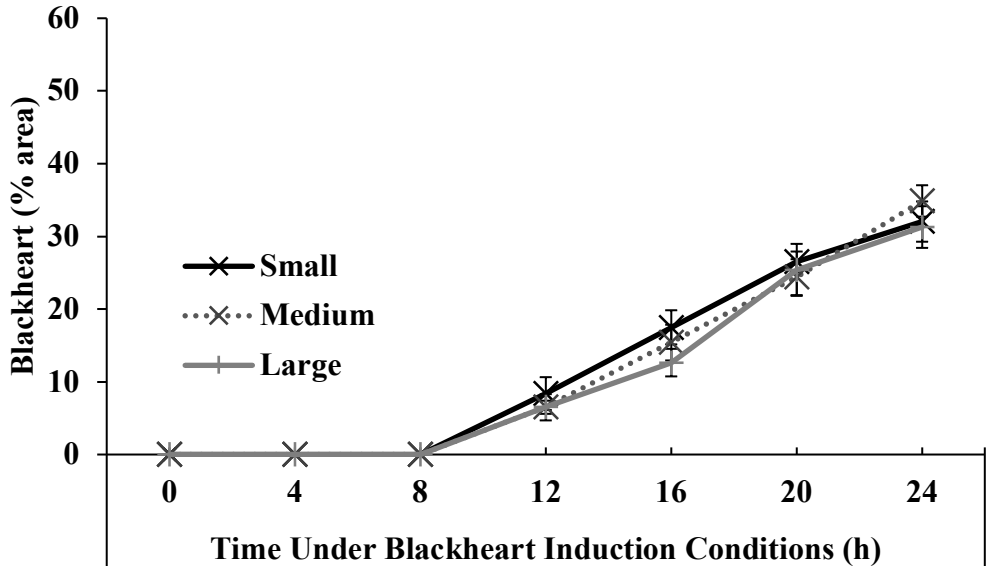


Figure 3.16: Effect of tuber size (5 cm width x 5 cm length "small"; 6.5 cm width x 7.5 cm length "medium"; 10 cm width x 12 cm length "large") on Blackheart in King Edward tubers stored for 3 months at 4°C. Error bars ± standard deviation, n=6.

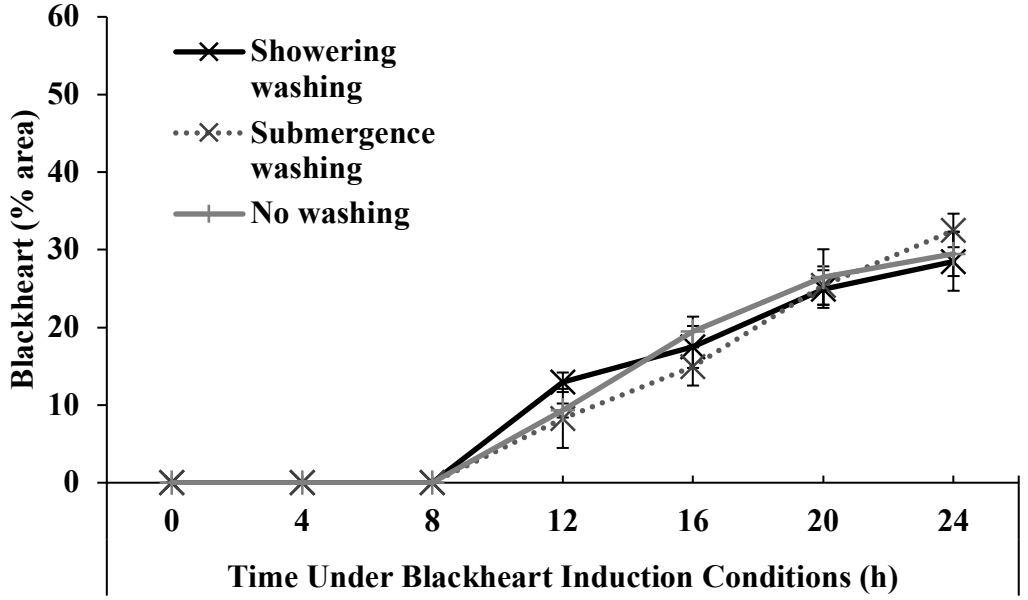


Figure 3.17: Effect of tuber washing treatment (no washing, submergence washing, showering) on Blackheart in King Edward tubers stored for 3 months at 4°C. Error bars ± standard deviation, n=5.

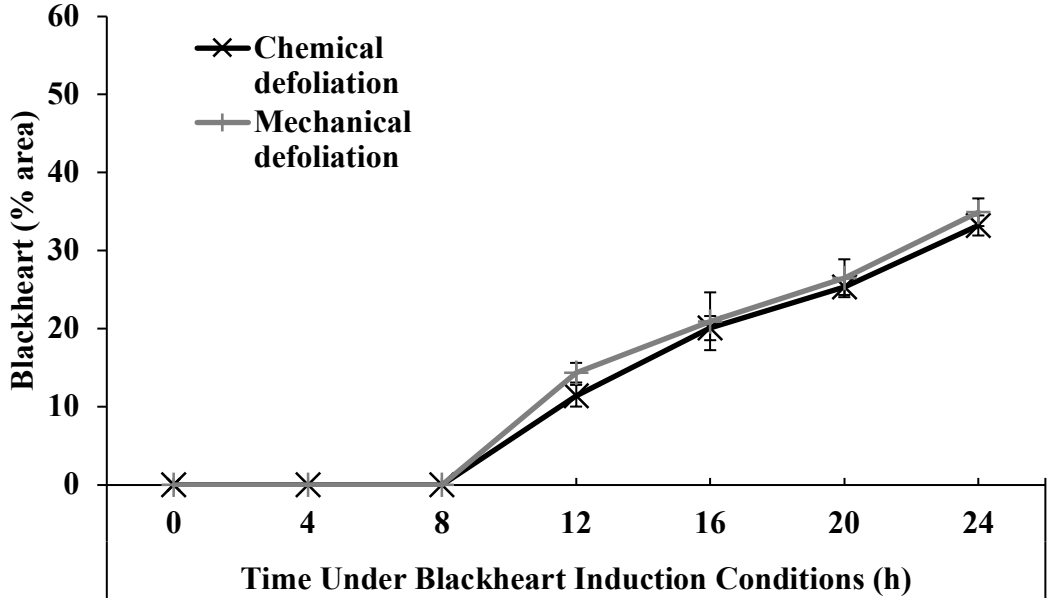


Figure 3.18: Effect of defoliation method (chemical defoliation or manual removal) on Blackheart in King Edward tubers stored at 4°C for 9 months. Error bars ± standard deviation, n=6.

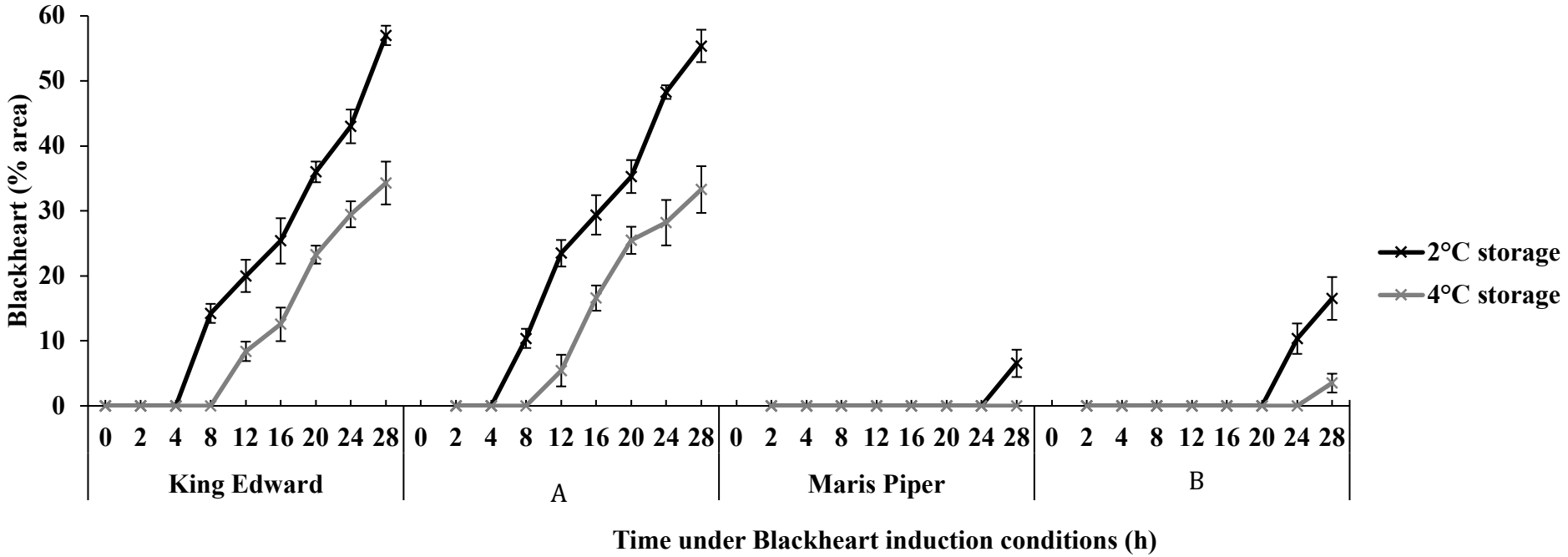


Figure 3.19: Effect of storage temperature (2°C versus 4°C) after 7 months on the development of Blackheart in different tuber varieties incubated under Blackheart induction conditions. Error bars represent standard deviation, n=8. A and B represent UK tuber varieties obsucred due to commercial sensitivity.

3.3 Discussion

3.3.1 There are Multiple Conditions that are Sufficient in Inducing Blackheart

As Blackheart was found in tubers stored at both 37 °C and 4°C (Table 3.2), it appears that high temperature is sufficient, but not necessary to induce Blackheart, despite previous literature (Bartholomew, 1913; Stewart & Mix, 1917; Davis, 1926; Briddon, 2015). The proportion of Blackheart affected tubers is positively correlated with high temperature induction conditions, for example an additional 12 h is required for Blackheart to develop in tubers under anoxia and at 4°C, versus tubers incubated under anoxia and 37°C (Table 3.2). Therefore, high induction temperatures appear to increase the propensity of tubers to develop Blackheart, but high temperatures alone are not essential requirements for the disorder to develop.

Similarly, anoxia also appears to increase Blackheart susceptibilities of tubers. All King Edward tubers incubated under anoxia at 37°C developed Blackheart in only 24 h, whereas no Blackheart was identified in tubers incubated for the same time at 37°C alone (Table 3.2). However, although anoxia is sufficient for Blackheart to develop, it is not a necessary condition as Blackheart is still observed in tubers stored in well-ventilated conditions if the temperature is high (Table 3.2).

CO_2 accumulation does not appear to affect Blackheart incidence; tubers stored at 4°C, under anoxia, and with 1.5 g of KOH acting as a CO_2 scrubber, having no significant difference in Blackheart incidence after 48 h (Table 3.2).

The longer tubers are stored under induction conditions, the higher the incidence of Blackheart. For example, tubers that are stored under anoxia at 4°C, significantly increase in Blackheart incidence over 12 h. However, it appears that tubers need to be stored for a minimum of three months before Blackheart can develop. Therefore, from these results (Table 3.2), storage length at 4°C longer than three months appears to be the only necessary condition for Blackheart to develop; this is correlated by the low number of complaints and Blackheart incidence in industry prior to Christmas (David Wright, Manor Fresh Ltd., pers. comm., 2014; Potato Research Council, 2016). It is not clear why tubers stored for less than three months/younger tubers are resistant to Blackheart.

Aside from tuber age, there are no other necessary conditions, and many sufficient conditions, for Blackheart to develop. The number of factors that affect Blackheart development indicates that multiple conditions, rather than a single cause, influence Blackheart.

Combining both high temperature (37°C) and anoxia results in the fastest induction and highest incidence of Blackheart in King Edward tubers, which is in line with many published methods of Blackheart induction and the hypothesis that Blackheart is caused by increased respiration (Bartholomew, 1913; Stewart & Mix, 1917; Davis, 1926; Briddon, 2015). As speed of induction was an important component of an optimal induction condition, tubers (stored for at least 3 months, Table 3.2) were incubated at 37°C and anoxia for 0-32 h to test these conditions as a Blackheart induction method (Figure 3.1). Tubers were then removed from the Blackheart

induction conditions, left for 12 h for pigmentation to develop and imaged (Chapter 2) (Figures 3.1 & 3.2). These images were then used to calculate the average percentage area of Blackheart affected tissue (Chapter 2) (Figure 3.3).

Heat damage appeared present in tubers induced for longer than 30 h, driving high variation due to the inclusion of other necrotic tissue in the image analysis measurements (Chapter 2). Therefore, only tubers induced for up to 24 h were used in future biochemical studies to avoid heat necrosis.

This induction method was able to produce Blackheart in a time-dependent manner where the disorder spread in percentage area with time. These conditions were able to to reliably induce Blackheart in all King Edward tubers after 12 h, and the low standard deviations around the mean percentage area of Blackheart quantified at each time point (12 h onwards, Figure 3.3) indicated that incubation at 37°C with anoxia resulted in a coordinated and reliable induction of Blackheart (Figure 3.3).

3.3.2 Blackheart Characterisations

In all tuber varieties Blackheart originated in the pith tissue in a single location (Figures 3.1 & 3.2), which was confirmed by non-destructive imaging of a King Edward tuber during Blackheart induction (Figures 3.5 & 3.6). This point of origin of Blackheart was not correlated with the distance from the tuber stolon nor the centre of the tuber; Blackheart affected tissue even extended into the pith rays and out towards the buds before spreading into the surrounding parenchyma tissue (Figures 3.1 & 3.2). The region of pigmented tissue always had a defined edge and was never diffuse

(Figures 3.1 & 3.2). Blackheart was never found in the cortex tissue, and the spread of the disorder over time was maintained within the vascular ring, except for the spread of Blackheart through the pith rays (Figures 3.1 & 3.2).

Blackheart affected tissue was largely firm to the touch and cavities in affected tissues were rarely found, except in tubers with very advanced Blackheart, as has previously been recorded (Kiaitsi, 2015; Briddon, 2015). Blackheart pigmentation was only present after tubers had been re-aerated and varied in colour from pink, brown, inky blue or dark black (Figures 3.1 & 3.2). The disorder was never visible externally and affected tubers were indistinguishable from unaffected potatoes.

Non-destructive imaging indicated that Blackheart affected tissue was structurally different from unaffected tissue (Figures 3.7 & 3.8); changes in ADC indicate that water is less freely diffusible in the pith tissue prior to the induction of Blackheart, when compared to the cortex and parenchyma combined however, the pith tissue displays the greatest ADC increase during incubation under Blackheart induction conditions (Figure 3.8). These changes in the ADC (Figure 3.8) and T1 weighting (Figure 3.7) appear to indicate that water becomes more freely diffusible in the pith tissue prior to the onset of Blackheart (Figure 3.3). This observation indicates that there are possible changes to pith tissue structural integrity, prior to the onset of Blackheart. These changes are reduced in the parenchyma and cortex (Figures 3.7 & 3.8). Due to the incubation of the tuber in a water jacket, it was difficult to distinguish the periderm of the tuber (Figure 3.5); therefore measurements taken at the edge of the tuber were used and due to the inability to reliably identify the tissue type, it was described as a combination of cortex and parenchyma tissues. However, the

combining of a Blackheart susceptible tissue (parenchyma) and resistant tissue (cortex) will likely mask tissue specific response. Therefore, it is possible that any changes observed to the T1 of the parenchyma and cortex (Figure 3.7) actually represent the parenchyma developing Blackheart, especially as these observations correlate with the later induction of Blackheart in the parenchyma (Figure 3.1).

3.3.3 Annual and Varietal Variations in Blackheart Susceptibility Exist

All varieties appear to increase in Blackheart susceptibility over time (Figures 3.9, 3.10 & 3.11), which correlates with the timing of consumer complaints and incidence in industry stores (Potato Research Council, 2016; Briddon, 2015; Kiaitsi, 2015; David Wright, Manor Fresh Ltd., pers. comm., 2014). However, the relative susceptibilities between varieties do not appear to vary over time, and no varieties switch between low and high susceptibility; for example, King Edward remains one of the most susceptible varieties, and Maris Piper one of the least susceptible after both three, six and nine months of long term storage (Figures 3.9, 3.10 & 3.11). Additionally it appears there are annual variations in the degree of Blackheart susceptibility within each variety (Figures 3.12, 3.13, 3.14 and 3.15) indicating that field conditions may have a potential role in Blackheart incidence.

It appears that different UK varieties have different susceptibilities to Blackheart, as measured by the time of Blackheart onset and the area of Blackheart affected tissue. The most resistant varieties under these induction conditions appear to be Maris Piper and B, with low extent of Blackheart and late onset of the disorder (after 24 h of Blackheart induction conditions) (Figures 3.9, 3.10 & 3.11). The most susceptible

varieties appear to be D, King Edward, A and E (Fig 3.9, 3.10 & 3.11). These findings correlate with industry observations; Maris Piper has previously been indicated to have a low relative susceptibility to Blackheart, and A one of the highest (A. Briddon, Potato Research Council, Pers. Comm.). As the tubers were grown and stored under identical conditions, these observations indicate that there are likely genetic variations that influence Blackheart susceptibility.

There appears to be a correlation between Blackheart susceptibility and tuber age/storage duration in all varieties (Figures 3.9, 3.10 & 3.11) as seen by the increasing percentage area of affected tuber tissue. However, the increase in Blackheart susceptibility appears to be consistent in all varieties as their relative susceptibilities do not appear to change over time; for example, both King Edward and Maris Piper remain as some of the most and least susceptible varieties after both three and nine months of long term storage (Figures 3.9 and 3.11) and both show a consistent 69% ±0.3% increase in Blackheart affected tissue.

Because there are practical limitations to the continued use of eight different varieties, two 'model' varieties were chosen to represent susceptible and resistant responses; for susceptible varieties King Edward was selected and for resistant varieties, Maris Piper. Two additional susceptible and resistant varieties, A and B respectively, were also continued throughout the project due to their similarities in response and for cases where additional comparisons were necessary. These varieties were chosen based on their relative susceptibilities and the low variation in the measurements. Additionally, both Maris Piper and King Edward are ubiquitous in the UK market and two of the most popular varieties consumed (Kiaitsi, 2015; Briddon, 2015) and

therefore their inclusion in this project will ensure industrial applicability. Other varieties were discounted based inconsistency in Blackheart induction: for example, after eight hours of induction conditions, Blackheart was present in only two of the four E tubers sampled (Figure 3.10) and there was variability in the extent of Blackheart in D tubers over time (Figure 3.9).

Alternatively, King Edward tubers showed a consistent onset of Blackheart and the disorder was present in all tubers after 12 h of induction conditions, throughout the year (Figures 3.9, 3.10 & 3.11). The area of Blackheart affected tissue also increased consistently with time under induction conditions. In Maris Piper, no Blackheart was observed before the onset of the disorder after <24 h under Blackheart induction conditions (Figures 3.9, 3.10 & 3.11).

3.3.4 Certain Industrial Practices Appear to Increase Blackheart Susceptibility

Annual variations observed in tubers stored under identical conditions (Figures 3.12, 3.13, 3.14 & 3.15) suggest that storage is not the only factor that influences Blackheart susceptibility. Various factors throughout the industrial food system are thought to influence Blackheart incidence during and after long term storage, however many were found to have no noticeable effect under this experimental method (Figures 3.16, 3.17 & 3.18).

However, storage of tubers at 2°C (versus 4°C) significantly increased Blackheart susceptibility (Figure 3.19), in line with the findings of Briddon (2015). There are multiple reasons why 2°C storage may increase Blackheart susceptibility; firstly, by

elevating tuber respiration rates (Burton, 1989) which have previously been linked to Blackheart (Chapter 1). Similarly, it appears that membrane permeability may be an important aspect of Blackheart (3.2.3) and electrolyte leakage and changes to membrane integrity increases at low temperatures (Spychalla & Desborough, 1990; Malone et al., 2006) which may affect this. Chilling injuries, physiologically similar to Blackheart, can be observed in soft fruit and other vegetables and are usually caused by improper membrane function at low temperatures (Zhou et al., 2014; Zhou et al., 2003). Alternatively, it is possible that the temperature transition, rather than the absolute temperature, affects Blackheart susceptibility, with tubers stored at 2°C experiencing a larger jump when transferred to Blackheart induction conditions (Malone et al., 2006). Additional work is required to explore and investigate this observation further.

3.4 Summary

The work in this chapter provides the first comprehensive and systematic characterisation of Blackheart. It was found that there are many conditions that are sufficient to induce Blackheart in tubers, however the only necessary condition is prior storage at 4°C for three months (although it is unclear if tuber age rather than storage is the significant factor). Blackheart was found to be a tissue dependent disorder, originating from a single point in the pith and spreading throughout the pith and into the parenchyma. Blackheart never appeared in the cortex tissues. Blackheart-affected tissues appear to have increased water movement, which is suggestive increased membrane permeability.

A Blackheart induction method, utilising 37°C and anoxia was used to identify varietal and annual differences, and was shown to be an effective experimental tool in identifying Blackheart susceptibilities demonstrating that there are underlying genotypic factors that affect susceptibility of tubers to Blackheart. Conditions including storing potato tubers at 2°C and the length of storage were identified industry-relevant factors that increase Blackheart susceptibility. However, it appears that there is no single underlying cause for Blackheart, and multiple conditions affect the disorder, which may explain the confusion in the literature surrounding the disorder and the difficulty in preventing or predicting Blackheart.

4 Blackheart Physiology and Biochemistry

4.1 Introduction

This chapter aims to explore and test the prevailing assumptions that are presented in the literature concerning Blackheart, despite the lack of experimental verification. These assumptions represent fundamental aspects of the underlying physiology and biochemistry of the condition. The objectives of the work described in this chapter are: firstly, to test the role of the enzyme PPO and the abundance of its phenolic substrates in Blackheart pigmentation; secondly, to explore the role of cell death and membrane integrity in Blackheart affected tissues; and thirdly, to investigate the link between respiration and Blackheart. The results from these investigations will be used to better understand the biochemical changes occurring in Blackheart and will feed in to the development of a hypothesis on the cause of the disorder.

4.1.1 Blackheart Pigmentation

Blackheart was originally proposed to be caused by tyrosinase activity (Bartholomew, 1913) although no evidential support for this theory was provided. However, the role of tyrosinase enzymes, particularly the Polyphenol Oxidase (PPO) family, in Blackheart development has remained unquestioned and is repeatedly stated as fact throughout the existing Blackheart literature (Bartholomew 1913; Davis 1926; Kiaitsi, 2015).

There are few possible enzymatic candidates that may be involved in Blackheart pigmentation; peroxidase (POD) enzymes are abundant in potato, and display some

polyphenolic oxidation activity (Nokthai et al., 2010), however POD enzyme activity does not correlate with potato browning (Cantos et al., 2002), and PPO is considered the predominant contributor to enzymatic browning in potatoes (Tsouvaltzis & Brecht, 2017). Additionally, there is some supportive evidence for the involvement of PPO in Blackheart; both the cresolase and catchetolase activity of PPO enzymes are oxygen dependent, and whilst characterising Blackheart (Chapter 3) it was shown that tubers needed to be aerated after incubation under Blackheart induction conditions for the pigmentation to develop.

PPO inhibition with high pH (Mosneaguta et al., 2012) or application of cysteine, a competitive inhibitor of PPO (Ali et al., 2015) could be utilised to test the role of PPO in Blackheart. However, application of cysteine could potentially affect the activity of number of metabolic processes and there are practical limitations to how an inhibitor could be applied to tissues throughout a bulky tuber organ prior to Blackheart development. Additionally, given the amyloplastidic localisation of PPO (Czaninski & Catesson, 1974; Partington et al., 1999) and spatial separation from the vacuolar aromatic substrates (Vámos Vigyázó & Haard, 2009; Czaninski & Catesson, 1974), catastrophic changes in cell ultrastructure would be associated with the involvement of PPO. The dramatic changes to cell physiology that would underlie PPO involvement in Blackheart mean that explicitly testing the role of PPO is necessary.

Genetic modification of tubers to supress expression of genes encoding PPO is the most direct strategy to test the involvement of PPO in Blackheart. However, generation of transgenic potato lines is a lengthy procedure and was initially considered to be impractical within the time frame of this D.Phil. project. However,

an American agri-company, J.R.Simplot, have recently developed potatoes with reduced PPO expression as a consequence of gene knockdown using intragenic RNAi, resulting in a bruise-resistant cultivar, approved for growth and sale by the United States Department of Agriculture (Rommens et al., 2006). Experiments exploring the role of PPO in Blackheart development were conducted in collaboration with J.R.Simplot on their GM Innate® tubers; Blackheart was induced in their GM Innate® tubers and the presence or absence of pigmentation recorded, providing information on the involvement of PPO.

4.1.2 J.R. Simplot Innate® Tubers

Innate® tubers were developed by J.R.Simplot to display less bruising due to the knockdown of *Ppo-5*, which encodes a tuber specific PPO enzyme. Additionally, Innate® tubers were developed to produce less acrylamide during cooking due to the additional knockdown of genes that encode asparagine synthase-1 (*Asn1*), phosphorylase-L (*PhL*) and starch associated (*R1*) enzymes. Knockdown of *Asn1* limits the production of asparagine, and *PhL* and *R1* reduce the accumulation of reducing sugars, the precursors to acrylamide. Innate® tubers therefore result in processed products that have more favourable fry colours, fewer bruises and less acrylamide.

The development of the GM Innate® tubers utilised the Innate® technology; Potato derived expression cassettes, promoters and spacers were combined with backbone elements of vector pSIM1278 (Figure 4.1). Both sense and antisense sequences, encoding truncated potato genes were incorporated, when expressed these produced

double stranded RNA transcripts which were subsequently degraded via the Dicer-RISC RNAi pathway, thereby reducing expression. Within the vector backbone was the isopentenyl isomerase (*Ipt*) marker, which conferred overexpression of cytokinin and subsequent stunted phenotypes (Rommens et al., 2004; Rommens et al., 2006; Ye et al., 2013).

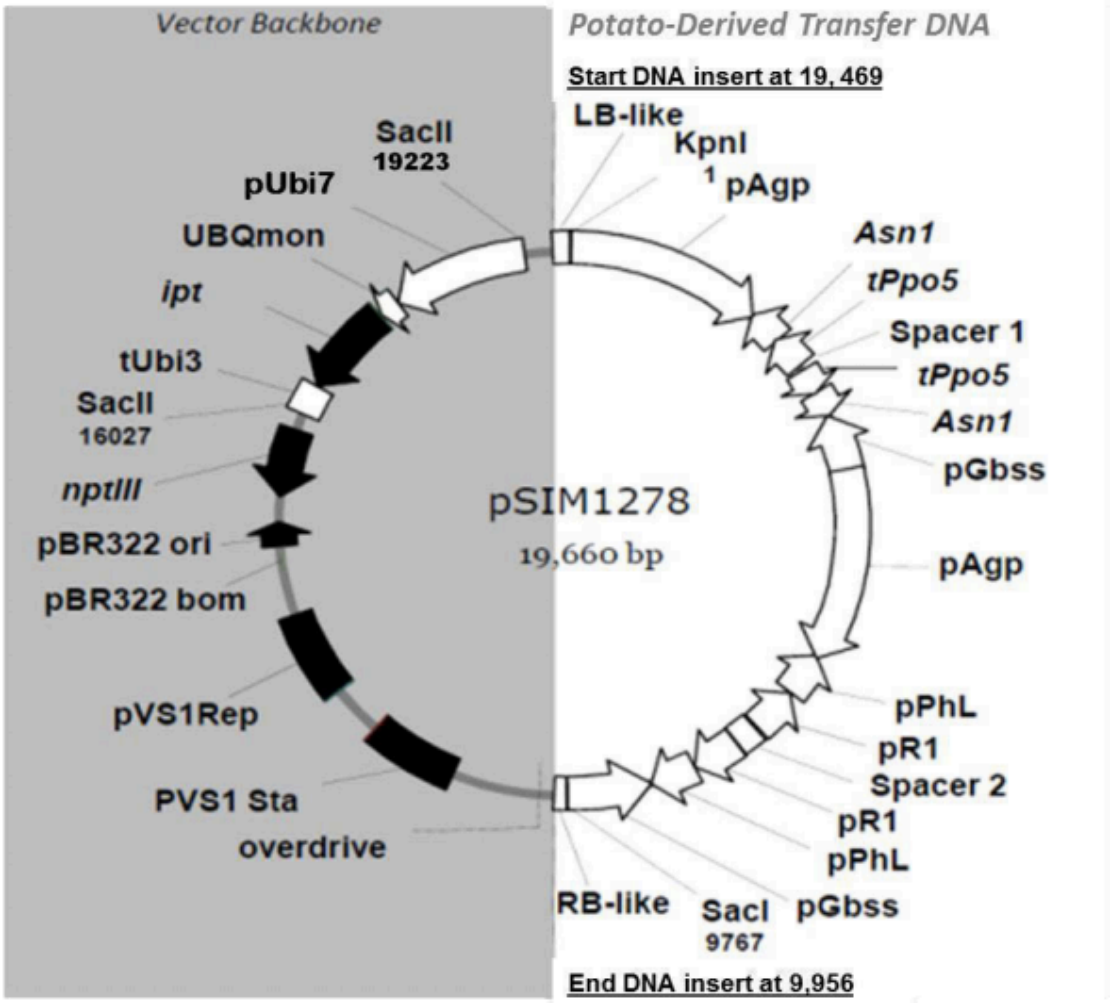


Figure 4.1 (from Ye et al., 2013) Two potato derived expression cassettes containing truncated sense and antisense asparagine synthase (*Asn1*) and the tuber specific Polyphenol Oxidase (*Ppo-5*) or phosphorylase-L (*PhL*) and starch associated (*R1*), were added to the pSIM1278 vector. The non-potato derived vector backbone contained an isopentenyl isomerase (*Ipt*) marker.

The resulting vector (Figure 4.1) was inserted into *Agrobacterium tumefaciens*, which then incorporated it into the potato genome, resulting in transformed potato varieties. Phenotypic screens were conducted and plants with stunted phenotypes removed, indicating incorporation of the vector backbone. Subsequent PCR and southern-blot hybridisations confirmed that the remaining lines were free from Agrobacterial backbone fragments, resulting in the production of purely cis-genic potato lines.

All Innate® transformed lines contained at least one functional *Asn1*/*Ppo-5* gene silencing cassette. These plants were shown to produce an array of unpolyadenylated RNA molecules which down-regulated transcript levels of the target genes. *Ppo-5* transcript levels, the gene of interest for this study, was shown to be knocked down (Figure 4.2) and PPO activity was reduced by up to 85% in Innate® transformed lines as measured by a catechol assay (Rommens et al., 2004; Rommens et al., 2006; Ye et al., 2013). In the Innate® lines used for this experiment the Agrobacterial inserts during transformation pre-emptively terminated before or within the second *R1*/*PhL* cassette, rendering it non-functional (Ye et al., 2013). Therefore, in all transformed material used in this study transcripts from *Asn-1* and *Ppo-5* significantly reduced, whereas *R1* and *PhL* transcript levels were comparable, or only slightly lower than those found in WT lines (Figure 4.2). This was confirmed by a lack of significant difference in reducing sugar abundance between Innate® and WT tubers (Jingsong et al. 2013) suggesting no phenotypic differences.

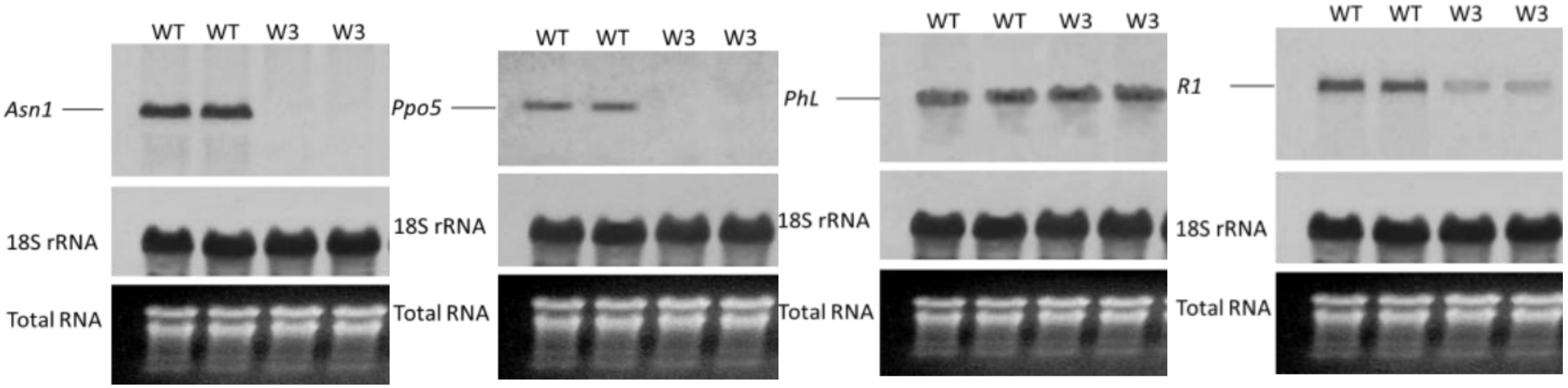


Figure 4.2 (modified from (Ye et al., 2013) Northern blot analysis RNA transcripts of *Asn1*, *Ppo-5*, *PhL* and *R1* in field grown tubers of both the WT Russet Burbank and W3 Innate Russet Burbank® (with vector pSIM1278) transformed lines. Compared with total RNA and the 18s rRNA benchmark.

However, an absence of visible pigmentation in Innate® tubers would not alone indicate that PPO causes Blackheart pigmentation, instead it could be possible that Innate® tubers do not develop Blackheart. This might occur due to varietal resistance, or the involvement of asparagine synthase and PPO in upstream Blackheart development. A way to identify the presence of Blackheart, independent of Blackheart pigmentation, will therefore be required.

4.1.3 Phenolic Metabolite Abundance and Distribution

PPO enzyme expression differs temporally and spatially in different tissues; PPO activity in potato tubers is greatest at the sub-epidermis and cortex tissues, declining in activity in the pith and parenchymal cells (Thygesen et al., 1995). Assuming PPO is responsible for Blackheart, then the distribution of pigmentation in the pith and parenchymal tissues is unlikely to be a simple consequence of PPO distribution. However, the concentration of phenolic PPO substrates has previously been linked to Blackheart (Jadhav et al., 1980; Kiaitsi, 2015) and PPO activity has been proposed to be largely substrate dependent (Murata et al. 1995). Additionally, cells surrounding Blackheart affected tissues stain strongly with Sudan IV (Reeve, 1968) which, despite non-specificity of the stain for lipids, was used to suggest that Blackheart tissues display a high abundance of suberin and phenolic compounds.

Tubers from stores displaying high incidence of Blackheart have been shown to have up to nine times higher levels of polyphenolic glycoalkaloids (Kiaitsi, 2015; Jadhav et al., 1980) and chlorogenic acid has been described as the “most important variable [in] differentiating potato stocks with different susceptibility to [Blackheart]” vis.

(Kiaitsi, 2015). However, the repeated misidentification of Blackheart in work completed by Kiaitsi (2015) (Chapter 3) renders this correlation inconclusive. Chlorogenic acid has been indicated as the most abundant potato phenolic compound making up 80-90% of total potato phenolic content, and largely localised to the periderm and cortex (Dao & Friedman, 1992). However, there appears to be no correlation between chlorogenic acid content and non-Blackheart potato tissue discoloration (Friedman, 1997).

Although the periderm has the highest phenolic content in tubers (Payyavula et al., 2015) the distribution of the aromatic amino acid tyrosine, a common substrate of PPO, is concurrent with the localization of Blackheart, with higher concentrations found in the pith of potato tubers (Reeve, 1968; Craft et al., 1958).

Phenolic metabolites also increase at low temperatures (Cheynier et al., 2012) along with up-regulation of phenolic-metabolite-synthesising enzymes, such as phenylalanine ammonia lyase (PAL) (Cheynier et al. 2012; Leyva et al. 1995) and these factors may influence the varying degrees of Blackheart susceptibility (Chapter 3). Similarly, there are clear varietal differences in phenolic metabolite abundances, which may also influence the varietal differences in Blackheart resistance and susceptibility. In addition, monophenol content is greatest after seven or eight months of potato storage (Blessington et al., 2010) and this correlates with increased Blackheart incidence (Chapter 3) (Briddon, 2015, David Wright, Manor Fresh Ltd. pers. comm).

Therefore, it is not clear if phenolic metabolite abundance correlates with Blackheart distribution, or if it can explain a potential increase in PPO activity. Quantifying the relative differences in phenolic metabolite abundance between Blackheart susceptible tissues, varieties and during Blackheart development, will aid in identifying any correlations and potential effects that phenolic concentration has on Blackheart development. This will be explored using untargeted GC-MS metabolomics, a common technique to separate, identify and quantify a wide variety of phenolic compounds in plant (Rohloff, 2015) and potato tissue (Akyol et al., 2016), including chlorogenic acid. Additionally, this untargeted approach will generate a metabolomics data set that can be scoured for changes in metabolites in the pith tissues of susceptible varieties during Blackheart induction, which may help direct future work.

4.1.4 Cell Death

Blackheart has long been assumed to consist of a region of necrosis within a tuber (Stewart & Mix, 1917; Bartholomew, 1913). However, it is a mark of how little is understood about Blackheart that the involvement of cell death has also never been experimentally demonstrated. Wounding-induced cell death has been shown to lead to a redistribution of PPO throughout the cell and vacuole (Partington et al., 1999). Despite different causes, this could help explain why necrotic disorders such as Blackspot (Stevens and Davelaar, 1997), heat necrosis and internal brown spot (Chi et al., 2015), as well as bruising, are observationally similar to Blackheart.

The involvement of PPO in generating Blackheart pigmentation would require dramatic changes to cell membrane physiology to allow enzyme-substrate mixing and

this loss of membrane integrity would likely affect cell viability. Evans blue is a common histological stain for cell viability due to its exclusion from tissues with intact cell membranes (Baker & Mock, 1994). However, as cells are able to tolerate some membrane leakage (Thalhammer et al., 2014) the degree, rather than presence/absence, of membrane permeability is also required to identify cell death. Additionally, cells may be able to repair membrane damage, and therefore multiple viability measurements will be considered in tandem to identify the role of cell death in Blackheart.

Changes in cell metabolism, including the redox and energy status of tissues, are common viability measurements (Riss et al., 2004) as sufficient energy and reducing power are necessary for cellular survival. Quantification of cellular adenylates and further measurements on the metabolic status of different tuber tissues will provide information on the metabolic activity of tissues during Blackheart induction conditions.

4.1.5 The Role of Respiration in Blackheart Susceptibility

High respiratory rates and cellular metabolic activity have long been associated with both increased Blackheart susceptibility and induction of Blackheart conditions (Stewart & Mix 1917; Davis 1926, Kiaitsi, 2015).

Tubers under Blackheart induction conditions can be assumed to also have increased respiratory rates; Blackheart induction methods (Chapter 3) including high temperatures lead to a general increase in enzymatic activity, and anoxia likely drives increased glycolytic flux via the Pasteur effect. As elevated respiration rates are likely

involved in the induction of Blackheart, it follows that high respiratory rates might also increase susceptibility of tubers to Blackheart. This line of thinking has influenced commercial practice and potato stores are frequently ventilated and monitored for changes in atmospheric concentration which might indicate elevated respiratory rates and thus, it is assumed, Blackheart incidence (Briddon, 2015; Kiaitsi, 2015; David Wright, Manor Fresh Ltd, pers. comm., 2014).

However, Briddon (2015) found no correlation between Blackheart susceptibility and the rate of CO_2 production by tubers post-harvest and concluded that "no effect of respiration rate could be linked to the development of Blackheart symptoms". Similarly, work completed by Kiaitsi (2015) concluded that "*a relationship between respiration rate and the incidence of* [Blackheart] *was not found as it was expected*". All previous experiments on respiratory rate and Blackheart susceptibility have explored changes in CO_2 production. However, respiration rates are not directly proportional to CO_2 release because many other reactions beyond the TCA cycle can produce CO_2; for example, temperature affects flux through the oxidative pentose-phosphate pathway and thus CO_2 production (Malone et al., 2006), without production of additional energy. Therefore, oxygen consumption may be a more appropriate measure of cellular respiration.

As the chosen Blackheart induction methods (Chapter 3) utilise anoxia, and can be reliably assumed to involve elevated respiratory rates without additional experimental testing, this chapter will focus on any correlations between the susceptibility of tubers to develop Blackheart and differences in oxygen consumption. It is not yet clear if elevated respiration rates are factors in Blackheart susceptibility, despite being the focus of Blackheart research and industry preventative measures.

4.2 Results

4.2.1 PPO and Blackheart Pigmentation

Blackheart was induced in both Simplot Innate® potato tubers with reduced PPO activity and the equivalent wild type US cultivars (cv. Snowden, Russet Ranger, Russet Burbank, Atlantic). Six tubers from each Simplot Innate® and WT cultivar lines were incubated under Blackheart induction conditions for 20 h and imaged (Chapter 2) (Figure 4.3) and Blackheart quantified (Chapter 2) (Figure 4.4).

In the Simplot Innate® lines, only slight discolouration of the pith tissue was visible (Figure 4.3) after incubation after 20 h of Blackheart induction conditions. However, strong Blackheart pigmentation was visible in all WT cultivars (Figures 4.3 & 4.4). Of the WT cultivars, Russet Ranger tubers displayed the highest susceptibility of Blackheart and Snowden the least (Figures 4.3 & 4.4).

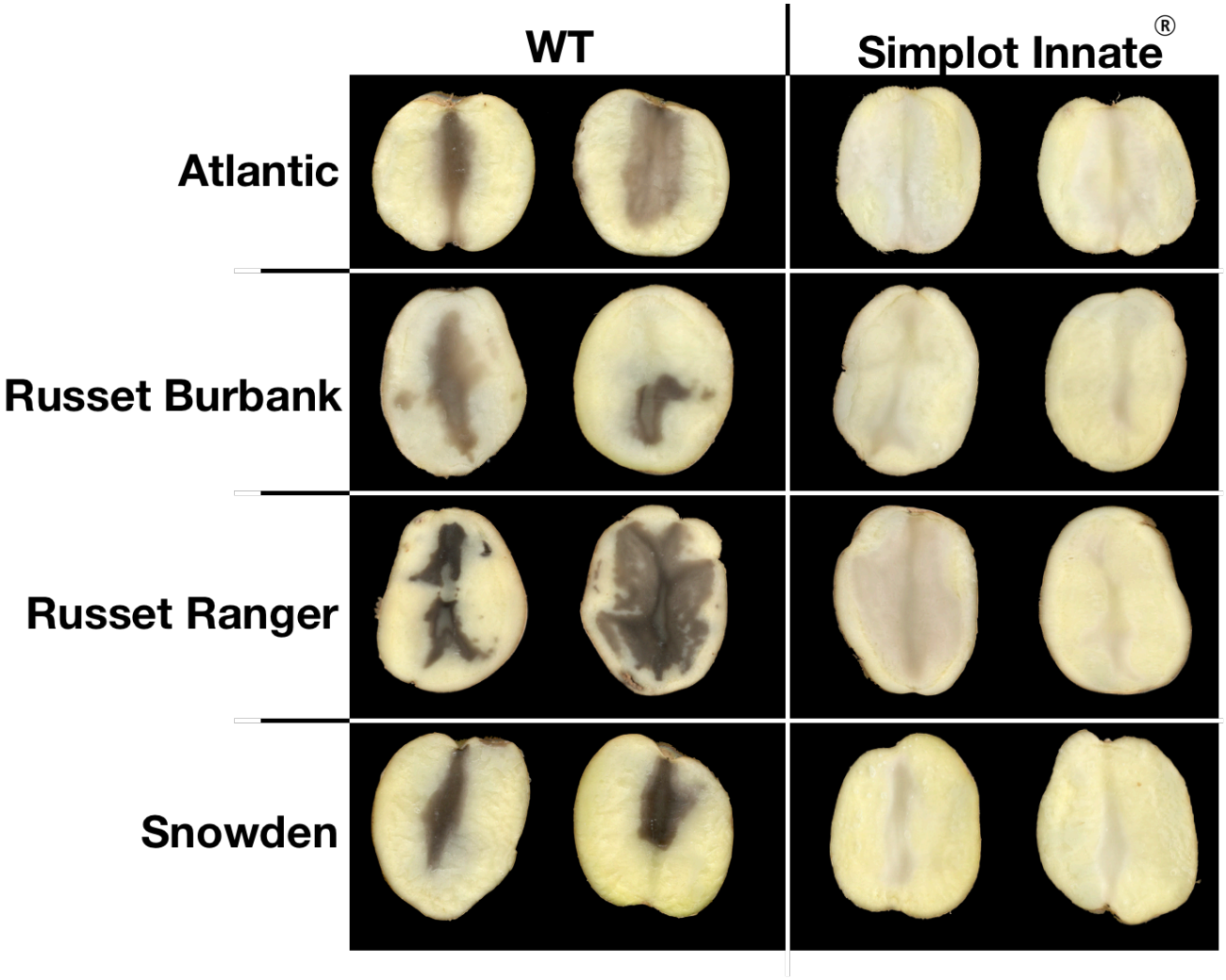


Figure 4.3: Appearance of Simplot Innate® potato tubers with knocked down Ppo-5 expression and the equivalent wild type US cultivars (cv. Snowden, Russet Ranger, Russet Burbank, Atlantic) after incubation under Blackheart induction conditions for 20 h.

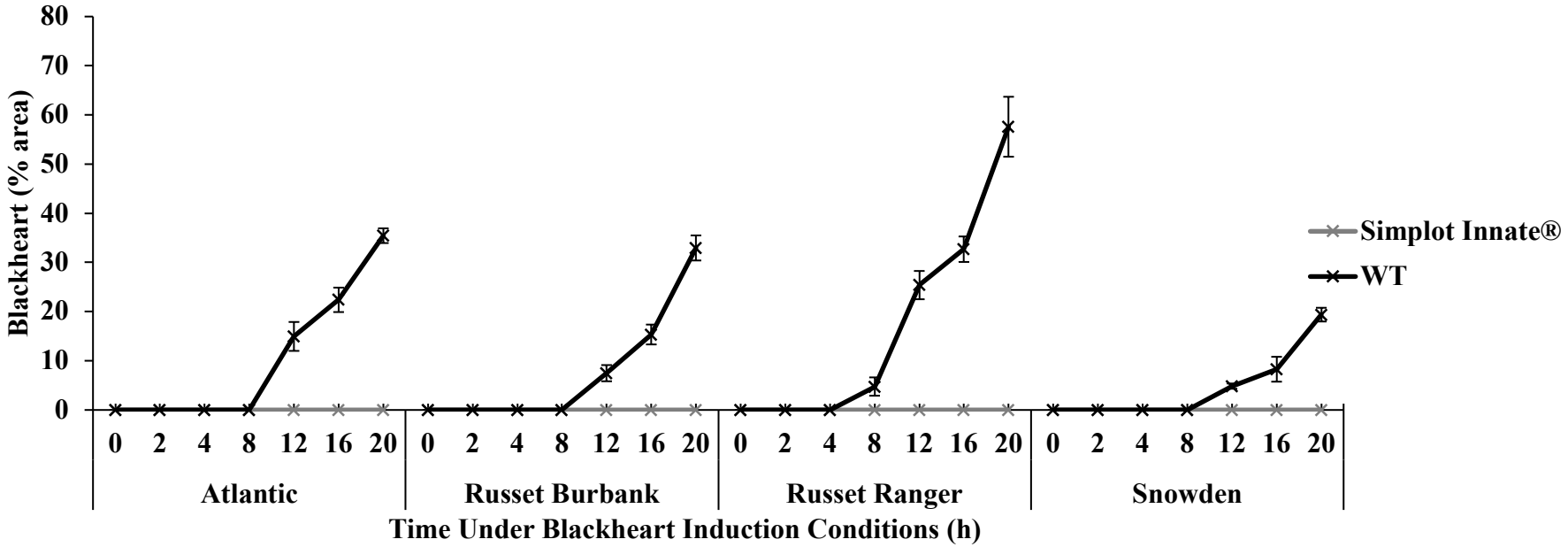


Figure 4.4: Quantified extent of Blackheart in Simplot Innate® potato tubers and the equivalent wild type US cultivars (cv. Snowden, Russet Ranger, Russet Burbank, Atlantic) after incubation under Blackheart induction conditions for 20 h. Error bars represent ± standard error of the mean, n = 6.

4.2.2 Phenolic Metabolite Abundance and Metabolomics

To measure relative differences in phenolic abundance between tissues of King Edward tubers during Blackheart induction untargeted GC-MS was used. Seven King Edward tubers were used for each time point, their metabolites extracted, derivatised and analysed using TagFinder software (Chapter 2). The metabolomics data was standardised by both fresh weight (FW) of the tissue and by amount of two internal standards (ribitol and norvaline), resulting in relative abundances of each metabolite per gram of fresh weight. The mean value of these was calculated from at least six biological replicates. Metabolite isomers and different derivatization products were combined to find the total abundance of each metabolite, and the sum of standard errors calculated.

A total of 272 metabolites including 39 phenolic metabolites, were detected and quantified and analyte-specific, non-parametric t-tests were conducted between samples using the Significant Analysis of Microarrays software (Tusher et al., 2001) to identify significant differences between specific time points (0 h, 12 h & 20 h of Blackheart induction conditions) and metabolites. The following data represents the sum of all derivatives of each phenolic metabolite that was found in at least three biological samples at each time point e.g. flavan-3-ol was only found in two biological samples at 12 and 18 h in the pith and was thus ommited.

After incubation under Blackheart induction conditions, tyrosine abundance was not significantly different in abundance in the pith or cortex (F test, $p = 0.873$), and the abundance of tyrosine declined linearly over time. Chlorogenic acid abundance

fluctuated in the pith and cortex throughout incubation under Blackheart induction conditions; there was no significant difference in chlorogenic acid abundance in the pith or cortex, except after 20 h of Blackheart induction conditions where chlorogenic acid abundance in the cortex was higher (Figure 4.6) (F test, p =0.493). The only phenolic compounds that were significantly higher in the pith throughout Blackheart induction conditions was cinnamic acid (Figure 4.7) (F test, p =0.03) and phenylalanine (Figure 4.5) (F test, p =0.029).

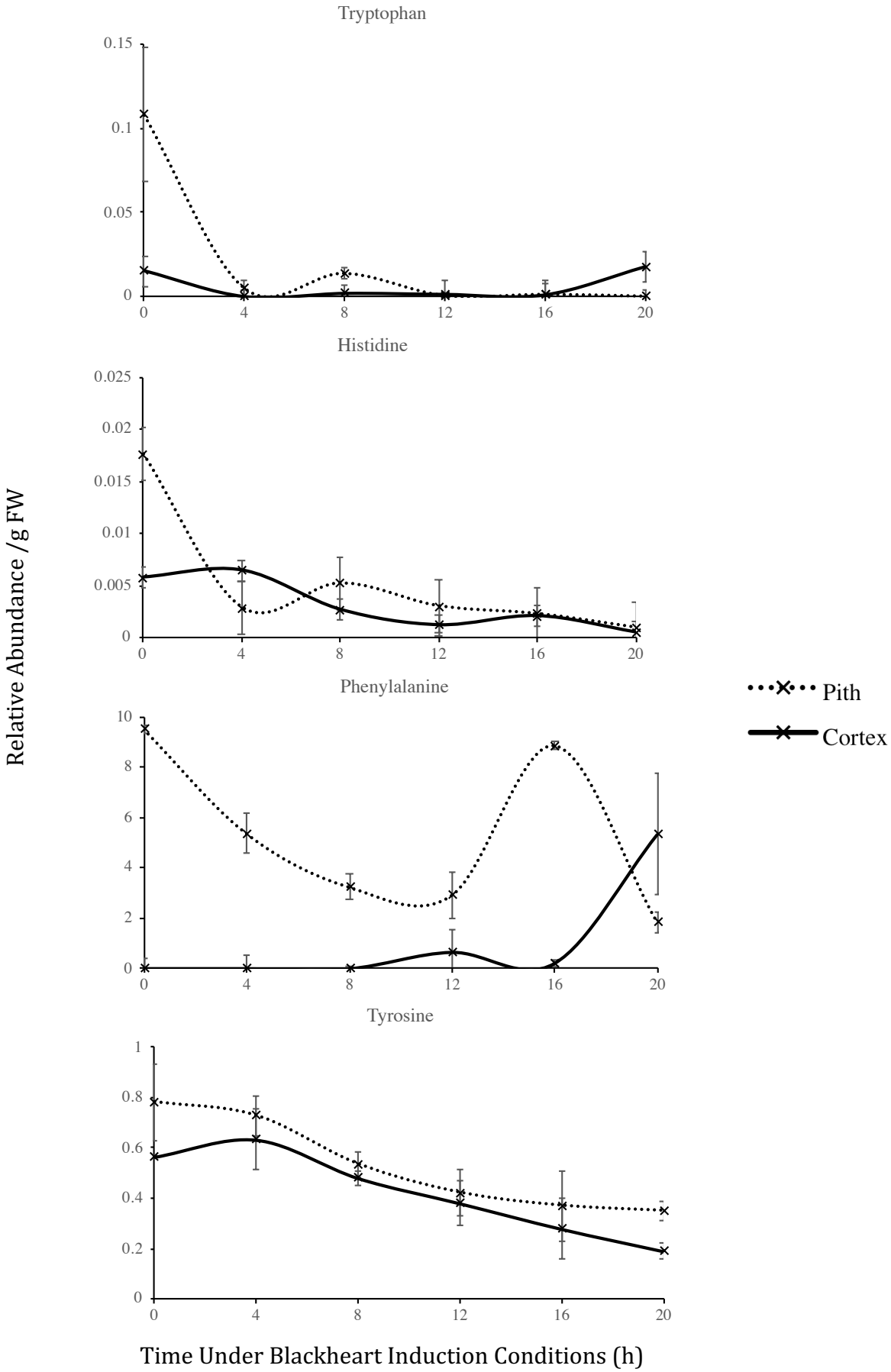


Figure 4.5: Mean phenolic amino acid abundance, relative to internal standards in pith and cortex tissues from six King Edward tubers and the sum of isomers /

derivitisation products for each metabolite. Error bars represent ± sum of standard error for each value.

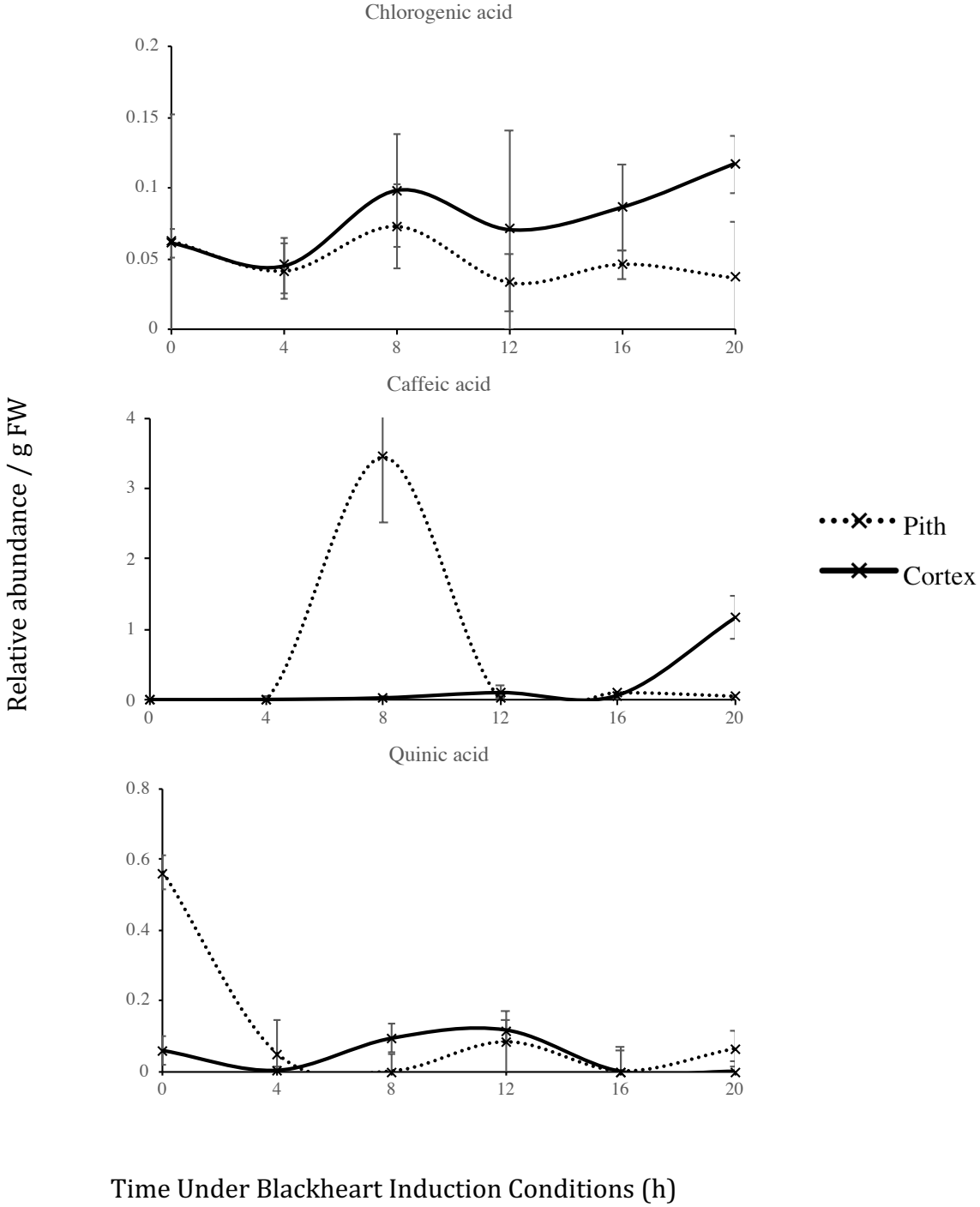


Figure 4.6 Mean abundances of Chlorogenic acid and precursosrs in pith and cortex tissues from six King Edward tubers and the sum of isomers/derivitisation products for each metabolite. Error bars represent ± sum of standard error for each value.

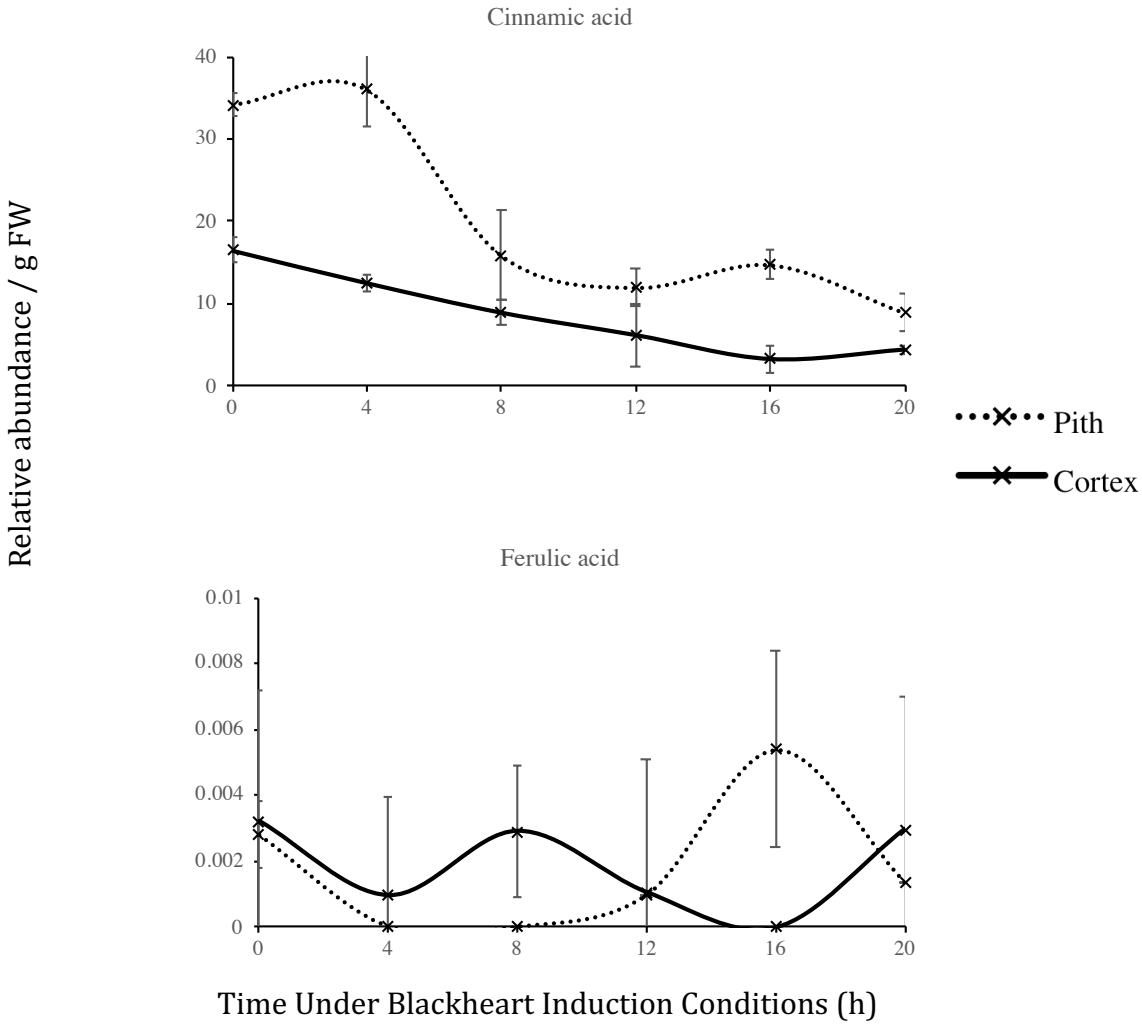


Fig 4.7: Mean abundances of phenylpropanoids in pith and cortex tissues from six King Edward tubers and the sum of isomers/derivitisation products for each metabolite. Error bars represent ± sum of standard error for each value.

4.2.3 Membrane Permeability

Evans blue is a non-permeable dye and can only stain cells with ruptured or permeable membranes (Baker and Mock, 1994). King Edward tubers were incubated under Blackheart induction conditions and immediately cut in half after removal from these incubation conditions. Half of the tuber was stained with Evans blue and the other half was wrapped in damp tissue to avoid desiccation and left for 12 h to develop Blackheart pigmentation before imaging (Chapter 2).

Evans blue strongly stained Blackheart affected tissue, immediately after removal from Blackheart induction conditions (Figure 4.8). The area of tissues stained with Evans blue correlated in shape, size and position to the area of Blackheart pigmentation, indicating Blackheart affected tissues had ruptured or permeable membranes. Unaffected tissues, such as the cortex, or pith tissues prior to the onset of Blackheart (8 h, Figure 4.8), showed significantly less staining, indicating these regions contained fewer ruptured cells or there was a lesser extent of membrane permeability.

Blackheart was induced in both Simplot Innate® potato tubers and the equivalent wild type US cultivars (cv. Snowden, Russet Ranger, Russet Burbank, Atlantic). After 20 h of Blackheart induction conditions, tubers were immediately cut in half after removal from these incubation conditions. Again, half of the tuber was stained with Evans blue and the other half was wrapped in damp tissue to avoid desiccation and left to develop Blackheart pigmentation (Figure 4.9) before imaging (Chapter 2).

WT US cultivars with Blackheart displayed similarly stained regions correlating in shape, size and position to the area of Blackheart pigmentation. However, Simplot Innate® potato tubers also displayed regions of intense Evans blue staining, despite the lack of Blackheart pigmentation (Figure 4.9).

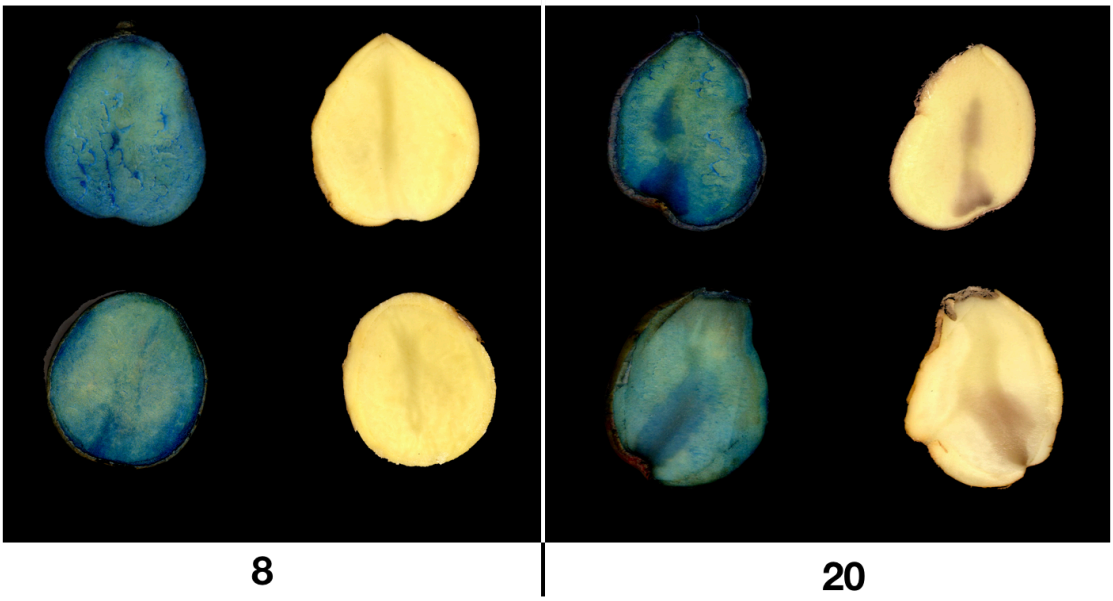


Figure 4.8: Appearance of King Edward tubers incubated under Blackheart induction conditions for 8 h or 20 h (Blackheart induced after 12 h). Half of each tuber was stained with a 1% Evans Blue solution for 30 minutes before imaging and the other was imaged after 12 h, allowing Blackheart pigmentation to develop.

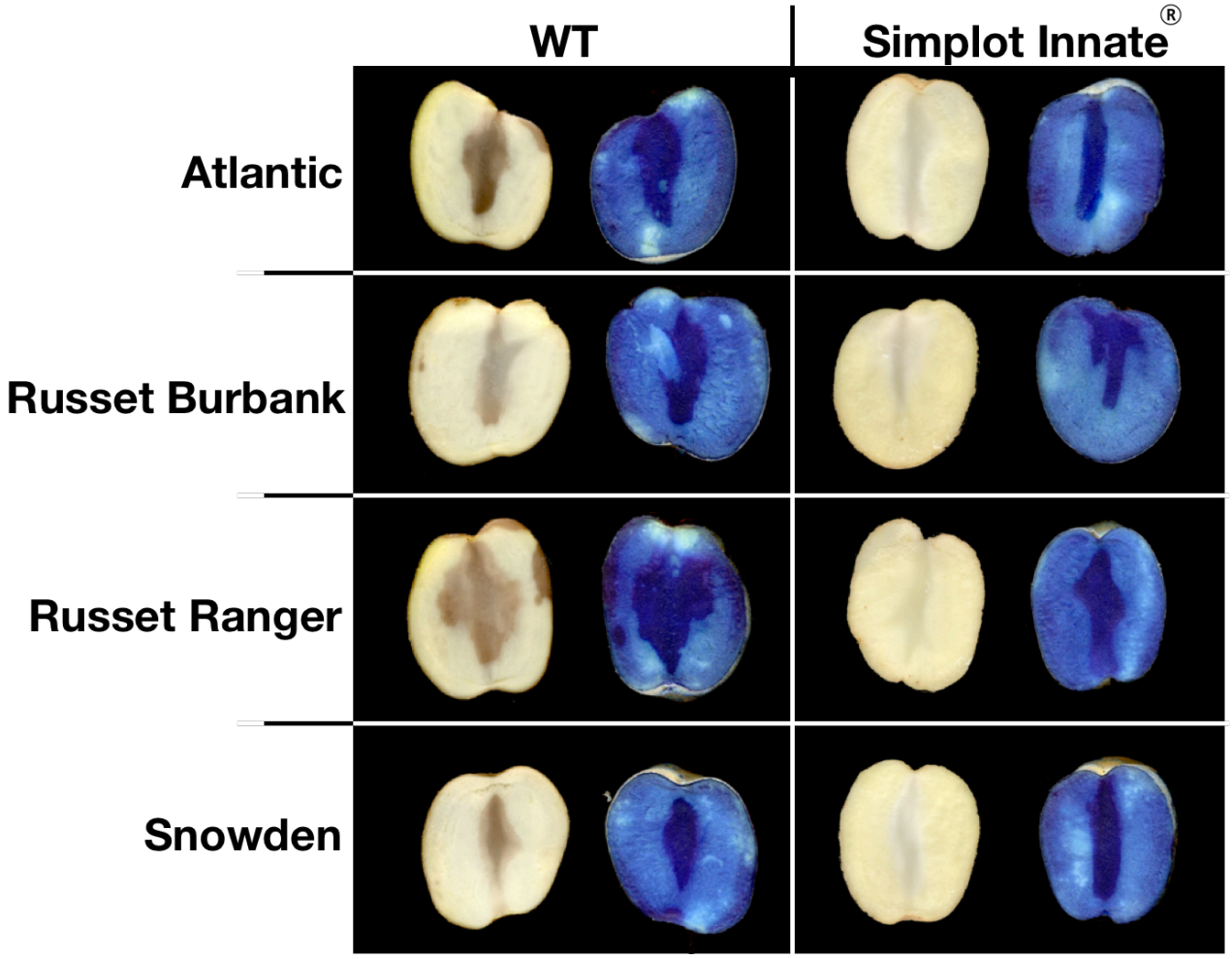


Figure 4.9: Appearance of Simplot Innate® potato tubers with knocked down Ppo-5 expression and the equivalent wild type US cultivars (cv. Snowden, Russet Ranger, Russet Burbank, Atlantic) after incubation under Blackheart induction conditions for 20 h. Half of each tuber was stained with a 1% Evans Blue solution for 30 minutes before imaging and the other was imaged after 12 h, allowing Blackheart pigmentation to develop.

4.2.4 Electrolyte Leakage

To assess the integrity of cell membranes during Blackheart induction, potato tissue discs from the pith, parenchyma and cortex tissues were taken from six King Edward tubers, stored at 4°C for three months and incubated under Blackheart induction conditions for the indicated time duration. These discs were then bathed in water and electrolyte leakage measured by recording the change in electrical conductivity of the solution, indicating the degree of membrane permeability in each tissue and condition type (Chapter 2).

In King Edward tubers, discs of pith tissue from tubers stored at 4°C for three months showed greater membrane leakage than parenchymal (t test, $p = 0.04$) or cortex tissues ($t = 2.99$, $p = 0.02$). All tissues showed increased rates of electrolyte leakage after incubation under Blackheart induction conditions (4 h, Figure 4.10),

After this transition (8 h-24 h, Figure 4.10) King Edward cortex tissues did not show any significant change in electrolyte leakage during Blackheart induction. However, both the pith and parenchymal tissues showed further increased electrolyte leakage as Blackheart developed, increasing in a linear fashion between 8-24 h (Figure 4.10). By 24 h, pith tissues displayed 97.01% electrolyte leakage, which was significantly greater than the parenchyma (mean= 83.81%, t-test, $p < 0.001$) and cortex (mean= 48.66%, t test, $p < 0.001$).

In contrast, in Maris Piper tubers, which are resistant to Blackheart induction, there were no significant differences in electrolyte leakage rates between tissues under Blackheart induction conditions, except after 24 h where the cortex tissue electrolyte leakage (mean=30.30%) was significantly lower than the pith (mean=42.01%, t test, p =>0.001) and parenchyma (mean=48.46%, t-test, p>0.001). The extent of electrolyte leakage in all tissues was lower in Maris Piper than in King Edward tubers (Figure 4.10).

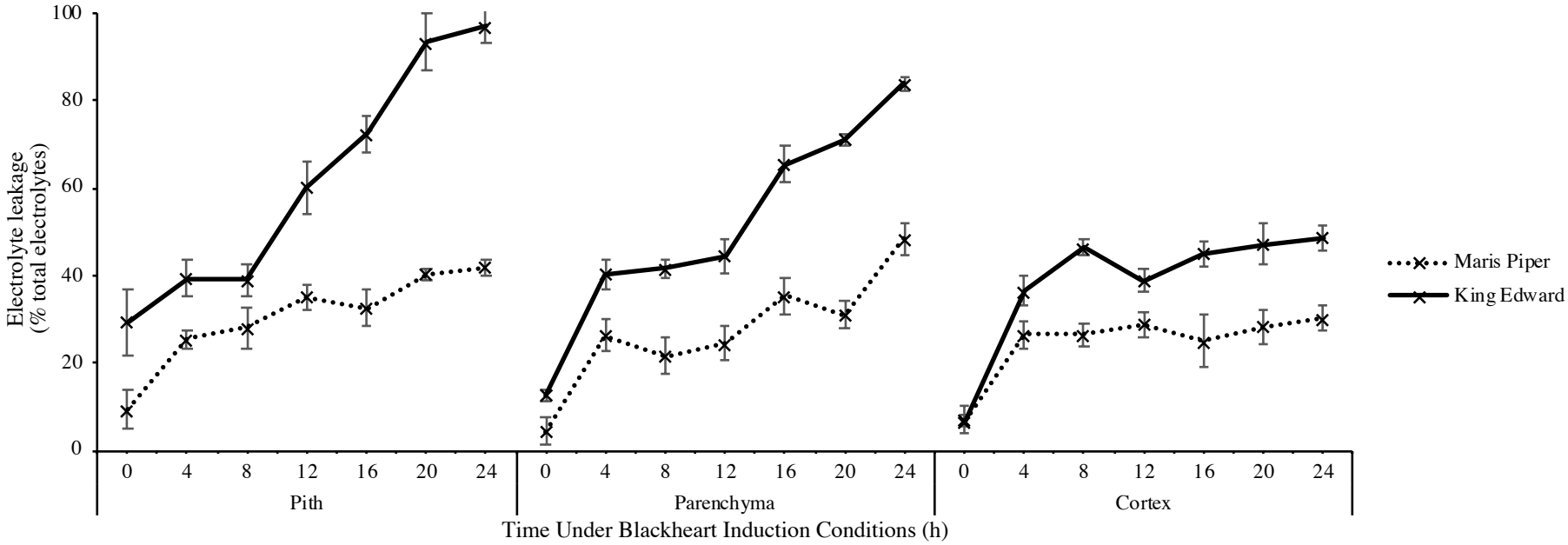


Figure 4.10 The mean electrolyte leakage, as a percentage of total cellular electrolytes, taken from the different tissue types of six King Edward and Maris Piper tubers throughout incubation under Blackheart induction conditions. Error bars represent ± standard error of the mean.

Blackheart is observed in the Pith tissue of King Edward tubers after 12 h of Blackheart Induction conditions, before spreading into the parenchyma. Blackheart was never observed in Maris Piper tubers or cortex tissues before 24 h of Blackheart induction conditions.

4.2.5 TTC Stain

TTC is a redox stain that is reduced to red formazan via the action of oxidoreductase enzymes, and thus frequently used to indicate cellular respiration (Riss et al., 2004; Faridnia et al., 2015), although other enzymes apart from the respiratory dehydrogenases can also contribute to total oxidoreductase activity. King Edward tubers were incubated under Blackheart induction conditions and immediately cut in half after removal from these incubation conditions. Half of the tuber was stained with TTC (Chapter 2) and the other half was wrapped in damp tissue to avoid desiccation and left for 12 h to develop Blackheart pigmentation (Figures 4.11, 4.12 and 4.13) before imaging.

Strong red staining of tissue by TTC was observed immediately after removal from Blackheart induction conditions (Figure 4.11). The area of tissues where TTC was not converted to a red formazan correlated in shape, size and position to the equivalent area of Blackheart pigmentation in the second tuber half (Figure 4.11). The tissues unaffected by Blackheart, such as the cortex and pith tissues prior to the onset of Blackheart, stained red indicating these regions were metabolically active (8 h, Figure 4.11). However, a lack of red formazan was also found in the pith tissues of some samples prior to the visible onset of Blackheart (10 h, Figure 4.12). Additionally, the extent of Blackheart affected tissue was sometimes smaller in area than the equivalent unstained region of TTC treated samples (20 h, Figure 4.12 and 4.13), indicating that metabolic changes were occurring in tissues prior to the onset or spread of Blackheart.

Blackheart induced Simplot Innate® potato tubers and their equivalent wild type US cultivars (cv. Snowden, Russet Ranger, Russet Burbank, Atlantic) were also stained with TTC. WT US cultivars with Blackheart displayed similarly stained regions, which roughly correlated in shape, size and position to the area of Blackheart pigmentation. However, Simplot Innate® potato tubers also displayed unstained regions, despite the lack of Blackheart pigmentation (Figure 4.13).

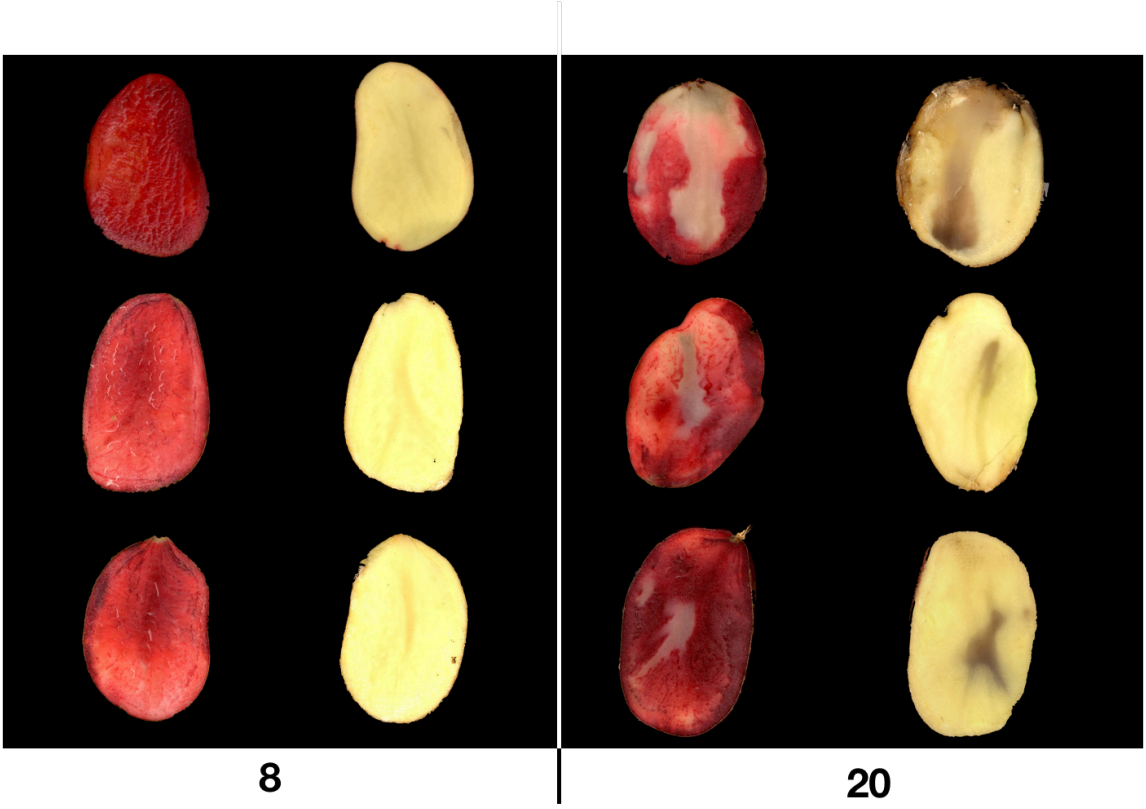


Figure 4.11: Appearance of King Edward tubers incubated under Blackheart induction conditions for 8 h or 20 h (Blackheart induced after 12 h). Half of each tuber was stained with a 1% TTC solution for 30 minutes before imaging and the other was imaged after 12 h, allowing Blackheart pigmentation to develop.



Figure 4.12: Appearance of King Edward tubers incubated under Blackheart induction conditions for 10 h or 24 h (Blackheart induced after 12 h). Half of each tuber was stained with a 1% TTC solution for 30 minutes before imaging and the other was imaged after 12 h, allowing Blackheart pigmentation to develop.

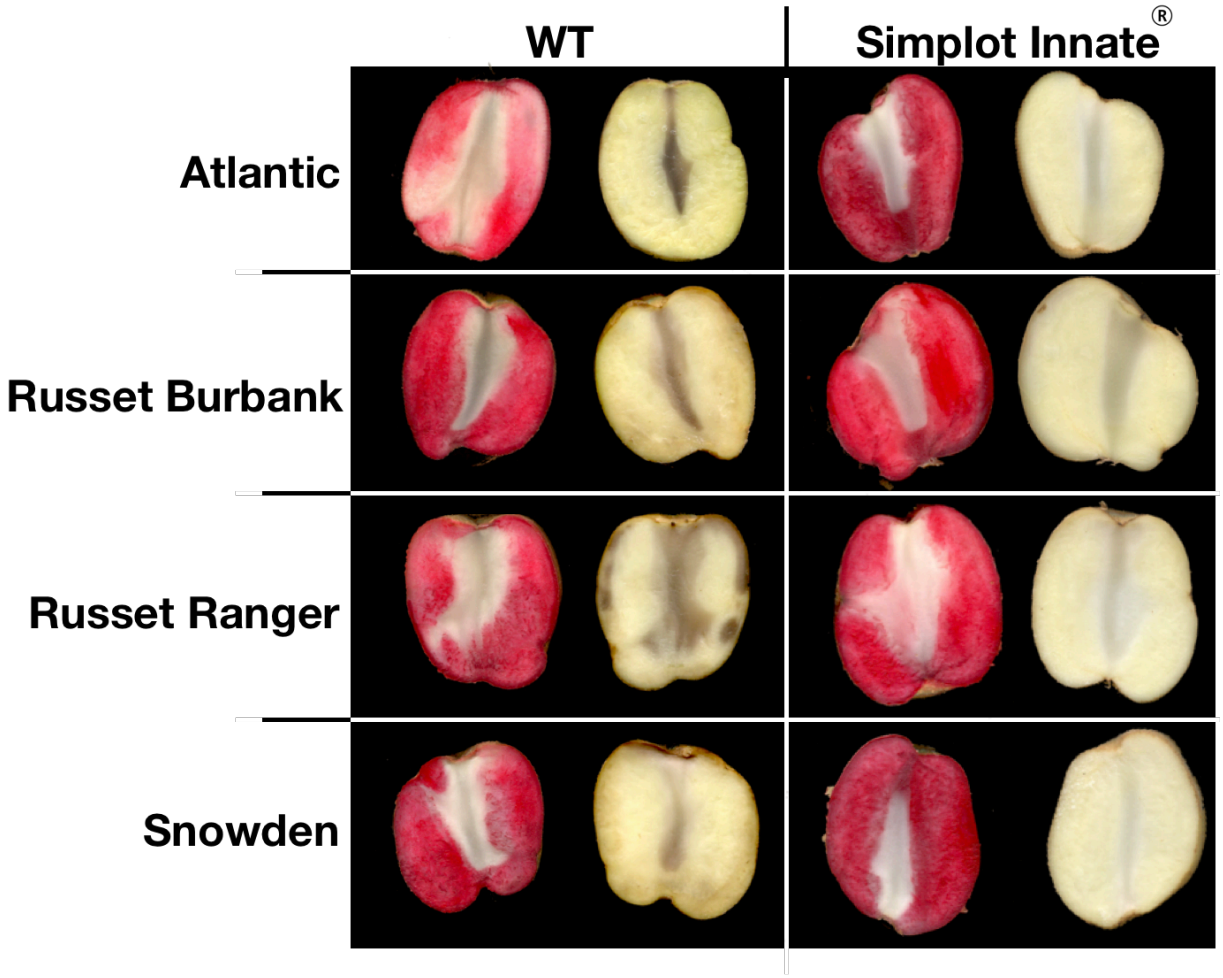


Figure 4.13: Appearance of Simplot Innate® potato tubers with knocked down Ppo-5 expression and the equivalent wild type US cultivars (cv. Snowden, Russet Ranger, Russet Burbank, Atlantic) after incubation under Blackheart induction conditions for 20 h. Half of each tuber was stained with a 1% TTC solution for 30 minutes before imaging and the other was imaged after 12 h, allowing Blackheart pigmentation to develop.

4.2.6 Adenylate Status

To assess cellular energy status during Blackheart induction, the levels of the adenylates ATP, ADP and AMP were measured using an assay based on the ATP dependent conversion of D-Luciferin to Oxyluciferin by a recombinant firefly luciferase assay (Chapter 2). Due to the difficulty of accurately recording and measuring adenylates in plant tissues, additional precautions were taken: eight biological replicates from King Edward or Maris Piper were used; all assays were confirmed to be in the linear range and above the maximum detection limit of 0.1 picomole ATP; additional samples from each tissue type at 0, 12 and 20 hours of Blackheart induction conditions were spiked with small amounts of adenylates and their recovery confirmed, ensuring any observed changes were not due to losses during extraction and assay. Values were compared with a standard curve of known adenylate concentrations to obtain adenylate abundance.

Both the ATP:ADP ratio and the adenylate energy budget are common metrics used to provide information on the energy status of biological samples (Riss et al., 2013). The Adenylate Energy Charge (AEC) provides additional information to the ATP:ADP ratio by simultaneously considering the concentration of all three adenine nucleotides (ATP, ADP and AMP) and the number of high energy phosphate bonds each contains (Chapter 2).

The concentrations of all nucleotides declined in all tissue types of King Edward tubers during Blackheart induction conditions (Figure 4.14). The cortex of King Edward tubers had the highest amount of ATP and ADP both prior to incubation

under Blackheart induction conditions (0 h, ATP + ADP = 35.67 nmol/g FW) and after 20 h of Blackheart induction conditions (20 h, ATP + ADP = 11.89 nmol/g FW) which was significantly higher than the equivalent amounts in the pith and cortex at each time point (t test, both 0 h and 20 h, $p>0.001$) (Figure 4.14).

Although all King Edward tissues showed reductions in ATP and ADP abundance under Blackheart induction conditions, the ATP and ADP abundance in the cortex was significantly greater than those in the pith (F test, ATP $p =0.001$, ADP $p =0.043$) and/or parenchyma (F test, ATP $p =0.01$, ADP $p =0.167$). This indicates that the cortex responds differently to Blackheart induction conditions, whereas the pith and parenchyma response is similar (F test, ATP $p =3.77$, ADP $p =0.659$), losing more ATP and ADP than the cortex during Blackheart induction.

The rate of adenylate decline in Maris Piper tuber tissue types was much less than in King Edward tubers (Figures 4.14 & 4.15), particularly after the onset of Blackheart induction conditions (0 h-4 h); between 4 h-20 h the rate of ATP decline in the pith of Maris Piper tubers was (0.13 nmol/g FW/h), significantly lower than that in the pith of King Edward tubers (0.36 nmol/g FW/h) (t test, $p =0.02$). Within the Maris Piper, the ATP and ADP abundance was not significantly different between any of the pith, parenchyma and cortex tissues (F test, $p>0.74$), indicating that the different tissue types did not respond differently under Blackheart induction conditions.

Importantly, the ATP:ADP ratio (Figure 4.16) and adenylate energy charge (Figure 4.17) in King Edward tubers were significantly higher in the cortex tissues, compared to both the pith (F test, ATP:ADP $p =0.001$, AEC $p =0.001$) and parenchyma (F test,

ATP:ADP p =0.01, AEC p =0.002). The pith and parenchyma response was not significantly different (F test, ATP:ADP p =0.571, AEC p =0.675). When compared to the ATP:ADP ratio and adenylate energy charge in the pith tissue of Maris Piper, the pith tissues of King Edward tubers were significantly lower (F test, ATP:ADP p =0.01, AEC p =0.021), indicating both varietal and tissue differences that correlate with Blackheart susceptibility.

The ATP:ADP ratios from WT and GM Innate® tubers are not significantly different within each tissue type (Figure 4.18) (F test, pith $p>0.348$, cortex $p>0.52$ from all varieties), indicating there is no affect of GM on the ATP:ADP ratio of tubers during Blackheart development. However, similar to the ATP:ADP ratios from Blackheart susceptible King Edward tubers, there is a significant difference between the ATP:ADP ratio between the pith and cortex of tubers during Blackheart induction (F test, $p<0.01$, from all varieties).

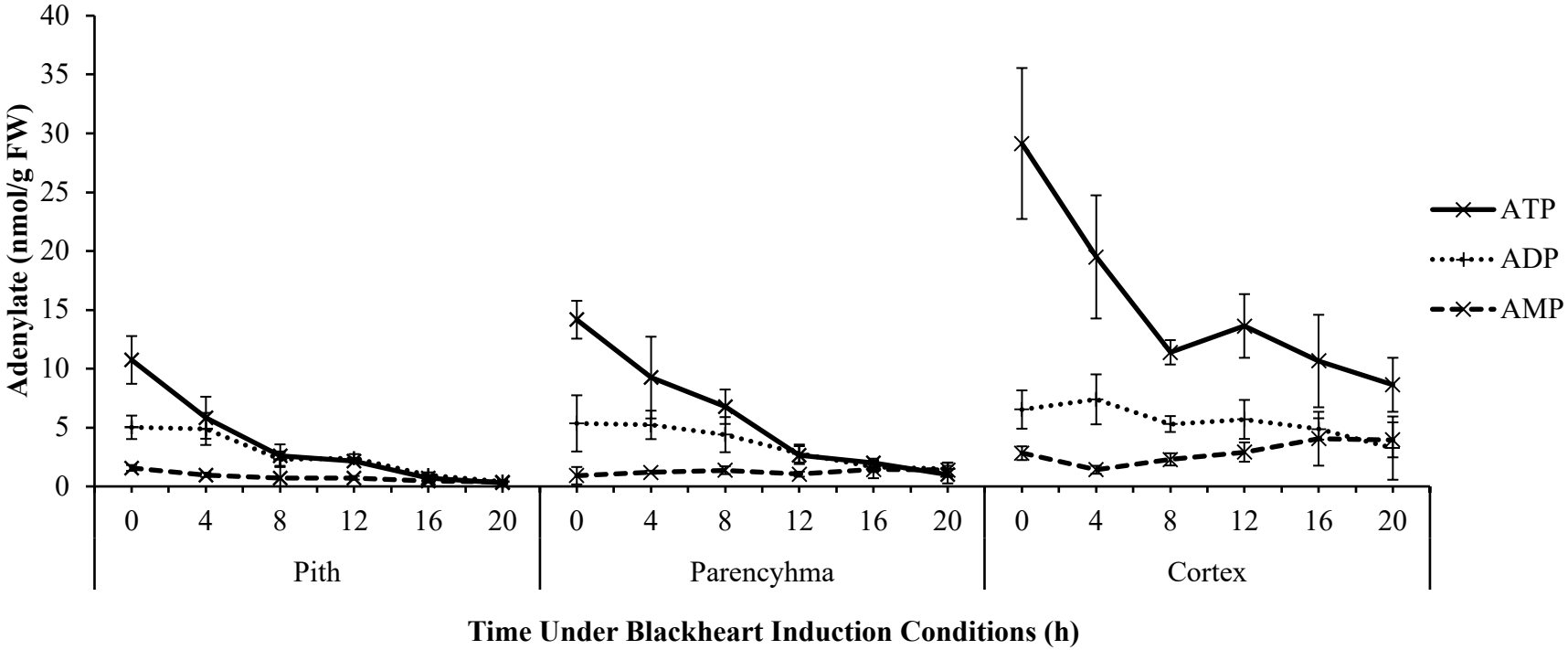


Figure 4.14: Mean adenylate concentration per gram of fresh weight in the pith, parenchyma and cortex tissues of eight King Edward tubers incubated under Blackheart induction conditions. Error bars represent ± standard error of the mean.

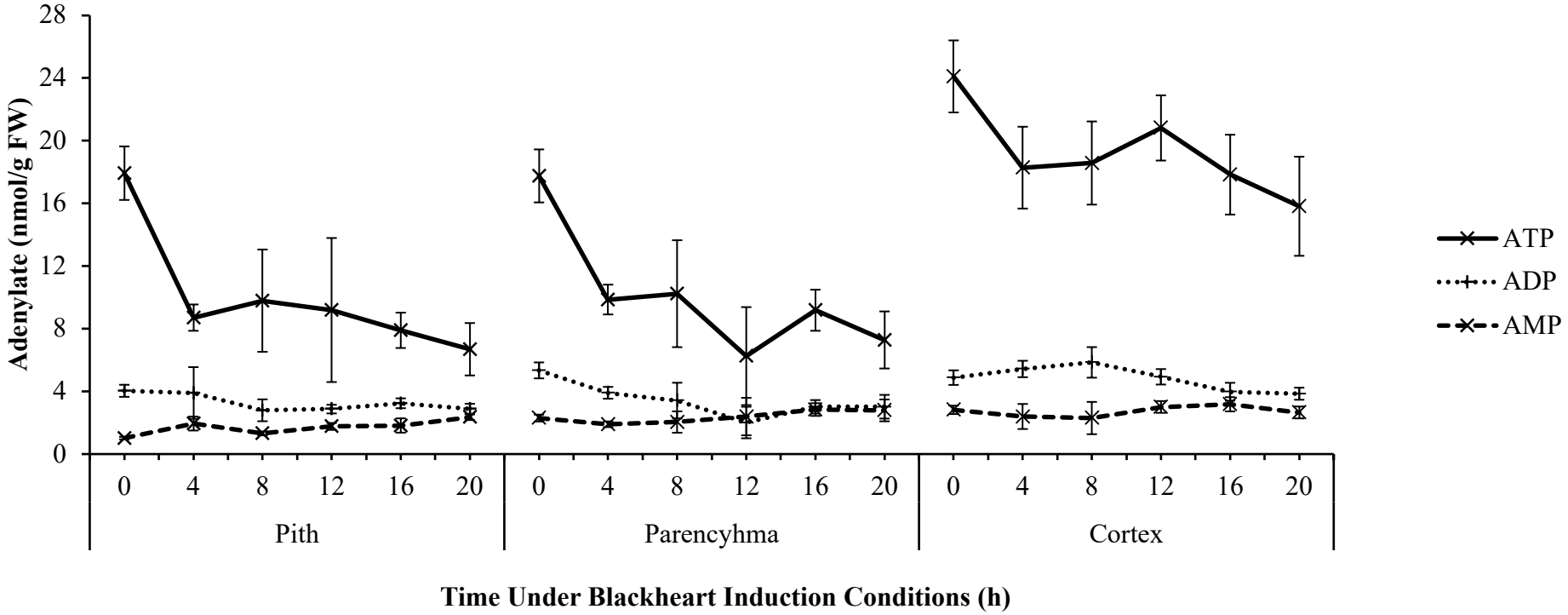


Figure 4.15: Mean adenylate concentration per gram of fresh weight in the pith, parenchyma and cortex tissues of eight Maris Piper tubers incubated under Blackheart induction conditions. Error bars represent ± standard error of the mean.

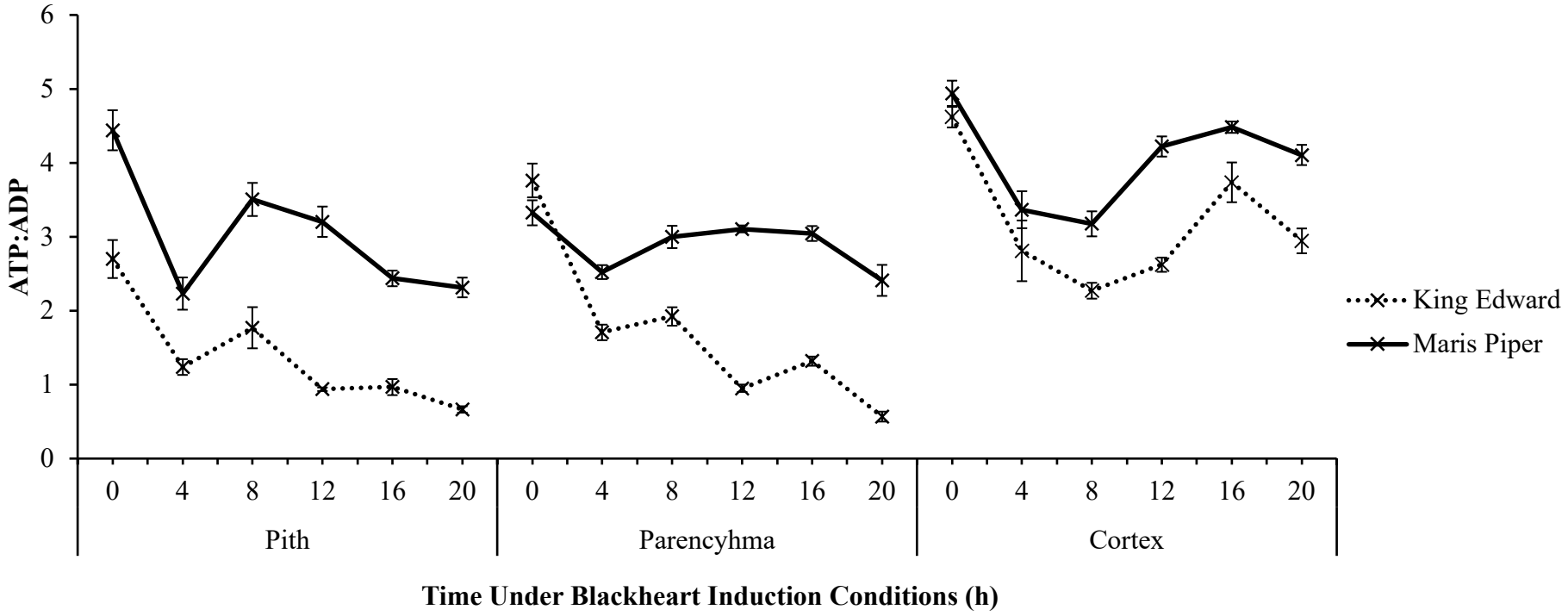


Figure 4.16: ATP:ADP ratio in the pith, parenchyma and cortex tissues of eight King Edward and Maris Piper tubers incubated under Blackheart induction conditions. Error bars represent ± standard error of the mean.

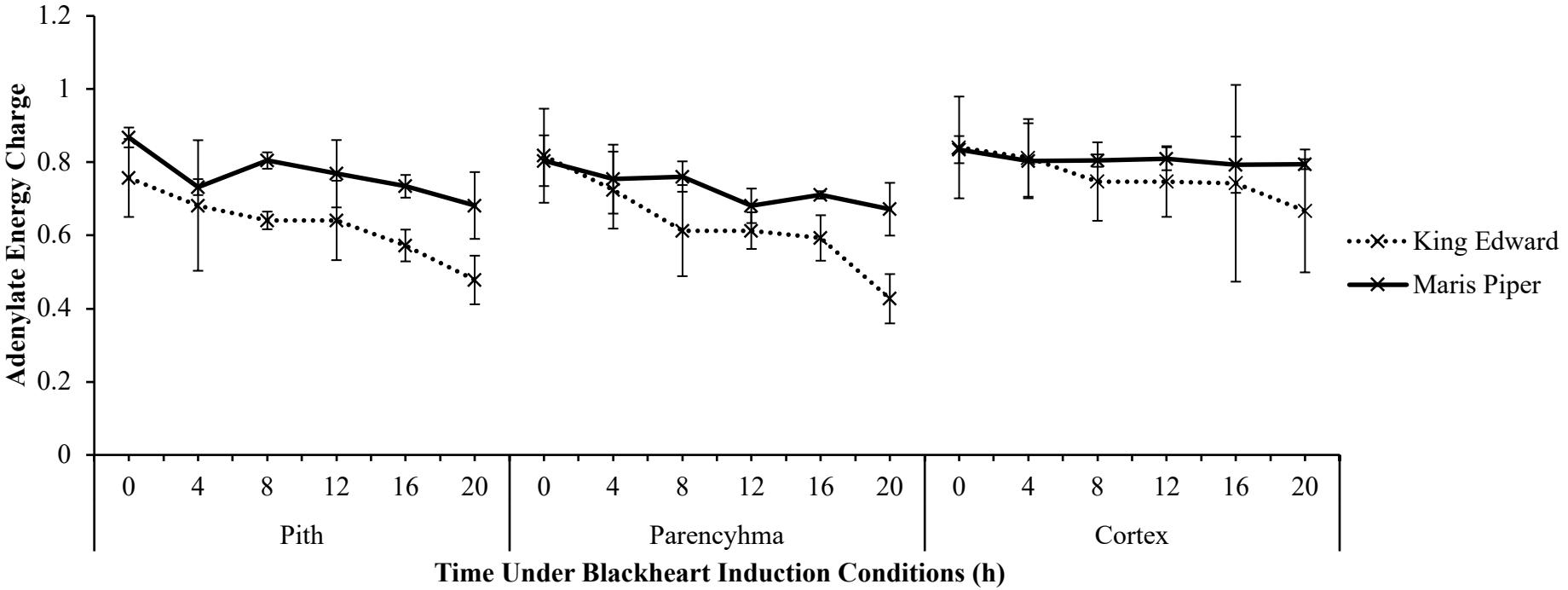


Figure 4.17: The Adenylate Energy Charge in the pith, parenchyma and cortex tissues of eight King Edward and Maris Piper tubers incubated under Blackheart induction conditions. Error bars represent ± standard error of the mean.

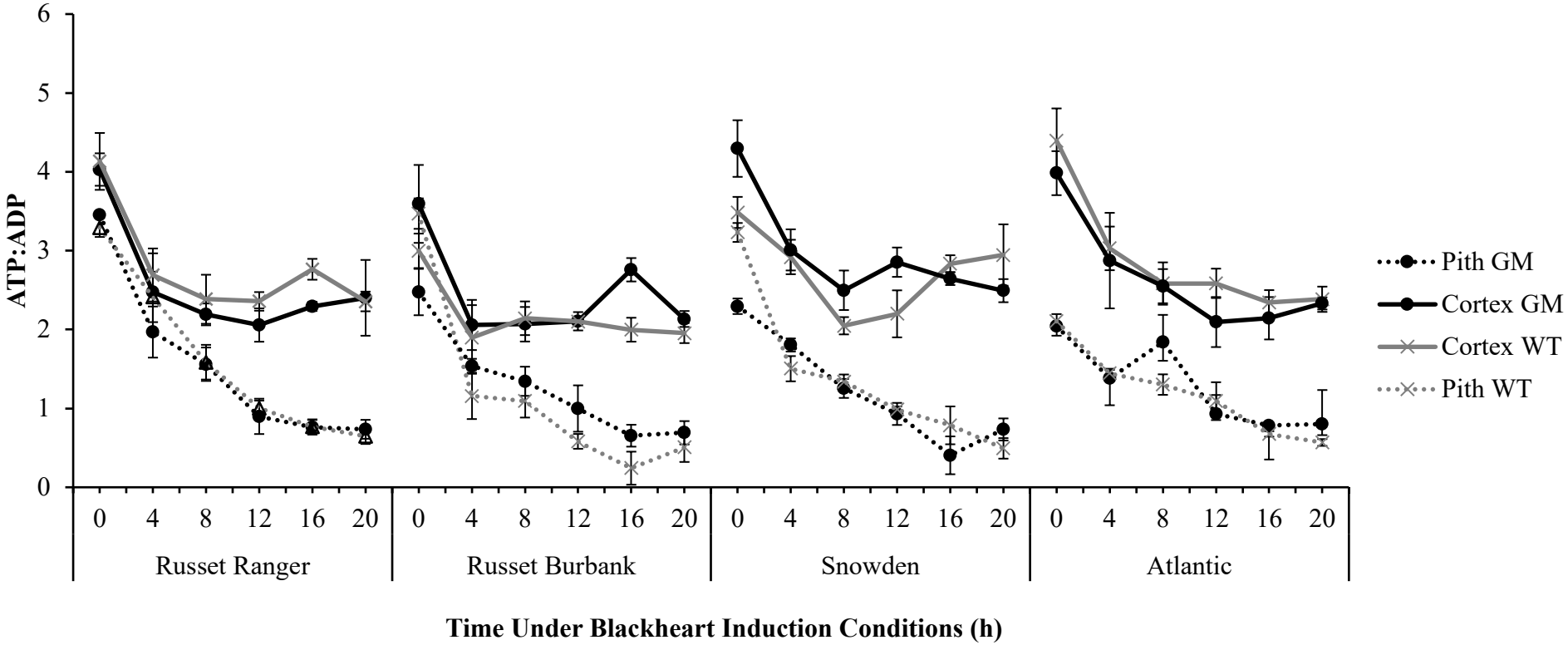


Figure 4.18: The ATP:ADP ratio in the pith and cortex tissues of eight tubers from both four tuber varieties from the US and their equivalent GM Innate® cultivars, incubated under Blackheart induction conditions. Error bars represent ± standard error of the mean.

4.2.7 Respiration Rate

Respiration rate was measured by sealing tubers in a gas-tight container and measuring the change in atmospheric oxygen within the container over time via a non-invasive Oxysense® oxygen analyser (Chapter 2). Tuber respiration rates were measured in three or 11-month old tubers, removed from under different storage conditions.

There was no significant difference in respiration rate between varieties in any of the measurements taken (Figures 4.19 & 4.20) (F test, $p<0.12$). However, significantly different respiration rates were identified between treatments (F test, $p>0.001$); the mean respiration rate across all tuber varieties at 2°C was (0.25 O_2%/h) 4°C (0.04 O_2%/h) and 37°C (0.86 O_2%/h).

Tuber respiration rate was significantly greater in tubers stored at 2°C for three months versus 4°C (t test, $p =0.001$) (Figure 4.19). Similarly, tubers that had been stored at 4°C for 11 months displayed greater respiration rates than those stored for three months (t test, $p =0.001$) (Figure 4.20). However, the highest respiration rate measured was in tubers stored at 37°C for 40 h (King Edward, 0.99 O_2%/h).

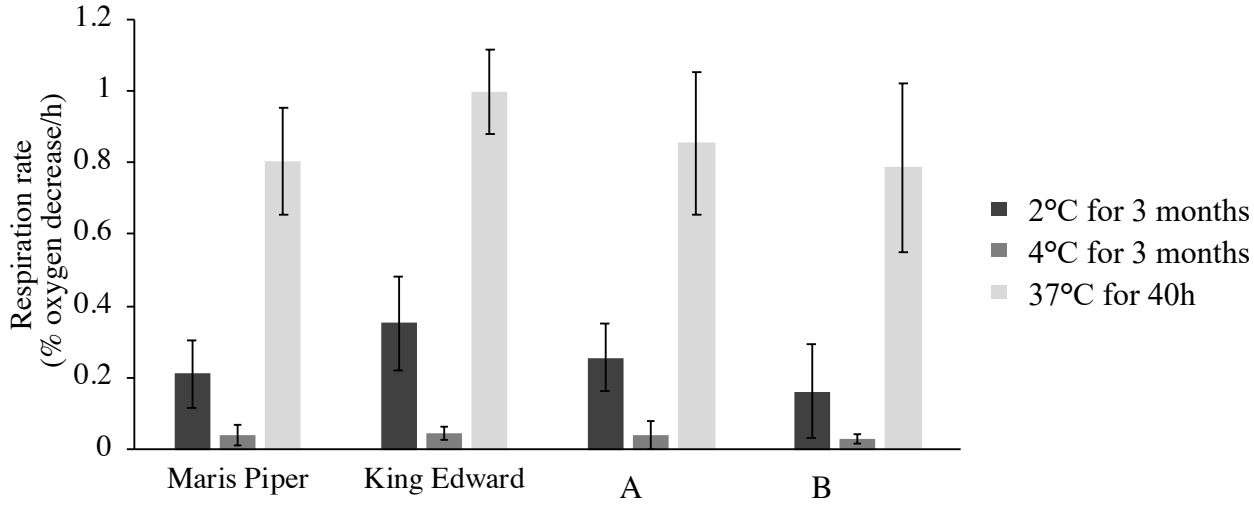


Figure 4.19: Respiration rates were measured in three-month old tubers stored at 2°C or 4°C for three months, or at 37°C for 40 h prior to measurements. The O_2% was measured from 3 hermetically sealed boxes containing 5 tubers both immediately after sealing and then after 4 h of incubation under each condition. Varieties A and B represent two UK varieties that have been obscured due to commercial sensitivity.

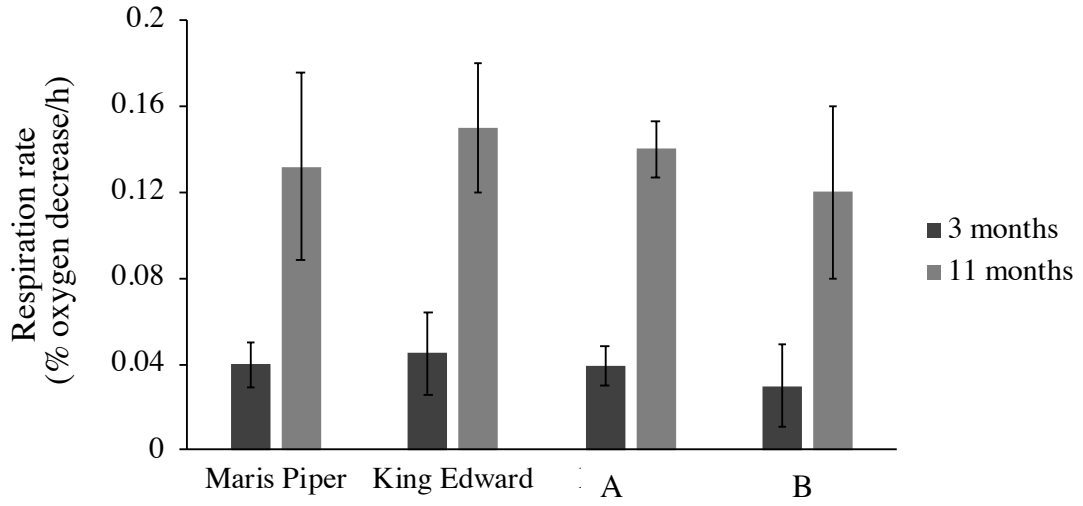


Fig 4.20: Respiration rates were measured in tubers stored at 4°C for 11 months prior to measurements. The O_2% was measured from three hermetically sealed boxes containing 5 tubers both immediately after sealing and then after 4 h of storage at 4°C. Varieties A and B represent two UK varieties that have been obscured due to commercial sensitivity.

4.3 Discussion

4.3.1 PPO Causes Blackheart Pigmentation

Experiments exploring the role of PPO in Blackheart development (4.2.1) were conducted on GM Innate ® tubers, developed by J.R. Simplot. Blackheart pigmentation did not occur in the Innate® *Ppo-5* knockout lines stored under Blackheart induction conditions, but was observable in the equivalent WT cultivars (Figure 4.3) which strongly suggests that the PPO enzyme that *Ppo-5* encodes causes Blackheart pigmentation. Additionally, the production of free radicals, which would indicate peroxidase activity, were not found to correlate with Blackheart induction, indicating PPO alone is responsible for the observable pigmentation (NBT and DAB staining in Supplementary data).

One caveat to this conclusion is the possible effect of the other genetic changes in the Innate lines (suppression *Asn-1* and *R1*). There is no obvious reason why the reduction in asparagine and sugar levels as a result of these genetic changes would impact upon Blackheart pigmentation since neither asparagine or sugars are substrates of PPO. It is conceivable that secondary changes in phenolic metabolites could have occurred, but for this to be responsible for the complete lack of pigmentation observed in the pith of Innate lines, all phenolic metabolites would have to be reduced to close to zero, which seems unlikely. Additionally, the down regulation of *Asn1*, nor *Ppo-5*, appeared to have no effect on the upstream causes of Blackheart; both Innate® and WT lines stored under Blackheart induction conditions are observationally identical when stained with Evans Blue and TTC (Figures 4.9 & 4.13) and display the

same ATP:ADP ratio response to Blackheart induction conditions (Figure 4.18). This suggests that the underlying changes to cell physiology and metabolism that occur during Blackheart development still occur in Innate® lines, despite a lack of visible pigmentation. There is also slight discolouration visible in the pith of Innate® tubers stored under Blackheart conditions (Figure 4.3), further indicating increased water content and cellular breakdown in the pith. Therefore, from these results, PPO driven pigmentation appears to be the final downstream effect in Blackheart. This involvement in Blackheart strongly suggests that changes in cell compartmentalisation and loss of membrane integrity occur during Blackheart development.

4.3.2 Phenolic Metabolite Abundance Does Not Appear to Have an Effect on Blackheart Susceptibility

For PPO substrate abundance to affect Blackheart incidence and susceptibility, the amount of phenolic metabolite/s would be expected to be greater in the pith of Blackheart susceptible varieties and lower in the cortex. Due to the lack of phenolic standard curves, absolute quantities of metabolites could not be calculated due to their likely differences in derivatization/ionisation efficiency. However, comparative analysis identified that the relative abundances of cinnamaic acid and phenylalanine (Figures 4.5 & 4.7) were greater in the pith prior to the induction of Blackheart relative to the cortex. Cinnamaic acid is produced from the conversion of phenylalanine (Figure 4.5) and ammonia by Phenylalanine Ammonia Lyase (PAL). PAL activity has been previously linked to enzymatic browning activity, by provision of downstream phenolic substrates for PPO (Vitti et al., 2011), however cinnamaic

acid itself appears to have inhibitory effects on potato PPO activity (Zhou et al., 2016) and therefore its abundance is unlikely to affect Blackheart distribution.

Tyrosine and chlorogenic acid are the main substrates for potato PPO due to abundance and PPO affinity (Stevens & Davelaar, 1997); chlorogenic acid makes up 90% the phenolic content of a tuber (Payyavula et al., 2015) and tyrosine is the most abundant building block of polyphenolic pigmentation (Stevens & Davelaar, 1997). However, neither chlorogenic acid nor tyrosine, significantly differ in amount between the pith or cortex of King Edward tubers (Figures 4.5 & 4.6).

Despite the previously proposed link between chlorogenic acid and Blackheart susceptibility (Kiaitsi, 2015) there is no direct evidence from this data that supports the hypothesis that phenolic metabolite concentrations influence the tissue-specific distribution or susceptibility of Blackheart. The changes to PPO activity that underlie Blackheart development in susceptible pith tissues are therefore likely to be due changes to the spatial separation of PPO and its substrates, rather than simply tuber substrate abundance and distribution.

4.3.3 Cell Death Occurs in the Susceptible Tissues During Blackheart Development

In Chapter 3, I proposed that the membrane permeability of Blackheart susceptible pith and parenchymal tissues increased during Blackheart development (Chapter 3), as apparent from increased water mobility, demonstrated by changes in the ACD and

T1-weighted MRI data for Blackheart affected pith and parenchymal tissues. This likely indicates loss of cellular compartmentalisation (Chapter 3).

The hypothesis that Blackheart involves changes to tissue structure is supported by the results presented in this chapter: histological staining of pith tissues of King Edward tubers with the non-permeable azo dye, Evans Blue, is suggestive of reduced membrane integrity and cell death (Mock & Baker, 1994). Due to the cell damage caused by slicing the tuber in half, all tissues were stained to some degree (Figures 4.8 & 4.9). However there was a clear increase in intensity of Evans blue staining beyond this background staining in Blackheart affected areas (Figures 4.8 & 4.9), indicating a greater abundance of damaged and non-viable cells.

Similarly, the extent of electrolyte leakage in the pith and parenchyma indicated complete cell death and loss of membrane function (Figure 4.10), corroborating the conclusions drawn from the distribution of the Evans blue stain (Figure 4.8). The viability threshold of electrolyte leakage, above which membrane permeability is assumed to be too great for cells to sustain or recover from, varies between tissue types and species; however, many tissues display a viability threshold of approximately 50% electrolyte leakage (Sage & Peixoto, 2015). Only the pith and parenchyma tissues of King Edward tubers displayed electrolyte leakage above 50% of the total tissue electrolytes, which correlated in time and distribution with Blackheart incidence at 12 h (Figure 4.10). Electrolyte leakage never exceed 50% of total electrolytes in any of the resistant tissues measured, including King Edward cortex tissues and all Maris Piper tissue types, supporting a possible electrolyte leakage viability threshold.

The ATP:ADP ratio of tubers under normoxia have previously been recorded to be 3:1, whereas under anoxia they fall to approximately 1:1 (Geigenberger et al., 2000). This is similar to the ratios that I observed in pith tissue for King Edward tubers: with an ATP:ADP ratio of just under 3:1 at time zero, which fell to around 1:1 during Blackheart induction (imposition of anoxia). Other tissues of King Edwards showed higher ATP:ADP ratios than this, but note that the sampling method used by Geigenberger et al. (2000) (longitudinal cores) leads to samples that are quantitatively dominated by pith tissue. The ATP:ADP ratio in the Blackheart susceptible pith and parenchymal tissues of King Edward tubers (Figure 4.16) and the pith tissue of the four varieties from the US (Russet Ranger, Russet Burbank, Atlantic, Snowden) (Figure 4.18) dropped below 1:1 after 12 h of Blackheart induction conditions, correlating with the induction of Blackheart in each variety (Chapter 3). ATP:ADP ratios below 1:1 indicate that ATP consumption exceeds production, signifying a cellular energy deficit and lack of cellular viability (Atkinson, 1968). All Blackheart resistant tissues maintain their ATP:ADP ratio above this 1:1 threshold (Figure 4.18). A threshold rate of ATP synthesis in tuber cell cultures under anoxia has previously been proposed (Rawyler et al., 1999); if ATP synthesis drops below 1.5-3% of that under normoxia (to approximately 10 μmol ATP per g/FW/h) cell death was shown to occur. The adenylate content of a cell cannot sustain itself beyond a few minutes, and ATP and ADP are rapidly catabolised (Roberts et al., 1984), therefore although this project only measured abundances, the declining adenylate contents (4.2.6) are indicative of reduced adenylate synthesis rates in Blackheart susceptible tissues. Therefore, these results and the work of Rawyler et al. (1999) support the existence of an ATP-synthesis-rate threshold in fermenting tubers, below which cell death occurs.

As well as reduced ATP:ADP ratios, declining ATP abundance has long been linked to cell death (Atkinson, 1968). In Blackheart susceptible tissues ATP declines by 21.3% prior to the induction of Blackheart (0 h-12 h), ultimately falling to just 3.5% of normal cellular ATP after 20 h of Blackheart induction conditions (Figure 4.14). Comparatively, the Blackheart resistant pith tissues from Maris Piper only decline by 37.3% (Figure 4.15). The ATP abundance in tissues with Blackheart, at 0.38nmol ATP, is orders of magnitude lower than the 20nmol/g/FW range of previously published ATP abundances in tubers stored under anoxia (Geigenberger et al., 2000).

Therefore, the extent of adenylate loss, adenylate abundance (Figure 4.14) and magnitude of membrane permeability (Figure 4.10) strongly indicate that susceptible tissues are dead after 20 h of Blackheart induction conditions. However, it may be possible that Blackheart susceptible tissues are still viable at 12 h and the degree of membrane leakage allows PPO-substrate mixing, without complete plasmolysis. Tissues continue to lose electrolytes and decline in ATP:ADP gradually after the onset of the disorder (12 h-20 h, Figures 4.10 & 4.14), rather than a cliff edge response. The observed gradual increase is likely to represent a growing proportion of dead cells within tissue discs and a non-homogeneous disc response, before total cells death at later time-points (Figure 4.10). Additionally, it is difficult to envisage how cells would be able to survive the extent of membrane damage that allows the diffusion of a 44 kDa PPO protein.

TTC is a common stain used to assess metabolic activity, and thus cell viability (Faridnia et al., 2015). Tetrazolium salts, are reduced by intracellular redox systems

into coloured insoluble derivatives. TTC accepts hydrogen atoms during NADH to NAD^+ oxidation via cellular oxoreductase enzymes, and is in turn reduced into a red formazan precipitate. As this process is reliant on a source of NADH and functional enzymatic activity, the coloured change provides information on the metabolic activity of tissues (Tan et al., 2015). The absence of formazan accumulation in the pith of susceptible tissues under Blackheart induction conditions (Figures 4.11, 4.12 & 4.13) suggests that there is reduced oxoreductase activity in these locations. Most oxoreductase activity is via enzymes in the mitochondrial electron transport chain and TCA cycle, however under anoxia TTC reduction would likely utilize lactate and alcohol dehydrogenases. It is possible that the Blackheart resistant tissues have greater fermentative flux which underpins the differential staining in the pith of a Blackheart susceptible variety. Alternatively, the positive charge of TTC facilitates uptake into cells via the plasma membrane potential (Tan et al., 2015). Instead the distribution of TTC staining could represent reduced chemiosmotic gradients in Blackheart susceptible tissues, either due to cell death and/or increased electrolyte leakage (Figure 4.10).

Collectively, the distribution of TTC and Evans blue staining, the electrolyte leakage and adenylate abundance all presented in this chapter strongly suggests that Blackheart involves cell death. Blackheart affected tissue has previously been proposed to be necrotic (Stewart & Mix, 1917; Bartholomew, 1913). However, the data that I have presented is insufficient to discriminate the type of cell death (i.e. necrotic versus programmed cell death). However, the sequential spread of Blackheart pigmentation, with a defined rather than a diffuse edge, is observationally

characteristic of the hypersensitive response in tubers (Gao et al., 2013) and thus could represent programmed cell death (PCD), as opposed to necrosis.

4.3.4 Respiration Rate and Blackheart Susceptibility

The use of O_2 depletion as a measure of respiratory rate could only be used to identify correlations between respiration and Blackheart susceptibility, rather than Blackheart induction due to the associated anoxic induction conditions. However, Blackheart induction conditions can be assumed to elevate respiration rate via elevated temperature (Figure 4.19) and the Pasteur effect.

Conditions that increase Blackheart susceptibility, such as tuber age or storage temperature (Chapter 3) (Briddon, 2015), also appear to drive elevated respiration rates in tubers (Figures 4.19 & 4.20). For example, potatoes stored at 2°C display increased susceptibility to Blackheart than those stored at 4°C (Chapter 3), correlating with elevated respiration rates as measured by both O_2 depletion (Figure 4.19) and CO_2 production (Burton, 1989).

These storage conditions do not appear to directly drive the onset of Blackheart, as the response of both Blackheart resistant and Blackheart susceptible varieties are not significantly different (Figures 4.19 & 4.20). However, it is possible that high respiration rates affect the degree of Blackheart susceptibility.

A potential explanation for this correlation could be that elevated respiratory rates are often driven by increased energy demands, lowering adenylate concentrations. The

adenylate threshold hypothesis proposed (4.3.3) emphasises the importance of the high initial ATP charge of Blackheart resistant tissues; the cortex tissue of King Edward tubers, and all tissues of the Blackheart resistant variety, Maris Piper, have significantly more ATP, and higher ATP:ADP ratios than Blackheart susceptible tissues (Figures 4.14 & 4.15). Therefore, if storage length or temperature decreases cellular adenylate abundances, then tubers are driven closer to the proposed threshold, increasing Blackheart susceptibility. This explanation can also help rationalise why a range of conditions affect Blackheart susceptibility, as many factors influence the energy status of cells.

It is not unreasonable to assume that the storage conditions that induce high respiratory rates also confer stress to potato tubers; it is probable that 2°C and 37°C temperatures, as well as extended dormancy in storage, are beyond the physiological ranges of potato tubers and therefore induce stress.

4.3.5 Do Increased Energy Demands, or a Reduced Energy Supply, Drive Blackheart Induction?

A decline in cellular ATP:ADP ratios could be driven by increased consumption or decreased production of ATP. Normally, cells equilibrate respiration and the flux through energy consuming pathways (Geigenberger et al. 2000; Zabalza et al., 2009). however, the declining ATP:ADP ratio under induction conditions indicates that Blackheart susceptible tissues are unable to maintain this balance (Figure 4.16).

It is possible that the declining ATP:ADP ratios in Blackheart susceptible tissues are driven by an inability to produce sufficient ATP under Blackheart induction conditions; high temperatures (Figure 4.19) and anoxia will force tissues into rapid fermentative respiration, which is substantially less efficient than aerobic respiration at producing ATP. Additionally, TTC staining suggests that Blackheart susceptible tissues may have less flux through the fermentative oxidoreductase enzymes under Blackheart induction conditions, and prior to the onset of Blackheart (Figure 4.12). Therefore, there may be reduced metabolic activity in pith tissues and ATP production in susceptible tissues under Blackheart induction conditions, driving cell death and membrane leakage.

Alternatively, it is possible that Blackheart induction conditions cause elevated energy demands in susceptible tissues. For example, it is possible that the increasing membrane permeability drives an increased consumption of ATP: energy is required to maintain cellular membrane function and physiology, the more electrolytes that leak from a membrane, the more ATP is utilised to pump ions and recover concentration gradients. Similarly, other energy-consuming processes such as biosynthesis or the removal of reactive oxygen species could be up-regulated in Blackheart susceptible tissues as a response of the high temperatures and/or stress of Blackheart induction conditions.

The rest of this thesis aims to identify the cause of cell death in Blackheart. Although it is not clear if the decline in ATP:ADP ratios or increases in membrane permeability occur first during Blackheart development, the lack of TTC staining in pith tissues appears to precede the onset of the disorder. Similarly, perturbation of ATP synthesis

in potato tubers has previously reduced membrane integrity, supporting this order of events (Crawford & Braendle, 1996; Rawyler et al., 1999). Based on these observations, this project will explore the hypothesis that metabolic limitations and/or insufficient energy supply drives cell death and Blackheart (Chapter 5).

4.4 Summary

Tubers with reduced Ppo-5 expression do not develop visible Blackheart symptoms indicating that PPO causes Blackheart pigmentation. This observation is further supported by changes in membrane permeability in the pith tissue of Blackheart affected tubers, which likely allows PPO-substrate mixing and subsequent pigmentation. There is no indication that the spatial distribution or abundance of phenolic substrates affects PPO activity.

During Blackheart induction, changes to the membrane permeability of pith tissues is correlated with a loss of energy homeostasis, ultimately driving cell death in Blackheart affected tissues. However, both Blackheart resistant varieties and tissue types are able to maintain energy homeostasis and membrane integrity during incubation under Blackheart induction conditions.

It is not yet clear if decreased energy supply to the pith tissue during Blackheart development limits the maintenance and function of membranes, or alternatively, if Blackheart induction conditions increase membrane permeability in the pith tissues, driving a higher energy demand. The remaining thesis chapters will aim to distinguish

between these two hypotheses of Blackheart development and differentiate between the cause and effect of the observations made in this chapter.

5 Does Insufficient Energy Production Lead to Blackheart?

5.1 Introduction

Blackheart susceptible tissues display declining adenylate energy status during the development of Blackheart. The adenylate energy charge and ATP:ADP ratios decline to such an extent that it is likely that this is responsible for the cell death that occurs during Blackheart (Chapter 4). It is currently unclear what drives this decline in cellular ATP:ADP ratios, because the consumption and production of energy in cells is normally well balanced (Geigenberger et al. 2000; Geigenberger, 2009). However, perturbations to potato ATP synthesis rates have previously been shown to be associated with increased membrane leakage and cell death (Crawford & Braendel, 1996; Rawyler et al. 1999). Therefore, the decline in ATP:ADP and reduction in membrane integrity in Blackheart susceptible tissues (Chapter 4) may be driven by an inability to produce sufficient ATP via respiration under Blackheart induction conditions. In the following sections, I discuss two alternative explanations as to why ATP synthesis could be decreased.

5.1.1 Insufficient Respiratory Substrates

The occurrence of Blackheart has previously been attributed to anoxic conditions (Bartholomew, 1913 Singh & Mathur, 1937; Briddon, 2015; Stewart & Mix, 1917; Kiaitsi, 2015) and tubers incubated under the Blackheart induction conditions chosen for this project (Chapter 3) can be assumed to be undergoing fermentative respiration due to the absence of oxygen. Under anoxic conditions, ATP is produced by

substrate-level phosphorylation and NAD^+ is regenerated during the conversion of pyruvate to lactate or ethanol. During anoxia, flux through the TCA cycle and mitochondrial respiration are significantly reduced (Rocha et al., 2010) and thus, less energy is produced; fermentative respiration produces only 2 mol ATP / mol glucose, as opposed to up to 36 mol ATP/ mol glucose under normoxia (Chapter 1).

The Pasteur effect is observed in several plant species (Gibbs & Greenway, 2003; Turner, 1951; Zabalza et al., 2009) and involves the rapid catabolism of carbohydrate reserves and increased glycolytic rate to meet cellular demands. Because of this, fermenting cells can use up to 20 times more glucose than those under normoxia (Kennedy et al., 1992). Under prolonged anoxia, this rapid catabolism may exhaust respiratory reserves completely (Gibbs & Greenway, 2003).

Given the likely accumulation of lower amounts of starch and sugars in central tissue tubers, it can be hypothesised that the Pasteur effect would exhaust carbohydrate reserves more rapidly in those tissues. Hence, one hypothesis is that the pith and parenchyma tissues are more susceptible to Blackheart due to more rapid exhaustion of carbohydrate reserves leading to an inability to maintain cellular energy balance and cell viability. This hypothesis is further supported by the recorded distributions of starch (Reeve, 1968; Sweetlove, 1995) and sugars (Bandana et al., 2016; Geigenberger, 2003) in potatoes, with lower abundances in central tissues. This distribution was proposed to be a hypoxic adaptation in the centre of tubers due to the diffusion pathway length between the tuber periderm and centre (Geigenberger et al., 2003). Imposed hypoxia was also demonstrated to reduce tuber tissue sugar contents in all potato tuber tissues (Geigenberger et al., 2003). Although Blackheart

pigmentation itself does not seem to be a function of tuber gaseous diffusion gradients (Chapter 3) it appears that pith and parenchymal tissues enter Blackheart induction conditions with fewer respiratory reserves, which may exacerbate their susceptibility. Therefore, it is possible that the higher abundance of respiratory substrates in Blackheart resistant cortex tissues sustains energy production and maintains the observed ATP:ADP ratios (Chapter 4) under Blackheart induction conditions.

Blackheart has long been associated with high respiratory rates (Chapter 4) (Stewart & Mix 1917; Davis 1926, Kiaitsi, 2015) and this proposed hypothesis can explain this correlation; elevated respiratory rates will require increased carbohydrate catabolism to provide respiratory substrates and may therefore ultimately increase Blackheart susceptibility. Tuber aging, storage at 2°C or high temperatures, and the rapid transition of tubers between temperatures all have been associated with high respiratory rates and evidence of increased Blackheart incidence (Chapter 4).

Tubers are over-wintering storage organs, providing carbohydrate and protein reserves that are mobilised during sprouting in the spring to support the growth of a new plant (Burton, 1989). During over-wintering, the tuber is dormant, but cell maintenance still requires energy and carbohydrate reserves are continually metabolised at low rates to support the dormant tissues during the winter (or during an imposed storage period in industry). This maintenance respiration could explain why Blackheart incidence and susceptibility increases with age/storage duration (Chapter 3), as older tubers have depleted respiratory reserves, and it may help explain why Blackheart is unable to be induced in tubers before a minimum of three months of storage (Chapter 3).

5.1.2 Respiratory Limitations

Although it appears that potato tubers do induce a Pasteur effect under anoxia, anoxic ATP synthesis is only 37.5% of the rate of ATP produced in normoxic potatoes (Geingenberger et al., 2003). Therefore, it is possible that, regardless of the abundance of respiratory reserves, susceptible tissues under Blackheart induction conditions have insufficient rates of ATP synthesis.

Additionally, there is some evidence supporting the presence of a metabolic limitation in Blackheart susceptible tissues, further limiting their ability to produce ATP under Blackheart induction conditions; the observable lack of TTC staining in pith tissues prior to the onset of Blackheart (Chapter 4) indicates that there may be reduced flux through the fermentative oxidoreductase enzymes of pith tissues under Blackheart induction conditions, which is indicative of a metabolic limitation. Previous work has identified reduced glycolytic flux in the centre of tubers due to hypoxia (Geigenberger et al., 2003).

Further support for the presence of a metabolic limitation in pith tissues of potato tubers can be found in the work of Malone et al. (2006), which demonstrated that cold storage (4°C) of potatoes resulted in dramatic respiratory changes, flux redistributions and reduced glycolytic rates, which were proposed to contribute to sugar accumulation via CIS (Chapter 1) (Malone et al., 2006). The sampling method utilised by Malone et al. (longitudinal cores) likely led to samples that were quantitatively dominated by pith tissue, and therefore these observations can be assumed to be

largely pith specific. Reductions in the glycolytic flux of tubers moved from 4°C storage to 25°C storage were observed, and shown to persist for at least 4 h after this transition. These conditions are similar to the transfer of tubers from 4°C storage into Blackheart induction conditions (37°C), or between 2-4°C cold stores in industry and approximately 22°C supermarkets, and therefore glycolytic fluxes may also be limited under these conditions. This reduction in glycolytic rate may limit the ability of tuber tissues to produce ATP, particularly if tissues are under anoxia and rely on rapid glycolytic flux via the Pasteur effect. Additionally, this hypothesis could explain why Blackheart cannot be induced unless tubers are first stored at low temperatures (Chapter 3).

Lastly, it is possible that even if there are no flux limitations and sufficient respiratory substrates, these may be inaccessible; sugar and starch are largely localised within vacuoles and amyloplasts, respectively, whereas glycolysis is mainly cytosolic (Farré et al., 2001). Therefore, it is possible that regardless of the abundance of respiratory substrates, ATP synthesis is limited by the availability of respiratory substrates in the cytosol.

5.1.3 Chapter Aims

The aim of the work described in this chapter was to investigate if the declining energy status of Blackheart susceptible tissues (Chapter 4) is caused by insufficient respiratory production of ATP. To do this, the work in this chapter will explore if Blackheart susceptible tissues have sufficient respiratory substrates during Blackheart development. For Blackheart to be driven by insufficient respiratory reserves in

susceptible tissues, it would be expected that the abundance of sugars and carbohydrates are significantly greater in the cortex versus the pith. Secondly, the work in this chapter aims to explore if any metabolic limitations exist that may reduce the rate of respiration and energy supply in susceptible tissues by identifying potential causes: firstly a glycolytic limitation could arise from the differential flux response of the pith and cortex to Blackheart induction conditions; and secondly, the Pasteur effect of Blackheart susceptible tissues may be limited by the maximal catalysis rate of glycolytic enzymes. For Blackheart to be driven by a limitation in the ability of susceptible tissues to produce ATP under Blackheart induction conditions, it would be expected that flux through glycolysis and fermentation is significantly greater in the cortex versus the pith. The results from this chapter will be used to refine the hypothesis behind the cause of cell death in Blackheart affected tissues.

5.2 Results

5.2.1 Fermentative Respiration

To confirm that tissues under Blackheart induction conditions were fermenting, the abundance of lactate was measured via untargeted GC-MS metabolomics (Chapter 2). Lactate accumulated in both the pith and cortex tissues after 4 h of incubation under Blackheart induction conditions indicating rapid onset of fermentation (Figure 5.1). There was no significant difference between the rate, or absolute amount, of lactate accumulation in the pith or cortex at any time point during incubation under Blackheart induction conditions (t tests, $p>0.8$). Lactate was present in similar abundances in the pith and cortex at 0 h of Blackheart induction conditions (t test, $p<0.00$).

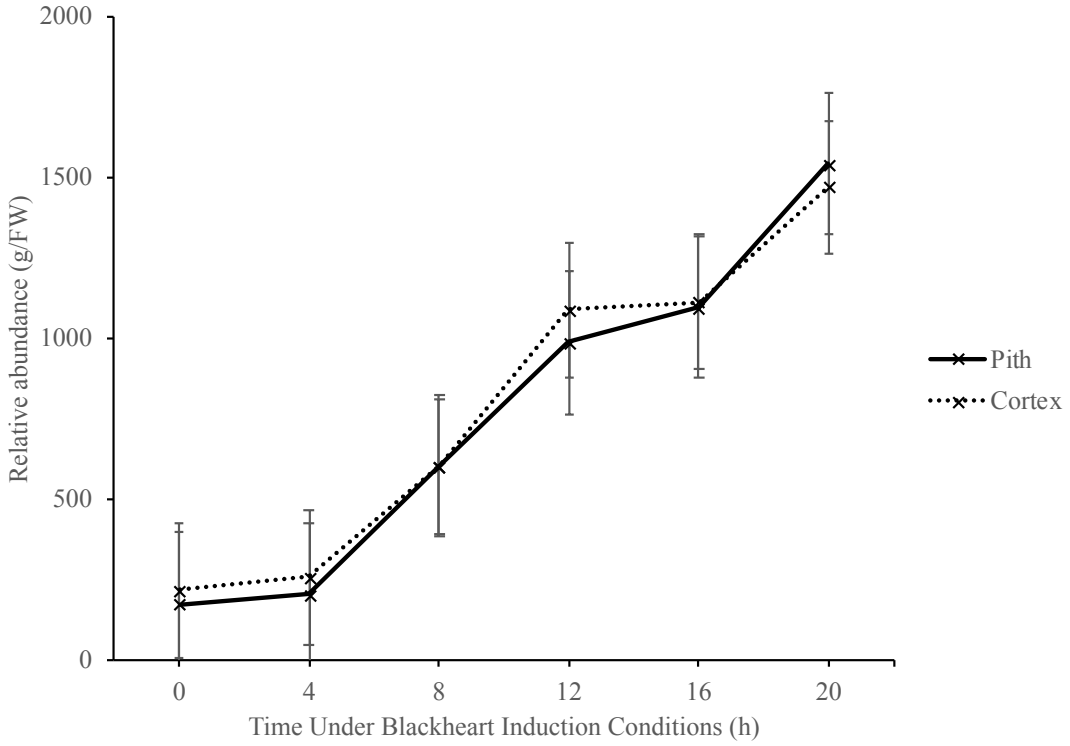


Figure 5.1: Abundance of lactate in pith and cortex tissues of King Edward tubers relative to internal standards and tissue weight during incubation under Blackheart induction conditions. Error bars ± standard error, n=6.

5.2.2 Quantification of Tuber Carbohydrate Reserves

The abundance of starch and sugars in the pith and cortex of King Edward tubers were measured by NADH-coupled spectrophotometric assays (Chapter 2). Starch was significantly greater in amount in the cortex of King Edward tubers than the pith (t tests, $p>0.00$), and did not significantly vary in either tissue type over time (F values, $p<0.8$) (Figure 5.2). Similar observations were found in the Blackheart resistant Maris Piper variety (data not shown).

Glucose, sucrose and fructose did not significantly differ between the pith and cortex tissues at any time point (Figure 5.3) (post-hoc multiple pairwise comparison t tests, $p>0.6$). However, transfer into Blackheart induction conditions (0 h versus all other time points, 4 h-20 h) resulted in a significant decline in the abundance of each sugar (F values, $p<0.012$) in both tissue types, to between 61-72% of the starting abundance in the pith, and 44-60% in the cortex.

When the sum abundance of total sugars (glucose, sucrose and fructose abundances combined) was considered, King Edward pith tissues had significantly more total sugars than the cortex (post-hoc multiple pairwise comparison t tests, $p>0.00$).

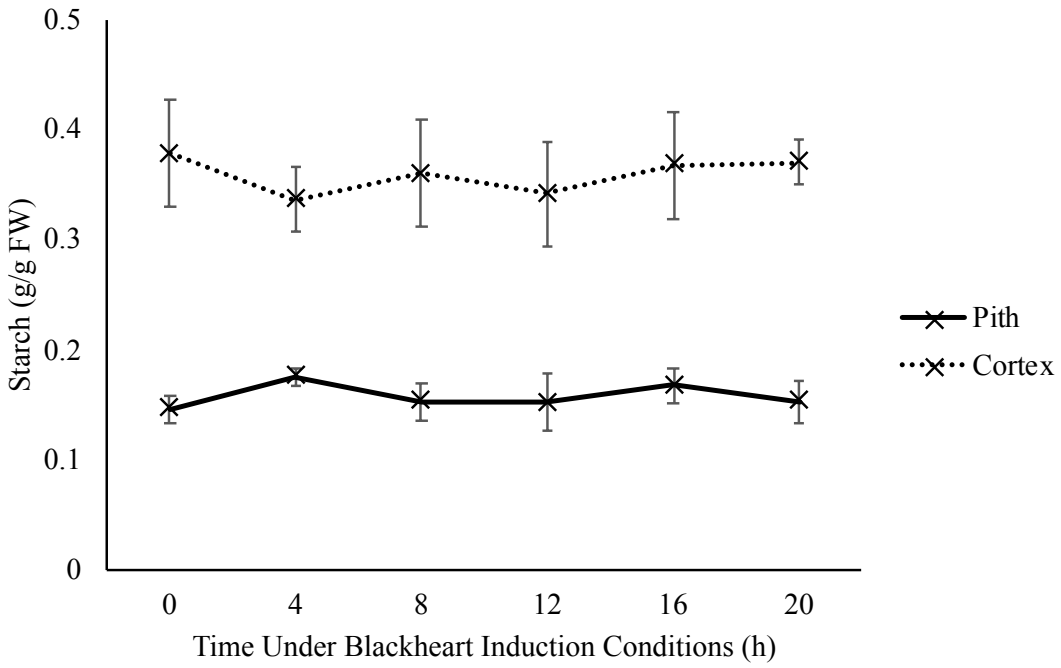


Figure 5.2: Abundance of starch in the pith and cortex of King Edward tubers incubated under Blackheart induction conditions. Error bars ± standard deviation, n=6.

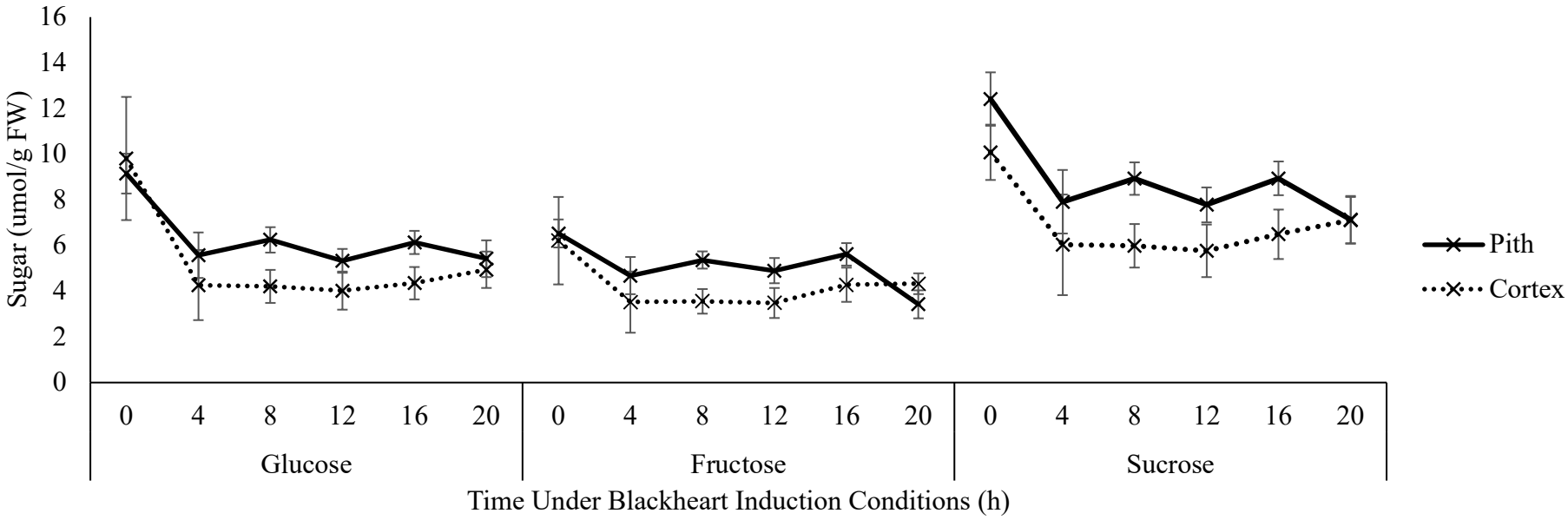


Figure 5.3: Abundance of glucose, fructose and sucrose in the pith and cortex of King Edward tubers incubated under Blackheart induction conditions. Error bars ± standard deviation, n>5.

5.2.3 Estimation of Fluxes Through Central Metabolism

King Edward tubers were incubated under Blackheart induction conditions (Chapter 2) for 0 h or 8 h before discs were taken from the pith and cortex tissues. These discs were then labelled with [U-^{14}C]glucose for 3 h whilst also under Blackheart induction conditions. Disc metabolism was then quenched, and tissues were fractionated as described in Chapter 2.

The recovery of the supplied ^{14}C label into the in soluble fraction was: Pith 0 h 45% ± 5.44%; Cortex 0 h 59.88% ± 4.11%; Pith 8 h 60.79% ± 3.5%; Cortex 8 h 55.15% ± 1.43%. The recovery of the supplied ^{14}C label into the insoluble fraction was: Pith 0 h 27.79% ± 1.48%; Cortex 0 h 32.04% ± 2.2%; Pith 8 h= 30.69% ± 5.24%; Cortex 8 h = 30.30% ± 2.25%. These recovery rates were comparative to those previously used and deemed sufficient for further analysis and fractionation (Malone et al., 2006).

To compare labelling patterns in different tissues and experimental conditions (0 h versus 8 h of Blackheart induction conditions) the ^{14}C recovered in each fraction was expressed as a percentage of the ^{14}C recovered in total fractions (minus glucose) from each sample, i.e. the percentage of metabolized ^{14}C (Table 5.1).

However, relative accumulation (Table 5.1) does not reflect the pool sizes of non-labeled metabolites and thus does not account for isotopic dilution (Malone et al., 2006). Therefore, to compensate for potential isotopic dilution, the specific activity of

the hexose phosphate pool was determined for both tissue types and time under Blackheart induction conditions. This was used to determine the rate of synthesis/carbon flux from the hexose phosphate pool into each fractioned metabolite class. The ^{14}C radioactivity in hexose phosphates was calculated by dividing the total radioactivity in the soluble neutral fraction by the total radioactivity in the acid phosphatase treated neutral fraction (Chapter 2). The specific activity of the hexose phosphate pool was calculated by dividing the radioactivity in the hexose phosphates by the total amount of hexose phosphates, which was then used to estimate the metabolic fluxes (nmol hexose phosphates/h) (Table 5.2).

For all samples, the specific activity of the hexose phosphate pool was a small proportion of the specific activity of the supplied labeled glucose, indicating dilution of the label by endogenous pools of sugars and sugar phosphates (Table 5.2). However, there was little variation in the specific activity of the hexose phosphate pools of different tissue types or incubation conditions (Table 5.2) (t test, $p>0.05$).

The ^{14}C radioactivity in various sugars was calculated as described in Chapter 2, and as follows: the ^{14}C radioactivity in fructose was calculated by subtracting the total radioactivity in the glucose oxidase treated neutral fraction from the total radioactivity in the hexokinase treated neutral fraction; the ^{14}C radioactivity in the total soluble sugars was calculated by adding the ^{14}C in sucrose with the ^{14}C in fructose, multiplied by two, which assumed that glucose was produced in an equimolar amount to fructose. The ^{14}C radioactivity in polysaccharides was calculated by the sum of the total radioactivity in the insoluble sugars, starch and cell wall. Flux into polysaccharides significantly declined in the pith tissues incubated under 8 h of

Blackheart induction conditions, versus 0 h, (t test, p =0.03) (Table 5.2).

The ^{14}C radioactivity in the phosphate esters was calculated by the subtraction of the total radioactivity in the soluble anionic fraction from the acid phosphatase treated cationic fraction. The sum of the total lipid, cell wall, starch, organic acids, phosphate esters, amino acids and protein was used to calculate the ^{14}C radioactivity into biosynthetic products; Flux into biosynthetic products significantly declined in the pith tissues incubated under 8 h of Blackheart induction conditions, versus 0 h, (t test, p =0.02), however no corresponding difference was found in the cortex tissues (t test, p =0.1) (Table 5.2).

The ^{14}C radioactivity into glycolytic products was calculated by the sum of the total CO_2, lipid, ethanol, organic acids, amino acids and protein. No significant difference was found between 0 h and 8 h of Blackheart induction conditions in the pith (t test, p =0.87) or cortex (t test, p =0.94). Similarly, within each time point neither the pith nor cortex were significantly different (0 h, t test, p =0.6) (8 h, t test, p =0.66).

Table 5.1: The effect of tissue type (pith versus cortex) and incubation under Blackheart induction conditions (0 h versus 8 h) on the metabolism of [U-^{14}C]glucose by King Edward tubers. n=4, ± standard deviation.

Metabolic fraction	**^{14}C in metabolic fractions from tuber discs (% metabolised ^{14}C)**			
	0 h + 3 h		**8 h + 3 h**	
	Pith	**Cortex**	**Pith**	**Cortex**
CO_2	3.03 ± 0.38	5.26 ± 1.34	4.17 ± 0.32	4.58 ± 0.33
Ethanol	0.03 ± 0.01	0.05 ± 0.01	3.34 ± 0.24	3.73 ± 0.33
Lipids	0.26 ± 0.06	0.38 ± 0.04	0.28 ± 0.02	0.25 ± 0.03
Sucrose	2.55 ± 0.60	3.99 ± 0.43	2.82 ± 0.12	2.39 ± 0.51
Hexose phosphates	2.93 ± 0.95	5.46 ± 2.13	3.91 ± 0.40	4.89 ± 0.61
Glucose	9.18 ± 1.38	10.43 ± 0.72	10.74 ± 0.67	11.49 ± 0.85
Fructose	1.12 ± 0.33	0.77 ± 0.29	1.13 ± 0.43	1.43 ± 0.49
Organic acids	0.63 ± 0.11	1.21 ± 0.18	0.33 ± 0.26	0.50 ± 0.40
Amino acids	1.30 ± 0.34	0.72 ± 0.18	0.51 ± 0.16	0.43 ± 0.13
Starch	0.91 ± 0.25	1.00 ± 0.16	0.66 ± 0.14	0.67 ± 0.22
Protein	0.17 ± 0.05	0.24 ± 0.05	0.22 ± 0.01	0.15 ± 0.02
Cell wall	0.12 ± 0.02	0.23 ± 0.03	0.17 ± 0.03	0.15 ± 0.05
Glycolytic products	5.41 ± 0.80	7.85 ± 1.22	8.86 ± 0.64	9.64 ± 0.98
Total soluble sugars	4.79 ± 1.12	5.53 ± 0.51	5.08 ± 0.83	5.24 ± 0.84
Polysaccharides	5.32 ± 1.27	6.76 ± 0.63	5.90 ± 0.97	6.06 ± 1.01
Biosynthetic products	3.38 ± 0.69	3.77 ± 0.49	2.16 ± 0.40	2.15 ± 0.40
Total absorbed	13.05 ± 1.34	6.79 ± 1.05	8.21 ± 0.17	9.00 ± 1.34
Total metabolised	12.81 ± 1.35	6.56 ± 1.07	7.96 ± 0.18	8.79 ± 1.32

Table 5.2: The effect of tissue type (pith versus cortex) and incubation under Blackheart induction conditions (0 h versus 8 h) on the metabolic flux in King Edward tubers, represented by the rate of accumulation of metabolites from the hexose phosphate pool calculated by the specific activity. n=4, ± standard deviation. *a* represents values in pith samples that are significantly different (p>0.05) between 0 h and 8 h, *b* represents values in pith tissues that are significantly different to cortex tissues within time points (0 h or 8 h)

Metabolic fraction	**Rate of accumulation of metabolites derived from hexose phosphate pool (nmol/g FW/h)**			
	0 h + 3 h		**8 h + 3 h**	
	Pith	**Cortex**	**Pith**	**Cortex**
CO_2	13.16 ± 1.41	11.79 ± 3.38	11.24 ± 1.05	13.01 ± 2.41
Ethanol	0.11 ± 0.04 *a*	0.12 ± 0.04	9.01 ± 0.71 *a*	10.65 ± 2.10
Lipids	1.10 ± 0.19	0.80 ± 0.10	0.75 ± 0.07	0.73 ± 0.018
Sucrose	10.73 ± 1.77	8.45 ± 0.88	7.58 ± 0.35	6.34 ± 0.95
Glucose	41.93 ± 8.89 *a b*	23.16 ± 4.74 *b*	28.99 ± 2.48 *a*	31.89 ± 4.13
Fructose	4.81 ± 1.23 *b*	1.88 ± 0.84 *b*	3.09 ± 1.30	3.80 ± 1.37
Organic acids	2.71 ± 0.48 *a*	2.47 ± 0.05	0.89 ± 0.71 *a*	1.82 ± 1.57
Amino acids	5.64 ± 1.49 *b*	1.55 ± 0.34 *b*	1.38 ± 0.42	1.22 ± 0.40
Starch	3.83 ± 0.95	2.21 ± 0.45	1.78 ± 0.43	1.74 ± 0.48
Protein	0.73 ± 0.15	0.50 ± 0.09	0.58 ± 0.02	0.42 ± 0.08
Cell wall	0.52 ± 0.07	0.47 ± 0.05	0.45 ± 0.09	0.39 ± 0.13
Total soluble sugars	20.35 ± 3.34 *a*	12.20 ± 2.15	13.77 ± 2.66 *a*	13.93 ± 1.90
Polysaccharides	24.70 ± 3.46 *a*	14.88 ± 2.54	15.99 ± 3.11 *a*	16.06 ± 2.27
Downstream glycolytic products	23.46 ± 3.12	17.22 ± 3.47	23.85 ± 1.99	27.84 ± 6.38
Biosynthetic products	14.54 ± 2.24 *a b*	7.99 ± 1.00 *b*	5.83 ± 1.14 *a*	6.32 ± 1.87
Specific activity (Bq/nmol % of applied glucose)	95.83 ± 3.70	99.83 ± 2.71	98.99 ± 3.99	104.53 ± 5.18

5.2.4 Maximum Glycolytic Enzyme Capacity

The maximum catalytic capacity of eight enzymes involved in fermentative respiration, glycolysis and production of respiratory substrates were measured via NADH coupled spectrophotometric assays (Chapter 2). Measurements from tissues taken from the pith tissue of King Edward tubers, incubated under Blackheart induction conditions for 0 and 8 h were compared (Figure 5.4). Enzyme activities were expressed using the units nmol/hour/g FW to allow comparison with fluxes calculated from the ^{14}C-labelling experiment (Section 5.2.3). There was no significant difference between the maximum catalytic capacities of any of the eight enzymes measured between 0 h and 8 h of Blackheart induction conditions (t tests, $p>0.82$). Maximum catalytic capacities of the enzymes were similar to those previously reported in potato tubers (Geigenberger et al., 1998; Veramendi et al., 2002; Burrell et al., 1994; Hajirezaei et al., 2000).

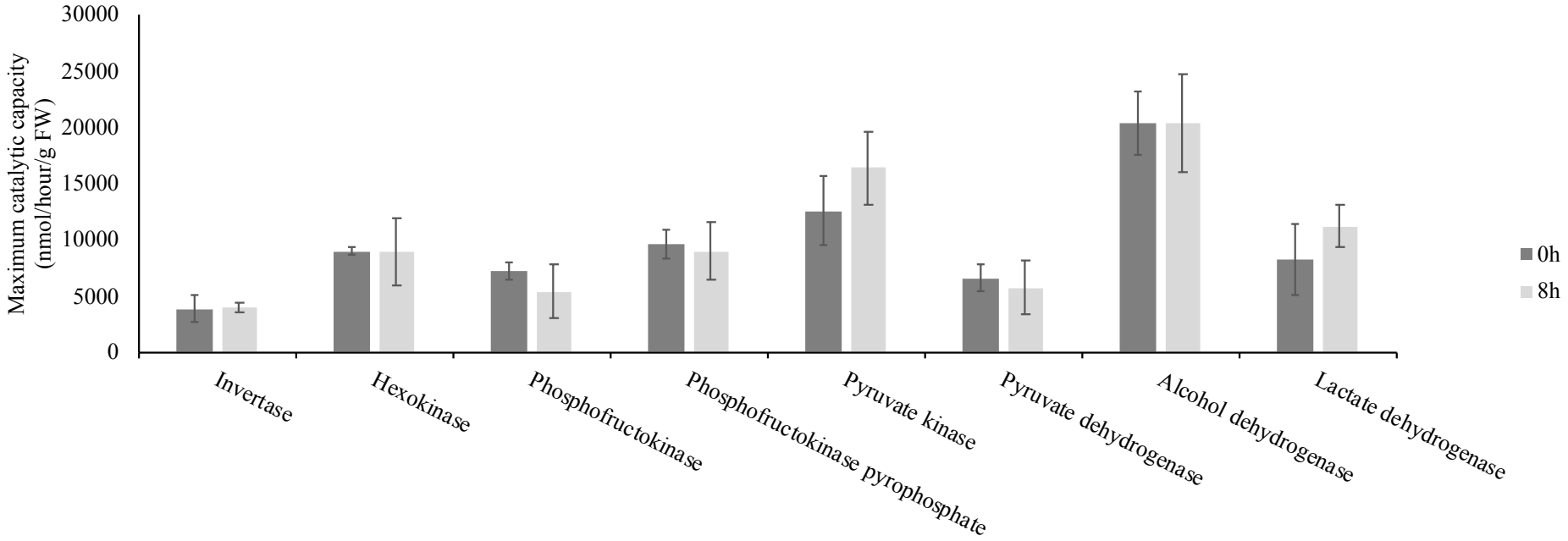


Figure 5.4: The maximum catalytic capacity of key glycolytic enzymes (nmol substrate turnover/hour/g fresh weight potato tissue) from pith tissues of King Edward tubers incubated under Blackheart induction conditions for 0 h or 8 h prior to measurements. Error bars ± standard deviation, n>6.

5.3 Discussion

5.3.1 Blackheart Susceptible Tissues Have Sufficient Carbohydrate Reserves

Both pith and cortex tissues appear to be fermenting under Blackheart induction conditions, due to the generation of lactate (Figure 5.1) and ethanol (Table 5.2). Despite previous studies proposing that central tissues are continually fermenting (Geigenberger et al., 2003) the relative abundance of lactate was not significantly different in the pith or cortex tissues (Figure 5.1), and nor was ethanol production greater in the pith tissues (Table 5.2), indicating no differential response in the tissues.

Both the cortex and pith tissues appeared to undergo fermentation after 4 h of Blackheart induction conditions (Figure 5.1), and this switch was met with an increased degradation of sugars, concurrent with a Pasteur effect. However, this decline was not sustained; no decline was observed in any of the sugars measured after 4 h of Blackheart induction conditions (4 h-20 h; Figure 5.3). It does not appear that these sugar reserves were maintained by increased starch turnover as no change in starch abundance (Figure 5.2) was observed in either the pith or cortex during Blackheart induction conditions. However, it is possible that the degree of starch abundance in potato tissues masked any visible degradation and a more sensitive method may have yielded different results.

Neither starch (Figure 5.2), nor sugars (Figure 5.3) were exhausted during incubation under Blackheart induction conditions; even after the visible onset of Blackheart (12 h) the abundance of carbohydrate reserves appeared sufficient. Additionally, pith

tissues displayed a significantly greater abundance of starch compared to the Blackheart resistant cortex. Therefore, from these results it appears that Blackheart susceptible tissues have sufficient abundance of respiratory substrates to maintain ATP synthesis throughout incubation under Blackheart induction conditions.

5.3.2 Blackheart Susceptible Tissues Show No Respiratory Limitations

The induction of Blackheart is not accompanied by a change in the rate of labelling of glycolytic or fermentative products during Blackheart induction (0-8 h), in either the pith nor cortex (Tables 5.2 & 5.3). This suggests that carbohydrate reserves remain accessible during incubation under Blackheart induction conditions (Figures 5.2 & 5.3) and no respiratory limitations are found in the pith tissues.

To maximum catalytic capacities of enzymes involved in fermentative respiration (chosen due to their roles in glycolytic regulation, substrate supply and energy production via fermentative respiration) were all notably greater than the fluxes towards metabolite pools derived from hexose phosphate pool (Tables 5.1 & 5.2); for example, in pith tissues incubated under Blackheart induction conditions for 8 h, only 23.85 ± 1.99 nmol of glycolytic products were produce per hour/g FW (Table 5.2), whereas the corresponding maximum catalytic capacities were much greater, with the lowest recorded rate at 3996 ± 492 nmol /h/g FW (Invertase) (Figure 5.4). However, the expression of fluxes relative to the specific activity of hexose phosphate pools (Table 5.2) assumes that no metabolic cycling occurs and that the hexose phosphate pools are at an isotopic steady state which is reached immediately during incubation.

Therefore the flux estimations (Table 5.2) are likely to be underestimated. Nevertheless, the very large difference between the flux measurements and maximum catalytic capacities recorded (Figure 5.4) suggest that, even with some underestimation of fluxes, it is likely that there is sufficient capacity within the metabolic network for larger fluxes.

No aspect of the results presented in this chapter support the hypothesis that pith tissues are unable to access their respiratory substrates, or that there is a limitation in glycolysis or the fermentative pathways that reduces ATP production during the development of Blackheart.

5.3.3 Insufficient Energy Production Does Not Appear to Drive Blackheart and Cell Death, However Increased Cellular Maintenance Demands Might

Both the rate of accumulation of lactate (Figure 5.1) and the estimated flux into the ethanol and CO_2 (Table 5.2) in the pith and cortex tissues under Blackheart induction are not significantly different. This indicates that, despite only the pith tissues developing Blackheart, the amount of ATP produced by Blackheart susceptible and resistant tissues under Blackheart induction conditions does not differ. Therefore, declining ATP:ADP ratios in pith tissues of Blackheart affected tubers (Chapter 4), does not appear to be caused by insufficient supply.

It was previously argued that, if the rate of supply of ATP did not significantly decrease in pith tissues during Blackheart induction conditions, then increases in ATP demand and utilisation would be expected instead (Chapter 4). Sources of ATP demand can generally be split into biosynthetic costs, i.e. the energy required for growth and building of complex molecules including proteins, cell walls and cell membranes, or into maintenance costs i.e. the energy required to maintain cellular function (Penning de Vries, 1975). From these results it appears that Blackheart susceptible tissues do not have elevated biosynthetic demands during Blackheart induction conditions; pith tissues display significantly decreased flux into biosynthetic products after incubation under Blackheart induction conditions (Table 5.2). This change in flux may be a diversion of carbon into energy producing pathways after application of Blackheart induction conditions and limitation of energy consuming reactions (Geigenberger, 2003). However, it indicates that energy demands from biosynthetic processes are unlikely to drive the declining ATP:ADP in pith tissues during Blackheart development (Chapter 4). Therefore, these results lead to the hypothesis that declining ATP:ADP ratios during Blackheart induction may instead be driven by increased maintenance costs.

5.4 Summary

Blackheart susceptible and Blackheart resistant tissues appear to produce the same amount of ATP during Blackheart induction conditions. No limitations in the rate of carbohydrate breakdown in pith tissues were observed, and there were sufficient reserves of accessible respiratory substrates throughout the development of Blackheart. The results in this chapter indicate that there are no limitations to the

production of energy in Blackheart susceptible tissues, and the declining energy status observed during Blackheart development is likely driven by ATP demands instead. Decreased flux into biosynthetic products in Blackheart susceptible tissues indicates that the ATP demands of maintenance costs may play a role in the declining ATP:ADP ratios observed during Blackheart development.

6 What Causes Increased Energy Demands in Blackheart Susceptible Tissues?

6.1 Introduction

It was previously proposed that the observed declines in ATP:ADP ratios of susceptible tissues during Blackheart development (Chapter 4) do not appear to be caused by reduced energy supply (Chapter 5) and thus appear to be instead driven by increased energy demands. Cellular energy demands can be separated into maintenance and biosynthesis costs (Penning de Vries, 1975). However, flux into biosynthetic products declined in susceptible tissues during Blackheart development, indicating that changes in maintenance processes may therefore drive increased energy demands and thus, a reduced adenylate energy charge.

6.1.1 Potential Causes of Increased Maintenance Costs

Maintenance costs are defined as the energy required for processes that are not associated with growth or a net increase in dry matter (Chiariello et al., 1989). These include: the general turnover and transport of organic compounds; the maintenance of ion gradients across membranes; and the physiological adjustment and repair of injury due to changes in the environment e.g. acclimation or both abiotic and biotic stress (Penning de Vries, 1974).

Most maintenance costs are calculated in photosynthetic (Lötscher et al., 2004) or rapidly growing tissues such as roots (Poorter et al., 1991), and therefore will not be representative of dormant storage organs such as potatoes. Additionally, the lack of

exogenous nutrient inputs into a harvested tuber means that a net increase in dry matter is not possible; therefore the biosynthetic fluxes observed in (Chapter 5) can be instead assumed to be result of the continual turnover of existing biomass. As the flux into 'biosynthetic products' declines during Blackheart development (Chapter 5), biomass turnover does not appear to be responsible for increased maintenance costs. Therefore, it is likely that either physiological adjustments to changing environments or ion gradient maintenance are possible causes of increased maintenance costs. The role of these two causes in the declining ATP:ADP ratio of Blackheart susceptible tissues will be addressed in this chapter.

6.1.2 Involvement and Respiratory Costs of Membrane Leakage in Blackheart

Membrane integrity and maintenance of ion gradients across lipid bilayers account for the majority of maintenance costs (Woods, 2014), and can make up almost 70% of plant respiration costs (Poorter et al., 1991). Ion and small molecule movement across the plasma membrane is an essential aspect of plant cell function, however a consequence of the fluidity of plasma membranes is ion leakage. Ion gradients are necessary for electrochemical potential and optimisation of conditions between intracellular compartments. Therefore, to maintain ion gradients in the face of continual basal leakage, ions are continually pumped back across membranes. Ions can be moved against their concentration gradient using ATP hydrolysis via primary or secondary active transport. In primary active transport carrier proteins can be directly phosphorylated via ATP hydrolysis, resulting in a conformational change and transport of molecules across the membrane. In secondary active transport, ATP

hydrolysis generates proton gradients across a membrane and the proton motive force pumps ions back across membranes via symport and antiport proteins. Active transport relies on ATPase enzymes, largely the P-ATPase in the plasma membrane and the V-ATPase in the vacuole.

It was previously shown that Blackheart susceptible tissues have increased electrolyte leakage prior to the onset of the disorder, and Blackheart pigmentation was only observed in tissues that displayed an electrolyte leakage ≥ 50% of total electrolytes (Chapter 4). Resistant varieties and tissue types appear to maintain membrane integrity during Blackheart development. It is not clear if electrolyte leakage increases prior to, or in tandem with, the onset of Blackheart (Chapter 4) however, these changes indicate that elevated costs from maintenance of ion leakage could be a contributing factor to declining ATP:ADP ratios. Alternatively, the declining ATP:ADP ratios may influence the ability of Blackheart susceptible tissues to restore membrane potentials.

It is possible that the elevated temperatures of the Blackheart induction conditions (37°C) drive this increased membrane leakage. Membrane fluidity increases at high temperatures and enables more movement of ions down their concentration gradients. Therefore, elevated temperatures drive increased respiratory costs and maintenance of ion gradients. Similarly, low temperatures (above freezing) can induce chilling injury which also results in increased membrane leakage (Wang, 1989; Parkin et al., 1989). Whilst the underlying cause of chilling injury is debated, temperature driven phase-transitions of cell membranes and a lack of membrane fluidity is thought to be the primary cause (Parkin et al., 1989). Chilling injury is dependent on the absolute

temperature the crop is exposed to, the duration of the exposure and the sensitivity of the crop to the temperature; chilling injury has been observed in potatoes stored at 1-0°C for several hours (Suslow & Voss, 1998) but also in tubers stored at 2-5°C for several months (Aguiar, 2012), and resulted in multiple symptoms, including Blackheart (Hruschka et al., 1969). This temperature dependent membrane leakage could explain why tubers stored at 2°C have increased susceptibility to Blackheart or why the disorder is only observed in tubers stored at 4°C for a minimum of three months (Chapter 3).

Lipid peroxidation may also contribute to low temperature membrane leakage in plants; tubers stored for over 7 months in 4°C were demonstrated to have reduced membrane integrity due to increased peroxidative damage to membrane lipids (Kumar & Knowles, 1993). Although this contribute to the age-related susceptibility of tubers to Blackheart, no increase in superoxide ions or H_2O_2 during potato Blackheart have been observed (Supplementary data), indicating that peroxidation is unlikely to drive Blackheart itself observed membrane leakage (Chapter 4).

6.1.3 Involvement and Respiratory Costs of Acclimation Responses in Blackheart

An important aspect of the temperature dependent nature of membrane leakage (6.1.3) is the varying degree of phospholipid fatty-acid saturation; a high proportion of polyunsaturated fatty acids leads to membranes that can retain fluidity at lower temperatures. However, altering phospholipid saturation levels requires breakdown and re-synthesis of the phospholipids, which typically takes several days (Falcone et

al., 2004). With short-term temperature transitions, mis-acclimated membranes become more rigid and phospholipids pack together tightly. This lack of fluidity enables electrolyte leak, particularly at the interface between the bilayer and membrane proteins (Brand et al., 2005), driving increased membrane permeability. To overcome this and maintain membrane function and ion gradients, tissues can acclimate to prolonged low temperatures by altering their degree of membrane lipid saturation. The steric effect of double bonds in fatty acid chains holds phospholipids further apart and increasing membrane fluidity. Similarly, the length of fatty acid chains effect membrane fluidity, with fewer stabilising van der Waal interactions between shorter hydrocarbons. Plants adjust the degree of phospholipid saturation and fatty acid length in response to changing temperatures and potato lipids have been demonstrated to become more desaturated when tubers are stored at lower temperatures (Sakai & Larcher, 1987).

The membrane acclimation response of plants to changing temperatures requires energy. Plants must remodel the plasma membrane by synthesising new lipids or modifying existing fatty acid chains via the Lands cycle. However, both reactions have high energy requirements; significant amounts of NADPH are required for the reduction of double bonds and ATP is required to generate the fatty acid substrate, malonyl-CoA. Additionally, acclimation to the new environment and synthesis of different metabolites drives an acclimation respiratory burst, where respiration rates significantly increase and then begin to fall after transition, as observed in potato tubers during storage (Spychalla & Desborough, 1990).

The potential role of acclimation in Blackheart and its effect on ATP:ADP ratios is twofold. Firstly, the transfer of tubers from 4°C cold storage to Blackheart induction conditions (37°C) may drive increased membrane permeability and thus ATP costs, due to the mis-acclimation of membranes to the new temperature. The degree of mis-acclimation could also explain why tubers stored at 2°C have increased susceptibility to Blackheart, or why the disorder is only observed in tubers that have been stored at 4°C prior (Chapter 3). Secondly, it is possible that the ATP costs of acclimation itself drive tissues below the proposed ATP:ADP ratio threshold and development of Blackheart (Chapter 4). Under these circumstances, it would be expected that Blackheart susceptible tissues have different membrane compositions, or acclimate slower, than resistant tissues and varieties.

6.1.2 Membrane Function Under Energy Stress

As well as the effects of temperature on membrane function, anoxia has been linked to increased membrane permeability. Reduction in both the absolute ATP abundance, and ATP synthesis rate via anoxic conditions have been shown to induce membrane damage in potato tuber cell cultures (Crawford & Braendle, 1996). Increased phospholipid breakdown and release of the FFA constituents indicated that lipid acyl hydrolase enzyme activity might be involved. However, these changes were also observed under normoxia when the ATP synthesis rate was artificially reduced, leading Rawyler et al., (1999) to propose that membrane lipid integrity relies on a threshold of ATP, below which a lipolytic acyl hydrolase (LAH) becomes activated. This threshold rate was suggested to be 1.5-3% of the overall theoretical ATP

synthesis rate under normoxia (Rawyler et al., 1999), which is comparable to the 93% decline in absolute ATP abundance observed in pith tissues during Blackheart (Chapter 4). The work in this thesis also indicates that Blackheart may be driven by a reliance on a threshold level of ATP, which correlated with increased membrane leakage and cell death in susceptible tissues (Chapter 4).

Additionally, lipid synthesis in potato tubers has been demonstrated to decline under anoxia largely due to the ATP and O_2 requirements fatty acid anabolism requires (Vartapetian et al., 1978; Brown & Beevers, 1987). A similar observation was made during storage under Blackheart induction conditions, where flux into lipids significantly declined after 8 h of Blackheart induction conditions, indicating decreased lipid synthesis (Chapter 5). The reduced flux into lipids observed in Blackheart susceptible tissues during the progression of Blackheart (Chapter 5) may further explain the reduced function of membranes; plant membranes are continually turned over (Steer, 1988) and if lipid synthesis is reduced, it is possible that the rate of membrane catabolism exceeds that of membrane anabolism. This is particularly pertinent if the rate of lipid degradation also increases via activation of LAH activity (Rawyler et al., 1999).

6.2 Chapter Aims

The aims of this chapter are to explore the connection between ATP:ADP ratios and membrane leakage in Blackheart susceptible tissues incubated under Blackheart induction. To do this, the role of increased maintenance costs will be considered, with a particular focus on the costs associated with maintenance of membrane gradients and acclimation responses. The work in this chapter will investigate the role of the

acclimation response by measuring respiratory rate and membrane composition in tuber under different temperature conditions and during Blackheart development. The importance of membrane gradient maintenance in Blackheart was indicated by the observation that susceptible tissues have increased electrolyte leakage prior to the onset of Blackheart (Chapter 4). The work in this chapter aims to investigate the cause of this membrane leakage by exploring the role of membrane hydrolysis, as previously described in anoxic tuber cells by Rawyler et al., (1999), as well as the role of reduced lipid synthesis in membrane function, as indicated by flux rates into lipids (Chapter 5). The work in this chapter will explore the metabolic costs of acclimation, or the costs of mis-acclimation, driven by the transfer of material from cold stores into Blackheart induction conditions, as factors that influence the consumption of ATP and Blackheart induction.

6.3 Results

6.3.1 Estimation of Flux Through Lipids

Reduced carbon flux into the lipid fraction of pith tissues under Blackheart induction conditions were previously observed (Chapter 5). To provide additional information, the labelled lipid fraction (as described in Chapter 5) was further fractionated via solid-phase extraction on aminopropyl columns into neutral lipid, FFAs and phospholipid components (Chapter 2) (Tables 6.1 & 6.2). The flux into the phospholipid component of pith tissues significantly declined between 0 h-8 h of Blackheart induction conditions (one sided t test, $p = 0.04$) by approximately 45%, whereas no change was observed in cortex tissues (t test, $p = 0.8$) (Table 6.2). This accounts for the majority of the reduced flux into pith tissue lipids. No significant change was observed in pith tissue flux into FFA between 0 h-8 h of Blackheart induction conditions, however it increased by approximately 29% in the cortex (one sided t test, $p = 0.02$) (Table 6.2). Blackheart induction conditions had no significant effect on the flux distributions into neutral lipids in any tissue type (Table 6.2).

Table 6.1 Effect of time under Blackheart induction conditions (0 h and 8 h) and tissue type (pith versus cortex) on the amount of ^{14}C incorporated into lipids (% of total metabolised U-^{14}C) by King Edward tubers. Each value is the mean ± standard errors, n=6 from tubers stored for 6 months prior to labelling.

		^{14}C incorporated into lipids (% of total metabolised U-^{14}C)			
		Total Lipids	**Neutral Lipids**	**FFA**	**Phospholipids**
0 h	**Pith**	0.261 ± 0.06	0.127 ± 0.019	0.063 ± 0.014	0.094 ± 0.021
	Cortex	0.374 ± 0.04	0.209 ± 0.028	0.089 ± 0.011	0.112 ± 0.018
8 h	**Pith**	0.277 ± 0.015	0.189 ± 0.109	0.085 ± 0.015	0.068 ± 0.01
	Cortex	0.253 ± 0.027	0.159 ± 0.012	0.095 ± 0.015	0.07 ± 0.016

Table 6.2 Effect of time under Blackheart induction conditions (0 h and 8 h) and tissue type (pith versus cortex) on the rate of accumulation of lipids derived from hexose-phosphate pool (nmol g/FW/h) into lipids by King Edward tubers. Each value is the mean ± standard errors, n=6 from tubers stored for 6 months prior to labelling. Asterisks indicate significant difference ($p>0.05$) between that value and all others in each lipid fraction.

		Rate of accumulation of lipids derived from hexose-phosphate pool (nmol g/FW/h)			
		Total Lipids	**Neutral Lipids**	**FFA**	**Phospholipids**
0 h	**Pith**	1.103 * ± 0.19	0.546 ± 0.058	0.273 ± 0.056	0.411 * ± 0.082
	Cortex	0.801 ± 0.103	0.430 ± 0.04	0.188* ± 0.016	0.239 ± 0.037
8 h	**Pith**	0.751 ± 0.067	0.511 ± 0.048	0.229 ± 0.042	0.184 ± 0.028
	Cortex	0.728 ± 0.176	0.432 ± 0.034	0.258 ± 0.041	0.196 ± 0.042

6.3.2 Quantification and Identification of Phospholipids and FFA Composition During Blackheart

Tubers were incubated under Blackheart induction conditions for 0-8 h and discs sampled from the pith and cortex tissues. Lipids were extracted via chloroform-methanol extraction and separated into FFA, phospholipids and neutral lipids via solid-phase extraction on aminopropyl columns (Chapter 2). Each fraction was quantified via both a SPV assay and GC-MS.

SPV assays involved the derivatisation of unsaturated lipids with sulphuric acid at high temperatures, producing carbonium ions. The addition of phosphor-vanillin generates a single pink chromophore per each unsaturated molecule which was used to estimate the amount of lipid in each fraction against a known concentration of oleic acid (C18:1). It should be noted that this method produces a single chromophore for each unsaturated molecule, regardless of the number of double bonds (Knight et al., 1972). Thus, as saturated lipid molecules cannot be measured through this assay, the results only yielded estimates of the abundance of each lipid class, rather than absolute amounts.

Therefore, GC-MS was used to quantify and ID each lipid from each fraction. Heptadecanoic acid was applied to each sample as an internal standard and fractions were derivatised to form Fatty Acid Methyl Esters (FAME's). Samples from each fraction were analysed using GC-MS and quantified via comparison to standard curves of each fatty acid and normalisation to fresh weight and the internal standard.

The pith and cortex tissues contained similar amounts of total lipids (t test, p =0.03), and phospholipids compromised 57-67% and 66% of these respectively. Pith tissue phospholipids declined in abundance after 8 h of Blackheart induction conditions (one sided t test, p<0.00), which was not observed in the cortex (t test, p =0.9). This decline was largely due to reduced abundance of phospholipids containing linoleic (C18:2) and linolenic acids (C18:3) in the pith tissues during Blackheart induction. Total phospholipids declined in the pith by 217 μg/g FW after 8 h of Blackheart induction conditions (Figures 6.1 & 6.3).

FFA compromised 2-5% and 2% of total lipids in the pith and cortex respectively. Cortex FFA did not change over time under Blackheart induction conditions (t test, p =0.8), however both linoleic (C18:2) and linolenic acids (C18:3) significantly increased in the pith (one sided t test, p<0.00). Total FFA increased in the pith by 65 μg/g FW after 8 h of Blackheart induction conditions (Figures 6.2 & 6.4).

Whereas GC-MS measurements involved the fragmentation of phospholipids into individual fatty acid constituents (Figure 6.3), the SVP assay measured each phospholipid. Proportional declines in phospholipid abundance and FFA increase were observed in the pith tissues (Figure 6.5) and a similar lack of change in resistant tissues and varieties (Figures 6.5 & 6.6). The ratio of FFA release to phospholipid decline during 0-8 h of Blackheart induction conditions in pith tissues of King Edward tubers was 2.18:1 (Figures 6.3 & 6.4). No significant changes were observed in the total lipids, phospholipids or FFA abundance in any Maris Piper tissues under Blackheart induction conditions (t tests, p>0.07) (Figure 6.5).

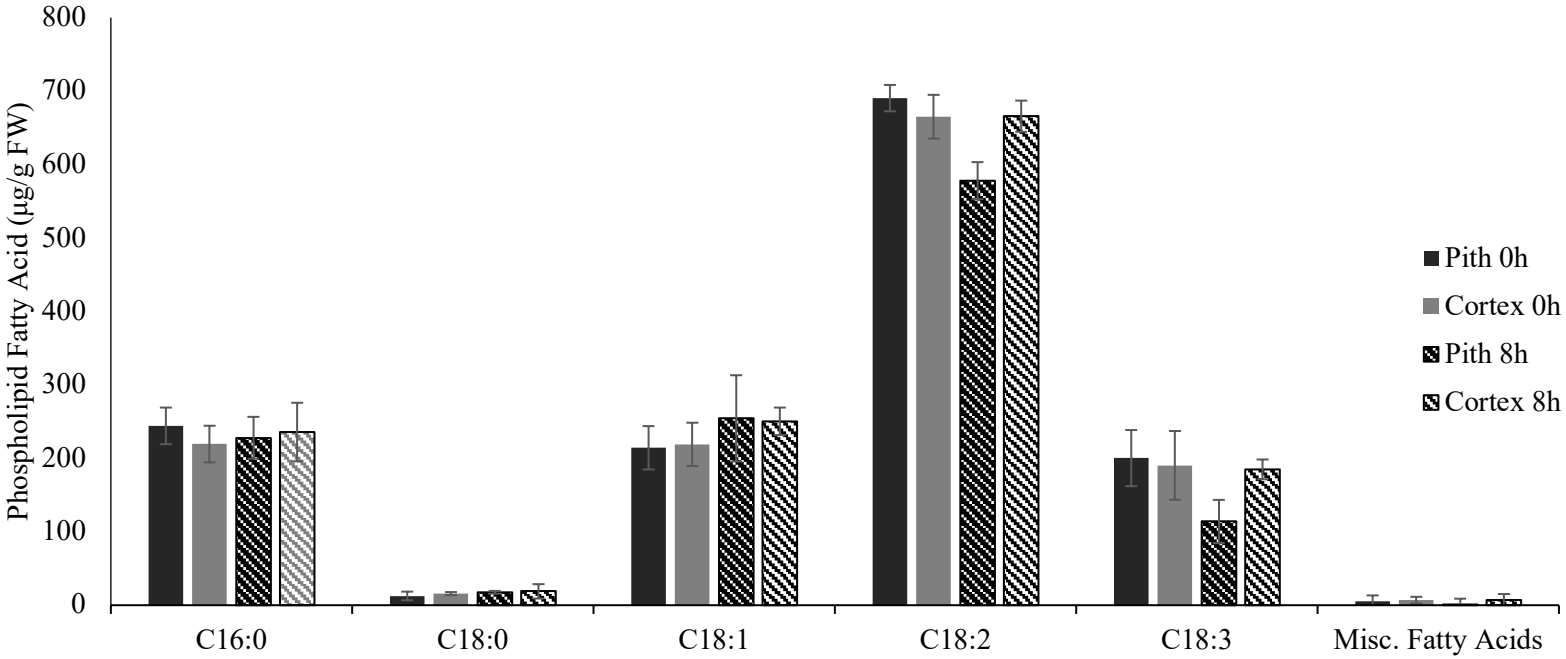


Figure 6.1: Phospholipid derived fatty acid identification and quantification (µg/g FW) via GC-MS in pith and cortex tissues of King Edward tubers incubated under Blackheart induction conditions (0 h versus 8 h) prior to analysis. n=6, error bars represent ± standard deviation.

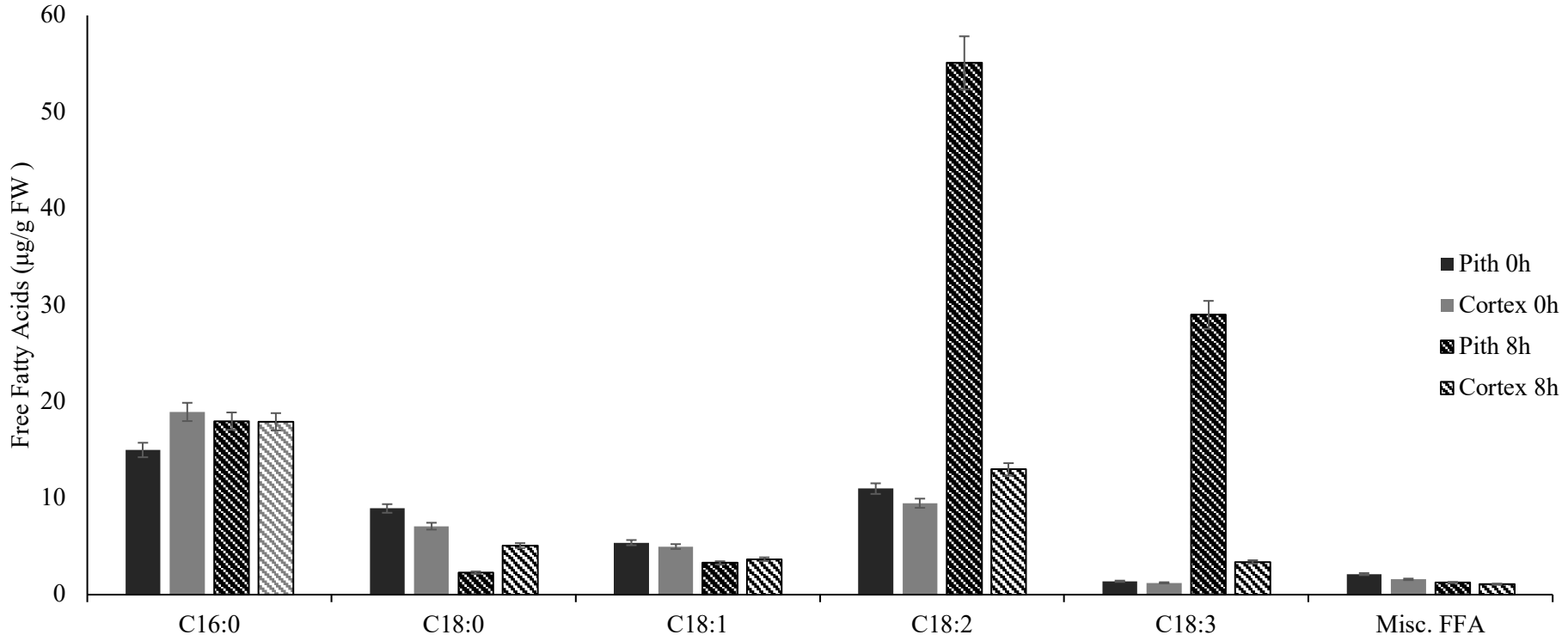


Figure 6.2: Fatty acid identification and quantification (µg/g FW) from the Free Fatty Acid fraction via GC-MS in pith and cortex tissues of King Edward tubers incubated under Blackheart induction conditions (0 h versus 8 h) prior to analysis. n=6, error bars represent ± standard deviation.

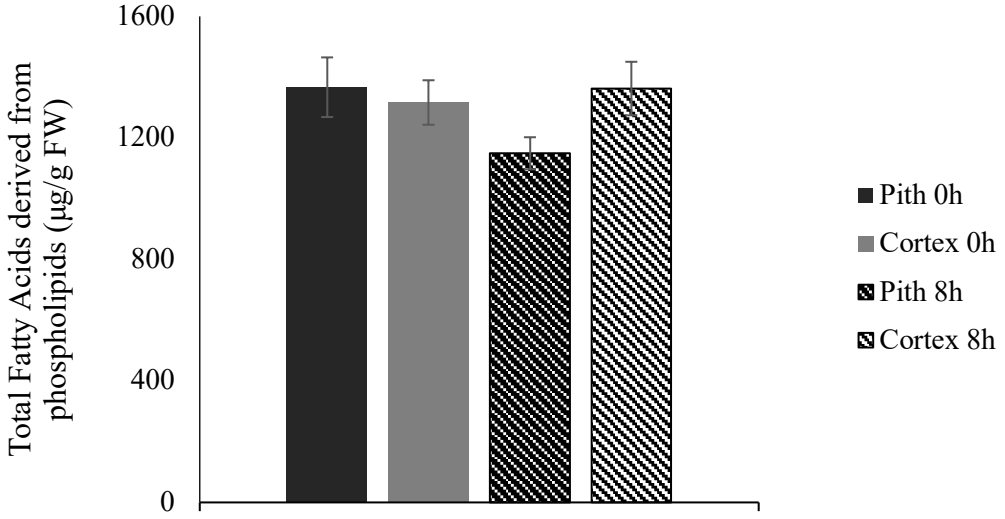


Figure 6.3: Total Fatty Acids derived from the phospholipid fraction (µg/g FW) via GC-MS in pith and cortex tissues of King Edward tubers incubated under Blackheart induction conditions (0 h versus 8 h) prior to analysis. n=6, error bars represent ± standard deviation.

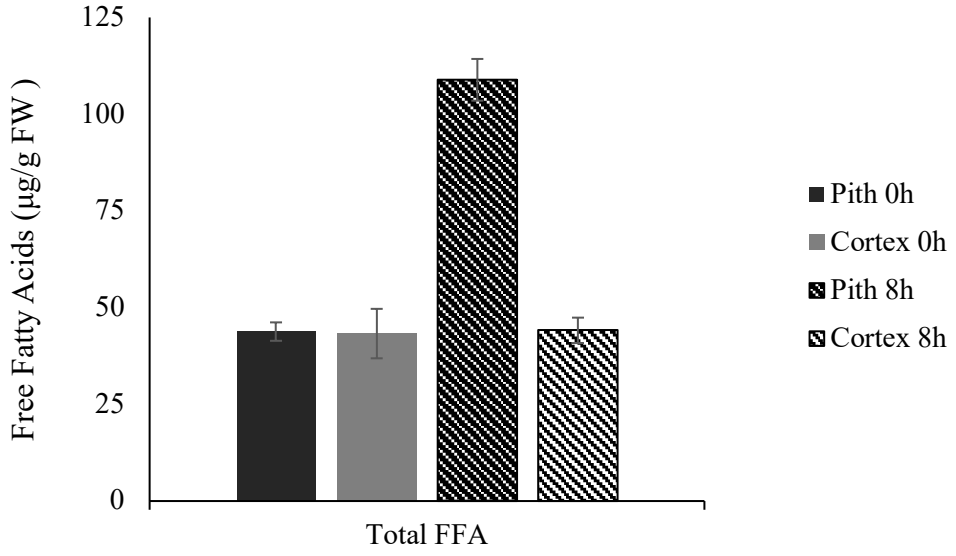


Figure 6.4: Total Fatty Acids derived from the FFA fraction (µg/g FW) via GC-MS in pith and cortex tissues of King Edward tubers incubated under Blackheart induction conditions (0 h versus 8 h) prior to analysis. n=6, error bars represent ± standard deviation.

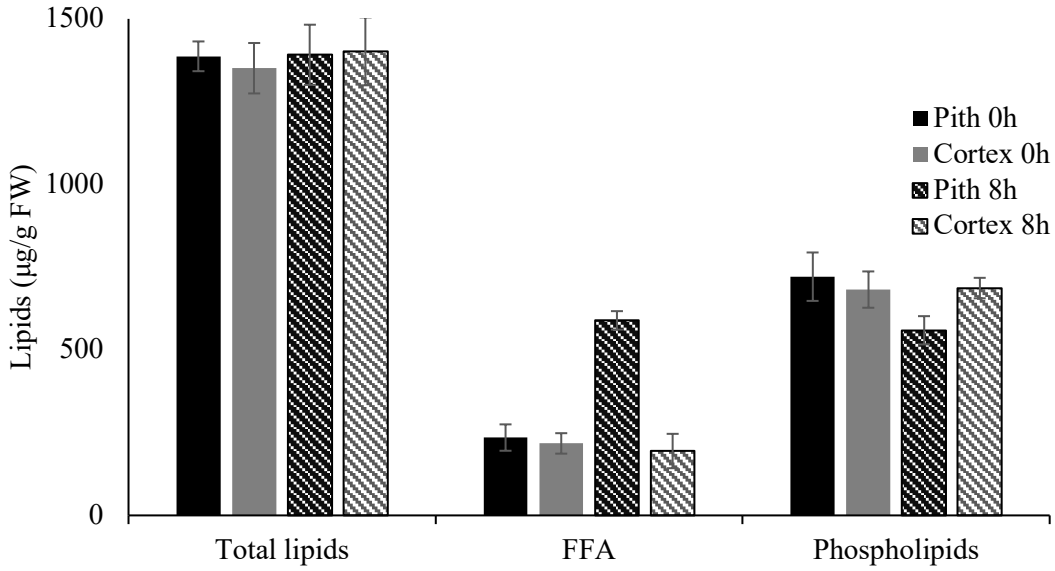


Figure 6.5: Total lipids in each fraction (µg/g FW) estimated via a SVP assay in pith and cortex tissues of King Edward tubers incubated under Blackheart induction conditions (0 h versus 8 h) prior to analysis. n=6, error bars represent ± standard deviation.

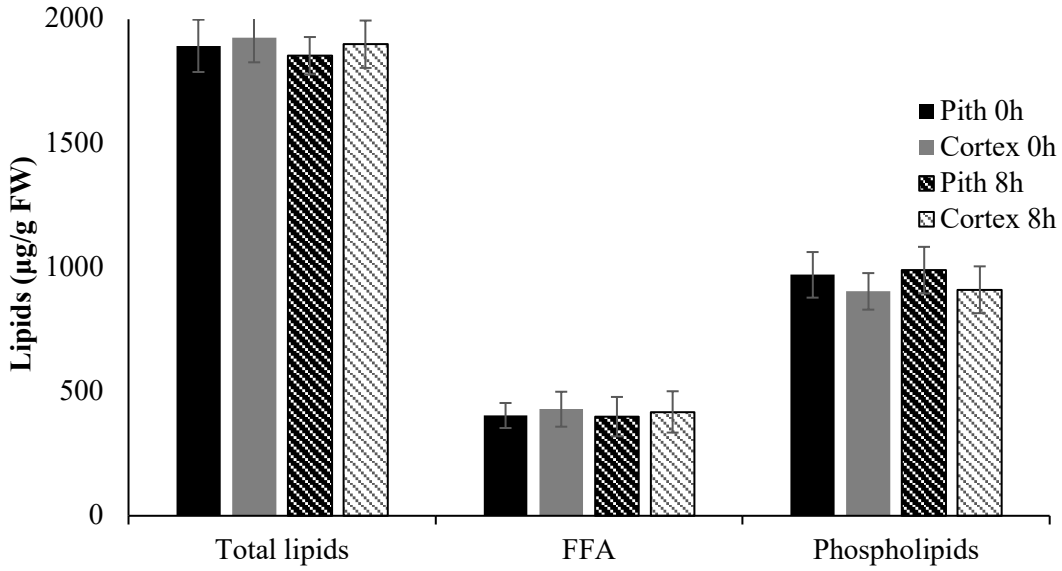


Figure 6.6: Total lipids in each fraction (µg/g FW) estimated via a SVP assay in pith and cortex tissues of Maris Piper tubers incubated under Blackheart induction conditions (0 h versus 8 h) prior to analysis. n=6, error bars represent ± standard deviation.

6.3.3 Effect of Storage Temperature on Membrane Permeability and Composition

The double bond index is a common measure of the length, saturation and abundance of fatty acids (Chapter 2); acclimated membranes at low temperatures have a greater double bond index than those at warmer temperatures (Sakai & Larcher, 1987). The double bond index of total fatty acids from the phospholipid fraction was calculated to assess the fluidity of the cell membrane in each sample. Pith tissues decreased in double bond index from 0-8 h of Blackheart induction conditions (Figure 6.7), due to the proportional loss of 18:2 and 18:3 fatty acids, and an overall decline in total phospholipids (Figure 6.1). Prior to Blackheart induction, 4°C stored pith tissues display a lower double bond index than either the pith or cortex tissues stored at 2°C (t tests, $p>0.04$). There was no significant difference (t test, $p =0.09$) in double bond indexes between the cortex and pith tissues stored at 2°C.

When 2°C stored tubers were compared to 4°C material both the pith (t test, $p =0.02$) and cortex (t test, $p =0.04$) had significantly greater electrolyte leakage (0 h, Figure 6.8). This difference was less pronounced after incubation under Blackheart induction conditions, and as previously observed (Chapter 4), both Blackheart susceptible tissues displayed greater electrolyte leakage than Blackheart resistant tissues (t tests, $p>0.05$).

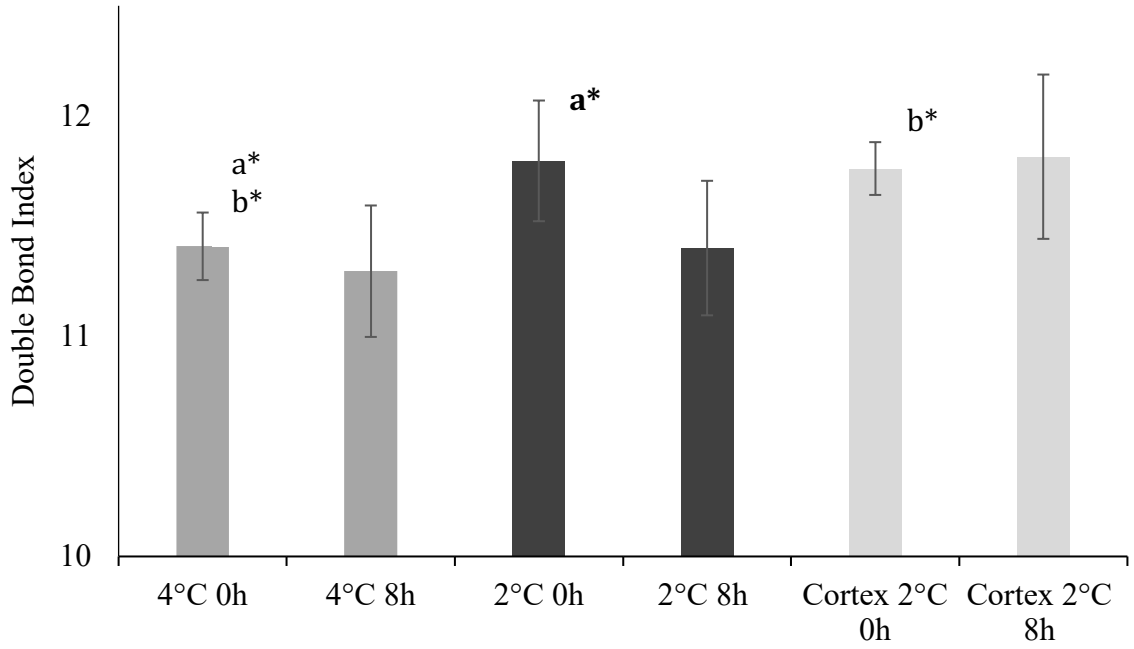


Figure 6.7: Double bond index of phospholipid fractions from King Edward tissues stored under different conditions (4°C for 8 months; 2°C for 8 months) before incubation under Blackheart induction conditions for 0 h-8 h. n>5, error bars represent ± standard errors. a* and b* are significantly different between eachother (t test, $p<0.05$).

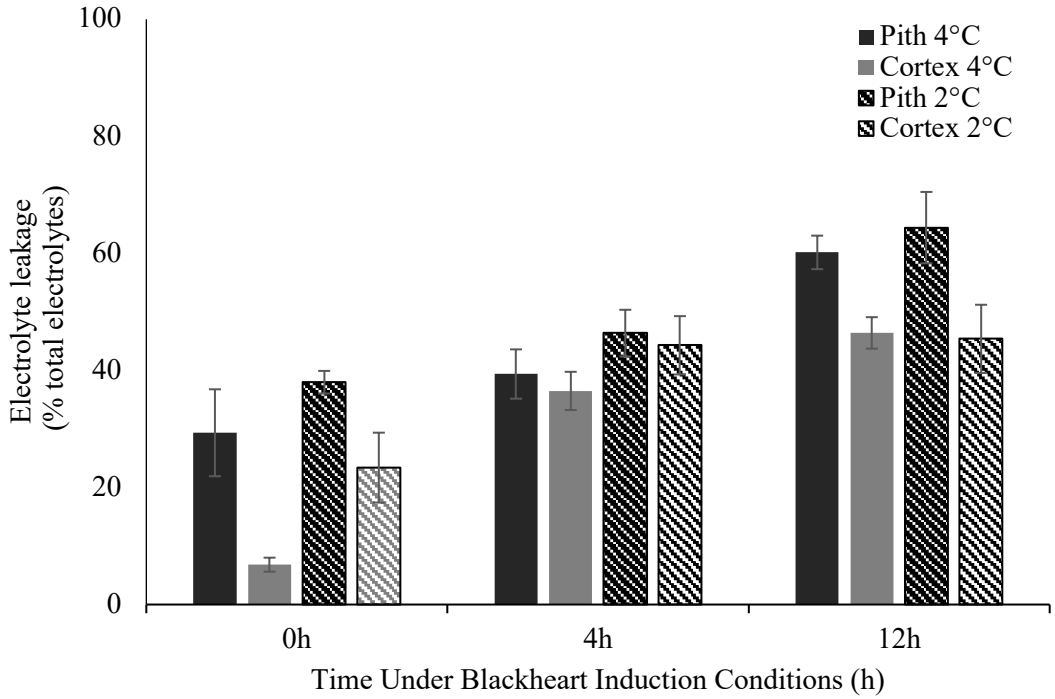


Figure 6.8: Electrolyte leakage of King Edward tissues stored under different conditions (4°C for 8 months; 2°C for 8 months) and times (0 h, 4 h and 12 h) before incubation under Blackheart induction conditions (37°C, anoxia) for 0 h-8 h. n=4, error bars represent ± standard errors.

6.3.4 Serine Hydrolase Activity Based Protein Profiling

Enzymes involved in the Lands cycle, connecting phospholipid breakdown and FFA release, are all members of the serine hydrolase enzyme family. Therefore, to investigate the direction the Lands cycle equilibrium had shifted under Blackheart induction conditions, and which enzymes were responsible for the altered membrane composition observed (6.3.3), *in vivo* ABPP involving the specific labelling of active serine hydrolase enzymes was conducted. Maris Piper and King Edward tubers were incubated under Blackheart induction conditions for 0 h or 8 h before discs were cut from pith and cortex tissues under a stream of N_2 and with a heat lamp ensuring Blackheart induction conditions were maintained. Discs were bathed in a buffered, isotonic system with 0.2 μM TAMARA FP probe, which binds covalently to accessible active sites of serine hydrolase enzymes. As TAMARA FP probes also contain a fluorescent tag, the intensity of fluorescence is relative to the activity of the serine hydrolase enzymes. Proteins were extracted, and the protein concentration used to standardise each sample before proteins were resolved via 15% SDS-PAGE gel electrophoresis. Gels were first imaged for in-gel fluorescence, representing the relative activity of the resolved serine hydrolase enzymes, before staining with coomassie, revealing the in-gel abundance of all resolved proteins.

The data demonstrates that the activity of a serine hydrolase enzyme, between 35-45 kDa in size, increased in pith tissues of King Edward tubers after Blackheart induction conditions (Figure 6.9). No changes in activity of this enzyme were

observed in Maris Piper tissues, or the cortex tissues of King Edward (Figures 6.9 & 6.10). No variation in the corresponding protein abundance (35-45 kDa) was observed (Figures 6.12). Quantification of the in-gel fluorescence and coomassie staining (Gel layouts in Supplementary Data) indicated that activity of the protein of interest increased by 21% after 8 h of Blackheart induction conditions in the pith tissue of King Edward tubers (Figure 6.11) which was significantly greater than the activity at 0 h in the pith of King Edward tubers (t-test, $p = 0.03$). However, there was no corresponding increase in protein abundance (Figure 6.12) and no significant changes between the cortex tissues of King Edward tubers after 0 or 8 h of Blackheart induction conditions (t-test, $p = 0.9$), or in the pith tissues of Maris Piper tubers after 0 or 8 h of Blackheart induction conditions.

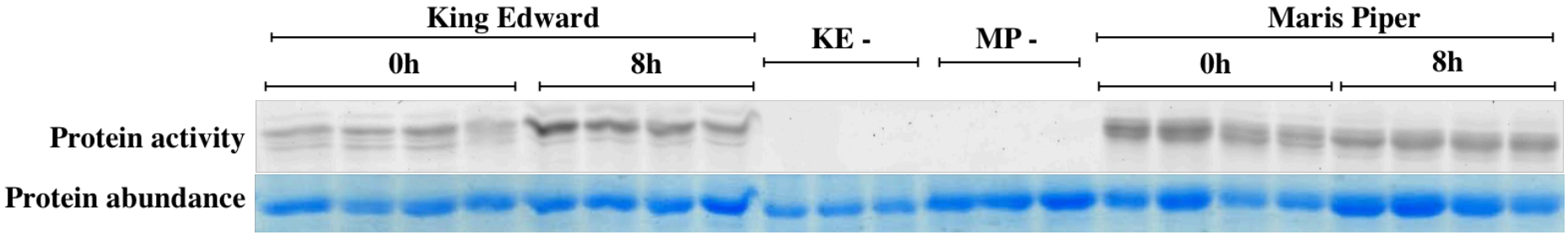


Figure 6.9 Activity of serine hydrolase enzymes and protein abundance from King Edward and Maris Piper pith tissues incubated under Blackheart induction conditions for 0 h or 8 h and then incubated with TAMRA-FP probe, or DSMO (negative controls; KE- and MP) for 15 minutes. Proteins were resolved via SDS-PAGE and TAMRA-FP labelling visualised via in-gel fluorescence imaging and relative protein abundance via in-gel coomassie staining. Image represents protein activity and abundance within the 35-45 kDa size range.

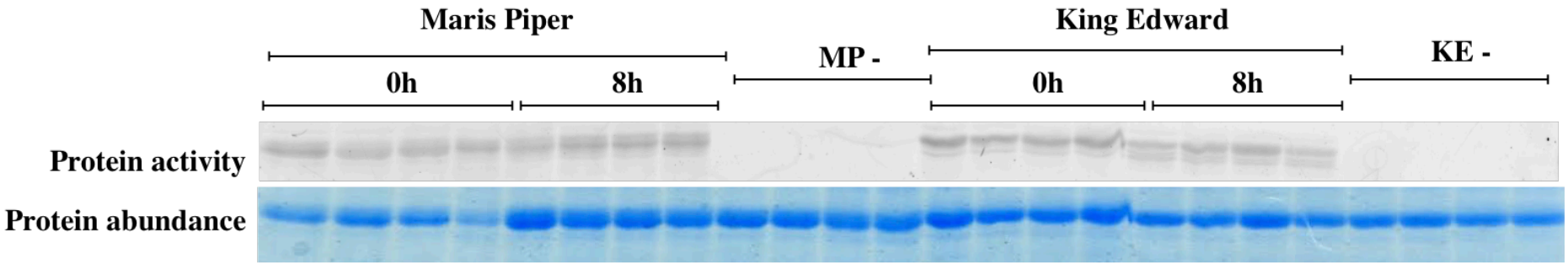


Figure 6.10 Activity of serine hydrolase enzymes and protein abundance from King Edward and Maris Piper cortex tissues incubated under Blackheart induction conditions for 0 h or 8 h and then incubated with TAMRA-FP probe, or DSMO (negative controls; KE- and MP) for 15 minutes. Proteins were resolved via SDS-PAGE and TAMRA-FP labelling visualised via in-gel fluorescence imaging, and relative protein abundance via in-gel coomassie staining. Image represents protein activity and abundance within the 35-45 kDa size range. n =4, negative controls represent n=3

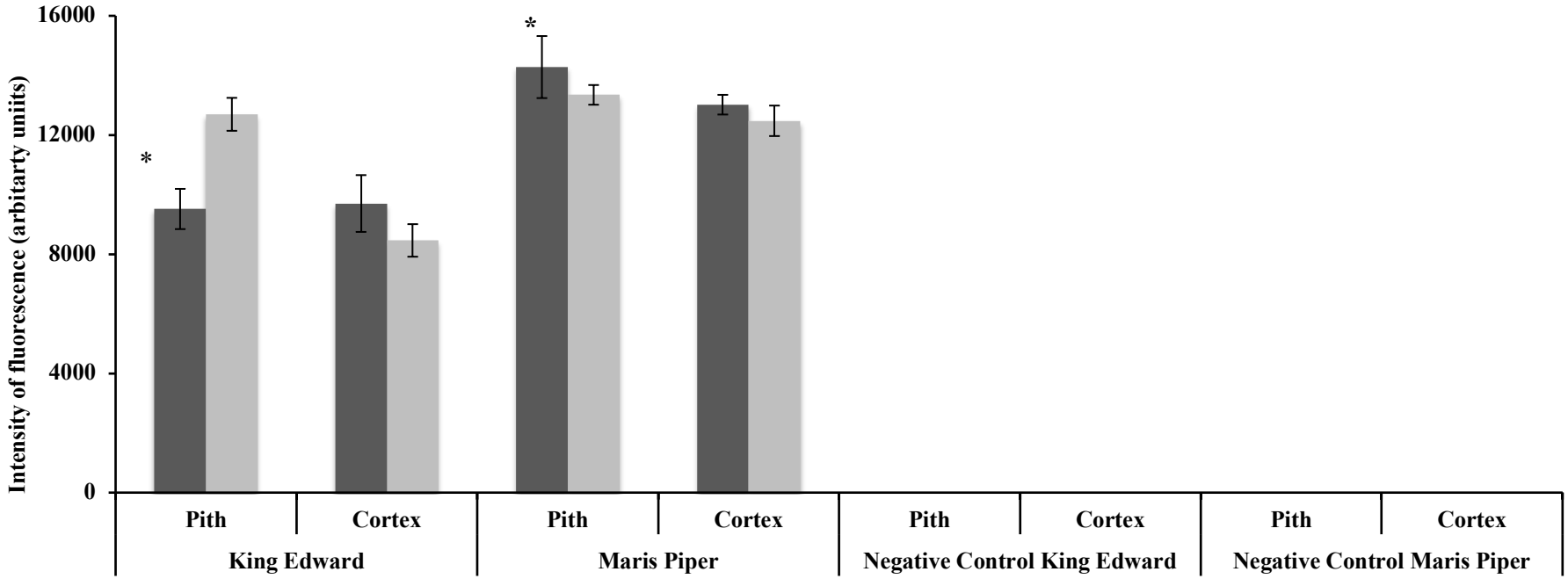


Figure 6.11 Intensity of fluorescence, representing activity of serine hydrolase enzyme of interest, in King Edward and Maris Piper pith and cortex tissues incubated under Blackheart induction conditions for 0 h or 8 h and then incubated with TAMRA-FP probe, or DSMO (negative controls) for 15 minutes. Asterisks represent significant differences between varietal measurements (t test, $p<0.05$), n=4.

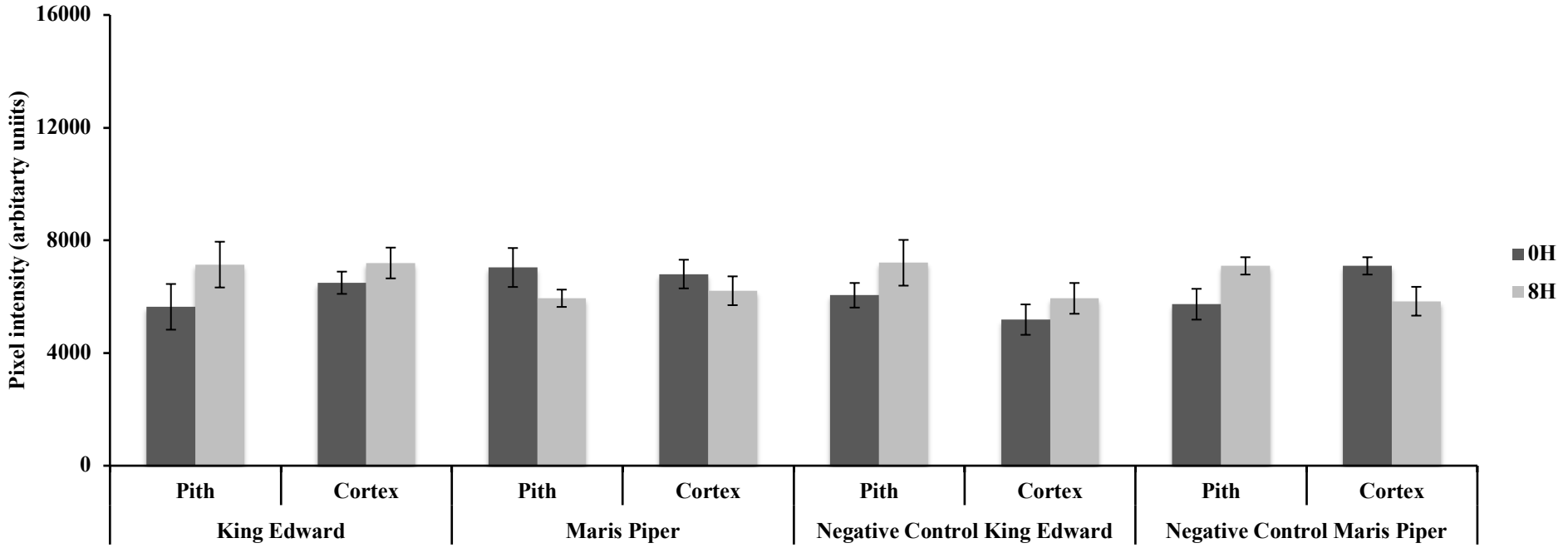


Figure 6.12 Abundance of protein at 35-45 kDa in King Edward and Maris Piper pith and cortex tissues incubated under Blackheart induction conditions for 0 h or 8 h and then incubated with TAMRA-FP probe, or DSMO (negative controls) for 15 minutes, n=4.

6.3.5 Serine Hydrolase Identification by Mass Spectrometry

To identify the specific protein responsible for the serine hydrolase activity observed in Figures 6.10 & 6.11), the protein band was excised, digested with trypsin and analysed by mass spectrometry. The protein band of interest (Figures 6.10 & 6.11), was actually the combination of two similarly sized bands (between 35-45 kDa) (Supplementary data). Therefore, a sample from pith tissues of King Edward tubers after 8 h of Blackheart induction conditions, was fractionated by SDS-PAGE with a longer run time to better resolve the two bands, which were then and the two excised separately. The larger band was labelled Band 1, and the smaller, Band 2. These bands were analysed via protein mass spectrometry by Dr Sabrina Liberatori at the Advanced Proteomics Facility at the Department of Biochemistry, University of Oxford (Chapter 2), which identified 203 proteins in Band 1, and 164 proteins in Band 2. Due to the specific labelling of the TAMRA-FP probe for serine hydrolase enzymes, non-serine hydrolase enzymes were ignored, resulting in 10 final possible proteins in Band 1, and eight in Band 2 (Table 6.3). Of these, all proteins were identified as members of the patatin protein family, except in both bands there was also a single pectin acetylesterase. The abundance (as measured by a spectral count index) of patatin was approximately 200x greater than the abundance of pectin acetylesterase in both bands (Table 6.3).

Table 6.3 Proteomic analysis and identification of protein bands of interest excised from gels as per (6.3.6). Each band was taken from a sample of King Edward pith tissues incubated under Blackheart induction conditions for 8 h.

Protein ID	Protein names	Mol. weight (kDa)	Band 1 Peptides	Band 2 Peptides	Sequence coverage Band 1 (%)	Sequence coverage Band 2 (%)	Intensity Band 1	Intensity Band 2
M1AGX5;Q3YJT5;Q2MY48;M1CUR3	Patatin	38.234	25	23	61.2	59.8	8.08E+10	5.56E+10
Q2MY45;Q2MY36;P15476;Q2MY42;P15477;Q2MY51;Q2MY41;Q2MY37;P11768;Q3YJT2	Patatin	42.614	26	22	60.1	60.1	5.76E+10	2.70E+10
Q42502;M1BFJ0;M1BFJ1	Patatin	42.465	23	22	54.9	53.6	3.08E+10	9.53E+09
Q3YJT4;Q2MY60;Q2MY59;Q2MY58;Q2MY50	Patatin	41.314	21	21	38.1	42.7	8.48E+09	3.81E+09
P07745	Patatin	42.49	23	19	52.8	52.8	5.10E+09	3.09E+09
M1C8D8;M1C8D9	Pectin acetylesterase	42.801	13	14	37.7	41.1	8.76E+08	5.67E+08
Q2MY44	Patatin	42.648	24	22	58	56.7	1.49E+08	2.06E+08
P15478	Patatin	42.338	14	14	24.6	24.9	3.97E+07	1.93E+07
Q2MY43;Q2MY56;Q2MY55	Patatin	42.686	9	0	25.6	0	3.46E+07	0
M1BFI9	Patatin	30.202	3	0	7.6	0	2.93E+06	0

6.4 Discussion

6.4.1 Cold Storage may Drive Increased Maintenance Costs under Blackheart Induction Conditions

Tubers stored at 2°C versus 4°C display greater membrane desaturation, indicating potentially increased acclimation costs via membrane remodelling at this lower temperature. This acclimation response is observed in both the cortex and pith tissues (Figure 6.7) and therefore, although 2°C storage and membrane acclimation correlates with increased Blackheart susceptibility, the associated costs do not appear to drive the decreased ATP:ADP ratios observed in Blackheart susceptible tissues.

Additionally, tubers stored at 2°C versus 4°C display increased membrane leakage (Figure 6.8) and respiratory rates (Chapter 4) when incubated under Blackheart induction conditions. The cause for this may be explained by the transition of tubers from low to warm temperatures and the increased maintenance costs that accompany membrane mis-acclimation; the differential membrane composition and degree of phospholipid saturation of tubers stored at 2°C versus 4°C (Figure 6.7) may render the membranes more poorly acclimated when tubers are transferred to warmer Blackheart induction conditions.

However, as pith and cortex tissues incubated under 2°C have similar membrane compositions and leakage, it is unlikely that membrane acclimation costs, or mis-acclimation costs, specifically drive Blackheart. However, the adenylate threshold hypothesis proposed (Chapter 4) emphasises the importance of the high initial ATP

abundance in Blackheart resistant tissues, and therefore tubers stored at 2°C may be driven closer to the proposed threshold, explaining the increased susceptibility of these tubers to develop Blackheart (Chapter 4).

6.4.2 Changes to Phospholipid Turnover Increases Prior to Blackheart Induction

The decline of flux into total lipids in the pith tissue of King Edward tubers between 0 h and 8 h of Blackheart induction conditions (Chapter 5) (Tables 6.1 & 6.2) appears to be predominantly caused by decreased carbon accumulation into pith tissue phospholipids. However, from the labelling experiment alone is not clear if this represents decreased phospholipid synthesis, or increased phospholipid turnover and subsequent dilution or movement of the radiolabel.

Results from GC-MS analysis and the SVP assays also indicate that phospholipid abundance decreases (Figures 6.1, 6.3 & 6.5). This decrease in pith tissue phospholipids containing linoleate and linolenate is matched with an increase in linoleate and linolenate FFA's (Figures 6.1 & 6.2). This correlation suggests phospholipid degradation into constituent FFA components occurs during Blackheart induction conditions. No increase in flux to FFA was observed (Table 6.2) indicating that the increased abundance arose from degradation of unlabelled substrates rather than *de novo* synthesis via the Kennedy pathway. Similar observations involving the accumulation of linoleic and linolenic acids in potato tubers under anoxia were identified by Rawyler et al., (1999) and were proposed to be driven by insufficient ATP synthesis.

6.4.2 Possible Causes of Increased Phospholipid Turnover During Blackheart Induction

From the flux measurements (Tables 6.1 & 6.2) and lipid quantification (Figures 6.1-6.6) alone, it is not clear if the degradation of phospholipids is driven by reduced synthesis of phospholipids via acyltransferases, or increased degradation via phospholipases. Rawyler et al., (1999) proposed that insufficient ATP synthesis activated a lipid acyl hydrolase, however their experiments did not consider the effect of reduced phospholipid synthesis.

The rapid change in phospholipid composition (Figure 6.1) is indicative of general hydrolysis rather than selective degradation of individual phospholipids, which is often observed during autophagy (Aubert et al., 1996). Both phospholipases and lipid acyl hydrolases (LAH) degrade phospholipids and are involved in the catabolic portion of the Lands cycle. The 2.18:1 ratio of FFA release to phospholipid decline (Figure 6.5) is indicative of a release of both hydrocarbon tails from each degraded phospholipid. As phospholipase A1 and A2 enzymes cleave individual hydrocarbon tails at the sn-1 or sn-2 positions of phospholipid glycerol backbones respectively (Matos & Pham-Thi, 2009; Galliard & Dennis, 1974), equal enzyme activities would be required to generate a 2:1 ratio. Phospholipase enzymes have been demonstrated to have different activities in potatoes (Senda et al., 1996) and due to the unlikeliness of enzyme activity coordination, it is more likely that this 2.18:1 ratio is caused by an enzyme that cleaves at both sn-1 and sn-2 positions, such as an LAH or phospholipase

B. A comparable ratio of 1.88:1 FFA release to phospholipid degradation was observed by Rawyler et al., (1999) in tuber cells under anoxia, resulting in the conclusion of the involvement of a LAH. Additionally, Rawyler et al., (1999) confirmed the absence of phospholipase A involvement by hydrolysis in a calcium free environment, the ion of which is required for phospholipase catalysis.

6.4.3 An Increase in Patatin Activity Appears to Drive Membrane Degradation During Blackheart Development

To investigate which direction the Lands cycle equilibrium had shifted, *in vivo* ABPP under Blackheart induction conditions was conducted, involving the specific labelling of active serine hydrolase enzymes (and thus encompassing acyltransferase, phospholipase and LAH enzymes). Incubation of tissues under Blackheart induction conditions indicated that a serine hydrolase between 35 and 45 kDa in size increased in activity in Blackheart susceptible tissues (Figures 6.9 & 6.11), but not in Blackheart resistant tissues or varieties (Figures 6.9, 6.10 & 6.11). Due to the apparent molecular weight and abundance of the protein it was thought to be patatin, which was further confirmed by MS (Table 6.3).

Although a pectin acetylesterase enzyme was also identified (Table 6.3), the abundance was approximately 200x less than that of patatin proteins, and therefore the changes in fluorescence and enzyme activity can be assumed to be caused by patatin. Patatin was found to be post translationally modified by the presence of two

different sized patatin bands when run for longer and on higher percentage acrylamide gels (Supplementary data).

Patatin is the storage protein of tubers and constitutes up to 40-60% of potato protein (Sonnewald et al., 1989). Patatin proteins have been demonstrated to have LAH activity (Racusen, 1984) but its *in vivo* activity in potatoes and involvement in lipid degradation is poorly characterised. Patatin is able to cleave at both the sn-1 and sn-2 positions (Senda et al., 1996; Canonne et al., 2011). Therefore, the correlation of patain activity and FFA release indicates that patatin is responsible for the 2.18:1 ratio (Figure 6.5) of FFA release to phospholipid degradation observed in Blackheart susceptible tissues during Blackheart development.

It should be noted that this conclusion does not exclude the possibility that there is also reduced phospholipid synthesis in Blackheart susceptible tissues during Blackheart development, via reduced acyltransferase activity. The decreased flux into phospholipids in pith tissues incubated under Blackheart induction conditions can be interpreted as decreased *de novo* synthesis. However, no fluorescence in the range of 65-67 kDa was observed during ABPP (Supplementary data) indicating that acyltransferase activity was low. However, the optimisation of ABPP for highly abundant proteins (allowing the analysis of patatin) may have limited the identification in activity changes of other serine hydrolase enzymes, and therefore the activity of acyltransferase may also contribute to membrane degradation.

6.4.3 Blackheart Affected Tissues Appear to Have Increased Maintenance Costs due to Membrane Leakage

Phospholipid abundance has been demonstrated to decrease by approximately 22.5% in pith tissues after 8 h under Blackheart induction conditions, which correlated with an increase in membrane leakage (Chapter 4). It is likely that this degree of phospholipid degradation affects membrane permeability and function, as cleaved hydrophilic phosphoglycerol heads will freely mix with the aqueous cell components. In potato tuber cell cultures the extent of the electrolyte leakage after phospholipid losses of 6-7% appeared to drive cell death (Crawford & Braendle, 1996). Therefore, it can be assumed that pith tissues under Blackheart induction conditions have increased maintenance costs due to membrane leakage. As the phospholipid abundance of Blackheart resistant varieties and tissue types does not decline (Figure 6.6), and the adenylate energy charge and degree of membrane leakage remains stable under Blackheart induction conditions (Chapter 4), these tissues do not appear to have increased maintenance costs.

6.5 Summary

Blackheart susceptible tissues have increased phospholipid degradation after 8 h of Blackheart induction conditions. This observation is correlated with an increase in patatin LAH activity, which is not observed in Blackheart resistant tissues or varieties. It is possible that patatin LAH activity drives this phospholipid degradation, although it is not clear why patatin activity changes during Blackheart development. This phospholipid degradation appears to be sufficient to explain the subsequent increase in membrane leakage previously observed during Blackheart development (Chapter 4). It is likely that this membrane degradation and leakage drives elevated

maintenance respiratory costs in Blackheart susceptible tissues, ultimately causing cell death.

7 Discussion

7.1 Summary of Research

Use of a Blackheart induction method enabled improved characterisation of Blackheart in *Solanum tuberosum*, demonstrating that the disorder is tissue specific. Both annual and varietal variations in Blackheart susceptibilities were found in modern potato varieties. The Blackheart induction method presented in this project allowed the identification of storage temperature and duration as conditions that increase Blackheart incidence and offers a tool to predict harvest susceptibility. Despite the prevailing thought that high temperatures and anoxia are required for Blackheart development, multiple conditions were identified as sufficient to induce Blackheart in tubers.

Tubers with reduced Ppo-5 expression did not develop visible Blackheart, providing the first empirical evidence for the role of PPO in Blackheart pigmentation. During the development of Blackheart, susceptible tissues rose above defined thresholds of membrane leakage and below thresholds of ATP:ADP ratios and adenylate energy charges, indicating cell death. The capacity for synthesis of ATP was altered in Blackheart affected tissues, as demonstrated by flux analysis and the abundance of respiratory substrates. However, the development of Blackheart correlates with increased membrane turnover and an upregulation of phospholipid cleavage in susceptible tissues, which is matched by increased patatin LAH activity. The increased respiratory demands that arise from this membrane degradation are proposed to drive the cell death and PPO pigmentation observed in Blackheart development.

7.2 Proposed Cause of Blackheart and Role of Patatin

From the research presented in this thesis, adenylate energy charges and ATP:ADP ratios are the first changes observed in susceptible tissues under Blackheart induction conditions (Chapter 4). Due to the timing of measurements, it is not known if patatin activation precedes or follows the observed changes in ATP abundance (Chapter 4 & 6). However, patatin activity and phospholipid degradation precede significant increases in membrane leakage (Chapter 4) and the order of these events implicates patatin activation as the driver. Ultimately it appears that resulting membrane leakage in Blackheart susceptible tissues drives in cell death and PPO-substrate mixing, causing Blackheart. However, from the results in this theses, and also within the literature, the underlying cause of patatin activation is unclear.

Reduced ATP synthesis rates have previously been implicated in the activation of potato LAH activity (Rawyler et al., 1999) which is likely to be patatin, however it is unclear what this underlying mechanism may be. Considering the implication of this proposed ATP threshold (Rawyler et al., 1999), its involvement could help explain many of the results presented in this thesis. Multiple conditions appear to both induce Blackheart, and increase the susceptibility of tubers to Blackheart (Chapter 3), indicating the involvement of a broad underlying mechanism. Of the conditions linked to increase Blackheart susceptibility, both through this thesis and anecdotally, most can be expected to have a negative impact on cellular ATP abundance. Therefore, such conditions may lower the ATP abundance and/or synthesis rates in tissues, bringing them closer to this potential patatin activating threshold.

Although regulation of patatin expression has been well characterised (Shewry, 2003) patain protein abundance does not appear to change over time (Chapter 6) and the rapid increase in activity (0-8 h) indicates that gene expression does not drive the observed activity increases (Chapter 6). Patatin post translational modification via glycosylation has been demonstrated to be involved in patatin activation (Shewry, 2003) and may drive changes in activity. Alternatively, storage proteins are often found in crystalline forms or protein bodies (Doye & Poon, 2005) and the activation of patatin could involve release from these insoluble states. During MRI imaging of tubers developing Blackheart, numerous regions of intense T1 weighted regions were observed to disappear during the development of Blackheart, concurrent with anhydrous bodies becoming more aqueous and disperse (Chapter 3). However, it is not yet known what may drive the increase activation of patatin observed (Chapter 6) and more work is required to confirm patatin as a driving force in Blackheart.

Blackheart could not be induced in certain potato varieties and tissue types, indicating that there may be genetic differences that convey resistance. Additionally, Blackheart could not be induced in tubers stored at 4°C for less than 3 months, although it is not clear if it is the storage duration or tuber age that drives this resistance. One explanation could be the importance of cold acclimation of tubers prior to transfer into Blackheart induction conditions (Chapter 6). An alternative explanation could involve tuber development; after approximately 3 months of stimulated “winter” conditions and tuber imposed endodormancy, sprout suppressants are required to induce ectodormancy. This transition and imposition of dormancy may drive developmental changes that increase the susceptibility of tubers to develop

Blackheart, for example as storage protein, patatin degradation and mobilisation may increase in order to nitrogen to sprouting buds.

The proposed cause of Blackheart, based on the observations of this thesis, implicate the role of increased membrane permeability which drives a reduction in cellular ATP:ADP ratios and adenylate energy charges. This membrane permeability appears to be driven by the activation of patatin and degradation of membrane phospholipids. It is possible that conditions that increase membrane permeability e.g. tuber age or storage temperature, and thus increase maintenance respiration costs have an effect of Blackheart susceptibility. Below a critical threshold, the consumption of ATP will drive cell death, and membrane rupture, allowing PPO-substrate mixing and Blackheart pigmentation.

7.3 Research Discussion: Future Work and Industrial Impact

The work in this project exploring the cause and control of Blackheart is largely unrivalled, particularly due to the dearth of literature around the disorder. All previous publications and industry prevention methods have been based on the first proposed cause of Blackheart in 1913 (Bartholomew, 1913); Blackheart was presented as "*asphyxiation*" of central tissues, driven by insufficient ventilation and heat. This project illustrated that neither CO_2 accumulation, O_2 abundance or high temperatures were necessary conditions for Blackheart to develop (Chapter 3) and thus gaseous diffusion does not appear to drive Blackheart. There was no difference to respiratory flux of tissues during Blackheart development (Chapter 5) indicating that "*asphyxiation*" did not cause Blackheart.

The identification of many sufficient factors for Blackheart to develop can explain the contradicting causes of Blackheart proposed in the literature (Bartholomew, 1913; Stewart & Mix, 1917; Singh & Mathur, 1937; Davis, 1926; Briddon, 2015) and current inability to prevent and predict the disease in industry (Briddon, 2015; Kiaitsi, 2015; David Wright, Manor Fresh Ltd., pers. comm., 2014); for example, both high and low storage temperatures were found to increase Blackheart susceptibility (Chapter 3), which is in line with previous work (Briddon, 2015). However, this project proposed that transferring tubers between temperatures, instead of the absolute temperature storage, was the predominant factor in increased Blackheart development. Similarly, this project provided empirical evidence that Blackheart susceptibility increases with tuber age and/or duration under storage conditions, supporting the anecdotal evidence observing the same effect in industry.

This thesis has shown that current industrial prevention methods have little empirical basis, and provides the first advancement in understanding the cause of Blackheart since 1913. With this improved knowledge, industry will be better able to prevent, predict and control the disorder; for example, avoidance of storing tubers at 2°C and gradual temperature transitions between stores require little effort from producers to instigate.

This project also provides the first characterisation of Blackheart as a tissue specific disorder, which spreads through the pith tissues from a single origin (Chapter 3). The varietal variations in Blackheart susceptibility and absence of the disorder in cortex tissues, indicates that there is likely a genetic component to the disorder. Future work

investigating conducting transcriptomic analysis could be used to explore expression profiles of susceptible and resistant varieties and tissues and identify any differences and the genetic basis of resistance.

Although multiple conditions have been shown to increase Blackheart susceptibility, the unifying link between them is that they all appear to increase tuber respiratory rate or membrane leakage. As Blackheart has been proposed to be caused by tissues falling beneath a 1:1 ratio of ATP:ADP, or increasing membrane permeability above a 50% electrolyte leakage threshold, it is possible that these conditions increase the susceptibility of tubers to Blackheart by bringing tissues closer to these thresholds. This project identifies phospholipid breakdown via patatin as a potential driving factor for this. It would be worthwhile to further explore the role of these thresholds in Blackheart development via artificial modification of the ATP:ADP ratio and electrolyte leakage of tissues via application of various concentrations of metabolic inhibitors or detergents and observing any increased Blackheart susceptibility. However, it is currently unclear how these would be supplied to tissues in intact tubers prior to Blackheart induction. These methods will further distinguish between the cause and effect of declining ATP concentrations and membrane leakage.

Additionally, the breadth of factors that affect Blackheart presents complications in completely avoiding the disorder in industry. Without additional research, solutions will be limited to prevention and prediction of the disorder; for example, selective breeding of current or novel varieties for reduced expression of PPO would offer growers and consumers a plethora of advantages, including absence of bruising or visible Blackheart pigmentation. Additional targets could include improved

temperature tolerance, specific membrane compositions or reduced/removed LAH activity of patatin via gene editing.

7.4 Limitations of This Research

Although a single underlying cause has been proposed for Blackheart in this thesis, multiple factors can cause cell death and drive PPO-substrate mixing and many disorders result in physiologically similar conditions to Blackheart e.g. bruising. The ubiquity of these downstream reactions limits the identification of a single Blackheart cause, and means that there may be multiple upstream origins of observationally identical conditions.

For practical reasons, this project utilised an induction method to generate Blackheart affected tubers for analysis. However, the chosen induction method is not representative of conditions observed in industry; at no point during the food system are tubers stored under anoxia and 37°C, although packaged tubers in consumers cupboards may provide similar conditions. It is possible that the biochemical measurements observed in this project are responses to these imposed induction conditions, and do not represent Blackheart observed in industry. However, the results from the induction method are consistent with anecdotal evidence and previously published research, supporting the applicability.

This project predominantly relied on the correlation of biochemical measurements with Blackheart onset, or comparison between susceptible and resistant tissue types and varieties. This correlatory approach was chosen as sampling for biochemical

analysis is destructive, preventing identification of Blackheart and measurements in the same tissues. Additionally, as this project was largely exploratory, this methodology yielded sufficient descriptive results to provide a springboard for future work. This limitation emphasises the importance of additional proof of concept experiments (as discussed in 7.3), which might include genetic modification of tuber patatin or artificial modification of tuber metabolism via application of inhibitors or hormones, providing stronger causative evidence.

An additional limitation of this correlatory approach is distinguishing between cause and effect; use of 4 h time course intervals further reduced the ability to establish an order of events during Blackheart development. Additional measurements, particularly around the point of Blackheart onset, would be beneficial.

7.5 Wider Impact of This Work

Potato tuber samples are frequently used as a heterotrophic tissue system in plant science research, however most sampling methodologies employ either: the use of longitudinal cores which are quantitively pith dominated; homogenisation of multiple tuber tissues; or fail to mention which tissues are sampled (Malone et al., 2006; Geigenberger, 2003). The work in this project has demonstrated that each tissue type has distinct responses and metabolism, and therefore potato tuber sampling methods should reflect this.

Loss of crop membrane integrity underlies many undesired issues in horticulture; membrane integrity has been linked to multiple post-harvest disorders such as aging,

waster loss, chilling injuries, ripening and resistance to pathogen infection (Parrish & Leopold, 1978; Maalekuu et al., 2006) . Additional information improving the current understanding of how membrane integrity is maintained, and the respiratory costs associated, has a far-reaching impact. The role of patatin, a ubiquitous protein found in many plants beyond potatoes (Shewry, 2003), has not previously been implicated in crop disorders and offers a novel research topic, with potential applicability to agricultural industries.

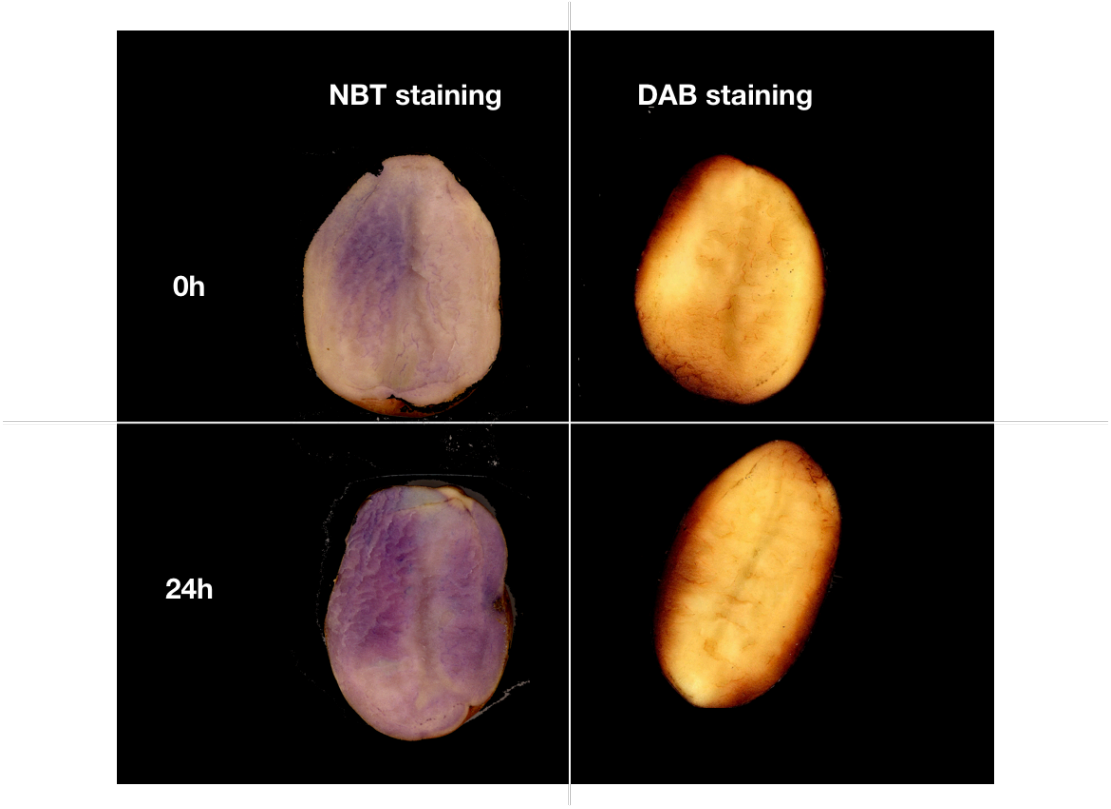
Potatoes are one of the world's most globally important crops, second only in consumption to rice and corn (Camire et al., 2009; FAO-STAT, 2018; FAO, 2009). Improved production, and with that improved storage of potatoes, offers *"a solution to increasing global food security",* as described by the Food and Agricultural Organisation (UN FAO, 2009). Therefore research into improved storage is of great importance.

Finally, current plant science research is dominated by a production-orientated approach to improving food security and over 95% of agricultural research funding goes towards increasing pre-harvest yields (Aulakh & Regmi, 2013; Kader, 2003). Current advances to increase potato yield focus on in-field issues and particularly yield losses from late blight (Singh et al., 2014). However, current aims to increase productivity of potatoes are ineffective without additional moves to reduce postharvest waste; almost all potato yield loss occurs beyond the field and in the UK 25-46% of tubers are losses occur between harvest and retail and an additional 49-74.5% of tuber waste occurs after purchasing (Terry et al., 2011). Blackheart is a significant cause of post-harvest potato waste, and one of the most important issues

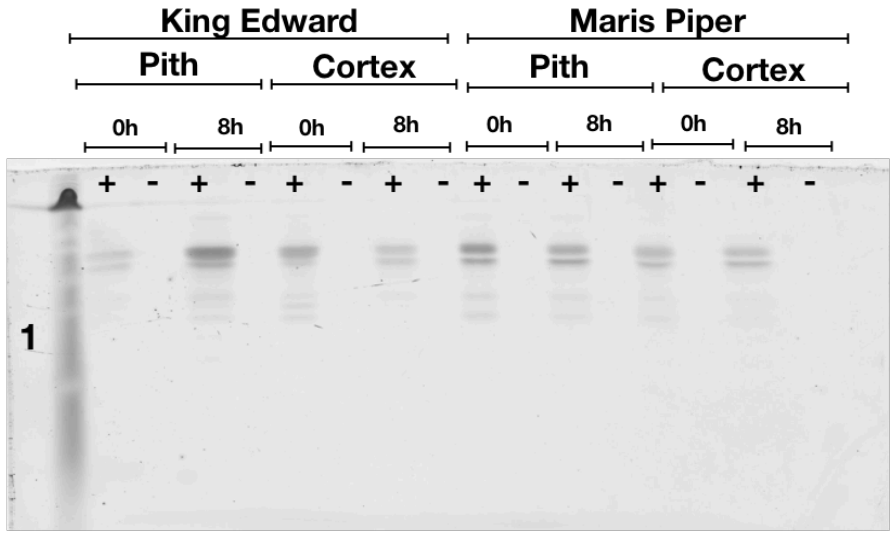
for the industry. Building on the new understanding of Blackheart proposed in this thesis, it is hoped that the disorder will be better managed in industry, resulting in less food waste, fewer consumer complaints and reduced reliance on imported tubers from supermarkets, as well as improving food security. This project emphasises the importance of funding of post-harvest crop research and the potential advances that can be achieved in such poorly researched areas.

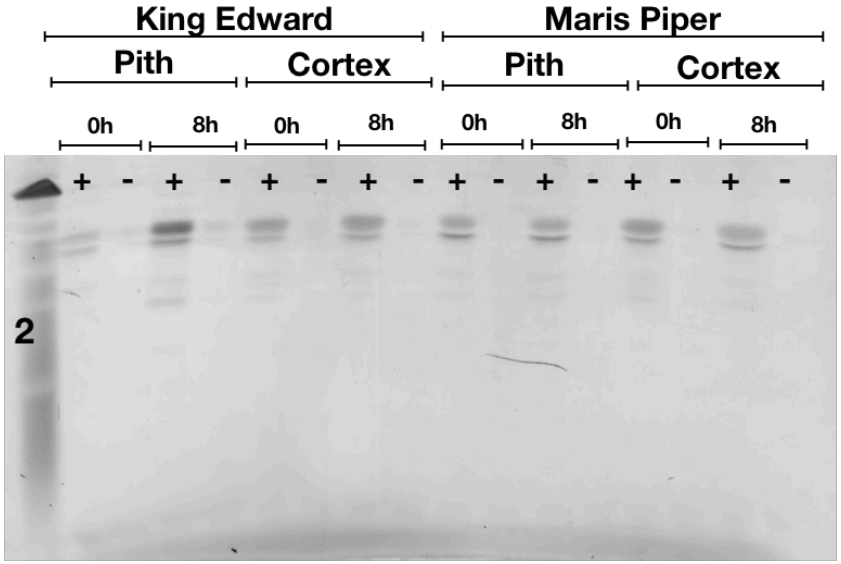
Supplementary Data

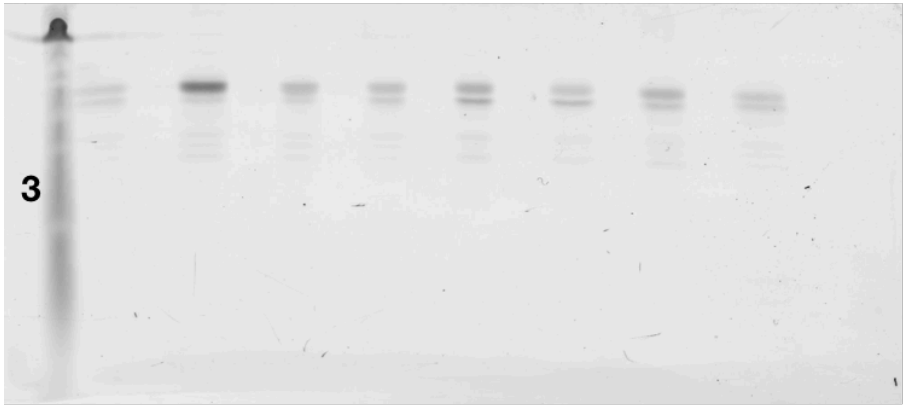
NBT and DAB staining of King Edward tubers during Blackheart development

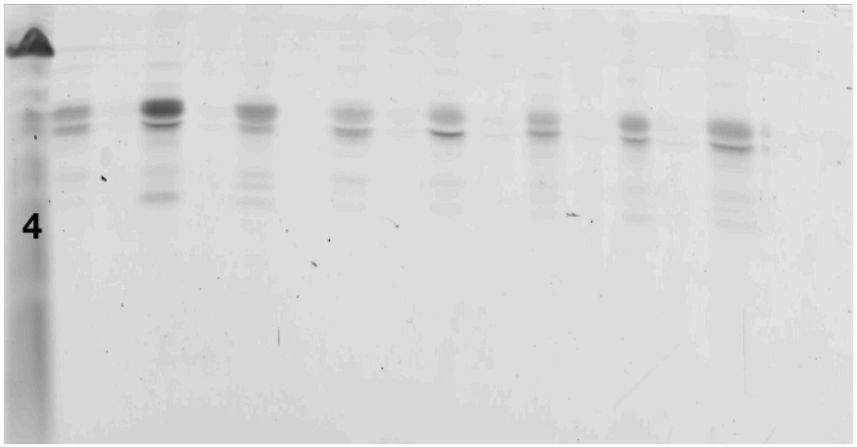


Activity of serine hydrolase enzymes from King Edward and Maris Piper pith tissues visualised via in-gel fluorescence imaging as per section 6.3.4.

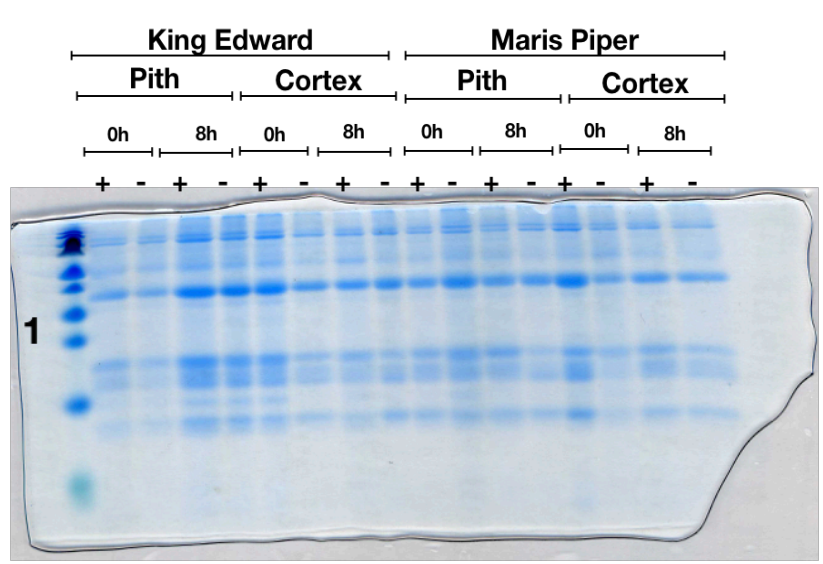


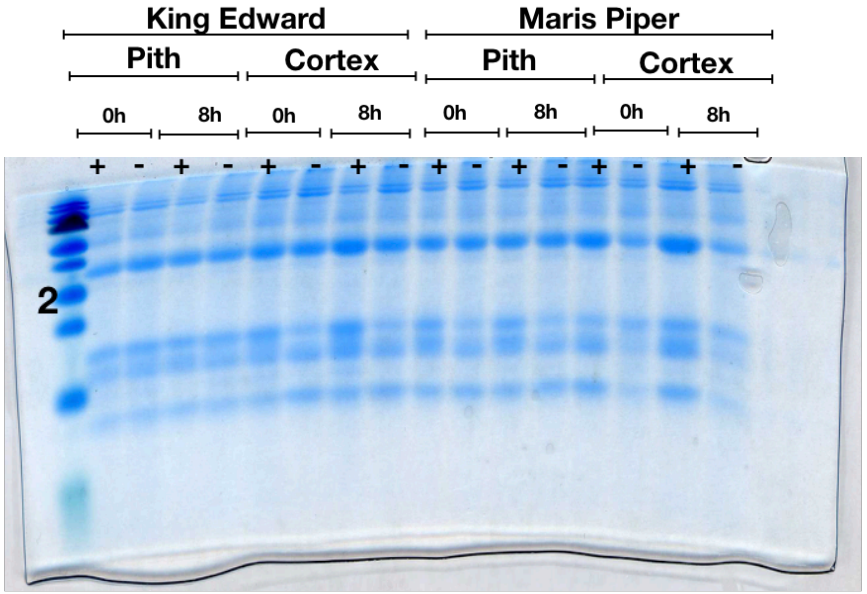


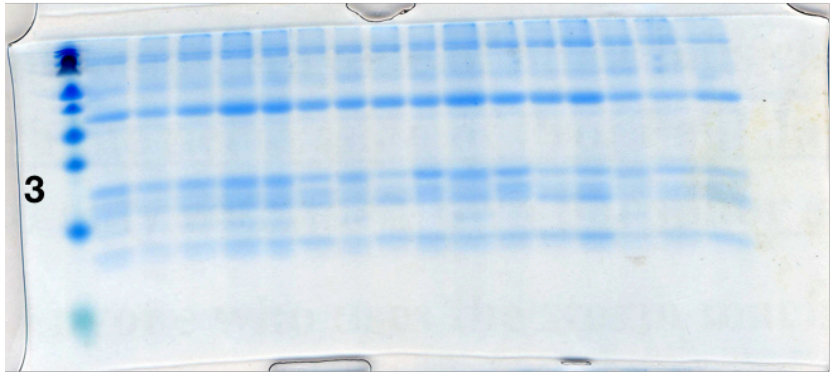


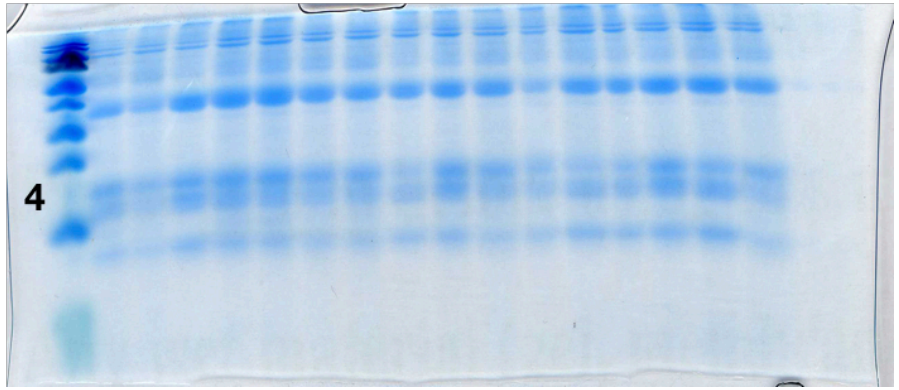


Abundance of proteins in King Edward and Maris Piper pith tissues visualised via in-gel Coomassie staining as per section 6.3.4.









Bibliography

Adrian Briddon (2014) Sutton Bridge Crop Storage Research, pers. comm.

Aguiar JL (2012) Symptoms of Frost, Freezing and Chilling Injury on Vegetables. Western Farm Press

Akyol H, Riciputi Y, Capanoglu E, Caboni MF, Verardo V (2016) Phenolic Compounds in the Potato and Its Byproducts: An Overview. Int J Mol Sci **17**: 835

Alexandratos N, Bruinsma J (2012) The 2012 Revision World Agriculture Towards 2030/2050: the 2012 Revision (Report). Rome. Global Perspective Studies Team FAO Agricultural Development Economics Division

Ali HM, El-Gizawy AM, El-Bassiouny REI, Saleh MA (2015) Browning Inhibition Mechanisms by Cysteine, Ascorbic Acid and Citric Acid, and Identifying PPO-Catechol-Cysteine Reaction Products. J Food Sci Technol **52**: 3651–3659

Appeldoorn NJG, de Bruijn SM, Koot-Gronsveld EAM, Visser RGF, Vreugdenhil D, van der Plas LHW (1997) Developmental Changes of Enzymes Involved in Conversion of Sucrose to Hexose-phosphate During Early Tuberisation of Potato. Planta **202**: 220–226

Arbon I, Brown C, Clarke C, Earp J, Fox T, Greenway D, Smith A, Stannard B, Warriner D, Whatley S, et al (2013) Global Food: Waste Not, Want Not (Report). UK Intstitute of Mechanical Engineers

Van As H (2006) Intact Plant MRI for the Study of Cell Water Relations, Membrane permeability, Cell-to-Cell and Long Distance Water Transport. J Exp Bot **58**: 743–756

Atkinson DE (1968) Energy Charge of the Adenylate Pool as a Regulatory Parameter. Interaction With Feedback Modifiers. Biochemistry **7**: 4030–4034

Aubert S, Gout E, Bligny R, Marty-Mazars D, Barrieu F, Alabouvette J, Marty F, Douce R (1996) Ultrastructural and Biochemical Characterization of Autophagy in Higher Plant Cells Subjected to Carbon Deprivation: Control by the Supply of Mitochondria with Respiratory Substrates. J Cell Biol **133**: 1251–1263

Aulakh J, Regmi A (2013) Post-Harvest Food Losses Estimation- Development of Consistent Methodology (Report). Rome. United Nations, FAO

Ausloos P, Clifton CL, Lias SG, Mikaya AI, Stein SE, Tchekhovskoi D V, Sparkman OD, Zaikin V, Zhu D (1999) The Critical Evaluation of a Comprehensive Mass Spectral Library. J Am Soc Mass Spectrom **10**: 287–299

Baker J, Mock NM (1994) An Improved Method for Monitoring Cell Death in Cell Suspension and Leaf Disc Assays using Evans Blue. Plant Cell Tissue Organ Cult **39**: 7–12

Bandana, Sharma V, Kaushik SK, Singh B, Raigond P (2016) Variation in Biochemical Parameters in Different Parts of Potato Tubers for Processing Purposes. J Food Sci Technol **53**: 2040–2046

Bartholomew E (1913) Black Heart of Potatoes. Phytopathology 3: 180-182

Bartholomew E (1914) A Pathological and Physiological Study of the Black Heart of Potato Tubers (Report). University of Wisconsin

BBSRC (2017) Secure Harvests - BBSRC (Website). https://bbsrc.ukri.org/research/briefings/food/secure-harvests/

Blessington T, Nzaramba MN, Scheuring DC, Hale AL, Reddivari L, Miller JC (2010) Cooking Methods and Storage Treatments of Potato: Effects on Carotenoids, Antioxidant Activity, and Phenolics. Am J Potato Res **87**: 479–491

Brand MD, Pakay JL, Ocloo A, Kokoszka J, Wallace DC, Brookes PS, Cornwall

EJ (2005) The Basal Proton Conductance of Mitochondria Depends on Adenine Nucleotide Translocase Content. Biochem J **392**: 353–362

Briddon A (2015) Blackheart - An Emerging Problem for the Potato Packing Industry (Report). Sutton Bridge Crop Storage Research

Brown DJ, Beevers H (1987) Fatty Acids of Rice Coleoptiles in Air and Anoxia. Plant Physiol **84**: 555–560

Burrell MM, Mooney PJ, Blundy M, Carter D, Wilson F, Green J, Blundy KS, Ap Rees T (1994) Genetic Manipulation of 6-Phosphofructokinase in Potato Tubers. Planta **194**: 95–101

Burton W (1989) The Potato, 3rd ed. Longman Scientific and Technical

Busch JM (1999) Enzymic Browning in Potatoes: a Simple Assay for a Polyphenol Oxidase Catalysed Reaction. Biochem Educ **27**: 171–173

Camire ME, Kubow S, Donnelly DJ (2009) Potatoes and Human Health. Crit Rev Food Sci Nutr **49**: 823–840

Canonne J, Froidure-Nicolas S, Rivas S (2011) Phospholipases in Action During Plant Defense Signaling. Plant Signal Behav **6**: 13–18

Cantos E, Tudela JA, Gil MI, Espín JC (2002) Phenolic Compounds and Related Enzymes Are Not Rate-Limiting in Browning Development of Fresh-Cut Potatoes. J Agric Food Chem **50**: 3015–3023

Cequier-Sánchez E, Rodríguez C, Dorta-Guerra R, Ravelo ÁG, Zárate R (2011) Echium Acanthocarpum Hairy Root Cultures, a Suitable System for Polyunsaturated Fatty Acid Studies and Production. BMC Biotechnol **11**: 42

Cheynier V, Sarni-Manchado P, Quideau S (2012) Recent Advances in Polyphenol Research. John Wiley & Sons Ltd.

Chi M, Liu C, Su Y, Tong Y, Liu H (2015) Bioinformatic Prediction of Upstream

MicroRNAs of PPO and Novel MicroRNAs in Potato. Can J Plant Sci **95**: 871–877

Chiariello NR, Mooney HA, Williams K (1989) Growth, Carbon Allocation and Cost of Plant Tissues. Plant Physiol. Ecol. Springer Netherlands, Dordrecht, pp 327–365

Couldwell DL, Dunford R, Kruger NJ, Lloyd DC, Ratcliffe RG, Smith AMO (2008) Response of Cytoplasmic pH to Anoxia in Plant Tissues with Altered Activities of Fermentation Enzymes: Application of Methyl Phosphonate as an NMR pH Probe. Ann Bot **103**: 249–258

Cox J, Mann M (2008) MaxQuant Enables High Peptide Identification Rates, Individualized ppb-Range Mass Accuracies and Proteome-Wide Protein Quantification. Nat Biotechnol **26**: 1367–1372

Cox J, Neuhauser N, Michalski A, Scheltema RA, Olsen J V., Mann M (2011) Andromeda: A Peptide Search Engine Integrated into the MaxQuant Environment. J Proteome Res **10**: 1794–1805

Craft CC, Siegelman HW, Butler WL (1958) Study of the Phenolic Compounds in Potato Tubers During Storage. Am Potato J **35**: 651–661

Crawford RMM, Braendle R (1996) Oxygen Deprivation Stress in a Changing Environment. J Exp Bot **47**: 145–159

Czaninski Y, Catesson AM (1974) Polyphenol Oxidases (Plants), 2nd ed. Reinhold, Van Nostrand, New York

Dao L, Friedman M (1992) Chlorogenic Acid Content of Fresh and Processed Potatoes Determined by Ultraviolet Spectrophotometry. J Agric Food Chem **40**: 2152–2156

Davis W (1926) Physiological Investigation of Black Heart of Potato Tuber. Bot Gaz

81: 323–360

Diop A, Caverly D (1998) Storage and Processing of Roots and Tubers in the Tropics (Report). United Nations FAO

Doye JPK, Poon WCK (2005) Protein Crystallization in Vivo (Report). University of Oxford

Falcone DL, Ogas JP, Somerville CR (2004) Regulation of Membrane Fatty Acid Composition by Temperature in Mutants of Arabidopsis with Alterations in Membrane Lipid Composition. BMC Plant Biol **4**: 17

FAO (2018) FAO STAT (Website). www.fao.org/faostat/

FAO (2009) New Light on a Hidden Treasure: End of Year Review (Report). United Nations FAO

Faridnia F, Burritt DJ, Bremer PJ, Oey I (2015) Innovative Approach to Determine the Effect of Pulsed Electric Fields on the Microstructure of Whole Potato Tubers: Use of Cell Viability, Microscopic Images and Ionic Leakage Measurements. Food Res Int **77**: 556–564

Farré EM, Tiessen A, Roessner U, Geigenberger P, Trethewey RN, Willmitzer L (2001) Analysis of the Compartmentation of Glycolytic Intermediates, Nucleotides, Sugars, Organic Acids, Amino Acids, and Sugar Alcohols in Potato Tubers Using a Nonaqueous Fractionation Method. Plant Physiol **127**: 685–700

Flexas J, Galmes J, Ribas-Carbo M, Medrano H (2005) The Effects of Water Stress on Plant Respiration. Plant Respir. Springer-Verlag, Berlin/Heidelberg, pp 85–94

Foley JA, Defries R, Asner GP, Barford C, Bonan G, Carpenter SR, Chapin FS, Coe MT, Daily GC, Gibbs HK, et al (2005) Global Consequences of Land Use. Science **309**: 570–574

Foley JA, Ramankutty N, Brauman KA, Cassidy ES, Gerber JS, Johnston M, Mueller ND, O'Connell C, Ray DK, West PC, et al (2011) Solutions for a Cultivated Planet. Nature **478**: 337–342

Friedman M (1997) Chemistry, Biochemistry, and Dietary Role of Potato Polyphenols. A Review. J Agric Food Chem **45**: 1523–1540

Funderburk HH, Lawrence JM (1964) Mode of Action and Metabolism of Diquat and Paraquat. Weeds **12**: 259–265

Galliard T, Dennis S (1974) Phospholipase, Galactolipase and Acyl Transferase Activities of a Lipolytic Enzyme from Potato. Phytochemistry **13**: 1731–1735

Gao L, Tu Z, Millett BP, Bradeen JM (2013) Insights into Organ-Specific Pathogen Defense Responses in Plants: RNA-Seq Analysis of Potato Tuber-Phytophthora infestans Interactions. BMC Genomics **14**: 340

Geigenberger P (2003a) Regulation of Sucrose to Starch Conversion in Growing Potato Tubers. J Exp Bot **54**: 457–465

Geigenberger P (2003b) Response of Plant Metabolism to Too Little Oxygen. Curr Opin Plant Biol **6**: 247–256

Geigenberger P, Fernie AR, Gibon Y, Christ M, Stitt M (2000) Metabolic Activity Decreases as an Adaptive Response to Low Internal Oxygen in Growing Potato Tubers. Biol Chem **381**: 723–740

Geigenberger P, Hajirezaei M, Geiger M, Deiting U, Sonnewald U, Stitt M (1998) Overexpression of Pyrophosphatase Leads to Increased Sucrose Degradation and Starch Synthesis, Increased Activities of Enzymes for Sucrose-Starch Interconversions, and Increased Levels of Nucleotides in Growing Potato Tubers. Planta **205**: 428–437

Gibbs J, Greenway H (2003) Review of Mechanisms of Anoxia Tolerance in Plants;

Growth, Survival and Anaerobic Catabolism. Funct Plant Biol **30**: 999–1063

Godfray HCJ, Beddington JR, Crute IR, Haddad L, Lawrence D, Muir JF, Pretty J, Robinson S, Thomas SM, Toulmin C (2010) Food Security: the Challenge of Feeding 9 Billion People. Science **327**: 812–818

Gustavsson J, Cederberg C, Sonesson U, Van Otterdijk R, Meybeck A (2011) Global Food Losses and Food Waste (Report). Dusseldorf. United Nations, FAO

Hajirezaei M, Takahata Y, Trethewey RN, Willmitzer L, Sonnewald U (2000) Impact of Elevated Cytosolic and Apoplastic Invertase Activity on Carbon Metabolism During Potato Tuber Development. J Exp Bot **51**: 439–445

Halket JM, Waterman D, Przyborowska AM, Patel RKP, Fraser PD, Bramley PM (2005) Chemical Derivatization and Mass Spectral Libraries in Metabolic Profiling by GC/MS and LC/MS/MS. J Exp Bot **56**: 219–43

Hargreaves JA, ap Rees T (1988) Turnover of Starch and Sucrose in Roots of Pisum sativum. Phytochemistry **27**: 1627–1629

Headford DWR, Douglas G (1967) Tuber Necrosis Following the Desiccation of Potato Foliage with Diquat. Weed Res **7**: 131–144

Hodges RJ, Buzby JC, Bennett B (2011) Postharvest Losses and Waste in Developed and Less Developed Countries: Opportunities to Improve Resource Use. J Agric Sci **149**: 37–45

Hruschka HW, Smith WL, Baker JE (1969) Reducing Chilling Injury of Potatoes by Intermittent Warming. Am Potato J **46**: 38–53

Jadhav SJ, Wu MT, Salunkhe DK (1980) Glycoalkaloids of Hollow Heart and Blackheart Potato Tubers. HortScience **15**: 147–148

Jolley R, Evans L, Makino N, Mason H (1974) Oxytyrosinase. J Biol Chem 335–345

Jordan CF (2002) Genetic Engineering, the Farm Crisis, and World Hunger. Bioscience **52**: 523–529

Kader AA (2003) A Perspective on Postharvest Horticulture (1978–2003). Hortscience **38**: 102–144

Kennedy RA, Rumpho ME, Fox TC (1992) Anaerobic Metabolism in Plants. Plant Physiol **100**: 1–6

Kiaitsi E (2015) Potato Stocks with Different Susceptibilities to Blackheart (PhD thesis). Cranfield University

King JC, Slavin JL (2013) White Potatoes, Human Health, and Dietary Guidance. Adv Nutr An Int Rev J **4**: 393S–401S

Klümper W, Qaim M (2014) A Meta-Analysis of the Impacts of Genetically Modified Crops. PLoS One **9**: e111629

Knight JA, Anderson S, Rawle JM (1972) Chemical Basis of the Sulfo-Phospho-Vanillin Reaction for Estimating Total Serum Lipids. Clin Chem **18**: 199

Kumar G, Knowles NR (1993) Changes in Lipid Peroxidation and Lipolytic and Free-Radical Scavenging Enzyme Activities during Aging and Sprouting of Potato (Solanum tuberosum) Seed-Tubers. Plant Physiol **102**: 115–124

Leyva A, Jarillo JA, Salinas J, Martinez-Zapater JM (1995) Low Temperature lnduces the Accumulation of Phenylalanine Ammonia-Lyase and Chalcone Synthase mRNAs of Arabidopsis thaliana in a Light-Dependent Manner'. Plant Physiol **108**: 39–46

Lipinski B, Hanson C, Lomax J, Kitinoja L, Waite R, Searchinger T (2013) Creating a Sustainable Food Future: Reducing Food Loss and Waste (Report). Washington

Lisec J, Schauer N, Kopka J, Willmitzer L, Fernie AR (2006) Gas

Chromatography Mass Spectrometry-Based Metabolite Profiling in Plants. Nat Protoc **1**: 387–396

Lobell DB, Schlenker W, Costa-Roberts J (2011) Climate Trends and Global Crop Production Since 1980. Science **333**: 616–620

Lötscher M, Klumpp K, Schnyder H (2004) Growth and Maintenance Respiration for Individual Plants in Hierarchically Structured Canopies of *Medicago sativa* and *Helianthus annuus* : the Contribution of Current and Old Assimilates. New Phytol **164**: 305–316

Luedemann A, Strassburg K, Erban A, Kopka J (2008) TagFinder for the Quantitative Analysis of Gas Chromatography - Mass Spectrometry (GC-MS)-Based Metabolite Profiling Experiments. Bioinformatics **24**: 732–737

Maalekuu K, Elkind Y, Leikin-Frenkel A, Lurie S, Fallik E (2006) The Relationship Between Water Loss, Lipid Content, Membrane Integrity and LOX Activity in Ripe Pepper Fruit After Storage. Postharvest Biol Technol **42**: 248–255

Malone JG, Mittova V, Ratcliffe RG, Kruger NJ (2006) The Response of Carbohydrate Metabolism in Potato Tubers to Low Temperature. Plant Cell Physiol **47**: 1309–22

Marangoni AG (2017) Low-Temperature Sweetening in Potato Tubers. Kinet. Anal. Food Syst. Springer International Publishing, Cham, pp 79–89

Matos AR, Pham-Thi A-T (2009) Lipid Deacylating Enzymes in Plants: Old Activities, New Genes. Plant Physiol Biochem **47**: 491–503

McMahon A, Lu H, Butovich IA (2013) The Spectrophotometric Sulfo-Phospho-Vanillin Assessment of Total Lipids in Human Meibomian Gland Secretions. Lipids **48**: 513

Miflin B (2000) Crop Improvement in the 21st Century. J Exp Bot **51**: 1–8

Millar AH, Whelan J, Soole KL, Day DA (2011) Organization and Regulation of Mitochondrial Respiration in Plants. Annu Rev Plant Biol **62**: 79–104

Mohamed I, Dudley R, Gregory A, Mouthaan R, Tian Z, Andrews P, Mellonie A (2016) Non-Destructive Testing for Blackheart Cavities in Potatoes with Microwave Radiation. 46th Eur. Microw. Conf. IEEE, pp 815–818

Mosneaguta R, Alvarez V, Barringer SA (2012) The Effect of Antibrowning Agents on Inhibition of Potato Browning, Volatile Organic Compound Profile, and Microbial Inhibition. J Food Sci **77**: C1234-40

Murata M, Noda I, Homma S (1995) Enzymatic Browning of Apples on the Market: Relationship Between Browning, Polyphenol Content, and Polyphenol Oxidase. Nippon Shokuhin Kagaku Kogaku Kaishi, **42**: 820–826

Nielsen TH, Deiting U, Stitt M (1997) A [beta]-Amylase in Potato Tubers Is Induced by Storage at Low Temperature. Plant Physiol **113**: 503–510

Nokthai P, Lee VS, Shank L (2010) Molecular Modeling of Peroxidase and Polyphenol Oxidase: Substrate Specificity and Active Site Comparison. Int J Mol Sci **11**: 3266–3276

Parkin KL, Marangoni A, Jackman RL, Yada RY, Stanley DW (1989) Chilling Injury: a Review of Possible Mechanisms. J Food Biochem **13**: 127–153

Parrish D, Leopold C (1978) On the Mechanism of Aging in Soybean Seeds. Plant Physiol **4**: 365–368

Partington JC, Smith C, Bolwell GP (1999) Changes in the Location of Polyphenol Oxidase in Potato (Solanum tuberosum L.) Tuber During Cell Death in Response to Impact Injury: Comparison With Wound Tissue. Planta **207**: 449–460

Paul MJ, Nuccio ML, Basu SS (2018a) Are GM Crops for Yield and Resilience

Possible? Trends Plant Sci **23**: 10–16

Paul MJ, Nuccio ML, Basu SS (2018b) Are GM Crops for Yield and Resilience Possible? Trends Plant Sci **23**: 10–16

Payyavula RS, Shakya R, Sengoda VG, Munyaneza JE, Swamy P, Navarre DA (2015a) Synthesis and Regulation of Chlorogenic Acid in Potato. Plant Biotechnol J **13**: 551–564

Payyavula RS, Shakya R, Sengoda VG, Munyaneza JE, Swamy P, Navarre DA (2015b) Synthesis and Regulation of Chlorogenic Acid in Potato: Rerouting Phenylpropanoid Flux in HQT-Silenced Lines. Plant Biotechnol J **13**: 551–564

Penning de Vries W (1975) The Cost of Maintenance Processes in Plant Cells. Ann Bot **39**: 77–92

Pfister-Sieber M, Brändle R (1995) Response of Potato Tubers to Hypoxia Followed by Reaeration. Potato Res **38**: 231–239

Pimentel D, Harvey C, Resosudarmo P, Sinclair K, Kurz D, McNair M, Crist S, Shpritz L, Fitton L, Saffouri R, et al (1995) Environmental and Economic Costs of Soil Erosion and Conservation Benefits. Science (80-) **267**: 1117–1123

Pimm SL, Raven P (2000) Extinction by Numbers. Nature **403**: 843–845

Plaxton WC (1996) The Organisation and Regulation of Plant Glycolysis. Annu Rev Plant Physiol Plant Mol Biol **47**: 47: 185-214

Poorter H, Werf A, Atkin OK, Lambers H (1991) Respiratory Energy Requirements of Roots Vary with the Potential Growth Rate of a Plant Species. Physiol Plant **83**: 469–475

Quested T, Parry A (2015) Household Food Waste in the UK (Report). WRAP

Racusen D (1984) Lipid Acyl Hydrolase of Patatin. Can J Bot **62**: 1640–1644

Ratcliffe RG (1994) In vivo NMR Studies of Higher Plants and Algae. Adv Bot Res

20: 43–123

Rawyler A, Pavelic D, Gianinazzi C, Oberson J, Braendle R (1999) Membrane Lipid Integrity Relies on a Threshold of ATP Production Rate in Potato Cell Cultures Submitted to Anoxia. Plant Physiol **120**: 293–300

Ray DK, Ramankutty N, Mueller ND, West PC, Foley JA (2012) Recent Patterns of Crop Yield Growth and Stagnation. Nat Commun **3**: 1293

Reeve RM (1968) Further Histological Comparisons of Black Spot, Physiological Internal Necrosis, Black Heart, and Hollow Heart in Potatoes. Am Potato J **45**: 391–401

Reid MS, Pratt HK (1972) Effects of Ethylene on Potato Tuber Respiration. Plant Physiol **49**: 252–5

Renz A, Merlo L, Stitt M (1993) Partial Purification from Potato Tubers of Three Fructokinases and Three Hexokinases Which Show Differing Organ and Developmental Specificity. Planta **190**: 156–165

Riss TL, Moravec RA, Niles AL, Duellman S, Benink HA, Worzella TJ, Minor L (2004) Cell Viability Assays (Bpok). Eli Lilly & Company and the National Center for Advancing Translational Sciences

Roberts JKM, Wemmer D, Jardetzky O (1984) Measurement of Mitochondrial ATPase Activity in Maize Root Tips by Saturation Transfer 31P Nuclear Magnetic Resonance. Plant Physiol **74**: 632–639

Rocha M, Licausi F, Araújo WL, Nunes-Nesi A, Sodek L, Fernie AR, van Dongen JT (2010) Glycolysis and the Tricarboxylic Acid Cycle are Linked by Alanine Aminotransferase During Hypoxia Induced by Waterlogging of Lotus japonicus. Plant Physiol **152**: 1501–1513

Rohloff J (2015) Analysis of Phenolic and Cyclic Compounds in Plants Using

Derivatization Techniques in Combination with GC-MS-Based Metabolite Profiling. Molecules **20**: 3431–3462

Rommens CM, Humara JM, Ye J, Yan H, Richael C, Zhang L, Perry R, Swords K (2004) Crop Improvement through Modification of the Plant's Own Genome. Plant Physiol **135**: 421–431

Rommens CM, Ye J, Richael C, Swords K (2006) Improving Potato Storage and Processing Characteristics through All-Native DNA Transformation. J Agric Food Chem **54**: 9882–9887

Rossouw D, Kossmann J, Botha FC, Groenewald J-H (2010) Reduced Neutral Invertase Activity in the Culm Tissues of Transgenic Sugarcane Plants Results in a Decrease in Respiration and Sucrose Cycling and an Increase in the Sucrose to Hexose Ratio. Funct Plant Biol **37**: 22–30

Sage RF, Peixoto MM (2016) Improved Experimental Protocols to Evaluate Cold Tolerance Thresholds in Miscanthus and Switchgrass Rhizomes. GCB Bioenergy **8**: 257–268

Sakai A, Larcher W (1987) Cold Acclimation in Plants. pp 97–137

Schindelin J, Arganda-Carreras I, Frise E, Kaynig V, Longair M, Pietzsch T, Preibisch S, Rueden C, Saalfeld S, Schmid B, et al (2012) Fiji: an Open-Source Platform for Biological-Image Analysis. Nat Methods **9**: 676–682

Schippers PA (1977) The Rate of Respiration of Potato Tubers During Storage. Potato Res **20**: 173–188

Scott GJ, Rosegrant MW, Ringler C (2000) Global Projections for Root and Tuber Crops to the Year 2020. Food Policy **25**: 561–597

Senda K, Yoshioka H, Doke N, Kawakita K (1996) A Cytosolic Phospholipase A2 From Potato Tissues Appears to be Patatin. Plant Cell Physiol **37**: 347–53

Serpen A, Gökmen V (2009) Evaluation of the Maillard Reaction in Potato Crisps by Acrylamide, Antioxidant Capacity and Color. J Food Compos Anal **22**: 589–595

Shewry PR (2003) Tuber storage proteins. Ann Bot **91**: 755–769

Sinclair TR, Purcell LC, Sneller CH (2004) Crop Transformation and the Challenge to Increase Yield Potential. Trends Plant Sci **9**: 70–75

Singh & Mathur (1937) Negative Corrleation Between the Occurance of Polyphenol Oxidase and Diastase and the Degree of Incidence of Blackheart of Potato. Phytopathology **27**: 992–1000

Slayton T (2009) Rice Crisis Forensics: How Asian Governments Carelessly Set the World Rice Market on Fire (Report). Centre for Global Development

Sonnewald U, Sturm A, Chrispeels MJ, Willmitzer L (1989) Targeting and Glycosylation of Patatin the Major Potato Tuber Protein in Leaves of Transgenic Tobacco. Planta **179**: 171–180

Sowokinos JR (2001) Biochemical and Molecular Control of Cold-Induced Sweetening in Potatoes. Am J Potato Res **78**: 221–236

Spychalla JP, Desborough SL (1990) Fatty Acids, Membrane Permeability, and Sugars of Stored Potato Tubers. Plant Physiol **94**: 1207–13

Steer MW (1988) Plasma Membrane Turnover in Plant Cells. J Exp Bot **39**: 987–996

Steffens J, Harel E, Hunt M (1994) Genetic Engineering of Plant Secondary Metabolism. Springer US, Boston, MA

Stevens H, Davelaar E (1997) Biochemical Potential of Potato Tubers To Synthesize Blackspot Pigments in Relation to Their Actual Blackspot Susceptibility. J Agric Food Chem **45**: 4221–4226

Stewart FC, Mix AJ (1917) Bulletin: Number 436: Blackheart and the Aeration of Potatoes in Storage (Report). Agricultural Experiment Station, New York State

Stitt M, Hurry V (2002) A Plant for all Seasons: Alterations in Photosynthetic Carbon Metabolism During Cold Acclimation in Arabidopsis. Curr Opin Plant Biol **5**: 199–206

Suslow T, Voss R (1998) Vegetables (Report). UC Postharvest Technology Center

Suzuki N, Mittler R (2006) Reactive oxygen species and temperature stresses: A delicate balance between signaling and destruction. Physiol Plant **126**: 45–51

Sweetlove L. (1995) The Control of Starch Synthesis (PhD thesis). University of Cambridge

Sweetlove L, Burrell M, ap Rees T (1996a) Characterization of Transgenic Potato (*Solanum tuberosum*) Tubers with Increased ADP Glucose Pyrophosphorylase. Biochem J **320**: 487–492

Sweetlove LJ, Burrell MM, ap Rees T (1996b) Starch Metabolism in Tubers of Transgenic Potato (*Solanum tuberosum*) With Increased ADP Glucose Pyrophosphorylase. Biochem J **320**: 493–498

Tan A, Berridge M, Herst P (2015) Tetrazolium Dyes as Tools in Cell Biology: New Insights Into Their Cellular Reduction. Biotechnol Annu Rev **11**: 127–152

Terry L, Mena C, Williams A, Jenney N, Whitehead P (2011) Mapping Fruit and Vegetable Waste Through the Retail and Wholesale Supply Chain (Report). Waste & Resources Action Programme

Thalhammer A, Hincha DK, Zuther E (2014) Measuring Freezing Tolerance: Electrolyte Leakage and Chlorophyll Fluorescence Assays. Methods Mol Biol **1166**: 15–24

Thygesen PW, Dry IB, Robinson SP (1995) Polyphenol oxidase in potato. A multigene family that exhibits differential expression patterns. Plant Physiol **109**: 525–531

Tilman D, Balzer C, Hill J, Befort BL (2011) Global Food Demand and the Sustainable Intensification of Agriculture. Proc Natl Acad Sci **108**: 20260–20264

Tolbert NE (1973) Activation of Polyphenol Oxidase of Chloroplasts. Plant Physiol **51**: 234–244

Tsouvaltzis P, Brecht JK (2017) Inhibition of Enzymatic Browning of Fresh-Cut Potato by Immersion in Citric Acid is Not Solely Due to pH Reduction of the Solution. J Food Process Preserv **41**: 128–129

Turner JS (1951) Respiration The Pasteur Effect in Plants. Annu Rev Plant Physiol **2**: 145–168

Tusher VG, Tibshirani R, Chu G (2001) Significance Analysis of Microarrays Applied to the Ionizing Radiation Response. Proc Natl Acad Sci U S A **98**: 5116–5121

United Nations DESA (2017) World Population Prospects: The 2017 Revision, Key Findings and Advance Tables (Report). New York

United Nations DESA (2015) Transforming Our World: the 2030 Agenda for Sustainable Development (Report). New York

United Nations FAO & OECD (2012) OECD-FAO Agricultural Outlook, 2012-2021 (Report). Rome

Valero E, Varón R, García-Carmona F (2000) Kinetics of a Self-Amplifying Substrate Cycle: ADP-ATP Cycling Assay. Biochem J **350**: 237

Vámos Vigyázó L, Haard N (2009) Polyphenol Oxidases and Peroxidases in Fruits and Vegetables. C R C Crit Rev Food Sci Nutr **15**: 49–127

Vartapetian BB, Mazliak P, Lance C (1978) Lipid Biosynthesis in Rice Coleoptiles Grown in the Presence or in the Absence of Oxygen. Plant Sci Lett **13**: 321–328

Veramendi J, Fernie AR, Leisse A, Willmitzer L, Trethewey RN (2002) Potato

Hexokinase 2 Complements Transgenic Arabidopsis Plants Deficient in Hexokinase 1 but Does Not Play a Key Role in Tuber Carbohydrate Metabolism. Plant Mol Biol **49**: 491–501

Vitti MCD, Sasaki FF, Miguel P, Kluge RA, Moretti CL (2011) Activity of Enzymes Associated with the Enzymatic Browning of Minimally Processed Potatoes. Brazilian Arch Biol Technol **54**: 983–990

VriesPenning D (1975) The Cost of Maintenance Processes in Plant Cells. Ann Bot **39**: 77–92

Wang CY (1989) Chilling injury of fruits and vegetables. Food Rev Int **5**: 209–236

Woods C (2014) Respiratory Carbon Loss in Plant Tissues Under Environmental Stress (PhD thesis). University of Oxford

Ye J, Weeks T, Yan H, Richael C, Duan H, Clark P, Collinge S (2013) Petition for Determination of Nonregulated Status for InnateTM Potatoes with Low Acrylamide Potential and Reduced Black Spot Bruise (Patent). 525

Yoruk R, Marshall MR (2003) Physiochemical Properties and Function of Plant Polyphenol Oxidase. J Food Biochem **27**: 361–422

Zabalza A, van Dongen JT, Froehlich A, Oliver SN, Faix B, Gupta KJ, Schmälzlin E, Igal M, Orcaray L, Royuela M, et al (2009) Regulation of Respiration and Fermentation to Control the Plant Internal Oxygen Concentration. Plant Physiol **149**: 1087–1098

Zhou L, Liu W, Xiong Z, Zou L, Chen J, Liu J, Zhong J (2016) Different Modes of Inhibition for Organic Acids on Polyphenoloxidase. Food Chem **199**: 439–446

Zhou Y, Dahler JM, Underhill SJ., Wills RB. (2003) Enzymes Associated With Blackheart Development in Pineapple Fruit. Food Chem **80**: 565–572

Zhou Y, Pan X, Qu H, Underhill SJR (2014) Low Temperature Alters Plasma

Membrane Lipid Composition and ATPase Activity of Pineapple Fruit During Blackheart Development. J Bioenerg Biomembr **46**: 59–69

Zhou Z, Zeng S, Li X, Zheng J (2015) Nondestructive Detection of Blackheart in Potato by Visible/Near Infrared Transmittance Spectroscopy. J Spectrosc **2015**: 1–9